UNIVERSIDADE ESTADUAL PAULISTA
"JÚLIO DE MESQUITA FILHO"
INSTITUTO DE BIOCIÊNCIAS – RIO CLARO

PROGRAMA DE PÓS-GRADUAÇÃO EM
ECOLOGIA, EVOLUÇÃO E BIODIVERSIDADE

SISTEMÁTICA E EVOLUÇÃO MORFOLÓGICA EM HOLOADENINAE (ANURA, BRACHYCEPHALOIDEA, CRAUGASTORIDAE)

ANA PAULA MOTTA

RIO CLARO – SP

2020

ANA PAULA MOTTA

SISTEMÁTICA E EVOLUÇÃO MORFOLÓGICA EM HOLOADENINAE (ANURA, BRACHYCEPHALOIDEA, CRAUGASTORIDAE)

Tese apresentada ao Instituto de Biociências do Câmpus de Rio Claro, Universidade Estadual Paulista, como parte dos requisitos para obtenção do título de Doutor em Ecologia, Evolução e Biodiversidade.

Orientador: Dr. Célio F. B. Haddad
Coorientador: Dr. José Manuel Padial

RIO CLARO – SP

2020

M921s

Motta, Ana Paula
Sistemática e evolução morfológica em Holoadeninae (Anura, Brachycephaloidea, Craugastoridae) / Ana Paula Motta. – Rio Claro, 2020

328 p. : il., tabs., fotos, mapas

Tese (doutorado) - Universidade Estadual Paulista (Unesp), Instituto de Biociências, Rio Claro
Orientador: Célio Fernando Baptista Haddad
Coorientador: José Manuel Padial

1. Biologia. 2. Zoologia. 3. Taxonomia (Zoologia). 4. Morfologia (Animais). I. Título.

Sistema de geração automática de fichas catalográficas da Unesp. Biblioteca do Instituto de Biociências, Rio Claro. Dados fornecidos pelo autor(a).

Essa ficha não pode ser modificada.

UNIVERSIDADE ESTADUAL PAULISTA

Câmpus de Rio Claro

CERTIFICADO DE APROVAÇÃO

TÍTULO DA TESE: SISTEMÁTICA E EVOLUÇÃO MORFOLÓGICA EM HOLOADENINAE (ANURA, BRACHYCEPHALOIDEA, CRAUGASTORIDAE)

AUTORA: ANA PAULA MOTTA VIEIRA
ORIENTADOR: CELIO FERNANDO BAPTISTA HADDAD
COORIENTADOR: JOSÉ MANUEL PADIAL

Aprovada como parte das exigências para obtenção do Título de Doutora em CIÊNCIAS BIOLÓGICAS (ZOOLOGIA), pela Comissão Examinadora:

Prof. Dr. CELIO FERNANDO BAPTISTA HADDAD
(Participaçao Virtual) Departamento de Zoologia /
UNESP - Instituto de Biociências de Rio Claro – SP

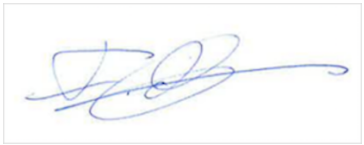

Prof. Dr. IGNACIO JOSÉ DE LA RIVA DE LA VIÑA (Participaçao Virtual)
Museo Nacional de Ciencias Naturales, Departamento de Biodiversidad y Biología Evolutiva / Madrid, Espanha

Profª Drª. MARÍA LAURA PONSSA (Participaçao Virtual) Tucumán, Argentina / CONICET-Fundación Miguel Lillo

Prof. Dr. MARIANE TARGINO ROCHA (Participaçao Virtual) Departamento de Vertebrados / Museu Nacional, Universidade Federal do Rio de Janeiro

Prof. Dr. HELIO RICARDO DA SILVA (Participaçao Virtual) Universidade Federal Rural do Rio de Janeiro / Rio de Janeiro-RJ

Rio Claro, 04 de dezembro de 2020

AVISO DE RESPONSABILIDADE NOMENCLATURAL

As alterações taxonômicas apresentadas neste documento, incluindo novos taxa, combinações e sinonímia, são rejeitadas como atos nomenclaturais e não estão disponíveis, de acordo com o Artigo 8.3 do Código Internacional de Nomenclatura Zoológica.

NOMENCLATURAL DISCLAIMER

The taxonomic changes presented herein, including new taxa, combinations, and synonymy, are disclaimed as nomenclatural acts and are not available, in accordance with Article 8.3 of the International Code of Zoological Nomenclature.

À minha mãe.

AGRADECIMENTOS

Agradeço imensamente ao meu orientador Prof. Célio F. B. Haddad e ao meu coorientador Prof. José M. Padial pela oportunidade de aprendizado e amadurecimento acadêmico. Aos amigos do laboratório de herpetologia da UNESP que foram parte muito importante desta experiência.

Aos membros da banca, que aceitaram o convite para avaliar e contribuir com meu trabalho.

A todos os curadores e gerentes das coleções que visitei por me proporcionarem toda a infraestrutura e ajuda necessárias, e aos que gentilmente forneceram material para ser analisado. Este trabalho não seria possível sem as coleções científicas.

Às agências de fomento que me proporcionaram a bolsa de doutorado e auxílios financeiros para pesquisa. A bolsa de doutorado foi concedida pelo Conselho Nacional de Desenvolvimento Científico e Tecnológico (CNPq) processo **141857/2016-1** (totalizando 14 meses) e pela Fundação de Amparo à pesquisa do Estado de São Paulo (FAPESP) processos **FAPESP 2017/08488-3**, **FAPESP (BEPE) 2018/10458-8**, e **FAPESP (BEPE) 2019/09537-3** (totalizando 41 meses).

À minha mãe, meu exemplo de luta. Obrigada pelo amor e apoio incondicionais.

Agradeço a todos que fizeram parte desta trajetória. Sou um pouco de cada canto que passei e de cada um que encontrei.

“Se procurar bem, você acaba encontrando
não a explicação (duvidosa) da vida,
mas a poesia (inexplicável) da vida.”

Carlos Drummond de Andrade

RESUMO

A subfamília Holoadeninae inclui gêneros em sua maioria distribuídos nos Andes (*Bryophryne*, *Lynchius*, *Microkayla*, *Niceforonia*, *Noblella*, *Oreobates*, *Phrynopus*, *Psychrophrynella*, *Qosqophryne*), assim como representantes na Amazônia, Cerrado e Mata Atlântica (*Barycholos*, *Euparkerella*, *Holoaden*, *Oreobates*). "*Eleutherodactylus*" *bilineatus* é incluída como *incertae sedis* nesta subfamília e seu estudo e comparação com os gêneros aos quais ela está relacionada ainda são necessários para resolver sua taxonomia. O gênero *Phrynopus* sofreu grandes mudanças na sua composição de espécies recentemente. Mesmo sendo um grupo com interessante variação em sua morfologia, caracteres morfológicos ainda não foram testados em um contexto filogenético e nenhuma sinapomorfia morfológica foi proposta para o gênero. Além disto, espécies do clado composto por *Phrynopus*, *Lynchius* e *Oreobates* apresentam interessante diversidade de formas e estão presentes em diferentes habitats distribuídos na América do Sul, constituindo um grupo ideal para o teste de diversas hipóteses evolutivas. Assim, o presente trabalho apresenta análises filogenéticas de evidência total utilizando dados genotípicos e fenotípicos para inferir as relações filogenéticas das espécies de *Phrynopus*, assim como dos gêneros de Holoadeninae; elucida as relações filogenéticas e a taxonomia de "*Eleutherodactylus*" *bilineatus*, e descreve um novo gênero de Holoadeninae; e mostra que a ocupação independente de habitats semelhantes é responsável pela convergência no formato do corpo das espécies de *Lynchius*, *Oreobates* e *Phrynopus*. Além disto, são feitas contribuições para a taxonomia dos gêneros *Lynchius* e *Oreobates*, que incluem a revisão de *O. heterodactylus* e *O. crepitans* e a descrição de uma nova espécie de *Oreobates* da Bolívia; descrição de uma nova espécie de *Lynchius* e uma nova espécie de *Oreobates* do Peru; e novos registros para a distribuição de *O. antrum*.

Palavras-chave: Convergência, Osteologia, Sistemática, Taxonomia, Terrarana.

ABSTRACT

The subfamily Holoadeninae includes genera mostly distributed in the Andes (*Bryophryne*, *Lynchius*, *Microkayla*, *Niceforonia*, *Noblella*, *Oreobates*, *Phrynopus*, *Psychrophrynella*, and *Qosqophryne*), as well as representatives in the Amazon, Cerrado and Atlantic Forest (*Barycholos*, *Euparkerella*, *Holoaden*, and *Oreobates*). "*Eleutherodactylus*" *bilineatus* is included in the subfamily as *incertae sedis* and its study and comparison with its relative genera are still necessary to resolve its taxonomy. The *Phrynopus* genus has recently undergone major changes in its composition. Even though it is a group with interesting variation in its morphology, morphological characters have not yet been tested in a phylogenetic context and no morphological synapomorphy has been proposed for the genus. In addition, species from the clade composed of *Phrynopus*, *Lynchius* and *Oreobates* have an interesting diversity of forms and are present in different habitats distributed in South America, constituting an ideal group for testing evolutionary hypotheses. This study includes total evidence phylogenetic analyses using genotypic and phenotypic data to infer the phylogenetic relationships of *Phrynopus*, as well as of the genera of Holoadeninae; elucidates the phylogenetic relationships and taxonomy of "*Eleutherodactylus*" *bilineatus*, describing a new genus of Holoadeninae; and shows that the independent occupation of similar habitats is responsible for the convergence in the body shape of species of *Lynchius*, *Oreobates* and *Phrynopus*. It also includes contributions to the taxonomy of *Lynchius* and *Oreobates*, which encompass the review of *O. heterodactylus* and *O. crepitans*, as well as the description of a new species of *Oreobates* from Bolivia; description of a new species of *Lynchius* and a new species of *Oreobates* from Peru; and new records for the distribution of *O. antrum*.

Keywords: Convergence, Osteology, Systematics, Taxonomy, Terrarana.

SUMÁRIO

INTRODUÇÃO GERAL 15
Referências 19

Seção 1 - Sistemática e Evolução Morfológica 21
Unmasking convergence in the high Andes: total evidence phylogeny of *Phrynopus* and phenotypic evolution in Holoadeninae (Anura: Brachycephaloidea) 22
Introduction 25
Materials and methods 30
Results 40
Discussion 43
Conclusions 56
References 57
Tables 70
Figure captions 88
Figures 90
Appendices 98

A new terraranan genus from the Brazilian Atlantic Forest with comments on the systematics of Brachycephaloidea (Amphibia: Anura) 119
Introduction 121
Materials and methods 123
Results 126
Discussion 130
References 134
Tables 143
Figure captions 146
Figures 148
List of supporting information 155
Appendix 163

Habitat rather than altitudinal shifts drive morphological evolution in a continental radiation of New World direct-developing frogs 164
Introduction 166
Materials and methods 168
Results 171
Discussion 172
References 176
Tables 182
Figure captions 184
Figures 186
Supplementary material 191

Seção 2 - Contribuições taxonômicas 203
On the identity of species of *Oreobates* (Anura: Craugastoridae) from central South America, with the description of a new species from Bolivia 204
Introduction 206
Materials and methods 210
Results 215
Discussion 234
References 241
Tables 250
Figure captions 259
Figures 262
Appendices 271

Two new species of terrestrial-breeding frogs (Anura: Brachycephaloidea) from Cordillera de Colán, Peru 275
Introduction 277
Materials and methods 279
Results 282
Discussion 295
References 299
Tables 305

Figure captions 307
Figures 309
Appendices 316

New distribution records of *Oreobates antrum* Vaz-Silva, Maciel, Andrade, and Amaro, 2018, a cave-associated species from the Seasonally Dry Tropical Forest in the Brazilian Cerrado (Anura: Brachycephaloidea: Craugastoridae) 319
References 322
Figures 324

CONCLUSÕES GERAIS 326

INTRODUÇÃO GERAL

O clado dos anuros neotropicais com ovos terrestres e desenvolvimento direto, superfamília Brachycephaloidea, é composto por mais de 1000 espécies e compreende em torno de um terço de todas as espécies de anuros descritas para o novo mundo (Frost, 2020). As espécies deste grupo, conhecido como terrarana, tem sido incluídas em diversas análises filogenéticas com diferentes abrangências taxonômicas, diferentes conjuntos de dados e diferentes métodos analíticos (Hedges et al. 2008; Pyron & Wiens, 2011; Padial et al. 2012; Padial et al. 2014; Heinicke et al., 2018; Jetz and Pyron, 2018). Todavia, as filogenias existentes são discordantes em diversos pontos, resultando em extensa instabilidade taxonômica em níveis de famílias, subfamílias e gêneros.

Em uma revisão recente de Brachycephaloidea, Padial et al. (2014) propuseram uma nova taxonomia para o grupo e reconheceram três famílias: Brachycephalidae, Craugastoridae e Eleutherodactylidae. A família Craugastoridae compreende 857 espécies distribuídas em 3 subfamílias, incluindo a subfamília Holoadeninae. Gêneros de Holoadeninae estão em sua maioria distribuídos nos Andes (*Bryophryne*, *Lynchius*, *Microkayla*, *Niceforonia*, *Noblella*, *Oreobates*, *Phrynopus*, *Psychrophrynella*, *Qosqophryne*), mas também incluem representantes na Amazônia, Cerrado e Mata Atlântica (*Barycholos*, *Euparkerella*, *Holoaden*, *Oreobates*).

Análises filogenéticas utilizando caracteres moleculares recuperaram a espécie *Ischnocnema bilineata* como pertencente a um clado incluindo os gêneros *Barycholos* e *Noblella*. Esta espécie foi removida do gênero *Ischnocnema* e incluída na família Holoadeninae como "*Eleutherodactylus*" *bilineatus* (Canedo & Haddad, 2012). A análise da morfologia desta espécie e comparação com os gêneros aos quais ela está relacionada ainda são necessários para resolver sua taxonomia.

Phrynopus é composto atualmente por 35 espécies com distribuição restrita aos Andes centrais do Peru. Lynch (1975) classificou espécies como pertencentes a *Phrynopus* baseado

principalmente em caracteres dos dígitos. Porém, a monofilia de *Phrynopus* (*sensu* Lynch, 1975) foi enfaticamente rejeitada em todas as análises filogenéticas moleculares (Hedges et al. 2008; Pyron & Wiens, 2011; Padial et al. 2012; Padial et al. 2014; Heinicke et al., 2018; Jetz and Pyron, 2018). Nenhum trabalho até então teve como foco uma revisão sistemática do gênero considerando sua diversidade morfológica, e as mudanças na composição de espécies de *Phrynopus* tem sido feitas principalmente com base em evidências moleculares.

O gênero *Phrynopus* tem sido recuperado em diferentes análises filogenéticas como parte de um clado que inclui os gêneros *Lynchius* e *Oreobates* (Hedges et al*.,* 2008; Padial et al*.*, 2009; Pyron & Wiens, 2011; Padial et al*.*, 2012; Padial et al., 2014). *Lynchius* foi proposto por Hedges et al. (2008) para um clado até então formado por três espécies: *Lynchius flavomaculatus* (Parker, 1938), *L. nebulanastes* (Cannatella, 1984) e *L. parkeri* (Lynch, 1975). Posteriormente, *Oreobates simmonsi* foi transferido para *Lynchius* (Padial et al. 2012) e três novas espécies foram descritas (Motta et al., 2016; Sánchez-Nivicela et al., 2019). Assim, o gênero é hoje composto por sete espécies distribuídas na Cordilheira Oriental no sul do Equador e Cordilheira de Huancabamba no norte do Peru, entre 1800m e 3100m de altitude.

Oreobates foi removido do sinônimo de *Ischnocnema* e revalidado por Caramaschi & Canedo (2006), que incluíram seis espécies no gênero. Após a revalidação, *Oreobates* teve um rápido aumento no número de espécies. Padial et al. (2008) apresentaram uma filogenia de *Oreobates* e classificaram 14 espécies de um clado como pertencentes ao gênero. Em uma revisão mais completa do gênero, Padial et al. (2012) apresentam evidências morfológicas e moleculares que suportam a existência de 22 espécies em *Oreobates*. O gênero é composto atualmente por 25 espécies distribuídas em diversos habitats, como Amazônia, Cerrado, além de florestas e vales nos Andes.

Apesar da suposta monofilia de *Lynchius*, *Oreobates* e *Phrynopus*, bem como a monofilia do clado formado por estes três gêneros, terem sido recuperados em diferentes

análises filogenéticas (Hedges et al*.,* 2008; Padial et al*.*, 2009; Pyron & Wiens, 2011; Padial et al*.*, 2012; Padial et al., 2014), a relação entre estes gêneros não é bem estabelecida e varia dependendo do dataset e método de análise empregado. Desta forma, apesar de evidências moleculares em análises filogenéticas terem conduzido um rápido crescimento no entendimento das relações filogenéticas e diversidade de espécies neste clado, ainda é necessário reverter a falta de evidências morfológicas, já que caracteres morfológicos nunca foram testados em um contexto filogenético e, portanto, sinapomorfias ainda não foram encontradas para o grupo.

Além disso, a evolução independente de características semelhantes em espécies que ocupam o mesmo habitat suporta a ideia de que evolução convergente está por trás de vários dos padrões recorrentes observados na variação morfológica em espécies de *Lynchius*, *Oreobates* e *Phrynopus* (Padial et al., 2012). Por exemplo, as duas espécies andinas do gênero *Oreobates* (*O. ayacucho* e *O. pereger*) se assemelham a *Lynchius* e *Phrynopus*, gêneros que têm distribuições relativamente pequenas e ecologicamente restritas nos Andes. Espécies de habitats mais secos, como Cerrado (*O. crepitans* e *O. heterodactylus*) ou vales secos andinos (*O. ibischi* e *O. discoidalis*), que frequentemente se empoleiram em vegetação baixa, têm corpo esbelto e apresentam longas extremidades com falanges terminais em forma de T e discos grandes nos dedos das mãos e dos pés. A semelhança entre espécies de *Oreobates* de florestas montanas e planícies amazônicas com *Lynchius simmonsi* (ou seja, pele com tubérculos, extremidades longas, cabeça relativemente grande e tubérculos plantares cônicos) também indica a evolução convergente como resultado da adaptação a ambientes florestais (Motta et al., 2016).

Desta forma, os objetivos deste projeto incluem: (I) realizar uma análise filogenética de evidência total utilizando dados genotípicos (sequências de DNA) e fenotípicos (morfologia externa, interna e osteologia) para inferir as relações filogenéticas das espécies de *Phrynopus* e de gêneros da subfamília Holoadeninae, assim como a evolução de caracteres neste grupo, (II)

elucidar as relações filogenéticas e a taxonomia de "*Eleutherodactylus*" *bilineatus*, (III) investigar se fatores ecológicos são os principais responsáveis pela morfologia convergente das espécies de *Lynchius*, *Oreobates* e *Phrynopus* ou se os padrões morfológicos são condicionados pelas relações filogenéticas, além de (IV) realizar revisões taxonômicas e descrições de novas espécies de *Lynchius* e *Oreobates*.

A tese está dividida em duas seções e cada seção inclui três capítulos. A primeira seção trata da sistemática e evolução morfológica em Holoadeninae, enquanto a segunda seção inclui colaborações taxonômicas para o grupo. Os capítulos foram formatados segundo modelo dos periódicos científicos aos quais os artigos foram ou serão submetidos.

Referências

CANEDO, C.; HADDAD, C. F. B. Phylogenetic relationships within anuran clade Terrarana, with emphasis on the placement of Brazilian Atlantic rainforest frogs genus *Ischnocnema* (Anura: Brachycephalidae). **Molecular Phylogenetics and Evolution**, v. 65, n. 2, p. 610–620, 2012.

CANNATELLA, D. C. Two new species of the leptodactylid frog genus *Phrynopus*, with comments on the phylogeny of the genus. **Occasional papers of the Museum of Natural History**, University of Kansas, v. 113, p. 1–16, 1984.

CARAMASCHI, U.; CANEDO., C. Reassessment of the taxonomic status of the genera *Ischnocnema* Reinhard and Lütken, 1862 and *Oreobates* Jiménez-de-la-Espada, 1872, with notes on the synonymy of *Leiuperus verrucosus* Reinhardt and Lütken, 1862 (Anura: Leptodactylidae). **Zootaxa**, v. 1116, p. 43–54, 2006.

HEDGES, S. B.; DUELLMAN, W. E.; HEINICKE, M. P. New World direct-developing frogs (Anura: Terrarana): Molecular phylogeny, classification, biogeography, and conservation. **Zootaxa**, v. 1737, p. 1–182, 2008.

HEINICKE, M. P.; LEMMON, A. R.; LEMMON, E. M.; MCGRATH, K.; HEDGES, S. B. Phylogenomic support for evolutionary relationships of New World direct-developing frogs (Anura: Terraranae). **Molecular Phylogenetics and Evolution**, v. 118, p. 145–155, 2018.

JETZ, W.; PYRON, R. A. The interplay of past diversification and evolutionary isolation with present imperilment across the amphibian tree of life. **Nature Ecology & Evolution**, v. 2, p. 850–858, 2018.

LYNCH, J. D. A review of the Andean leptodactylid frog genus *Phrynopus*. **Occasional Papers of the Museum of Natural History, University of Kansas,** v. 35, p. 1–51, 1975.

MOTTA, A. P.; CHAPARRO, J. C.; POMBAL JR., J. P.; GUAYASAMIN, J. M.; DE LA RIVA, I.; PADIAL, J. M. Molecular phylogenetics and taxonomy of the Andean genus *Lynchius* Hedges, Duellman, and Heinicke, 2008 (Anura: Craugastoridae). **Herpetological Monographs**, v. 30, p. 119–142, 2016.

PADIAL, J. M.; CHAPARRO, J. C.; DE LA RIVA, I. Systematics of *Oreobates* and the *Eleutherodactylus discoidalis* species group (Amphibia, Anura), based on two mitochondrial DNA genes and external morphology. **Zoological Journal of the Linnean Society**, v. 152, p. 737–773, 2008.

PADIAL, J. M.; CASTROVIEJO-FISHER, S.; DE LA RIVA, I. The phylogenetic relationships of *Yunganastes* revisited (Anura: Terrarana). **Molecular Phylogenetics and Evolution**, v. 52, p. 911–915, 2009.

PADIAL, J. M.; CHAPARRO, J. C.; CASTROVIEJO-FISHER, S.; GUAYASAMIN, J. M.; LEHR, E.; DELGADO A. J.; VAIRA, M.; TEIXEIRA JR., M.; AGUAYO-VEDIA, C. R.; DE LA RIVA, I. A revision of species diversity in the Neotropical genus *Oreobates* (Anura: Strabomantidae), with the description of three new species from the Amazonian slopes of the Andes. **American Museum Novitates**, v. 3752, p. 1–55, 2012.

PADIAL, J. M.; GRANT, T.; FROST, D. R. Molecular systematics of terraranas (Anura: Brachycephaloidea) with an assessment of the effects of alignment and optimality. **Zootaxa**, v. 3825, p. 1–132, 2014.

PARKER, H. W. The vertical distribution of some reptiles and amphibians in southern Ecuador. **Annals and Magazine of Natural History**, v. 11, n. 2, p. 438–450, 1938.

PYRON, R. A.; WIENS, J. J. A large-scale phylogeny of Amphibia including over 2800 species, and a revised classification of extant frogs, salamanders, and caecilians. **Molecular Phylogenetics and Evolution**, v. 61, p. 543–583, 2011.

SÁNCHEZ-NIVICELA, J. C.; URGILÉS, V. L.; NAVARRETE, M. J.; YÁNEZ-MUÑOZ, M. H.; RON, S. R. A bizarre new species of *Lynchius* (Amphibia, Anura, Strabomantidae)

135 from the Andes of Ecuador and first report of *Lynchius parkeri* in Ecuador. **Zootaxa**, v. 4567,
136 p. 1–24, 2019.

Seção 1

Sistemática e Evolução Morfológica

Unmasking convergence in the high Andes: total evidence phylogeny of *Phrynopus* and phenotypic evolution in Holoadeninae (Anura: Brachycephaloidea) †

Ana Paula Motta[1*], José Manuel Padial[2], Pablo Venegas[3], Mariana Lyra[1], Célio Fernando Baptista Haddad[1]

[1]Laboratório de Herpetologia, Departamento de Biodiversidade e Centro de Aquicultura (CAUNESP), Instituto de Biociências, Universidade Estadual Paulista, Av. 24A 1515, CEP 13506-900, Rio Claro, São Paulo, Brazil

[2]Department of Herpetology, American Museum of Natural History, Central Park West & 79th street, New York, NY 10024, USA.

[3]División de Herpetología, Centro de Ornitología y Biodiversidad (CORBIDI), Urb. Huertos de San Antonio, Surco, Lima, Peru

***Corresponding author**. E-mail: apmottah@gmail.com

Short running title: Total evidence phylogeny of *Phrynopus*

†Manuscrito preparado para ser submetido no periódico *Cladistics*

Abstract

Phrynopus was considered for decades the high Andean direct-developing frog genus par excellence and its presumed monophyly bore the implicit assumption that a single ancestral lineage had colonized and radiated through the Andes from Bolivia to Colombia. The monophyly of the genus was rejected with the advent of molecular phylogenetics and its monophyletic version was restricted to the slopes of the Central Andes in Peru. The number of known species has grown quickly but not so our understanding of species relationships and phenotypic evolution. The possible convergences that drove the former non-monophyletic taxonomy have not been tested, and the evolutionary character transformations resulting from this extensive Andean radiation have not been inferred and discussed. Likewise, synapomorphies for *Phrynopus* and other Holoadeninae genera remain unknown. In this study we reconstruct the history of species and of character transformations through a total evidence phylogenetic analysis, unprecedented in both characters and taxa, combining 15 genes and 101 phenotypic characters for 79 species of Holoadeninae. Our analyses recovered a monophyletic *Phrynopus*, sister to a clade including *Lynchius* and *Oreobates*. We found low support for *Phrynopus* but due to the wildcard behavior of *P. thompsoni*, a terminal with missing data. By reassessing our morphological knowledge of *Phrynopus* and other Holoadeninae genera with a broad Neotropical distribution we found a complex evolutionary scenario involving multiple instances of repeated evolution of the same character states and not restricted to high Andean groups as originally thought. We also found that researchers have been tricked by symplesiomorphies while diagnosing genera. For example, our results show that some features of digits that have been used to diagnose *Phrynopus* actually represent symplesiomorphies but that a knob-shaped terminal phalange is a derived state and probably constitutes a synapomorphy for the genus. Nonetheless, we found multiple novel phenotypic synapomorphies for groups for which they were so far unknown. We also found

that even though all *Phrynopus* are earless, the loss of tympanum is not coincidental with loss of acoustic communication and earless species probably use extratympanic pathways for the transfer of airborne sound to the inner ear. We also found that a sagittal-hinge pelvis griddle is shared among all holoadeninaes and therefore different locomotor modes are not necessarily the result of different configurations of the pelvic girdle. These results provide ample opportunity for further exploration of phenotypic traits and hypothesis-testing on morphological evolution.

Keywords: Craugastoridae, convergence, evolution, morphology, osteology, parallelism, terrarana, wildcard.

Introduction

The high Andes are rich in frog species, and direct-developing frogs or terraranas are the most diverse among them, both on the forested slopes and above the tree line (De la Riva, 2020). An interesting aspect of terraranan species occurring at high elevations is that they share a similar external morphology, the "phrynopoid" morphology: small frogs, with short limbs, rounded bodies and simple digits (i.e. no discs) (De la Riva, 2020). This pattern drove systematists to consider species distributed in the high Andes from Colombia to Bolivia as part of a single natural group, the genus *Phrynopus* Peters, 1873 (Lynch, 1975). *Phrynopus* became the direct-developing frog genus of the high Andes par excellence; it included all similarly looking species from high elevations and excluded dissimilar ones from those same areas as well as similarly looking ones from low elevations. It also carried forward the hypothesis that a single ancestral lineage had radiated through the roughed landscape of the high Andes.

The diversity of high Andean frogs has turned out to be not only unexpectedly high, but their relationship and phenotypic diversity far more complex than we thought (Hedges et al., 2008; De la Riva et al., 2017; De la Riva, 2020). As soon as molecular evidence was applied, the monophyly of *Phrynopus* was challenged (Lehr et al., 2005; Heinicke et al., 2007), and further analyses led to drastic changes in its composition and the erection of multiple taxa to remedy non-monophyly (Hedges et al., 2008).

The monophyly of different compositions of *Phrynopus* has been challenged (Hedges et al., 2008; Padial et al., 2012), while, paradoxically, the more and more restricted *Phrynopus* has become more and more rich in species diversity (Frost, 2020). There seems to be no end to new species both of *Phrynopus* and high Andean terraranas as we sample the intricate expanses of still understudied slopes of the Andes (De la Riva et al., 2017).

Our understanding of species diversity grows quickly, but not so our understanding of phenotypic variation and the evolution of high Andean frogs. *Phrynopus* and close relatives (*Oreobates* Jiménez de la Espada, 1872 and *Lynchius* Hedges, Duellman, and Heinicke, 2008) remain "molecular genera" lacking, as far as we know, distinctive morphological traits that could be pinpointed as synapomorphies. Species are assigned to these genera either by affinities inferred through DNA or based on distribution plus external appearance. Further, the pathways of phenotypic evolution that led to similar morphologies remain poorly understood. No study has attempted to reconstruct any aspect of the phenotype in high Andean frogs in a phylogenetic context. The only information available is scattered in species descriptions and early systematic accounts of species. We simply ignore how phenotypic traits have evolved, how many times similar phenotypic traits originated and at what level of the phylogeny, what traits are synapomorphies of what clades, and what evolutionary history may lie underneath such interesting pattern of similarity among distant relatives living in grasslands and elfin forests.

In this study we perform phylogenetic analysis that combines all available DNA sequence data for *Phrynopus* and close relatives with a dataset of external and internal morphology, unprecedented in both characters and taxa. We use this phylogenetic reconstruction to infer the history of changes in phenotypic traits for Holoadeninae and to discuss possible evolutionary scenarios for the evolution of these traits in the context of Neotropical biogeography, but also to identify synapomorphies for *Phrynopus* and related genera.

History and current understanding of Phrynopus

Our concept of *Phrynopus* dates back to Lynch's (1975) definition of a putative natural group of 14 species, among which he subsumed as synonyms *Niceforonia* Goin and

240 Cochran, 1963 and *Noblella* Barbour, 1930 (Table S1). The number of species of *Phrynopus*
241 grew quickly with additions of species from Bolivia and Peru (Cannatella, 1984; Hedges,
242 1990; De la Riva, 1992; Ardila- Robayo et al., 1996; Harvey and Ergueta-Sandoval, 1998;
243 Duellman, 2000; Lehr et al., 2000; Aguayo-Vedia and Harvey, 2001; Lehr, 2001; Lehr et al.,
244 2002a; Lehr and Aguilar, 2002; Lehr et al., 2002b; Lehr and Aguilar, 2003; Table S1), but no
245 phylogenetic analyses addressed relationships.

246 A test of the monophyly of *Phrynopus* based on DNA sequences was first provided by
247 Lehr et al. (2005a). Their analysis recovered three clades: Central Peru (species still placed in
248 *Phrynopus*), Bolivia (species now placed in *Microkayla* De la Riva, Chaparro, Castroviejo-
249 Fisher, and Padial, 2017), and Northern Peru (species now placed in *Lynchius* Hedges,
250 Duellman, and Heinicke, 2008). In order to get a monophyletic *Phrynopus* they removed
251 *Phrynopus carpish* and *P. simonsii* from the genus. Later on, new species were described
252 (Lehr et al., 2005b; Lehr, 2006; Chaparro et al., 2007; De la Riva, 2007; Lehr, 2007;
253 Duellman and Hedges, 2008), *Noblella* was removed from the synonym of *Phrynopus* (De la
254 Riva et al., 2008), and some species thought to be *Phrynopus* were transferred to genera of
255 distantly related families: *Eleutherodactylus* (family Eleutherodactylidae; Lehr, 2006; Lehr
256 and Aguilar, 2006), *Pleurodema* (family Leptodactylidae; Lehr, 2006), and *Melanophryne*
257 (now synonym of *Ctenophryne*, family Microhylidae; Lehr and Trueb, 2007).

258 The DNA sequence analyzes by Hedges et al. (2008) also rejected the monophyly of
259 *Phrynopus*, at that point a genus of 44 species (Table S1). Their analyses revealed a complex
260 scenario where high-elevation species lineages with similar phenotypes had independent
261 origins. The non-monophyletic *Phrynopus* had to be split into a number of genera. Species
262 were transferred to *Bryophryne* Hedges, Duellman, and Heinicke, 2008; *Hypodactylus*
263 Hedges, Duellman, and Heinicke, 2008 (now in the synonym of *Niceforonia*); *Lynchius*
264 Hedges, Duellman, and Heinicke, 2008; *Niceforonia* Goin and Cochran, 1963; and

Psychrophrynella Hedges, Duellman, and Heinicke, 2008. *Phrynopus* was thus reduced to a clade of 19 nominal and two unnamed species occurring in the upper humid forests and grasslands of the Cordillera Oriental in Peru.

Since the reorganization of the genus, 19 new species have been named under this new concept of *Phrynopus* (Chaparro et al., 2008; Trueb and Lehr, 2008; Lehr and Oroz, 2012; Lehr et al., 2012; Mamani and Malqui, 2014; Chávez et al., 2015; Rodriguez and Catenazzi, 2017; Lehr et al., 2017; Lehr and Rodriguez, 2017; von May et al., 2018; Venegas et al., 2018; Chávez et al., 2020). Two species, *Phrynopus curator* and *P. nicoleae,* turned out to be synonyms of *P. tribulosus* (von May et al., 2018), while *P. ayacucho* was transferred to *Oreobates* (Padial et al., 2012).

Phrynopus currently comprises 35 species distributed in the Cordilleras Oriental and Central of Peru and is restricted to a region between 6º and 12º of latitude along the slopes of the Central Andes (Venegas et al., 2018; Figure 1). Species have been recorded at elevations between 2600–4490 m, though most of them show very restricted distributions, both horizontally and vertically, and rarely overlap (Rodriguez and Catenazzi, 2017).

Phylogenetic analyses have supported the monophyly of *Phrynopus* as currently defined, although with incomplete taxon sampling, and the genus has consistently been recovered as part of a clade including the genera *Lynchius* and *Oreobates* (Padial et al., 2009; Pyron and Wiens, 2011; Padial et al., 2012; Padial et al., 2014; Motta et al., 2016; De la Riva et al., 2017; Heinicke et al., 2018; Venegas et al., 2018). Several internal relationships as well as the relationship with closely related clades differ among analyses. For example, molecular phylogenetic analyses have placed *Phrynopus* as either the sister group of *Lynchius* (Padial et al., 2009), *Oreobates* (Padial et al., 2012; Venegas et al., 2018), or *Lynchius* and *Oreobates* (Hedges et al., 2008; Pyron and Wiens 2011; Padial et al., 2014; Motta et al., 2016; De la Riva et al., 2017; Heinicke et al., 2018).

290 The classification of families and subfamilies of Brachycephaloidea (Frost et al.,
291 2006) has also faced many changes since Hedges et al. (2008) rearranged the taxonomy of the
292 group, in part due the shifting position of the clade comprising *Lynchius*, *Oreobates*, and
293 *Phrynopus*. This clade was recovered by Hedges et al. (2008) within a clade that also included
294 *Pristimantis*, *Strabomantis*, and *Niceforonia*, and the six genera were considered part of the
295 subfamily Strabomantinae. However, even though the bootstrap support for the clade
296 including *Lynchius*, *Oreobates*, and *Phrynopus* was high (99%), support for relationship
297 among genera in this clade ranged from 19 to 66%. Later Padial et al. (2014) recovered
298 *Lynchius*, *Oreobates*, and *Phrynopus* as the sister clade of Holoadeninae *sensu* Hedges et al.
299 (2008) and transferred these three genera to this subfamily. Heinicke et al. (2018) found a
300 topology congruent with Hedges et al. (2008), but included *Lynchius*, *Oreobates*, *Phrynopus*,
301 and *Pristimantis* in the subfamily Pristimantinae, while *Strabomantis* and *Niceforonia* were
302 transferred to their own subfamily: Strabomantinae and Hypodactylinae, respectively.
303 Terraranan genera have been supported by molecular evidence but pose a challenge
304 for classifications based on morphology. Although Hedges et al. (2008) provided a new
305 diagnosis for *Phrynopus*, they failed to find morphological synapomorphies, and DNA
306 analysis remains the only unambiguous way to allocate species to this genus. In the absence
307 of molecular data, species have still been tentatively allocated to *Phrynopus* on the basis of
308 overall similarity and geographical distribution (Trueb and Lehr, 2008; Lehr and Oroz, 2012;
309 Mamani and Malqui, 2014; Chávez et al., 2015; Rodriguez and Catenazzi, 2017; Lehr and
310 Rodriguez, 2017). The use of these auxiliary criteria is nonetheless objectionable because the
311 external morphologies of species living in high altitude grasslands look similar and has led to
312 misplacing several species in *Phrynopus* that turned out to belong to distantly related families
313 (see above). Fortunately, ongoing studies of the internal anatomy of terraranan frogs (e.g.,
314 Taboada et al., 2013) are leading to the discovery of synapomorphies at different levels and

315 increasing taxon and character sampling will probably lead to further discoveries and a better
316 picture of morphological variation across clades.
317 The study of the osteological diversity of craugastorid anurans also seems to be
318 promising in finding combinations of features that may support the monophyly of genera
319 (Trueb and Lehr, 2008). However, comparing osteological characters among species of
320 *Phrynopus* and its closely related genera is still difficult as we have limited information
321 available (i.e., morphological data for only five species of *Phrynopus,* three of *Lynchius*, and
322 four of *Oreobates*; see Trueb and Lehr, 2008; Motta et al., 2016).
323
324 **Material and Methods**
325 *Taxon sampling*
326 For the ingroup we sampled 24 out of 34 nominal species of *Phrynopus* and seven
327 unnamed species, including *Phrynopus* spI and *Phrynopus* sp. of von May et al. (2018). Three
328 of the nominal species and five of the unnamed species are included in a phylogenetic
329 analysis for the first time: *Phrynopus dagmarae*, *P. thompsoni*, *P. valquii*, *Phrynopus* sp. 1,
330 *Phrynopus* sp. 2, *Phrynopus* sp. 3, *Phrynopus* sp. 4, and *Phrynopus* sp. 5.
331 The genus *Phrynopus* is closely related to the genera *Lynchius* and *Oreobates* (e.g.,
332 Hedges et al. 2008; Pyron and Wiens, 2011; Canedo and Haddad, 2012; Padial et al., 2012;
333 Padial et al., 2014; Motta et al., 2016; De la Riva et al., 2017; Heinicke et al., 2018; Venegas
334 et al., 2018). Hence, with the exception of one species for which molecular data is not
335 available (*Oreobates zongoensis*), our outgroup includes all nominal species of *Lynchius*
336 (seven species) and *Oreobates* (24 species). We also sampled representative species of all
337 genera of Holoadeninae (*sensu* Padial et al., 2014), except *Qosqophryne* (not available at the
338 time of analysis). We used two criteria to sample species: selected taxa (1) represent the
339 diversity of the subfamily, including representatives of the independent lineages of

phrynopoid frogs, and (2) have sequences available on GenBank and specimens available for external morphology and osteological data. Specifically, species included in our outgroup are *Barycholos pulcher*, *Ba. ternetzi*, *Bryophryne cophites*, *"Eleutherodactylus" bilineatus*, *Euparkerella brasiliensis, Holoaden bradei, Microkayla guillei*, *M. kempffi*, *M. wettsteini, Niceforonia brunnea*, *Ni. elassodiscus*, *Ni. nana*, *Ni. nigrovittata*, *Ni. peraccai, Noblella heyeri*, *No. lochites,* and *Psychrophrynella usurpator*. We rooted all our analyses with the distant species *Haddadus binotatus*. Total taxon sampling includes 79 species of Holoadeninae and the root.

Morphological characters sampling

Character sampling and coding. Our goal was to include characters that have been considered important for the taxonomy of Holodeninae, as well as those that are related to different functions in this group. We explored the characters that reflected variation among brachycephaloid clades (Lynch, 1971; Lynch, 1975; Duellman and Lehr, 2009) and complemented the matrix with characters that have been used to study non-brachycephaloid frogs (Grant et al., 2006; Ponssa, 2008; Reilly and Jorgensen, 2011; Barrionuevo, 2017), as well as novel characters and character-states discovered in the course of our study.

Our final sample for morphological data includes 61 species for external morphology and 43 for osteology (Table 1). Following the conceptual definition of characters as transformation series (Grant and Kluge, 2004), the final phenotypic matrix includes 101 characters, 10 multistate, of which 8 were considered additive. We used Mesquite (Maddison and Maddison, 2015) to edit the matrix. All characters and character-states, as well as information about character selection and definition, are listed in Appendix 1. The phenotypic dataset employed in the analyses is given in Appendix S1.

Phenotypic character data was obtained from specimens housed in the herpetological collection of AMNH (American Museum of Natural History, New York, USA), CM (Carnegie Museum of Natural History, Pittsburgh, USA), CORBIDI (Centro de Ornitología y Biodiversidad, Lima, Peru), KU (Biodiversity Institute, Kansas University, Lawrence, USA), MACN (Museo Argentino de Ciencias Naturales "Bernardino Rivadavia", Buenos Aires, Argentina), MCZ (Museum of Comparative Zoology of Harvard University, Cambridge, USA), MHNCP (Universidad Nacional de San Antonio Abad del Cusco, Cusco, Peru), MNRJ (Museu Nacional, UFRJ, Rio de Janeiro, Brazil), MUSM (Museo de Historia Natural, Universidad Nacional Mayor de San Marcos, Lima, Peru), MZUSP (Museu de Zoologia, USP, São Paulo, Brazil), UFMT (Universidade Federal do Mato Grosso, Cuiabá, Brazil), and ZUEC (Museu de História Natural, UNICAMP, Campinas, Brazil). A list of studied material is provided in Appendix 2.

Osteological characters were coded from dry skeletons and/or cleared and stained specimens housed in the herpetological collection of KU, MNRJ, and MCZ. For one species (*Lynchius megacephalus*) we obtained osteological data from the literature (Sánchez-Nivicela et al., 2019). Following the procedures of Taylor and Van Dyke (1985), we cleared and double-stained specimens of five species: *"Eleutherodactylus" bilineatus*, *Barycholos ternetzi*, *Oreobates antrum*, *O. berdemenos*, and *O. heterodactylus*.

Osteological data was also obtained through micro-computed tomography (microCT) Scan images for 20 species (Table 1). The images collected by the CT scanner were compiled and processed in the software VGStudio MAX to create a 3D model that was visualized in the software MeshLab (Cignoni et al., 2008) and used to score osteological character states.

Sampling characters historically used to define Phrynopus.— Lynch (1975) included the "simple-toed" high-elevation Andean frogs as part of *Phrynopus*, and the shape of tips of

digits was considered a diagnostic characteristic, while the shape of terminal phalanges was not considered useful to separate *Phrynopus* (*sensu* Lynch, 1975) from *Eleutherodactylus*. Thirty years later, Lehr´s (2005) observations indicated otherwise; he stated that that the shape of tips of digits was not useful to distinguish genera, while shape of terminal phalanges was a useful character to distinguish *Eleutherodactylus*, *Phrynopus*, and *Phyllonastes* (now *Noblella*). In their revision of terraranan frogs, Hedges et al. (2008) also used these characters to define genera, listing digits narrow, rounded, or bulbous, circumferential groves absent, and terminal phalanges knob shaped as diagnostic characteristics of *Phrynopus*. They also described terminal phalanges knob-shaped for *Oreobates* and terminal phalanges knob-shaped or weakly T-shaped for *Lynchius*. Furthermore, the characteristics of the terminal phalanges and tips of digits are still being used to assign species to the genus when molecular data is not available (Lehr and Oroz, 2012; Chavez et al., 2015; Lehr and Rodriguez, 2017; Rodriguez and Catenazzi, 2017).

The terminology employed for the shape of terminal phalanges has been mostly a reflection of the experience or interpretation of the author, and no definition for the terminology used is available (Lehr, 2006). For example, Lynch (1972) reported knobbed terminal phalanges for *Phrynopus juninensis*, while Cannatella (1985) considered the terminal phalanges of the same specimen as T-shaped. A similar discrepancy is found in the terminology used to describe the terminal phalanges of *Lynchius flavomaculatus*. In its original description, Parker (1938) described the terminal phalange as T-shaped (same state found by us), while Lynch (1969) considered it knob-shaped. The inconsistency in the terminology is commonly due to the extension of lateral processes of the terminal phalanges. The term T-shaped is used for the characteristic terminal phalanges of *Eleutherodactylus* with large lateral processes. However, in some species the lateral processes are not as developed as in most species of *Eleutherodactylus* and some authors classify them as intermediate between

T-shaped and knob-shaped or vestigial T-shaped phalanges. Hence, the classification relies on the researcher perception of whether the lateral process of the terminal phalanges is developed enough to be called T-shaped. In order to avoid this subjectivity, we considered terminal phalanges with lateral processes (regardless of their length) as T-shaped and classified the terminal phalanges without lateral processes according to the shape of the tip of the phalange as knobbed, spade, pointed or rounded (see Appendix 1).

Characters related to vomer were critical for the taxonomic decisions of Lynch (1975) regarding *Phrynopus*. Lynch considered that vomers characteristics did not support the separation of *Noblella* from *Niceforonia* and *Phrynopus* and, thus, included *Niceforonia* and *Noblella* in the synonym of *Phrynopus*. However, vomer characters were used to define groups in *Phrynopus* (*sensu* Lynch, 1975): the *P. flavomaculatus* group (*brunneus*, *columbianus*, *flavomaculatus*, *parkeri*, *peraccai*, *pereger*) has prevomerine teeth and associated processes; in the *P. peruvianus* group (only *peruvianus*) prevomerine teeth, dentigerous processes, and dentigerous ramus are absent; in the *P. simonsii* group (*nanus* and *simonsii*) prevomerine teeth and processes are present or absent, when absent, the dentigerous ramus is not reduced in size; and the *P. peruanus* group (*cophites*, *laplacai*, *montium*, *peruanus*, and *wettsteini*) lacks prevomerine teeth and dentigerous processes (except in *peruanus*), and the dentigerous ramus is thin and sliver-like. More recently, even after the rearrangement of *Phrynopus* by Hedges et al. (2008), Trueb and Lehr (2008) listed vomer characteristics as important features to distinguish *Phrynopus* from *Lynchius*: well-developed dentate vomers of *Lynchius* in contrast with vomers lacking dentigerous processes in *Phrynopus*.

Likewise, shape and size of nasals vary among genera. Lynch (1975) pointed out the similarities of nasals in *Phrynopus montium* and *P. peruanus* (“widely separated and relatively small”) compared to *Lynchius flavomaculatus*, *L. parkeri*, and *Oreobates pereger*

439 ("in contact and large"). Trueb and Lehr (2008) listed small nasals that do not overlap with
440 the sphenethmoid as a useful character to distinguish *Phrynopus* from *Lynchius*.
441 Other characters also have been considered promising in defining groups. Lynch
442 (1971) considered the variation in the shape of the hyoid plate among species of
443 Leptodactylidae (at that time including species now split into14 families; De la Riva, 2020) as
444 impressive, and some of the potentially useful characters considered were the shape of the
445 alary process and variation in the posterolateral process.
446
447 *Sampling characters to study function*. Evolutionary histories of some characters have been
448 discussed with regard to their function. *Phrynopus* comprises a radiation of earless frogs,
449 which means that most species lack the tympanic middle ear, composed of columella,
450 tympanic annulus, and tympanic membrane. The middle ear transmits sound waves to the
451 inner ear and we analyzed the presence and absence of its structures to better understand the
452 evolution of the middle ear in Holoadeninae.
453 Species of *Phrynopus*, as well as species of other genera of Holoadeninae, use habitat
454 differently and show different locomotor modes. Different configurations of pelvic girdle are
455 correlated with locomotor modes in anurans, and three functional pelvic-bauplans are
456 proposed: lateral-bender morph (associated with walking, burrowing, and hopping frogs),
457 fore-aft-slider morph (associated to burrowing, walking, hopping, climbing, and aquatic
458 frogs), and sagittal-hinge morph (associated to jumping frogs) (Emerson, 1979; Emerson,
459 1982; Reilly and Jorgensen, 2011; Jorgensen and Reilly, 2013). The pelvic morphs are
460 defined by the states of four characters: sacral diapophyseal expansion, dorsal iliac ridge,
461 sacro-urostylic articulation, and urostyle dorsal ridge (Reilly and Jorgensen, 2011). We
462 include those four characters in our matrix to understand pelvic girdle evolution in
463 Holoadeninae.

Molecular character sampling

We include newly produced sequences and sequences available on GenBank of 15 genes for a total of 78 species of Holoadeninae. Tissue samples or DNA sequences were not available for *Phrynopus thompsoni*, which was scored for morphological data only. Mitochondrial DNA genes include the protein-coding cytochrome b (cytb) and cytochrome c oxidase subunit I (COI), and the rRNA genes 12S and 16S. Nuclear genes include the protein-coding genes chemokine receptor 4 (CXCR4), two exons of cellular myelocytomatosis (c-myc), histone H3 (HH3), sodium-calcium exchanger 1 (NCX1), propiomelanocortin A (POMC), recombination-activating protein 1 (RAG1), rhodopsin (Rhod), seven-in-absentia (SIA), solute carrier family 8 member 3 (SLC8A3), and tyrosinase precursor (Tyr), and the noncoding nuclear gene 28S. These gene fragments were available to most of our terminals and have been successfully used in several phylogenetic studies of Brachycephaoidea (Hedges et al., 2008; Padial et al., 2014). Sequences for 12S, 16S, COI, RAG1, and Tyr genes were newly produced for this study. Accession numbers for all sequences produced and used in this study are listed in Appendix 3.

DNA amplification and sequencing

We extracted total DNA from ethanol preserved tissues, following standard high-salt protocol adapted for microcentrifuge tubes (Maniatis et al., 1982; Lyra et al., 2017). We amplified two mitochondrially encoded gene fragments: one including the partial sequences of 12S rRNA, tRNA-val and 16S rRNA genes (H1 fragment) and a fragment of the cytochrome c oxidase I (COI); and two nuclear genes: partial sequences of tyrosinase (TYR), and partial sequences of recombination activating 1 (RAG-1). Amplifications were carried out in a 22 µl reaction using Ampliqon Taq DNA Polymerase Master Mix (Ampliqon A/S, Odense M, Denmark), with primers listed in Table S2. For the mitochondrial genes we

followed polymerase chain reactions (PCR) conditions described in Lyra et al. (2017) (UP reaction protocol). For nuclear genes we used the following PCR cycling protocol: 3min of denaturation at 95ºC, followed by 45 cycles of 20s of denaturation at 95ºC plus 20s of annealing at 56ºC plus 1 min of extension at 68ºC, followed by 3 min of final extension at 68ºC, and stored at 12ºC. PCR products were purified using an enzimatic reaction containing 1 unit of Exonuclease I and 0.5 unit of Alcaline phosphatase (Thermo Fisher Scientific Inc.) and were sent to Macrogen, Inc., Seoul, Repuiblic of Korea, for sequencing. Sequence files were checked for quality and contigs were assembled using Geneious R11 (Biomatters).

Phylogenetic analysis

Sequences were first aligned in MAFFT v.7 (Katoh and Standley, 2013; under the G-INS-i strategy) and partitioned into fragments of equal length separated by conserved regions with no gaps and few or no nucleotide substitutions (we used Geneious 11.1.2 to visualize and edit the sequences; Kearse et al., 2012). This strategy generated putatively homologous fragments where length variation among DNA sequences was due to insertions and/or deletions of nucleotides, which is a requisite for tree alignment in POY (Wheeler et al., 2006). After the removal of gaps implied by MAFFT from sequence fragments, tree alignment of unaligned sequences was performed under parsimony with equal weights for all classes of transformations using direct optimization (DO; Wheeler, 1996; Wheeler et al., 2006) and iterative pass optimization (IPO; Wheeler, 2003) algorithms in POY 5.1.1 (Wheeler et al., 2015). Tree searches were first conducted using DO under the command “search”, which implements an algorithm based on random addition sequence Wagner builds, subtree pruning and regrafting (SPR), and tree bisection and reconnection (TBR) branch swapping (see Goloboff, 1996, 1999), parsimony ratcheting (Nixon, 1999) and tree fusing (Goloboff, 1999), running consecutive rounds of searches within a specified run-time, storing the shortest trees

514 of each independent run and performing a final round of tree fusing on the pooled trees. Some
515 searches implemented the command “auto_static_approx”, which evaluates sequence
516 fragments and transforms characters into static homologies when the number of indels is low
517 and stable between topologies. This command was applied to the last set of searches and was
518 not implemented during the last round of swap under iterative pass. The optimal tree found
519 during driven searches was swapped using IPO (Wheeler, 2003). As we have observed that
520 POY 4.1.2 or POY 5.1.1 does not always report all equally parsimonious trees when large
521 datasets are analyzed, the optimal alignment resulting from IPO was converted into a data
522 matrix (i.e. implied alignment: Wheeler, 2003) and driven searches were conducted in TNT
523 (Goloboff et al., 2008) until a stable strict consensus was reached at least three times (see
524 below for details of driven searches in TNT).
525 We calculated Goodman–Bremer (GB) values (Goodman et al., 1982; Bremer, 1988;
526 see Grant and Kluge, 2008) for each supported clade in TNT using the optimal tree-alignment
527 matrix and the parameters specified in the bremer.run macro (available at http://
528 www.zmuc.dk/public/phylogeny/tnt/), which begins by searching for trees N steps longer than
529 the optimum (ten random addition sequence Wagner builds and TBR swapping saving two
530 trees per replicate), using inverse constraints for each node of the most parsimonious tree.
531 Swapping of each constrained search was limited to 20 min and constrained searches were
532 repeated three times as specified in the default settings of the bremer.run macro. We also
533 calculated parsimony jackknife frequencies (Farris et al., 1996) for each supported clade by
534 resampling the tree-alignment matrix. We caution that, as in analyses of similarity-alignment
535 matrices, the resulting clade frequencies are conditional on this particular alignment and not
536 the data themselves. Given that the tree-alignment matrix is derived from the optimal tree, the
537 resulting clade frequencies are expected to be higher than would be obtained from matrices
538 aligned according to different guide trees (e.g. a UPGMA or neigbor-joining tree, as in

539 MAFFT and Clustal, respectively). We calculated parsimony jackknife frequencies (JF) from
540 1000 pseudoreplicates searches using driven searches, gaps treated as fifth state, and removal
541 probability of 0.36 (≈ e–1) (Farris et al., 1996).

542 On the basis of the arguments of Kluge and Grant (2006), molecular and phenotypic
543 characters were also treated under equal weights in our total evidence analysis, but they were
544 analyzed as a static matrix. We combined morphological and molecular data from different
545 conspecific specimens into a single terminal to represent a species. Uncorrected p-distances
546 were estimated in Mega v4.0 (Tamura et al. 2007) for the aligned 16S fragment. Character
547 optimizations were visualized using Mesquite v.3.03 (Maddison and Maddison, 2019).

548 Taxa scored as missing for the majority of characters are expected to be highly
549 unstable in phylogenetic parsimony analyses (wildcard behavior), affecting both the
550 resolution of the consensus tree and the support for the recovered relationships (Wilkinson,
551 2003; Padial et al., 2014; Goicoechea et al. 2016). Our dataset includes a terminal (*P.*
552 *thompsoni*) that lacks molecular data, representing a large amount of missing data. In order to
553 test the effects of including this terminal in our analyses, we also performed independent
554 analyses for a dataset excluding *P. thompsoni* following the same steps described above. We
555 consider the results of the total evidence analyses including all terminals (TE) to be the
556 phylogenetic hypothesis (species relationships) that best explains trait variation, and the
557 results from the analyses excluding *P. thompsoni* (EXT) were solely used to identify the
558 contributions of this terminal to unresolved relationships and/or low support values in the total
559 evidence analysis.
560

561 **Results**

562 *Phylogeny*

563 Total evidence parsimony tree searches (TE) identified an optimal tree of 12512 steps
564 that was visited 5865 times during 3537 rounds of build þ TBR, 32562 of fusing, and 1873 of
565 ratchet. A round of swapping under iterative pass optimization recovered a single tree of
566 12491 steps. Additional searches of the tree-alignment in TNT found one additional tree of
567 the same length and strict consensus in shown in Figure 3.

568 TE analyses recovered a monophyletic *Phrynopus* as the sister group of a clade
569 including the monophyletic genera *Lynchius* and *Oreobates* (Figure 3A). We found high
570 support for *Lynchius* (JF = 100%; GB = 50), *Oreobates* (JF = 100%; GB = 13), and the clade
571 including both genera (JF = 100%; GB = 24). On the other hand, we found low support for
572 *Phrynopus* (JF = 89%; GB = 1) and the clade including *Lynchius*, *Oreobates*, and *Phrynopus*
573 (JF = 91%; GB = 3). Within the rest of the outgroup, all testable genera were recovered as
574 monophyletic, with high support. *Niceforonia* is sister to the clade composed by *Microkayla*
575 and *Psychrophrynella*, which is in turn sister to a clade including *Bryophryne*, *Noblella*,
576 *Barycholos*, and *"Eleutherodactylus" bilineatus*. The sister group of this entire clade is the
577 clade including *Lynchius*, *Oreobates*, and *Phrynopus*. The clade formed by *Holoaden* and
578 *Euparkerella* is sister to all other genera of Holoadeninae. Overall, those relationship have
579 high support, except the clade including *Euparkerella* and *Holoaden* (JF = 93%; GB = 3), and
580 the relationship of this clade with all the other genera (JF = 93%; GB = 3).

581 Our TE analyses support the three nominal species (*Phrynopus dagmarae*, *P.*
582 *thompsoni*, and *P. valquii*) and five unnamed species (*Phrynopus* sp. 1, *Phrynopus* sp. 2,
583 *Phrynopus* sp. 3, *Phrynopus* sp. 4, and *Phrynopus* sp. 5) as part of *Phrynopus*. Within
584 *Phrynopus*, *P. peruanus* forms a clade with *Phrynopus* spI that is sister to all other species.
585 *Phrynopus auriculatus* and *P. mariellaleo* form a clade that is the sister group of the

586 remaining 27 species. Our TE analyses recover *Phrynopus dagmarae* as sister species of a
587 clade composed by *P. tribulosus* and *P. thompsoni*. *Phrynopus valquii* is sister to a clade
588 comprising 18 species of *Phrynopus* that includes early diverging *Phrynopus* sp. 1 and
589 *Phrynopus* sp. 2. *Phrynopus* sp. 3 is recovered as sister to *P. barthlenae* and uncorrected p-
590 distance between them is 4%; *Phrynopus* sp. 4 is recovered as sister to a clade including *P.*
591 *montium* and *P. juninensis*; *Phrynopus* sp. 5 is recovered as sister to *P. heimorum* and
592 uncorrected p-distance is 4%.

593 The conflicts among the two topologies of TE analyses are restricted to the position of
594 *Phrynopus pesantesi*, which is recovered as either the sister species of *P. barthlenae* and
595 *Phrynopus* sp. 3 or the sister species of a clade including *P. barthlenae*, *Phrynopus* sp. 3, *P.*
596 *horstpauli*, *Phrynopus* sp. 4, *P. montium*, and *P. juninensis* (Figrues 3A and S1).

597 The EXT analyses recovered the same relationships among genera as the TE analyses
598 (Figure 3B). The two analyses differed mostly regarding some internal relationships among
599 species in *Lynchius*, *Oreobates*, and *Phrynopus*. In *Phrynopus*, the discrepancies are related to
600 the position of *P. valquii*, the sister species *P. montium* and *P. juninensis*, and the sister
601 species *P. horstpauli* and *P. bufoides*. The EXT analyses (excluding the wildcard *P.*
602 *thompsoni*) also recovered a monophyletic *Phrynopus* as the sister group of a clade including
603 the monophyletic genera *Lynchius* and *Oreobates*. We found high support for *Lynchius* (JF =
604 100%; GB = 37), *Oreobates* (JF = 100%; GB = 21), and the clade including both genera (JF =
605 100%; GB = 34) in the EXT analyses. We also found high support for *Phrynopus* (JF = 100%;
606 GB = 28) and the clade including *Lynchius*, *Oreobates*, and *Phrynopus* (JF = 100%; GB =
607 49).
608

609 *Phenotypic synapomorphies of* Phrynopus *and comments on outgroups*

610 Two character states optimized as synapomorphies of *Phrynopus*: omosternum
611 entirely cartilaginous (character 10, state 0) and acute anterior ala of vomer (character 42,
612 state 2). The knob-shaped terminal phalanges optimize as a synapomorphy of the clade
613 including all *Phrynopus* but *P. peruanus* and *P.* spI (because character states for those species
614 are unknown), with a reversal to T-shaped phalanges in a clade including *P. barthlenae*, *P.*
615 *horstpauli*, *P. juninensis*, *P. montium*, *Phrynopus* sp. 3, and *Phrynopus* sp. 4. We found the
616 absence of middle ear structures (characters 48, 49, and 50) as synapomorphies of the clade
617 including all species of *Phrynopus* but *P. auriculatus*, *P. mariellaleo*, *P. peruanus*, and *P.* spI
618 (middle ear structures present in those species).

619 Although our goal was not to address the phenotypic evolution of all genera of
620 Holoadeninae, our dataset allows us to pinpoint some interesting findings concerning
621 characters of outgroup taxa. The presence of finger pads (character 74, state 1) is a
622 synapomorphy of *Oreobates* within Holodaneninae. The relationship of *Lynchius* and
623 *Oreobates* as sister groups is supported by three synapomorphies: nasals large and close to
624 each other (character 30, state 2; character 31, state 0) and elongate, slender, pointed
625 zygomatic ramus of squamosal (character 46, state 0). We did not find a synapomorphy for
626 the clade including *Lynchius*, *Oreobates*, and *Phrynopus*, nor for the genus *Lynchius*.

627 Our optimizations indicate four synapomorphies for *Niceforonia*: terminal phalange
628 rounded (character 6, state 4); anterior terminus of omosternum blunt (character 9, state 2),
629 and nasals large and close to each other (character 30, state 2; character 31, state 0). The clade
630 excluding *Niceforonia nana* is supported by three additional synapomorphies: neural spine
631 imbricated (character 17, state 2), dorsolateral folds present (character 59, state 1), and
632 occipital-scapular fold present (characters 65, state 1). For *Microkayla* we found the contact
633 of nasal and maxilla (character 28, state 1) as potentially synapomorphic, however, we

634 sampled three out of the 25 species known for the genus (*M. guillei*, *M. kempffi*, and *M.*
635 *wettsteini*).

636 Our optimizations indicate six synapomorphies for the clade including *Noblella heyeri*
637 and *N. lochites*: pointed terminal phalanges (character 6, state 3); small, triangular nasals
638 (character 31, state 2); quadratojugal and maxilla not overlapping (character 38, state 1);
639 anterior ala and dentigerous process of vomer absent (character 42, state 0; character 43, state
640 0); and zygomatic ramus inconspicuous, poorly defined (character 46, state 5). However,
641 *Noblella* is here represented by two out of the 16 species included in this genus and they are
642 part of the *Noblella* Northern Clade (*sensu* Reyes-Puig et al., 2019).

643 The sister group of *Noblella* is the clade including *Barycholos* and
644 "*Eleutherodactylus*" *bilineatus*, and the relationship of these two genera is supported by six
645 synapomorphies: nasals large and close to each other (character 30, state 2; character 31, state
646 0); long cultriform process of parasphenoid (character 40, state 1); vomerine teeth present
647 (character 41, state 1); broad dentigerous process of vomer (character 43, state 2); and finger
648 pads present (character 74, state 1). Our optimizations indicate four synapomorphies for
649 *Barycholos*: alary process of hyoid present (character 2, state 1); dorsolateral and
650 supratympanic folds present (character 59, state 1; character 62, state 1); and plantar
651 supernumerary tubercles present (character 88, state 1).

652

653 **Discussion**

654 Phrynopus *relationships*

655 The monophyly of *Phrynopus* is supported by two phenotypic synapomorphies
656 (omosternum entirely cartilaginous and acute anterior ala of vomer). The knob-shaped
657 terminal phalange is a putative synapomorphy for the genus, but resolution is pending until
658 the shape of the terminal phalange is known for *P. peruanus* and *P*. spI, species that form a

659 clade that has been consistently recovered as sister group of all other *Phrynopus* (Venegas et
660 al., 2018; von May et al., 2018; Catenazzi et al., 2020). As mentioned before, the analyses
661 excluding *Phrynopus thompsoni* recovered the same relationships among genera as the total
662 evidence analyses. Within *Phrynopus*, the removal of *P. thompsoni* increases resolution, since
663 there is no conflict in the position of *P. pesantesi*, the species responsible for the polytomy in
664 the strict consensuses in the TE analyses. The wildcard behavior of *P. thompsoni* is more
665 conspicuous in the support values. The removal of this terminal from the matrix increases
666 Goodman–Bremer support values considerably, particularly for the unsupported clades in TE
667 analyses. Chiefly among clades that showed higher values of support when we excluded *P.*
668 *thompsoni* is the clade including all species of *Phrynopus* and the clade including *Lynchius*,
669 *Oreobates*, and *Phrynopus*. The support for *Phrynopus* increased from GB = 1 to GB = 28,
670 while the support for the clade including *Lynchius*, *Oreobates*, and *Phrynopus* increased from
671 GB = 3 to GB = 49. Therefore, our results indicate that *P. thompsoni*, the terminal with
672 missing data, behaves as a wildcard, and its effects are mostly on Goodman–Bremer support
673 values, while our inference is impacted only in a few interspecific relationships inside
674 *Lynchius*, *Oreobates*, and *Phrynopus*.

675 We recovered pairs of species that have been consistently found as sister species: *P.*
676 *auriculatus* and *P. mariellaleo*; *P. bracki* and *P. badius*; *P. juninensis* and *P. montium*; and *P.*
677 *miroslawae* and *P. tautzorum*. Sister species are usually geographically distant (e.g. *P.*
678 *auriculatus* and *P. mariellaleo* occur in localities that are 540 km apart) and associated to
679 different habitats (e.g. *P. miroslawae* occur in elfin forests and *P. tautzorum* in puna). With
680 the exception of two pairs of species (*P. juninensis* and *P. montium*; *P. daemon* and *P.*
681 *unchog*), species known to occur sympatrically are not recovered as sister species. *Phrynopus*
682 *dagmarae* is sympatric to *P. daemon*, *P. horstpauli*, *P. kauneorum*, and *P. vestigiatus*, but was

683 not recovered as the sister species of any of those species. *Phrynopus valquii* is sympatric to
684 *P. anancites*, but the relationship of the two species could not be accessed.
685 We also provide the strongest test for the relationship between *Phrynopus* and
686 *Lynchius* and *Oreobates*. The relationship of *Lynchius* and *Oreobates* as sister genera is
687 supported by three phenotypic synapomorphies. Intergeneric relationships within the clade
688 (*Phrynopus* (*Lynchius* + *Oreobates*)) are in agreement with those recovered in the recent
689 studies involving large parts of Holoadeninae (Padial et al., 2014; Motta et al., 2016; De la
690 Riva et al., 2017, Venegas et al., 2018).
691
692 *Evolution of character complexes historically used to diagnose* Phrynopus *and other*
693 *Holoadeninae genera*
694 The characteristics of the terminal phalanges and tips of digits have been the major
695 character complexes used in *Phrynopus* classification, as well as in most Holoadeninae
696 genera. Our results show that some features of digits that have been used to diagnose
697 *Phrynopus* actually represent symplesiomorphies. The absence of pads and circumferential
698 grooves on tips of fingers used to diagnose *Phrynopus* (Lynch, 1975; Hedges et al., 2008) are
699 indeed shared by all the species of the genus. However, absence is the ancestral state for
700 Holoadeninae for both characters (characters 74 and 75), with seven transformations to
701 presence of pads and four transformations to presence of circumferential grooves on tips of
702 fingers across the genera of Holoadeninae (Figure 4).
703 On the other hand, the knob-shaped terminal phalange, a character state also used to
704 diagnose *Phrynopus* (Hedges et al., 2008), is a derived state and probably constitutes a
705 synapomorphy for the genus (though information for *P. peruanus* is missing). The
706 optimization of the shape of terminal phalanges (character 6) recovers T-shaped terminal
707 phalange as the ancestral state for Holoadeninae with transformations from T-shaped to knob-

shaped in *Phrynopus*, to spade-shaped in *Euparkerella*, to rounded in *Microkayla kempffi* and in *Niceforonia*, and to pointed in the clade including *Noblella heyeri* and *No. lochites* (Figure 4). In *Lynchius*, the transformation to pointed phalange occurs either in *L. megacephalus* and *L. simmonsi* independently, or in the ancestral species of the genus with a subsequent reversal to T-shaped (Figure 4).

Our analyses indicate that the shape of terminal phalanges is not correlated to the shape of fingers disc, nor is the shape of fingers disc correlated to the presence/absence of pads and circumferential grooves. The tips of fingers are not necessarily expanded when the terminal phalanges are T-shaped (e.g. several species of *Oreobates*), circumferential grooves are not always present when pads are present (e.g. *Oreobates lundbergi*), and pads are present in expanded and unexpanded tips (e.g. *Oreobates granulosus* and *O. remotus*). In all species of Holoadeninae included in our analyses, tips of fingers are not expanded (character 73), except in *Oreobates antrum*, *O. chiquitanus*, *O. heterodactylus*, *O. ibischi*, *O. remotus*, and *O. yanucu*. These species occur in rocky outcrops and caves and the expanded tips of fingers are apparently correlated to their climbing habits, as the specimens have been found at up to 1.8 m above the ground and climbing stalagmites inside caves (Kohler and Padial, 2016; Vaz-Silva et al., 2018; Motta et al., 2020).

The shape of finger subarticular tubercles has also been considered an important character to diagnose genera of Holoadeninae. Species of *Phrynopus* share the rounded fingers subarticular tubercle. However, this is also a symplesiomorphy of the genus, as the optimization of shape of finger subarticular tubercles (characters 78) recovers the round shape as the ancestral state for Holoadeninae. The presence of prominent conical subarticular tubercles and prominent supernumerary tubercles associated with the axis of fingers and toes have been proposed as morphological synapomorphies for *Oreobates* (Padial et al., 2008). Conical fingers subarticular tubercles are recovered as either a synapomorphy of the clade

733 including *Lynchius* and *Oreobates*, or a synapomorphy of *Oreobates* with an independent
734 transformation in *Lynchius simmonsi*. The same optimization was found for conical toes
735 subarticular tubercles (character 87) and for conical plantar supernumerary tubercles
736 (character 88).

737 Shape and size of nasals have also been used to distinguish *Phrynopus* from other
738 Holoadeninae genera (Trueb and Lehr, 2008). Our optimizations of those characters
739 (characters 30 and 31) recovered medium-sized nasals separated from each other as the
740 ancestral state for Holoadeninae, and this character state is actually a symplesiomorphy of
741 *Phrynopus* species (Figure 5). The optimization of size and shape of nasals also indicate that
742 transformation can lead both to reduction and increase in the degree of ossification of these
743 structures in Holoadeninae. There is one transformation to small nasals (in *Noblella*) and at
744 least three transformations to large nasals (in *Niceforonia*, the clade including *Lynchius* and
745 *Oreobates*, and the clade including *Barycholos* and *"Eleutherodactylus" bilineatus*). Large
746 nasals are usually correlated with medial contact between the two bones, while the separation
747 between nasals may be due reduction of bone or to an anterior extension of the sphenethmoid
748 (Lynch, 1971). The sphenethmoid extends to the tip of nostril in *Noblella*, *Microkayla*, and
749 *Niceforonia*, genera with small, medium, and large nasals, respectively. Therefore, in
750 Holoadeninae the separation of nasals is mostly related to the reduction of the bone, and
751 sphenethmoid extending to the tip of nostril does not imply in separation of the nasals.

752 Characteristics of vomer have also been considered important features to distinguish
753 *Phrynopus*. For example, *Lynchius* has well-developed dentate vomers in contrast with
754 vomers lacking dentigerous processes in *Phrynopus* (Trueb and Lehr, 2008). However, loss or
755 apparent loss of the prevomerine teeth is not an uncommon phenomenon in brachycephaloids
756 (Lynch, 1968). Our optimization recovers the presence of vomerine teeth as the ancestral state
757 for Holoadeninae (character 41), with transformations to absence of vomerine teeth in

758 *Noblella*, in *Euparkerella*, in *Bryophryne cophites*, in *Microkayla*, and in a clade of
759 *Phrynopus* including all species but *P. auriculatus*, *P. mariellaleo*, *P. peruanus*, and *P.* spI
760 (Figure 6). There is one reversal to presence of vomerine teeth in a clade including *Phrynopus*
761 *dagmarae*, *P. interstinctus*, and *P. vestigiatus*.

762 Large and toothed vomers have been considered a primitive state and the reduction
763 and loss of vomers a derived condition (Lynch, 1971) and our analyses support that
764 hypothesis for Holoadeninae. The optimization of shape of dentigerous process of vomer
765 (characters 43) recovers the broad process as the ancestral state for Holoadeninae (Figure 6).
766 Dentigerous process of vomer is lost independently twice: in *Noblella* and in
767 *Psychrophrynella usurpator*. Transformation from broad to thick dentigerous process of
768 vomer occurs in *Euparkerella*, in *Bryophryne cophites*, in *Microkayla*, and in *Phrynopus*. The
769 thick dentigerous process of vomer optimizes ambiguously on the common ancestor of all
770 *Phrynopus* but is unambiguously optimized as the ancestral state of the clade including all
771 species of *Phrynopus* but *P. auriculatus*, *P. mariellaleo*, *P. peruanus*, and *P.* spI. Moreover,
772 reduction in the size of the vomer does not necessarily mean that the vomerine teeth are lost
773 (Lynch, 1971). In *Phrynopus*, transformation to thick dentigerous process may have taken
774 place in the ancestral of all species *Phrynopus* and, hence, before the loss of vomerine teeth,
775 or in the ancestral of the clade including all species of *Phrynopus* but *P. auriculatus*, *P.*
776 *mariellaleo*, *P. peruanus*, and *P.* spI. Therefore, even though the reduction in the size of
777 vomer does not imply loss of the vomerine teeth, it precedes it (Figure 6).

778 The variation in the shape of the hyoid plate among the brachycephaloids is
779 impressive and some of the characters considered potentially useful are the shape of the alary
780 process and variation in the posterolateral process (Lynch, 1971). For example, the
781 relationship between *Euparkerella* and *Holoaden* was suggested based on the similarities of
782 the hyoid plate shape in these genera (Lynch, 1971) and hyoid characters have also been

783 considered critical in diagnosing genera (Motta et al., in press). The only species of
784 *Phrynopus* for which we have data for the hyoid plate is *P. montium*. In this species, as well
785 as in *Oreobates* species, the alary process of hyoid is present, while all species of *Lynchius*
786 lost this process. The absence of alary process is rare in Holoadeninae: it has been lost in
787 *Lynchius*, the clade including *Euparkerella* and *Holoaden*, the clade including
788 *"Eleutherodactylus" bilineatus* and *Noblella*, and in *Psychrophrynella usurpator*. However,
789 the optimization of alary process of hyoid (character 2) is ambiguous, mostly due lack of data
790 for that character in Holoadeninae. Alary process of hyoid absent is a putative synapomorphy
791 for *Lynchius*. Nevertheless, that can only be confirmed once we gather more data on the
792 presence and absence of this structure to determine the ancestral and derived states for this
793 character.
794
795 *Unmasking convergence in Holoadeninae*
796 The phylogenetic framework provided by our analyses enables a new interpretation of
797 morphological variation and allows us to discuss evolutionary hypotheses on patterns of
798 morphological diversity and geographical distribution in light of phylogeny. Even though the
799 affinities we found in Holoadeninae are consistent with previous phylogenetic hypotheses, the
800 inclusion of morphological data brings new perspectives on the phenotypic evolution of this
801 Neotropical group.
802 Morphological similarities in high Andean species led most authors to deduce that the
803 similar traits evolved independently as the result of adaptation to the same habitat, and those
804 species share the phrynopoid morphology. Aside from body shape, characteristics that have
805 been used to define the phrynopoid morphology include shape of terminal phalanges, pads
806 and discs on digits, and middle ear (Lynch, 1975; Lehr, 2005; Lehr et al., 2005; De la Riva,
807 2007; Rodriguez and Catenazzi, 2017; De la Riva, 2020). Our analyses showed that

808 researchers have been tricked by symplesiomorphies and revealed a different scenario for the
809 evolution of those characters in the phrynopoid genera (i.e., *Bryophryne*, *Microkayla*,
810 *Phrynopus*, and *Psychrophrynella*). The absence of pad and circumferential groove on digits,
811 for long considered evidence of convergence in high Andean species, actually represent
812 ancestral states shared by those species (Figure 4). On the other hand, the knobbed terminal
813 phalange as found in *Phrynopus* is a derived state but was not found in any other genera
814 (Figure 4), and the absence of tympanum, also a derived state, is only shared by *Bryophryne*
815 (Figure 7).

816 Nevertheless, our analyses also unmasked convergence in character states that,
817 interestingly, were used by Lynch (1975) to define groups of species (i.e., character states of
818 the vomer and nasal bones) but overlooked by several subsequent studies addressing
819 convergence (Lehr, 2005; Lehr et al., 2005; De la Riva, 2020). Lynch (1975) was tricked by
820 symplesiomorphies when defining *Phrynopus* and by convergence when defining groups of
821 species, but his observations on osteological variation hidden under similar external traits
822 provide a general framework for the study of convergence in Holoadeninae. Species groups
823 were proposed mainly based on characteristics of vomer, ear, and nasals. The *P. peruanus*
824 group (*sensu* Lynch, 1975) included species that are now part of *Bryophryne*, *Microkayla*, and
825 *Phrynopus*, and species of this group converge in having acute anterior ala of vomer, thick
826 dentigerous process of vomer, and lack of vomerine teeth. Interestingly, those same character
827 states are shared by *Euparkerella*, a genus from the Brazilian Atlantic Forest. The *P.*
828 *flavomaculatus* group included species that are now part of *Lynchius*, *Niceforonia*, and
829 *Oreobates*, and species of this group converge in having large nasals close to each other or in
830 contact. However, those same character states are shared by the non-Andean clade *Barycholos*
831 and *"Eleutherodactylus" bilineatus*.

832 By reassessing our morphological knowledge of Holoadeninae genera we show that
833 evolutionary history of characters considered convergent is more complex than we believed.
834 The repeated evolution of the same character states is a common phenomenon in
835 Holoadeninae and is not restricted to high Andean groups. Moreover, it represents a case of
836 parallel evolution, because all the events involve the same ancestral state giving rise to the
837 same derived state.
838
839 *Tympanic middle ear evolution and acoustic communication*
840 Complete loss of tympanic middle ear is widespread among anurans, occurring
841 independently at least 35 times in species of no fewer than 20 anuran families (Pereyra et al.,
842 2016). Our optimization recovers the presence of columella, tympanic annulus, and tympanic
843 membrane as the ancestral state for Holoadeninae (characters 48, 49, and 50), with one
844 transformation resulting in the loss of the tympanic membrane in *Lynchius nebulanastes* and
845 *L. parkeri*, and four transformations involving the loss of the three structures: in the clade
846 including *Euparkerella* and *Holoaden*, in *Bryophryne cophites*, in *Niceforonia nana*, and in a
847 clade of *Phrynopus* including all species but *P. auriculatus*, *P. mariellaleo*, *P. peruanus*, and
848 *P.* spI. There is no reversal resulting in the acquisition of tympanic middle ear (Figure 7).
849 The presence of a middle ear is not a necessary condition for hearing in anurans.
850 Earless frogs actually have a hearing capacity comparable to species with tympanum, and use
851 extratympanic pathways involving lungs, the opercular system, the oral cavity, or bone
852 conduction (Boistel et al., 2013; Hetherington and Lindquist, 1999; Lombard and Straughan,
853 1974; Hetherington, 1992). It has been proposed that in *Phrynopus* "only the eared species are
854 known to produce advertisement calls (i.e., earless species do not produce calls)" and, thus,
855 that "*Phrynopus* comprise a radiation lacking both the communication signal (advertisement
856 calls) and sensory system (tympanic membrane and annulus)" (von May et al., 2018, pp. 3–4).

857 However, data available and, equally important, missing data for acoustic communication in
858 *Phrynopus* species do not support that hypothesis.

859 Even though von May et al. (2018, p. 18) affirm that "to date, the only species known
860 to produce advertisement calls are *P. auriculatus*, *P. peruanus*, and *Phrynopus* spI" (eared
861 species), the earless species *P. bracki* also had its advertisement call described long before
862 their study (Hedges, 1990). Moreover, information about acoustic communication in earless
863 species of *Phrynopus* was available in natural history notes of species descriptions. A male
864 specimen of *Phrynopus pesantesi* was observed calling in captivity and emitted a release call
865 when disturbed (Lehr et al., 2005), and males of *P. badius* and *P. curator* were heard calling
866 from the leaf litter and among mosses (Lehr et al., 2012). Therefore, even in the absence of a
867 middle ear, earless species of *Phrynopus* seem to use acoustic communication and probably
868 use extratympanic pathways for the transfer of airborne sound to the inner ear.

869 Morever, due to the limited evidence on acoustic communication mechanisms in
870 *Phrynopus*, it seems premature to affirm that the lack of tympanum results in the inability to
871 produce acoustic signals in species of this genus. Most species of *Phrynopus* have a cryptic
872 mode of life restricted to leaf litter and moss layers, making it difficult to find and observe the
873 behavior of individuals (Lehr and Oróz, 2012). As a consequence, many species are known
874 only from the type locality, have been observed in the field once or are known from a limited
875 number of specimens (Lehr and Oróz, 2012; Rodriguez and Catenazzi, 2017). As a matter of
876 fact, for some species of *Phrynopus* only one male has been collected (*P. lapidoides*, *P.*
877 *unchog*, *P. anancites*, *P. capitalis*, *P. personatus*, *P. daemon*, and *P. chaparroi*), while for
878 others only females are known (*P. miroslawae*, *P. thompsoni*, and *P. vestigiatus*). Thus, both
879 limited number of specimens and behavioral observations makes it difficult to drag any firm
880 conclusion about the correlation between the lack of tympanum and acoustic communication.

881 On the other hand, we can affirm that the loss of tympanum is not coincident with lack
882 of advertisement calls in the clade that includes the genera *Euparkerella* and *Holoaden*. All
883 species of *Euparkerella* and two out of four species of *Holoaden* are known to produce calls
884 (Martins, 2010; Martinelli and Toledo, 2016; Hepp et al., 2015). The genus *Bryophryne* also
885 comprises a radiation of earless species. In addition to *Bryophryne cophites*, tympanum has
886 been lost in *Br. bakersfield*, *Br. bustamantei, Br. quellokunka*, *Br. tocra*, and *Br. wilakunka*,
887 species that were recovered as part of the same clade (De la Riva et al., 2017). In *Bryophryne*
888 the loss of tympanum also does not precludes the production of acoustic signals, as at least
889 two of earless species have been heard calling: *Br. bakersfield* (Chaparro et al., 2007) and *Br.*
890 *bustamantei* (Chaparro et al., 2015).
891 Aside from some scattered losses that represent autapomorphies, the middle ear
892 structures were completely lost in only one more group of Brachycephaoidea: the genus
893 *Brachycephalus* (Pereyra et al., 2016). In this clade of miniaturized frogs, the loss of
894 tympanum is also not coincident with lack of advertisement calls, as advertisement calls have
895 been described for 12 out of the 36 named species of the genus (Bornschein et al., 2019). It
896 has been suggested that two species of *Brachycephalus* (*B. ephippium* and *B. pitanga*) are
897 unable to perceive their own calls, as they produce calls outside their hearing sensitivity
898 (Goutte et al., 2017). However, males of those species have the ability to synchronize calls,
899 avoiding acoustic overlap with a conspecific male, and males have been recorded emitting
900 advertisement calls antiphonally even when individuals are mutually hidden from one another
901 (Tandel et al., 2014; personal observations). The ability to synchronize calls in the absence of
902 visual signals strongly suggests that *B. ephippium* and *B. pitanga* can hear their conspecific
903 vocalizations. In contrast to the middle ear, in individuals of both species the body surface
904 overlaying the lungs shows patterns of tissue displacement that correlated with the
905 advertisement call frequency (Goutte et al., 2017). One hypothesis for the perception of

906 acoustic signals is that the pronounced attenuation of sound energy when the sound penetrates
907 the lateral body wall and enters the lung (Lindquist et al., 1998) might promote a reduction in
908 the frequency of the sound that is transferred to the inner ear that reaches the species
909 sensitivity range.

910 The loss of only the tympanic membrane has also not precluded the production of
911 mating calls in *Lynchius* (Cannatella, 1984; Duellman and Lehr, 2009). However, in contrast
912 with species that lack all three tympanic structures, in *Lynchius nebulanastes* and *L. parkeri*
913 the middle ear can still be used as a hearing pathway, because the acoustic function of the
914 tympanic annulus is retained even in the absence of tympanic membrane (Wever, 1985).
915
916 *Pelvic girdle evolution and locomotion in Holoadeninae*

917 Species of *Phrynopus*, as well as species of other genera of Holoadeninae, occupy
918 different habitats and microhabitats and show different locomotor modes. Most species of
919 *Phrynopus* primarily move by walking or by short jumps. Nevertheless, some species are
920 more agile and capable of jumping (e.g. *P. curator*), and one species (*P. horstpauli*) is
921 arboreal (Lehr et al., 2012; von May et al., 2018). *Oreobates* species also show a wide variety
922 of locomotion behaviors. There are species that climb low vegetation, rocky outcrops, and
923 stalagmites (e.g. *O. antrum*), species that live in the leaf litter and jump and quickly maneuver
924 at the ground level (e.g. *O. lehri*), and slow-moving frogs adapted to cold grasslands (e.g. *O.*
925 *ayacucho*) (Padial et al., 2012; Kohler and Padial, 2016; Motta et al., 2020).

926 Different configurations of pelvic girdle are correlated with locomotor modes in
927 anurans. The lateral-bender morph (associated with walking, burrowing, and hopping frogs) is
928 considered the basal and general condition for frogs and the sagittal-hinge morph (associated
929 to jumping frogs) is a derived condition, implying that walking/hopping is the ancestral
930 locomotor mode and jumping appears later (Reilley and Jorgensen, 2011). Nevertheless,

931 pelvic girdle patters may also be family specific, and species with the same articulation
932 morphology may show differences in the degree of movement (Emerson, 1979). States of
933 characters of sagittal-hinge morph (characters 18–21) are shared by all species of
934 Holoadeninae and, thus, the pelvic morph does not vary among species with different
935 locomotor modes.

936 The pelvic type seems to be conservative in Brachycephaloidea species. The only
937 species ever described as a *Phrynopus* that had expanded diapophyses was, in fact, a species
938 of the family Microhylidae (Lehr and Trueb, 2007). Jorgensen and Reilley (2013) analyzed
939 species of terraranan frogs and found that species of the families (*sensu* Hedges et al., 2008)
940 Eleutherodactylidae (represented by *Eleutherodactylus coqui*), Strabomantidae (represented
941 by *Barycholos pulcher*, *Holoaden bradei, Oreobates quixensis*, *Lynchius flavomaculatus*,
942 *Pristimantis altae*, and *Strabomantis anomalus*), and Craugastoridae (represented by
943 *Craugastor crassidigitus*) have the same pelvic type (sagittal-hinge pelvis) and are all
944 considered jumpers, while Brachycephalidae (represented by *Brachycephalus ephippium*) has
945 the non-sagittal-hinge pelvis and is considered walker/hopper.

946 It is important to note that other characteristics of the pelvic girdle are also related to
947 locomotor mode. For example, the crests of ilium and urostyle have larger areas in jumper
948 species when compared to hopper species (Ponssa et al., 2018). However, the species of the
949 genera included in that study (family Leptodactylidae) have different kinds of pelvic girdle,
950 and, thus, the same pattern might not be found in Holoadeninae. Even though we did not
951 measure the area of the crests, they apparently show no tendency on having different areas.
952 Studies exploring the adaptations to a variety of use of habits by species of Holoadeninae are
953 scarce and deserve attention.
954

Conclusions

The present analysis is the most comprehensive phylogenetic analysis of *Phrynopus* to date and allowed us to fill some gaps on our understanding of trait evolution in this genus and its relatives. Our analyses support the monophyly of *Phrynopus*, sister to a clade including the genera *Lynchius* and *Oreobates*. These analyses provide the strongest test to date of these relationships as well as the relationships of species in these genera. We also discovered phenotypic synapomorphies for *Phrynopus* and related genera unknown to date. Our results also revealed that the evolution of phenotypic characters in Holoadeninae render character states used to diagnose *Phrynopus* and other genera in the past as symplesiomorphies. We were able to show that repeated evolution of a character state is a common phenomenon in Holoadeninae and is not restricted to high Andean groups and, hence, that selective pressures resulting from the colonization of high Andean environments is not necessarily the only process driving the evolution of similar morphologies. However, since the events involved the same ancestral state giving rise to the same derived state, we provide support for the hypothesis that similar phenotypes are parallelisms, the causes of which remain unknown. All in all, we were able to answer some long standing questions such as what traits are synapomorphic for what clades and which are simplesiomorphies; how many times similar traits originated and at what level of the phylogeny; and, in turn, what confused us in the first time and what evolutionary history may lie underneath such interesting pattern of similarity among distant relatives. Therefore, our results provide a strong foundation for further exploration and understanding of morphological evolution in terraranas. We hope our findings will encourage future study of osteological diversity in this group. After all, “although it is more difficult to gather data about bones, they have fascinating functional and evolutionary stories to tell” (Trueb and Lehr, 2008; p.23).

Acknowledgments

For allowing access to material under their care we thank F. Burbrink, C. Raxworthy, and D. Kizirian (AMNH), Stephen Rogers (CM), P. Venegas (CORBIDI), R. Brown, R. Glor, and L. Welton (KU), Julian Faivovich (MACN), J. Hanken, J. Rosado, and J. Martinez (MCZ), J. Chaparro (MUBI), J. Pombal Jr. and M. Cardoso (MNRJ), C. Aguilar (MUSM), T. Grant and A. Benetti (MZUSP), F. Franco (UFMT), F. Toledo (ZUEC). APM thanks São Paulo Research Foundation (FAPESP) for her PhD scholarship (grants #2017/08488-3 and #2018/10458-8); MCZ for the Ernst Mayr Travel Grant; and AMNH for the Collection Study Grant. FAPESP (grant #2013/50741-7) and Conselho Nacional de Desenvolvimento Científico e Tecnológico (CNPq; grant #306623/2018-8) provided financial support to CFBH.

References

Aguayo-Vedia, C.R. and Harvey, M.B., 2001. Dos nuevas especies de *Phrynopus* (Anura: Leptodactylidae) de los bosques nublados de Bolivia. Rev. Biol. Trop. 49, 333–345.

Ardila-Robayo, M.C., Ruiz-Carranza, P.M. and Barrera-Rodriguez, M., 1996. Una nueva especie de *Phrynopus* (Amphibia, Anura, Leptodactylidae) de La Cordillera Central Colombiana. Lozania. Bogotá 67, 1–10.

Barrionuevo, J.S., 2017. Frogs at the summits: phylogeny of the Andean frogs of the genus *Telmatobius* (Anura, Telmatobiidae) based on phenotypic characters. Cladistics 33, 41–68.

Boistel, R., Aubin, T., Cloetens, P., Peyrin, F., Scotti, T., Herzog, P., Gerlach, J., Pollet, N., Aubry, J., 2013. How minute sooglossid frogs hear without a middle ear. Proc. Natl. Acad. Sci. U.S.A. 110, 15360–15364.

1003 Bornschein, M.R., Rollo Jr., M.M., Pie, M.R., Confetti, A.E. and Ribeiro, L.F., 2019.
1004 Redescription of the advertisement call of *Brachycephalus tridactylus* (Anura:
1005 Brachycephalidae). Phyllomedusa 18: 3–12.
1006 Bremer, K., 1988. The limits of amino acid sequence data in angiosperm phylogenetic
1007 reconstruction. Evolution 42, 795–803.
1008 Canedo, C. and Haddad, C.F.B., 2012. Phylogenetic relationships within anuran clade
1009 Terrarana, with emphasis on the placement of Brazilian Atlantic rainforest frogs genus
1010 *Ischnocnema* (Anura: Brachycephalidae). Mol. Phylogenetics Evol. 65, 610–620.
1011 Cannatella, D.C., 1984. Two new species of the leptodactylid frog genus *Phrynopus*, with
1012 comments on the phylogeny of the genus. Occas. Pap. Mus. Nat. Hist. Univ. Kans.
1013 113, 1–16.
1014 Cannatella, D.C., 1985. The systematic status of *Syrrhophus juninensis* Shreve (Anura:
1015 Leptodactylidae). Proc. Biol. Soc. Wash. 98, 774–777.
1016 Catenazzi, A., Mamani, L., Lehr, E. and von May, R., 2020. A new genus of terrestrial-
1017 breeding frogs (Holoadeninae, Strabomantidae, Terrarana) from southern Peru.
1018 Diversity 12, 1–17.
1019 Chaparro, J.C., De la Riva, I., Padial, J.M., Ochoa, J.A. and Lehr, E., 2007. A new species of
1020 *Phrynopus* from Departamento Cusco, southern Peru (Anura: Brachycephalidae).
1021 Zootaxa 1618, 61–68.
1022 Chaparro, J.C., Padial, J.M. and De la Riva, I., 2008. Two sympatric new species of
1023 *Phrynopus* (Anura: Strabomantidae) from Yanachaga Chemillen National Park
1024 (central Peruvian Andes). Zootaxa 1761, 49–58.
1025 Chaparro, J.C., Padial, J.M., Gutiérrez, R.C. and De la Riva, I., 2015. A new species of
1026 Andean frog of the genus *Bryophryne* from southern Peru (Anura: Craugastoridae) and

its phylogenetic position, with notes on the diversity of the genus. Zootaxa 3994, 94–108.

Chávez, G., Santa Cruz, R., Rodríguez, D. and Lehr, E., 2015. Two new species of frogs of the genus *Phrynopus* (Anura: Terrarana: Craugastoridae) from the Peruvian Andes. Amphib. Reptile Conserv. 9, 15–25.

Chávez, G., García Ayachi, L.A. and Catenazzi, A., 2020. A new species of frog (Terrarana, Strabomantidae, *Phrynopus*) from the Peruvian Andean grasslands. PeerJ 8 (e9433), 1–14.

Cignoni, P., Callieri, M., Corsini, M., Dellepiane, M., Ganovelli, F. and Ranzuglia G., 2008. MeshLab: an Open-Source Mesh Processing Tool. Eurographics Italian Chapter Conference, 129–136.

De la Riva, I., 1992. A new species of *Phrynopus* from Bolivia (Anura: Leptodactylidae). Herpetologica 48, 111–114.

De la Riva, I., 2007. Bolivian frogs of the genus *Phrynopus*, with the description of twelve new species (Anura: Brachycephalidae). Herpetol. Monogr. 21, 241–277.

De la Riva, I., 2020. Unexpected beta-diversity radiations in highland clades of Andean Terraranae frogs In: Rull, V., Carnaval, A., (Eds.), Neotropical Diversification: Patterns and Processes. Fascinating Life Sciences. Springer Nature Switzerland, AG. pp. 741–764.

De la Riva, I., Chaparro, J.C. and Padial, J.M., 2008. The taxonomic status of *Phyllonastes* Heyer and *Phrynopus peruvianus* (Noble) (Lissamphibia, Anura): resurrection of *Noblella* Barbour. Zootaxa 1685, 67–68.

De la Riva, I., Chaparro, J.C., Castroviejo-Fisher, S., and Padial, J.M., 2017. Underestimated anuran radiations in the high Andes: five new species and a new genus of

1051 Holoadeninae, and their phylogenetic relationships (Anura: Craugastoridae). Zool. J.
1052 Linn. Soc. 182, 129–172.
1053 Duellman, W.E., 2000. Leptodactylid frogs of the genus *Phrynopus* in northern Peru with
1054 descriptions of three new species. Herpetologica 56, 273–285.
1055 Duellman, W.E. and Hedges, S.B., 2008. Two minute species of *Phrynopus* (Lissamphibia:
1056 Anura) from the Cordillera Oriental in Peru. Zootaxa 1675, 59–66.
1057 Duellman, W.E. and Lehr, E., 2009. Terrestrial-breeding frogs (Strabomantidae) in Peru.
1058 Natur und Tier-Verlag, Germany.
1059 Emerson, S.B., 1979. The ilio-sacral articulation in frogs: form and function. Biol. J. Linn.
1060 Soc. 11, 153–168.
1061 Emerson, S.B., 1982. Frog postcranial morphology: identification of a functional complex.
1062 Copeia 3, 603–613.
1063 Farris, J.S., Albert, V.A., Kallersjo, M., Lipscomb, D. and Kluge, A.G., 1996. Parsimony
1064 jackknifing outperforms neighbor-joining. Cladistics 12, 99–124.
1065 Frost, D.R., 2020. Amphibian Species of the World: an Online Reference, Version 6.0.
1066 American Museum of Natural History, New York, NY.
1067 http://research.amnh.org/herpetology/amphibia/index.html (accessed on 21 July 2020).
1068 Frost, D.R., Grant, T., Faivovich, J., Bain, R.H., Haas, A., Haddad, C.F.B., De Sá, R.O.,
1069 Channing, A., Wilkinson, M., Donnellan, S.C., Raxworthy, C.J., Campbell, J.A.,
1070 Blotto, B.L., Moler, P., Drewes, R.C., Nussbaum, R.A., Lynch, J.D., Green, D.M. and
1071 Wheeler, W.C., 2006. The amphibian tree of life. Bull. Am. Mus. Nat. Hist. 297, 1–
1072 370.
1073 Goicoechea, N., Frost, D.R., De la Riva, I., Pellegrino, K.C., Sites Jr, J., Rodrigues, M.T.
1074 Padial, J.M., 2016. Molecular systematics of teioid lizards

(Teioidea/Gymnophthalmoidea: Squamata) based on the analysis of 48 loci under tree-alignment and similarity ‐ alignment. Cladistics 32, 624–671.

Goloboff, P.A., 1996. Methods for faster parsimony analysis. Cladistics 12, 199–220.

Goloboff, P.A., 1999. Analyzing large data sets in reasonable times: solutions for composite optima. Cladistics 15, 415–428.

Goloboff, P.A., Farris, J.S., Nixon, K.C., 2008. TNT, a free program for phylogenetic analysis. Cladistics 24, 774–786.

Goodman, M., Weiss, M.L., Czelusniak, J., 1982. Molecular evolution above the species leve, branching patterns, rates, and mechanisms. Syst. Zool. 31, 376–399.

Goutte, S., Mason, M.J., Christensen-Dalsgaard, J., Montealegre-Z, F., Chivers, B.D., Sarria-S, F.A., Antoniazzi, M.M., Jared, C., Sato, L.A. and Toledo, L.F., 2017. Evidence of auditory insensitivity to vocalization frequencies in two frogs. Sci. Rep. 7, 12121.

Grant, T. and Kluge, A.G, 2004. Transformation series as an ideographic character concept. Cladistics 20, 23–31.

Grant, T. and Kluge, A.G., 2008. Clade support measures and their adequacy. Cladistics, 24, 1051–1064.

Grant, T., Frost, D.R., Caldwell, J.P., Gagliardo, R., Haddad, C.F.B., Kok, P.J.R., Means, D.B., Noonan, B.P., Schargel, W.E. and Wheeler, W.C., 2006. Phylogenetic systematics of dart-poison frogs and their relatives (Amphibia: Athesphatanura: Dendrobatidae). Bull. Am. Mus. Nat. Hist. 299, 1–262

Harvey, M.B. and Ergueta-Sandoval, P., 1998. A new species of *Phrynopus* (Anura: Leptodactylidae) from elfin forest in the Bolivian Andes. J. Herpetol. 32: 536–540.

Hedges, S.B., 1990. A new species of *Phrynopus* (Anura: Leptodactylidae). Copeia 1990, 108–112.

1099 Hedges, S.B., Duellman, W.E. and Heinicke, M.P., 2008. New World direct-developing frogs
1100 (Anura: Terrarana): molecular phylogeny, classification, biogeography, and
1101 conservation. Zootaxa 1737, 1–182.
1102 Heinicke, M.P., Duellman, W.E. and Hedges, S.B., 2007. Major Caribbean and Central
1103 American frog faunas originated by oceanic dispersal. Proc. Natl. Acad. Sci. U.S.A.
1104 104, 10092–10097.
1105 Heinicke, M.P., Lemmon, A.R., Lemmon, E.M., McGrath, K. and Hedges, S.B., 2018.
1106 Phylogenomic support for evolutionary relationships of New World direct-developing
1107 frogs (Anura: Terraranae). Mol. Phylogenet. Evol. 118, 145–155.
1108 Hepp, F., de Carvalho-e-Silva, S.P., de Carvalho-e-Silva, A.M.P.T. and Folly, M., 2015. A
1109 fifth species of the genus *Euparkerella* (Griffths, 1959), the advertisement calls of *E.*
1110 *robusta* Izecksohn, 1988 and *E. tridactyla* Izecksohn, 1988, and a key for the
1111 *Euparkerella* species (Anura: Brachycephaloidea: Craugastoridae). Zootaxa 3973,
1112 251–270.
1113 Hetherington, T.E., 1992. The effects of body size on the evolution of the amphibian middle
1114 ear. In: Webster, D.B., Fay, R.R. and Popper, A.N. (Eds.), The evolutionary biology of
1115 hearing. Springer-Verlag New York, USA. pp. 421–437.
1116 Hetherington, T.E. and Lindquist, E.D., 1999. Lung-based hearing in an “earless” anuran
1117 amphibian. J. Comp. Physiol. A 184, 395–401.
1118 Jorgensen, M.E. and Reilly, S.M., 2013. Phylogenetic patterns of skeletal morphometrics and
1119 pelvic traits in relation to locomotor mode in frogs. J. Evol. Biol. 26, 929–943.
1120 Katoh, K. and Standley, D.M., 2013. MAFFT multiple sequence alignment software version
1121 7: Improvements in performance and usability. Mol. Biol. Evol. 30, 772–780.
1122 Kearse, M., Moir, R., Wilson, A., Stones-Havas, S., Cheung, M., Sturrock, S., Buxton, S.,
1123 Cooper, A., Markowitz, S., Duran, C., Thierer, T., Ashton, B., Meintjes, P.,

1124 Drummond, A., 2012. Geneious Basic: an integrated and extendable desktop software
1125 platform for the organization and analysis of sequence data. Bioinformatics 28,1647–
1126 1649.
1127 Kluge, A.G. and Grant, T., 2006. From conviction to anti–superfluity, old and new
1128 justifications for parsimony in phylogenetic inference. Cladistics 22, 276–288.
1129 Köhler, J. and Padial, J.M., 2016. Description and phylogenetic position of a new (singleton)
1130 species of *Oreobates* Jiménez de la Espada, 1872 (Anura: Craugastoridae) from the
1131 Yungas of Cochabamba, Bolivia. Ann. Carnegie. Mus. 84, 23–38.
1132 Lehr, E., 2001. A new species of *Phrynopus* (Anura: Leptodactylidae) from the eastern
1133 Andean slopes of central Peru. Salamandra 37, 11–20.
1134 Lehr, E., 2005. A new species of the *Eleutherodactylus nigrovittatus* group (Anura:
1135 Leptodactylidae) from Andean Peru. Herpetologica 61, 199–208.
1136 Lehr, E., 2006. Taxonomic status of some species of Peruvian *Phrynopus* (Anura:
1137 Leptodactylidae), with the description of a new species from the Andes of southern
1138 Peru. Herpetologica 62, 331–347.
1139 Lehr, E., 2007. New eleutherodactyline frogs (Leptodactylidae: *Pristimantis*, *Phrynopus*)
1140 from Peru. B. Mus. Comparat. Zool. Cambridge, Massachusetts 159, 145–178.
1141 Lehr, E. and Aguilar, C., 2002. A new species of *Phrynopus* (Amphibia, Anura,
1142 Leptodactylidae) from the puna of Maraypata (Departamento de Huánuco, Peru).
1143 Zoologische Abhandlungen. Staatliches Museum für Tierkunde in Dresden 52, 57–64.
1144 Lehr, E. and Aguilar, C., 2003. A new species of *Phrynopus* (Amphibia, Anura,
1145 Leptodactylidae) from the puna of Maraypata (Departamento de Huánuco, Peru).
1146 Zoologische Abhandlungen. Staatliches Museum für Tierkunde in Dresden 53, 87–92.
1147 Lehr, E. and Aguilar, C., 2006. The taxonomic status of *Phrynopus pereger* Lynch 1975
1148 (Amphibia, Anura, Leptodactylidae). Zootaxa 1284, 53–60.

1149 Lehr, E. and Oróz, A., 2012. Two new species of *Phrynopus* (Anura: Strabomantidae) from
1150 the Cordillera de Carpish in central Peru (Departamento de Huánuco). Zootaxa 3512,
1151 53–63.
1152 Lehr, E. and Rodríguez, D., 2017. Two new species of Andes frogs (Craugastoridae:
1153 *Phrynopus*) from the Cordillera de Carpish in central Peru. Salamandra 53, 327–338.
1154 Lehr, E. and Trueb, L., 2007. Diversity among New World microhylid frogs (Anura:
1155 Microhylidae): morphological and osteological comparisons between *Nelsonophryne*
1156 (Günther 1901) and a new genus from Peru. Zool. J. Linn. Soc. 149, 583–609.
1157 Lehr, E., Köhler, G. and Ponce, E., 2000. A new species of *Phrynopus* from Peru (Amphibia,
1158 Anura, Leptodactylidae). Senckenbergiana Biologica 80, 205–212.
1159 Lehr, E., Aguilar, C. and Köhler, G., 2002a. Two sympatric new species of *Phrynopus*
1160 (Anura: Leptodactylidae) from a cloud forest in the Peruvian Andes. J. Herpetol. 36,
1161 208–216.
1162 Lehr, E., Rodríguez, D. and Córdova, J.H., 2002b. A new species of *Phrynopus* (Amphibia,
1163 Anura, Leptodactylidae) from the Cordillera de Carpish (Departamento de Huánuco,
1164 Peru). Zoologische Abhandlungen. Staatliches Museum für Tierkunde in Dresden 52,
1165 65–70.
1166 Lehr, E., Müller, A. and Fritzsch, G., 2005a. Analysis of Andes frogs (*Phrynopus*,
1167 Leptodactylidae, Anura) phylogeny based on 12S and 16S mitochondrial rDNA
1168 sequences. Zool. Scr. 34, 593–603.
1169 Lehr, E., Lundberg, M. and Aguilar, C., 2005b. Three new species of *Phrynopus* from central
1170 Peru (Amphibia: Anura: Leptodactylidae). Copeia 2005, 479–491.
1171 Lehr, E., Moravec, J. and Cusi, J.C., 2012. Two new species of *Phrynopus* (Anura,
1172 Strabomantidae) from high elevations in the Yanachaga-Chemillén National park in
1173 Peru (Departamento de Pasco). ZooKeys 235, 51–71.

1174 Lehr, E., von May, R., Moravec, J. and Cusi, J.C., 2017. A new species of *Phrynopus*
1175 (Amphibia, Anura, Craugastoridae) from upper montane forests and high Andean
1176 grasslands of the Pui Pui Protected Forest in central Peru. ZooKeys 713, 131–157.
1177 Lindquist, E.D., Hetherington, T E. and Volman, S.F., 1998. Biomechanical and
1178 neurophysiological studies on audition in eared and earless harlequin frogs (*Atelopus*).
1179 J. Comp. Physiol. 183, 265–271.
1180 Lombard, R.E. and Straughan, I.R., 1974. Functional aspects of anuran middle ear structures.
1181 J. Exp. Biol. 61, 71–93.
1182 Lynch, J.D., 1968. Systematic status of some Andean leptodactylid frogs with a description of
1183 a new species of *Eleutherodactylus*. Herpetologica 24, 289–300.
1184 Lynch, J.D., 1969. Taxonomic notes on Ecuadorian frogs (Leptodactylidae:
1185 *Eleutherodactylus*). Herpetologica 25, 262–274.
1186 Lynch, J.D., 1971. Evolutionary relationships, osteology, and zoogeography of leptodactyloid
1187 frogs. Misc. Publ. Museum Nat. Hist. Univ. Kansas 53, 1–238.
1188 Lynch, J.D., 1972. Generic partitioning of the South American leptodactylid frog genus
1189 *Eupsophus* Fitzinger 1843 (sensu lato). Bull. South. Calif. Acad. Sci. 71, 2–11.
1190 Lynch, J.D., 1975. A review of the Andean leptodactylid frog genus *Phrynopus*. Occas. pap.
1191 Mus. Nat. Hist. 35, 1–51.
1192 Lyra, M.L., Haddad, C.F.B. and Azeredo-Espin, A.M.L., 2017. Meeting the challenge of
1193 DNA barcoding Neotropical amphibians: polymerase chain reaction optimization and
1194 new COI primers. Mol. Ecol. Resour. 17, 966–980.
1195 Maddison, W. P. and Maddison, D.R., 2019. Mesquite: a modular system for evolutionary
1196 analysis. Version 3.61. Accessible at http://www.mesquiteproject.org
1197 Mamani, L. and Malqui, S., 2014. A new species of *Phrynopus* (Anura: Craugastoridae) from
1198 the central Peruvian Andes. Zootaxa 3838, 207–214.

1199 Maniatis T., Fritsch, E.F. and Sambrook, J., 1982. Molecular cloning: a laboratory manual.
1200 Cold Spring Harbor Laboratory, New York, USA.
1201 Martinelli, A. and Toledo, L.F., 2016. The last scream: the distress call of a probably extinct
1202 Brazilian anuran (*Holoaden bradei* Lutz, 1958). Zootaxa 4184, 383–385.
1203 Martins, I. A., 2010. Natural history of *Holoaden luederwaldti* (Amphibia: Strabomantidae:
1204 Holoadeninae) in southeastern of Brazil. Zoologia 27, 40–46.
1205 Motta, A.P., Chaparro, J.C., Pombal Jr., J.P., Guayasamin, J.M., De la Riva, I. and Padial,
1206 J.M., 2016. Molecular phylogenetics and taxonomy of the Andean genus *Lynchius*
1207 Hedges, Duellman, and Heinicke, 2008 (Anura: Craugastoridae). Herpetol. Monogr.
1208 30, 119–142.
1209 Motta, A.P., Lyra, M.L., Gazoni, T., Parise-Maltempi, P.P. and Haddad, C.F.B., 2020. New
1210 distribution records of *Oreobates antrum* Vaz-Silva, Maciel, Andrade, and Amaro,
1211 2018, a cave-associated species from the Seasonally Dry Tropical Forest in the
1212 Brazilian Cerrado (Anura: Brachycephaloidea: Craugastoridae). Herpetol. Notes 13,
1213 561–563.
1214 Motta, A.P., Taucce, P.P.G., Haddad, C.F.B. and Canedo, C., in press. A new terraranan
1215 genus from the Brazilian Atlantic Forest with comments on the systematics of
1216 Brachycephaloidea (Amphibia: Anura). J. Zoolog. Syst. Evol. Res.
1217 Nixon, K.C., 1999. The parsimony ratchet, a new method for rapid parsimony analysis.
1218 Cladistics 15, 407–414.
1219 Padial, J.M., Chaparro, J.C. and De la Riva, I., 2008. Systematics of *Oreobates* and the
1220 *Eleutherodactylus discoidalis* species group (Amphibia, Anura), based on two
1221 mitochondrial DNA genes and external morphology. Zool. J. Linn. Soc. 152, 737–773.
1222 Padial, J.M., Castroviejo-Fisher, S. and De la Riva, I., 2009. The phylogenetic relationships of
1223 *Yunganastes* revisited (Anura: Terrarana). Mol. Phylogenet. Evol. 52, 911–915.

1224 Padial, J.M., Chaparro, J.C., Castroviejo-Fisher, S., Guayasamín, J.M., Lehr, E., Delgado,
1225 A.J., Vaira, M., Teixeira, Jr, M., Aguayo, R. and De la Riva, I., 2012. A revision of
1226 species diversity in the Neotropical genus *Oreobates* (Anura: Strabomantidae), with
1227 the description of three new species from the Amazonian slopes of the Andes, and the
1228 proposal of candidate species. Am. Mus. Novit. 3752, 1–55.
1229 Padial, J.M., Grant, T. and Frost, D.R., 2014. Molecular systematics of terraranas (Anura:
1230 Brachycephaloidea) with an assessment of the effects of alignment and optimality
1231 criteria. Zootaxa 3825, 1–132.
1232 Parker, H.W., 1938. The vertical distribution of some reptiles and amphibians in southern
1233 Ecuador. Ann. Mag. Nat. Hist. 2, 438–450.
1234 Pereyra, M.O., Womack, M.C., Barrionuevo, J.S., Blotto, B.L., Baldo, D., Targino, M.,
1235 Ospina-Sarria, J.J., Guayasamin, J.M., Coloma, L.A., Hoke, K.L., Grant, T. and
1236 Faivovich, J., 2016. The complex evolutionary history of the tympanic middle ear in
1237 frogs and toads (Anura). Sci. Rep. 6, 34130.
1238 Ponssa, M.L., 2008. Cladistic analysis and osteological descriptions of the frog species in the
1239 *Leptodactylus fuscus* species group (Anura, Leptodactylidae). J. Zoolog. Syst. Evol.
1240 Res. 46, 249–266.
1241 Pyron, R.A. and Wiens, J.J., 2011. A large-scale phylogeny of Amphibia including over 2800
1242 species, and a revised classification of extant frogs, salamanders, and caecilians. Mol.
1243 Phylogenet. Evol. 61, 543–583.
1244 Reilly, S.M. and Jorgensen, M.E., 2011. The evolution of jumping in frogs: morphological
1245 evidence for the basal anuran locomotor condition and the radiation of locomotor
1246 systems in crown group anurans. J. Morphol. 272, 149–168.

1247 Rodríguez, L.O. and Catenazzi, A., 2017. Four new species of terrestrial-breeding frogs of the
1248 genus *Phrynopus* (Anura: Terrarana: Craugastoridae) from Río Abiseo National Park,
1249 Peru. Zootaxa 4273, 381–406.
1250 Sánchez-Nivicela, J.C., Urgilés, V.L., Navarrete, M.J., Yánez-Muñoz, M.H. and Ron, S.R.,
1251 2019. A bizarre new species of *Lynchius* (Amphibia, Anura, Strabomantidae) from the
1252 Andes of Ecuador and first report of *Lynchius parkeri* in Ecuador. Zootaxa 4567, 1–
1253 24.
1254 Taboada, C., Grant, T., Lynch, J.D. and Faivovich, J., 2013. New morphological
1255 synapomorphies for the New World direct-developing frogs (Amphibia: Anura:
1256 Terrarana). Herpetologica 69, 342–357.
1257 Tamura, K., Dudley, J., Nei, M. and Kumar, S., 2007. MEGA4: Molecular Evolutionary
1258 Genetics Analysis (MEGA) software version 4.0. Mol. Biol. Evol. 24, 1596–1599.
1259 Tandel, M.C.F.F., S. Loibel, E.G. Oliveira and C.F.B. Haddad. 2014. Diferenciação de 3 tipos
1260 de vocalizações (cantos) na espécie *Brachycephalus pitanga*. Revista da Estatística da
1261 Universidade Federal de Ouro Preto 3: 374–386.
1262 Taylor, W.R. and Van Dyke, G.C., 1985. Revised procedures for staining and clearing small
1263 fishes and other vertebrates for bone and cartilage study. Cybium 9, 107–19.
1264 Trueb, L. and Lehr, E., 2008. A new species of *Phrynopus* (Anura, Strabomantidae) from
1265 Peru, with comments on the osteology of the genus. Phyllomedusa 7, 11–24.
1266 Vaz-Silva, W., Maciel, N.M., de Andrade, S.P. and Amaro, R.C., 2018. A new cryptic species
1267 of *Oreobates* (Anura: Craugastoridae) from the seasonally dry tropical forest of central
1268 Brazil. Zootaxa 4441, 89–108.
1269 Venegas, P.J., Barboza, A.C., De la Riva, I. and Padial, J.M., 2018. A new species of
1270 *Phrynopus* from the northeastern Andes of Peru, its phylogenetic position, and notes

1271 on the relationships of Holoadeninae (Anura: Craugastoridae). Zootaxa 4446, 501–
1272 524.
1273 von May, R., Lehr, E. and Rabosky, D.L., 2018. Evolutionary radiation of earless frogs in the
1274 Andes: molecular phylogenetics and habitat shifts in high-elevation terrestrial
1275 breeding frogs. PeerJ 6, e4313.
1276 Wever, E.G., 1985. The amphibian ear. (Princeton University Press, 1985).
1277 Wheeler, W.C., 1996. Optimization alignment, the end of multiple sequence alignment in
1278 phylogenetics? Cladistics 12, 1–10.
1279 Wheeler, W.C., 2003. Iterative pass optimization of sequence data. Cladistics 19, 254–260.
1280 Wheeler, W.C., Aagesen, L., Arango, C.P., Faivovich, J., Grant, T., D'haese, C., Janies, D.A.,
1281 Smith, W.L., Varon, A., Giribet, G., 2006. Dynamic homology and phylogenetic
1282 systematics: a unified approach using POY. American Museum of Natural History,
1283 New York, NY. ISBN 0-913424-58-7.
1284 Wheeler, W.C., Lucaroni, N., Hong, L., Crowley, L.M., Varon, A., 2015. POY version 5:
1285 phylogenetic analysis using dynamic homologies under multiple optimality criteria.
1286 Cladistics 31, 189–196.
1287 Wilkinson, M., 2003. Missing entries and multiple trees: instability, relationships, and support
1288 in parsimony analysis. J. Vertebr. Paleontol. 23, 311–323.

1289 **Tables**

1290 **Table 1**. List of character sets sampled for species included in the phylogenetic analysis.

1291 Osteological data were collected from cleared and stained specimens (CS), dry skeletons (DS)

1292 and 3DM models (3DM).

Species	Molecular	External Morphology	Osteology
Barycholos pulcher	x	x	CS
Barycholos ternetzi	x	x	CS
Bryophryne cophites	x	x	CS
"Eleutherodactylus" bilineatus	x	x	CS
Euparkerella brasiliensis	x	x	CS
Haddadus binotatus	x	-	-
Holoaden bradei	x	x	CS
Lynchius flavomaculatus	x	x	CS
Lynchius megacephalus	x	-	Drawing*
Lynchius nebulanastes	x	x	CS
Lynchius oblitus	x	x	-
Lynchius parkeri	x	x	CS
Lynchius simmonsi	x	x	3DM
Lynchius tabaconas	x	x	-
Microkayla guillei	x	x	3DM
Microkayla kempffi	x	x	3DM
Microkayla wettsteini	x	x	CS
Niceforonia brunnea	x	x	3DM
Niceforonia elassodiscus	x	x	3DM
Niceforonia nana	x	x	CS
Niceforonia nigrovittata	x	x	3DM
Niceforonia peraccai	x	x	CS
Noblella heyeri	x	x	CS
Noblella lochites	x	x	3DM
Oreobates amarakaeri	x	x	-
Oreobates antrum	x	x	CS
Oreobates ayacucho	x	x	-
Oreobates barituensis	x	-	-
Oreobates berdemenos	x	x	CS
Oreobates chiquitanus	x	-	CS
Oreobates choristolemma	x	-	-
Oreobates cruralis	x	x	3DM
Oreobates discoidalis	x	x	CS and 3DM
Oreobates gemcare	x	x	-
Oreobates granulosus	x	x	-
Oreobates heterodactylus	x	x	CS
Oreobates ibischi	x	-	-
Oreobates lehri	x	x	3DM
Oreobates lundbergi	x	x	-

Oreobates machiguenga	x	x	3DM
Oreobates madidi	x	-	-
Oreobates pereger	x	x	CS
Oreobates quixensis	x	x	CS
Oreobates remotus	x	-	-
Oreobates sanctaecrucis	x	-	-
Oreobates sanderi	x	x	3DM
Oreobates saxatilis	x	x	-
Oreobates yanucu	x	-	-
Phrynopus auriculatus	x	x	3DM
Phrynopus badius	x	x	-
Phrynopus barthlenae	x	x	-
Phrynopus bracki	x	-	-
Phrynopus bufoides	x	x	-
Phrynopus daemon	x	x	-
Phrynopus dagmarae	x	x	3DM
Phrynopus heimorum	x	x	-
Phrynopus horstpauli	x	x	3DM
Phrynopus interstinctus	x	x	-
Phrynopus inti	x	-	-
Phrynopus juninensis	x	x	CS
Phrynopus kauneorum	x	x	3DM
Phrynopus mariellaleo	x	x	-
Phrynopus miroslawae	x	x	-
Phrynopus montium	x	x	CS
Phrynopus peruanus	x	x	Dry skeleton
Phrynopus pesantesi	x	x	-
Phrynopus sp	x	-	-
Phrynopus sp. 1	x	-	-
Phrynopus sp. 2	x	-	-
Phrynopus sp. 3	x	-	-
Phrynopus sp. 4	x	-	-
Phrynopus sp. 5	x	-	-
Phrynopus spI	x	-	-
Phrynopus tautzorum	x	x	-
Phrynopus thompsoni	-	x	3DM
Phrynopus tribulosus	x	x	3DM
Phrynopus unchog	x	x	-
Phrynopus valquii	x	x	3DM
Phrynopus vestigiatus	x	x	-
Psychrophrynella usurpator	x	x	CS and 3DM
TOTAL	**79**	**61**	**43**

1293

1294 **Table S1**. Taxonomic history of *Phrynopus* since Lynch's (1975) reorganization of the genus.

Reference	Taxonomic acts	Composition of *Phrynopus* after taxonomic acts	N
Lynch 1975	Redefines the genus *Phrynopus*, includes *Niceforonia* and *Noblella* in the synonym of the genus, and describes four new species: *P. brunneus*, *P. cophite*s, *P. parkeri*, and *P. pereger*	*P. brunneus, P. columbianus, P. cophites, P. flavomaculatus, P. laplacai, P. montium, P. nanus, P. parkeri, P. peraccai, P. pereger, P. peruanus, P. peruvianus, P. simonsii,* and *P. wettsteini*	14
Cannatella 1984	Describes two new species: *P. lucida* and *P. nebulanaste*s	*P. brunneus, P. columbianus, P. cophites, P. flavomaculatus, P. laplacai, P. lucida, P. montium, P. nanus, P. nebulanaste*s, *P. parkeri, P. peraccai, P. pereger, P. peruanus, P. peruvianus, P. simonsii,* and *P. wettsteini*	16
Cannatella 1985	Transfers *Telmatobius juninensis* to *Phrynopus*	*P. brunneus, P. columbianus, P. cophites, P. flavomaculatus, P. juninensis, P. laplacai, P. lucida, P. montium, P. nanus, P. nebulanaste*s, *P. parkeri, P. peraccai, P. pereger, P. peruanus, P. peruvianus, P. simonsii,* and *P. wettsteini*	17
Lynch 1986	Describes *P. bagrecito*	*P. bagrecito, P. brunneus, P. columbianus, P. cophites, P. flavomaculatus, P. juninensis, P. laplacai, P. lucida, P. montium, P. nanus, P. nebulanaste*s, *P. parkeri, P. peraccai, P. pereger, P. peruanus, P. peruvianus, P. simonsii,* and *P. wettsteini*	18

Hedges 1990	Describes *P. bracki*	*P. bagrecito, P. bracki, P. brunneus, P. columbianus, P. cophites, P. flavomaculatus, P. juninensis, P. laplacai, P. lucida, P. montium, P. nanus, P. nebulanaste*s, *P. parkeri, P. peraccai, P. pereger, P. peruanus, P. peruvianus, P. simonsii,* and *P. wettsteini*	19
De la Riva 1992	Describes *P. kempffi*	*P. bagrecito, P. bracki, P. brunneus, P. columbianus, P. cophites, P. flavomaculatus, P. juninensis, P. kempffi, P. laplacai, P. lucida, P. montium, P. nanus, P. nebulanaste*s, *P. parkeri, P. peraccai, P. pereger, P. peruanus, P. peruvianus, P. simonsii,* and *P. wettsteini*	20
Ardila-Robayo et al. 1996	Describe *P. adenobrachius*	*P. adenobrachius, P. bagrecito, P. bracki, P. brunneus, P. columbianus, P. cophites, P. flavomaculatus, P. juninensis, P. kempffi, P. laplacai, P. lucida, P. montium, P. nanus, P. nebulanaste*s, *P. parkeri, P. peraccai, P. pereger, P. peruanus, P. peruvianus, P. simonsii,* and *P. wettsteini*	21
Harvey and Ergueta-Sandoval 1998	Describe *P. pinguis*	*P. adenobrachius, P. bagrecito, P. bracki, P. brunneus, P. columbianus, P. cophites, P. flavomaculatus, P. juninensis, P. kempffi, P. laplacai, P. lucida, P. montium, P. nanus, P. nebulanaste*s, *P. parkeri, P. peraccai, P. pereger, P. peruanus, P. peruvianus, P. pinguis, P. simonsii,* and *P. wettsteini*	22
Duellman 2000	Describes *P. fallaciosus, P. spectabilis,* and *P. thompsoni*	*P. adenobrachius, P. bagrecito, P. bracki, P. brunneus, P. columbianus, P. cophites, P. fallaciosus, P. flavomaculatus, P. juninensis, P. kempffi, P. laplacai, P. lucida, P. montium, P. nanus, P. nebulanaste*s, *P. parkeri, P. peraccai, P. pereger, P. peruanus, P. peruvianus, P. pinguis, P. simonsii, P. spectabilis, P. thompsoni,* and *P. wettsteini*	25

Lehr et al. 2000	Describe *P. horstpauli*	*P. adenobrachius, P. bagrecito, P. bracki, P. brunneus, P. columbianus, P. cophites, P. fallaciosus, P. flavomaculatus, P. horstpauli, P. juninensis, P. kempffi, P. laplacai, P. lucida, P. montium, P. nanus, P. nebulanaste*s, *P. parkeri, P. peraccai, P. pereger, P. peruanus, P. peruvianus, P. pinguis, P. simonsii, P. spectabilis, P. thompsoni,* and *P. wettsteini*	26
Aguayo-Vedia and Harvey 2001	Describe *P. adenopleurus* and *P. iatamasi*	*P. adenobrachius, P. adenopleurus, P. bagrecito, P. bracki, P. brunneus, P. columbianus, P. cophites, P. fallaciosus, P. flavomaculatus, P. horstpauli, P. iatamasi, P. juninensis, P. kempffi, P. laplacai, P. lucida, P. montium, P. nanus, P. nebulanaste*s, *P. parkeri, P. peraccai, P. pereger, P. peruanus, P. peruvianus, P. pinguis, P. simonsii, P. spectabilis, P. thompsoni,* and *P. wettsteini*	28
Lehr 2001	Describes *P. heimorum*	*P. adenobrachius, P. adenopleurus, P. bagrecito, P. bracki, P. brunneus, P. columbianus, P. cophites, P. fallaciosus, P. flavomaculatus, P. heimorum, P. horstpauli, P. iatamasi, P. juninensis, P. kempffi, P. laplacai, P. lucida, P. montium, P. nanus, P. nebulanaste*s, *P. parkeri, P. peraccai, P. pereger, P. peruanus, P. peruvianus, P. pinguis, P. simonsii, P. spectabilis, P. thompsoni,* and *P. wettsteini*	29
Lehr et al. 2002a	Describe *P. dagmarae* and *P. kauneorum*	*P. adenobrachius, P. adenopleurus, P. bagrecito, P. bracki, P. brunneus, P. columbianus, P. cophites, P. dagmarae, P. fallaciosus, P. flavomaculatus, P. heimorum, P. horstpauli, P. iatamasi, P. juninensis, P. kauneorum, P. kempffi, P. laplacai, P. lucida, P. montium, P. nanus, P. nebulanaste*s, *P. parkeri, P. peraccai, P. pereger, P. peruanus, P. peruvianus, P. pinguis, P. simonsii, P. spectabilis, P. thompsoni,* and *P. wettsteini*	31

Lehr and Aguilar 2002	Describe *P. barthlenae*	*P. adenobrachius, P. adenopleurus, P. bagrecito, P. barthlenae, P. bracki, P. brunneus, P. columbianus, P. cophites, P. dagmarae, P. fallaciosus, P. flavomaculatus, P. heimorum, P. horstpauli, P. iatamasi, P. juninensis, P. kauneorum, P. kempffi, P. laplacai, P. lucida, P. montium, P. nanus, P. nebulanaste*s, *P. parkeri, P. peraccai, P. pereger, P. peruanus, P. peruvianus, P. pinguis, P. simonsii, P. spectabilis, P. thompsoni,* and *P. wettsteini*	32
Lehr et al. 2002b	Describe *P. carpish*	*P. adenobrachius, P. adenopleurus, P. bagrecito, P. barthlenae, P. bracki, P. brunneus, P. carpish, P. columbianus, P. cophites, P. dagmarae, P. fallaciosus, P. flavomaculatus, P. heimorum, P. horstpauli, P. iatamasi, P. juninensis, P. kauneorum, P. kempffi, P. laplacai, P. lucida, P. montium, P. nanus, P. nebulanaste*s, *P. parkeri, P. peraccai, P. pereger, P. peruanus, P. peruvianus, P. pinguis, P. simonsii, P. spectabilis, P. thompsoni,* and *P. wettsteini*	33
Lehr and Aguilar 2003	Describe *P. tautzorum*	*P. adenobrachius, P. adenopleurus, P. bagrecito, P. barthlenae, P. bracki, P. brunneus, P. carpish, P. columbianus, P. cophites, P. dagmarae, P. fallaciosus, P. flavomaculatus, P. heimorum, P. horstpauli, P. iatamasi, P. juninensis, P. kauneorum, P. kempffi, P. laplacai, P. lucida, P. montium, P. nanus, P. nebulanaste*s, *P. parkeri, P. peraccai, P. pereger, P. peruanus, P. peruvianus, P. pinguis, P. simonsii, P. spectabilis, P. tautzorum, P. thompsoni,* and *P. wettsteini*	34

Lehr 2005	Transfers *P. lucida* and *P. nebulanastes* to *Eleutherodactylus*	*P. adenobrachius, P. adenopleurus, P. bagrecito, P. barthlenae, P. bracki, P. brunneus, P. carpish, P. columbianus, P. cophites, P. dagmarae, P. fallaciosus, P. flavomaculatus, P. heimorum, P. horstpauli, P. iatamasi, P. juninensis, P. kauneorum, P. kempffi, P. laplacai, P. montium, P. nanus, P. parkeri, P. peraccai, P. pereger, P. peruanus, P. peruvianus, P. pinguis, P. simonsii, P. spectabilis, P. tautzorum, P. thompsoni,* and *P. wettsteini*	32
Lehr et. al. 2005a	Transfer *P. simonsii* to *Eleutherodactylus* and remove *P. carpish* from *Phrynopus*	*P. adenobrachius, P. adenopleurus, P. bagrecito, P. barthlenae, P. bracki, P. brunneus, P. columbianus, P. cophites, P. dagmarae, P. fallaciosus, P. flavomaculatus, P. heimorum, P. horstpauli, P. iatamasi, P. juninensis, P. kauneorum, P. kempffi, P. laplacai, P. montium, P. nanus, P. parkeri, P. peraccai, P. pereger, P. peruanus, P. peruvianus, P. pinguis, P. spectabilis, P. tautzorum, P. thompsoni,* and *P. wettsteini*	30
Lehr et al. 2005b	Describe *P. bufoides*, *P. paucari* and *P. pesantesi*	*P. adenobrachius, P. adenopleurus, P. bagrecito, P. barthlenae, P. bracki, P. brunneus, P. bufoides, P. columbianus, P. cophites, P. dagmarae, P. fallaciosus, P. flavomaculatus, P. heimorum, P. horstpauli, P. iatamasi, P. juninensis, P. kauneorum, P. kempffi, P. laplacai, P. montium, P. nanus, P. parkeri, P. paucari, P. peraccai, P. pereger, P. peruanus, P. peruvianus, P. pesantesi, P. pinguis, P. spectabilis, P. tautzorum, P. thompsoni,* and *P. wettsteini*	33

Lehr 2006	Describes *P. boettgeri;* transfers *P. flavomaculatus* and *P. fallaciosus* to *Eleutherodactylus*; transfers *P. spectabilis* to *Pleurodema*; includes *P. laplacai* in the synonym of *P. wettsteini*	*P. adenobrachius, P. adenopleurus, P. bagrecito, P. barthlenae, P. boettgeri, P. bracki, P. brunneus, P. bufoides, P. columbianus, P. cophites, P. dagmarae, P. heimorum, P. horstpauli, P. iatamasi, P. juninensis, P. kauneorum, P. kempffi, P. montium, P. nanus, P. parkeri, P. paucari, P. peraccai, P. pereger, P. peruanus, P. peruvianus, P. pesantesi, P. pinguis, P. tautzorum, P. thompsoni,* and *P. wettsteini*	30
Lehr and Aguilar 2006	Transfer *P. pereger* to *Eleutherodactylus*	*P. adenobrachius, P. adenopleurus, P. bagrecito, P. barthlenae, P. boettgeri, P. bracki, P. brunneus, P. bufoides, P. columbianus, P. cophites, P. dagmarae, P. heimorum, P. horstpauli, P. iatamasi, P. juninensis, P. kauneorum, P. kempffi, P. montium, P. nanus, P. parkeri, P. paucari, P. peraccai, P. peruanus, P. peruvianus, P. pesantesi, P. pinguis, P. tautzorum, P. thompsoni,* and *P. wettsteini*	29
Lehr 2007	Describes *P. kotosh*, *P. oblivius*, and *P. ayacucho*	*P. adenobrachius, P. adenopleurus, P. ayacucho, P. bagrecito, P. barthlenae, P. boettgeri, P. bracki, P. brunneus, P. bufoides, P. columbianus, P. cophites, P. dagmarae, P. heimorum, P. horstpauli, P. iatamasi, P. juninensis, P. kauneorum, P. kempffi, P. kotosh*, *P. montium, P. nanus, P. oblivius*, *P. parkeri, P. paucari, P. peraccai, P. peruanus, P. peruvianus, P. pesantesi, P. pinguis, P. tautzorum, P. thompsoni,* and *P. wettsteini*	32

Heinicke et al. 2007	Remove *P. brunneus* and *P. peraccai* from *Phrynopus*	*P. adenobrachius, P. adenopleurus, P. ayacucho, P. bagrecito, P. barthlenae, P. boettgeri, P. bracki, P. bufoides, P. columbianus, P. cophites, P. dagmarae, P. heimorum, P. horstpauli, P. iatamasi, P. juninensis, P. kauneorum, P. kempffi, P. kotosh*, *P. montium, P. nanus, P. oblivius*, *P. parkeri, P. paucari, P. peruanus, P. peruvianus, P. pesantesi, P. pinguis, P. tautzorum, P. thompsoni,* and *P. wettsteini*	30
De la Riva 2007	Describes *P. ankohuma, P. chacaltaya, P. condoriri, P. guillei, P. harveyi, P. iani, P. illampu, P. illimani, P. kallawaya, P. katantika, P. quimsacruzis*, and *P. saltator*	*P. adenobrachius, P. adenopleurus, P. ankohuma, P. ayacucho, P. bagrecito, P. barthlenae, P. boettgeri, P. bracki, P. bufoides, P. chacaltaya, P. columbianus, P. condoriri, P. cophites, P. dagmarae, P. guillei, P. harveyi, P. heimorum, P. horstpauli, P. iani, P. iatamasi, P. illampu, P. illimani, P. juninensis, P. kallawaya, P. katantika, P. kauneorum, P. kempffi, P. kotosh*, *P. montium, P. nanus, P. oblivius*, *P. parkeri, P. paucari, P. peruanus, P. peruvianus, P. pesantesi, P. pinguis, P. quimsacruzis*, *P. saltator*, *P. tautzorum, P. thompsoni,* and *P. wettsteini*	42
Chaparro et al. 2007	Describe *P. bustamantei*	*P. adenobrachius, P. adenopleurus, P. ankohuma, P. ayacucho, P. bagrecito, P. barthlenae, P. boettgeri, P. bracki, P. bufoides, P. bustamantei*, *P. chacaltaya, P. columbianus, P. condoriri, P. cophites, P. dagmarae, P. guillei, P. harveyi, P. heimorum, P. horstpauli, P. iani, P. iatamasi, P. illampu, P. illimani, P. juninensis, P. kallawaya, P. katantika, P. kauneorum, P. kempffi, P. kotosh*, *P. montium, P. nanus, P. oblivius*, *P. parkeri, P. paucari, P. peruanus, P. peruvianus, P. pesantesi, P. pinguis, P. quimsacruzis*, *P. saltator*, *P. tautzorum, P. thompsoni,* and *P. wettsteini*	43

De la Riva et al. 2008	Remove *Noblella* from the synonym of *Phrynopus*, transferring *P. peruvianus* to *Noblella*	*P. adenobrachius, P. adenopleurus, P. ankohuma, P. ayacucho, P. bagrecito, P. barthlenae, P. boettgeri, P. bracki, P. bufoides, P. bustamantei*, *P. chacaltaya, P. columbianus, P. condoriri, P. cophites, P. dagmarae, P. guillei, P. harveyi, P. heimorum, P. horstpauli, P. iani, P. iatamasi, P. illampu, P. illimani, P. juninensis, P. kallawaya, P. katantika, P. kauneorum, P. kempffi, P. kotosh*, *P. montium, P. nanus, P. oblivius*, *P. parkeri, P. paucari, P. peruanus, P. pesantesi, P. pinguis, P. quimsacruzis*, *P. saltator*, *P. tautzorum, P. thompsoni,* and *P. wettsteini*	42
Duellman and Hedges 2008	Describe *P. auriculatus* and *P. tribulosus*. Also define *Phrynopus sensu stricto*	*P. adenobrachius, P. adenopleurus, P. ankohuma, P. auriculatus, P. ayacucho, P. bagrecito, P. barthlenae, P. boettgeri, P. bracki, P. bufoides, P. bustamantei*, *P. chacaltaya, P. columbianus, P. condoriri, P. cophites, P. dagmarae, P. guillei, P. harveyi, P. heimorum, P. horstpauli, P. iani, P. iatamasi, P. illampu, P. illimani, P. juninensis, P. kallawaya, P. katantika, P. kauneorum, P. kempffi, P. kotosh*, *P. montium, P. nanus, P. oblivius*, *P. parkeri, P. paucari, P. peruanus, P. pesantesi, P. pinguis, P. quimsacruzis*, *P. saltator*, *P. tautzorum, P. thompsoni, P. tribulosus*, and *P. wettsteini*	44

Hedges et al. 2008	Transfer *P. bustamantei* and *P. cophites* to *Bryophryne*; *P. adenobrachius*, *P. columbianus*, and *P. nanus* to *Hypodactylus* (now *Niceforonia*); *P. parkeri* to *Lynchius*; *P. adenopleurus, P. ankohuma, P. bagrecito, P. boettgeri, P. chacaltaya, P. condoriri, P. guillei, P. harveyi, P. iani, P. iatamasi, P. illampu, P. illimani, P. kallawaya, P. katantika, P. kempffi, P. quimsacruzis, P. saltator, P. pinguis,* and *P. wettsteini* to *Psychrophrynella*	*P. auriculatus, P. ayacucho, P. barthlenae, P. bracki, P. bufoides, P. dagmarae, P. heimorum, P. horstpauli, P. juninensis, P. kauneorum, P. kotosh*, *P. montium, P. oblivius*, *P. paucari, P. peruanus, P. pesantesi, P. tautzorum, P. thompsoni, P. tribulosus*, *Phrynopus* sp. 1, and *Phrynopus* sp. 2	21
Chaparro et al. 2008	Describe *P. miroslawae* and *P. nicoleae* (*Phrynopus* sp. 1 and *Phrynopus* sp. 2 from Hedges et al. 2008)	*P. auriculatus, P. ayacucho, P. barthlenae, P. bracki, P. bufoides, P. dagmarae, P. heimorum, P. horstpauli, P. juninensis, P. kauneorum, P. kotosh*, *P. miroslawae, P. montium, P. nicoleae, P. oblivius*, *P. paucari, P. peruanus, P. pesantesi, P. tautzorum, P. thompsoni,* and *P. tribulosus*	21
Trueb and Lehr 2008	Describe *P. lechriorhynchus*	*P. auriculatus, P. ayacucho, P. barthlenae, P. bracki, P. bufoides, P. dagmarae, P. heimorum, P. horstpauli, P. juninensis, P. kauneorum, P. kotosh*, *P. lechriorhynchus, P. miroslawae, P. montium, P. nicoleae, P. oblivius*, *P. paucari, P. peruanus, P. pesantesi, P. tautzorum, P. thompsoni,* and *P. tribulosus*	22

Padial et al. 2012	Transfer *P. ayacucho* to *Oreobates*	*P. auriculatus, P. barthlenae, P. bracki, P. bufoides, P. dagmarae, P. heimorum, P. horstpauli, P. juninensis, P. kauneorum, P. kotosh*, *P. lechriorhynchus, P. miroslawae, P. montium, P. nicoleae, P. oblivius*, *P. paucari, P. peruanus, P. pesantesi, P. tautzorum, P. thompsoni,* and *P. tribulosus*	21
Lehr and Oroz 2012	Describe *P. interstinctus* and *P. vestigiatus*	*P. auriculatus, P. barthlenae, P. bracki, P. bufoides, P. dagmarae, P. heimorum, P. horstpauli, P. interstinctus, P. juninensis, P. kauneorum, P. kotosh*, *P. lechriorhynchus, P. miroslawae, P. montium, P. nicoleae, P. oblivius*, *P. paucari, P. peruanus, P. pesantesi, P. tautzorum, P. thompsoni, P. tribulosus*, and *P. vestigiatus*	23
Lehr et al. 2012	Describe *P. badius* and *P. curator*	*P. auriculatus, P. badius*, *P. barthlenae, P. bracki, P. bufoides, P. curator*, *P. dagmarae, P. heimorum, P. horstpauli, P. interstinctus, P. juninensis, P. kauneorum, P. kotosh*, *P. lechriorhynchus, P. miroslawae, P. montium, P. nicoleae, P. oblivius*, *P. paucari, P. peruanus, P. pesantesi, P. tautzorum, P. thompsoni, P. tribulosus*, and *P. vestigiatus*	25
Mamani and Malqui 2014	Describe *P. chaparroi*	*P. auriculatus, P. badius*, *P. barthlenae, P. bracki, P. bufoides, P. chaparroi, P. curator*, *P. dagmarae, P. heimorum, P. horstpauli, P. interstinctus, P. juninensis, P. kauneorum, P. kotosh*, *P. lechriorhynchus, P. miroslawae, P. montium, P. nicoleae, P. oblivius*, *P. paucari, P. peruanus, P. pesantesi, P. tautzorum, P. thompsoni, P. tribulosus*, and *P. vestigiatus*	26

Chavez et al. 2015	Describe *P. daemon* and *P. valquii*	*P. auriculatus, P. badius*, *P. barthlenae, P. bracki, P. bufoides, P. chaparroi, P. curator*, *P. daemon, P. dagmarae, P. heimorum, P. horstpauli, P. interstinctus, P. juninensis, P. kauneorum, P. kotosh*, *P. lechriorhynchus, P. miroslawae, P. montium, P. nicoleae, P. oblivius*, *P. paucari, P. peruanus, P. pesantesi, P. tautzorum, P. thompsoni, P. tribulosus*, *P. valquii*, and *P. vestigiatus*	28
Rodriguez and Catenazzi 2017	Describe *P. anancites*, *P. capitalis*, *P. dumicola* and *P. personatus*	*P. anancites*, *P. auriculatus, P. badius*, *P. barthlenae, P. bracki, P. bufoides, P. capitalis*, *P. chaparroi, P. curator*, *P. daemon, P. dagmarae, P. dumicola, P. heimorum, P. horstpauli, P. interstinctus, P. juninensis, P. kauneorum, P. kotosh*, *P. lechriorhynchus, P. miroslawae, P. montium, P. nicoleae, P. oblivius*, *P. paucari, P. personatus, P. peruanus, P. pesantesi, P. tautzorum, P. thompsoni, P. tribulosus*, *P. valquii*, and *P. vestigiatus*	32
Lehr et al. 2017	Describe *P. inti*	*P. anancites*, *P. auriculatus, P. badius*, *P. barthlenae, P. bracki, P. bufoides, P. capitalis*, *P. chaparroi, P. curator*, *P. daemon, P. dagmarae, P. dumicola, P. heimorum, P. horstpauli, P. interstinctus, P. inti, P. juninensis, P. kauneorum, P. kotosh*, *P. lechriorhynchus, P. miroslawae, P. montium, P. nicoleae, P. oblivius*, *P. paucari, P. personatus, P. peruanus, P. pesantesi, P. tautzorum, P. thompsoni, P. tribulosus*, *P. valquii*, and *P. vestigiatus*	33

Lehr and Rodriguez 2017	Describe *P. lapidoides* and *P. unchog*	*P. anancites*, *P. auriculatus, P. badius*, *P. barthlenae, P. bracki, P. bufoides, P. capitalis*, *P. chaparroi, P. curator*, *P. daemon, P. dagmarae, P. dumicola, P. heimorum, P. horstpauli, P. interstinctus, P. inti, P. juninensis, P. kauneorum, P. kotosh*, *P. lapidoides*, *P. lechriorhynchus, P. miroslawae, P. montium, P. nicoleae, P. oblivius*, *P. paucari, P. personatus, P. peruanus, P. pesantesi, P. tautzorum, P. thompsoni, P. tribulosus*, *P. unchog*, *P. valquii*, and *P. vestigiatus*	35
Von May et al. 2018	Include *P. curator* and *P. nicoleae* in the synonym of *P. tribulosus*	*P. anancites*, *P. auriculatus, P. badius*, *P. barthlenae, P. bracki, P. bufoides, P. capitalis*, *P. chaparroi, P. daemon, P. dagmarae, P. dumicola, P. heimorum, P. horstpauli, P. interstinctus, P. inti, P. juninensis, P. kauneorum, P. kotosh*, *P. lapidoides*, *P. lechriorhynchus, P. miroslawae, P. montium, P. oblivius*, *P. paucari, P. personatus, P. peruanus, P. pesantesi, P. tautzorum, P. thompsoni, P. tribulosus*, *P. unchog*, *P. valquii*, and *P. vestigiatus*	33
Venegas et al. 2018	Describe *P. mariellaleo*	*P. anancites*, *P. auriculatus, P. badius*, *P. barthlenae, P. bracki, P. bufoides, P. capitalis*, *P. chaparroi, P. daemon, P. dagmarae, P. dumicola, P. heimorum, P. horstpauli, P. interstinctus, P. inti, P. juninensis, P. kauneorum, P. kotosh*, *P. lapidoides*, *P. lechriorhynchus, P. mariellaleo, P. miroslawae, P. montium, P. oblivius*, *P. paucari, P. personatus, P. peruanus, P. pesantesi, P. tautzorum, P. thompsoni, P. tribulosus*, *P. unchog*, *P. valquii*, and *P. vestigiatus*	34

Chavez et al. 2020	Describe *P. remotum*	*P. anancites*, *P. auriculatus, P. badius*, *P. barthlenae, P. bracki, P. bufoides, P. capitalis*, *P. chaparroi, P. daemon, P. dagmarae, P. dumicola, P. heimorum, P. horstpauli, P. interstinctus, P. inti, P. juninensis, P. kauneorum, P. kotosh*, *P. lapidoides*, *P. lechriorhynchus, P. mariellaleo, P. miroslawae, P. montium, P. oblivius*, *P. paucari, P. personatus, P. peruanus, P. pesantesi, P. remotum, P. tautzorum, P. thompsoni, P. tribulosus*, *P. unchog*, *P. valquii*, and *P. vestigiatus*	35

References for this section:

Aguayo-Vedia, C.R. and Harvey, M.B., 2001. Dos nuevas especies de *Phrynopus* (Anura: Leptodactylidae) de los bosques nublados de Bolivia. Rev. Biol. Trop. 49, 333–345.

Ardila-Robayo, M.C., Ruiz-Carranza, P.M. and Barrera-Rodriguez, M., 1996. Una nueva especie de *Phrynopus* (Amphibia, Anura, Leptodactylidae) de La Cordillera Central Colombiana. Lozania. Bogotá 67, 1–10.

Cannatella, D.C., 1984. Two new species of the leptodactylid frog genus *Phrynopus*, with comments on the phylogeny of the genus. Occas. Pap. Mus. Nat. Hist. Univ. Kans. 113, 1–16.

Cannatella, D.C., 1985. The systematic status of *Syrrhophus juninensis* Shreve (Anura: Leptodactylidae). Proc. Biol. Soc. Wash. 98, 774–777.

Chaparro, J.C., De la Riva, I., Padial, J.M., Ochoa, J.A. and Lehr, E., 2007. A new species of *Phrynopus* from Departamento Cusco, southern Peru (Anura: Brachycephalidae). Zootaxa 1618, 61–68.

Chaparro, J.C., Padial, J.M. and De la Riva, I., 2008. Two sympatric new species of *Phrynopus* (Anura: Strabomantidae) from Yanachaga Chemillen National Park (central Peruvian Andes). Zootaxa 1761, 49–58.

Chávez, G., Santa Cruz, R., Rodríguez, D. and Lehr, E., 2015. Two new species of frogs of the genus *Phrynopus* (Anura: Terrarana: Craugastoridae) from the Peruvian Andes. Amphib. Reptile Conserv. 9, 15–25.

Chávez, G., García Ayachi, L.A. and Catenazzi, A., 2020. A new species of frog (Terrarana, Strabomantidae, *Phrynopus*) from the Peruvian Andean grasslands. PeerJ 8 (e9433), 1–14.

De la Riva, I., 1992. A new species of *Phrynopus* from Bolivia (Anura: Leptodactylidae). Herpetologica 48, 111–114.

De la Riva, I., 2007. Bolivian frogs of the genus *Phrynopus*, with the description of twelve new species (Anura: Brachycephalidae). Herpetol. Monogr. 21, 241–277.

De la Riva, I., Chaparro, J.C. and Padial, J.M., 2008. The taxonomic status of *Phyllonastes* Heyer and *Phrynopus peruvianus* (Noble) (Lissamphibia, Anura): resurrection of *Noblella* Barbour. Zootaxa 1685, 67–68.

1317 Duellman, W.E., 2000. Leptodactylid frogs of the genus *Phrynopus* in northern Peru with descriptions of three new species. Herpetologica 56,
1318 273–285.
1319 Duellman, W.E. and Hedges, S. B., 2008. Two minute species of *Phrynopus* (Lissamphibia: Anura) from the Cordillera Oriental in Peru.
1320 Zootaxa 1675, 59–66.
1321 Harvey, M.B. and Ergueta-Sandoval, P., 1998. A new species of *Phrynopus* (Anura: Leptodactylidae) from elfin forest in the Bolivian Andes. J.
1322 Herpetol. 32: 536–540.
1323 Hedges, S.B., 1990. A new species of *Phrynopus* (Anura: Leptodactylidae). Copeia 1990, 108–112.
1324 Hedges, S.B., Duellman, W.E. and Heinicke, M.P., 2008. New World direct-developing frogs (Anura: Terrarana): Molecular phylogeny,
1325 classification, biogeography, and conservation. Zootaxa 1737, 1–182.
1326 Heinicke, M.P., Duellman, W.E. and Hedges, S.B., 2007. Major Caribbean and Central American frog faunas originated by oceanic dispersal.
1327 Proc. Natl. Acad. Sci. U.S.A. 104, 10092–10097.
1328 Lehr, E., 2001. A new species of *Phrynopus* (Anura: Leptodactylidae) from the eastern Andean slopes of central Peru. Salamandra 37, 11–20.
1329 Lehr, E., 2005. A new species of the *Eleutherodactylus nigrovittatus* group (Anura: Leptodactylidae) from Andean Peru. Herpetologica 61, 199–
1330 208.
1331 Lehr, E., 2006. Taxonomic status of some species of Peruvian *Phrynopus* (Anura: Leptodactylidae), with the description of a new species from
1332 the Andes of southern Peru. Herpetologica 62, 331–347.
1333 Lehr, E., 2007. New eleutherodactyline frogs (Leptodactylidae: Pristimantis, *Phrynopus*) from Peru. B. Mus. Comparat. Zool. Cambridge,
1334 Massachusetts 159, 145–178.
1335 Lehr, E. and Aguilar, C., 2002. A new species of *Phrynopus* (Amphibia, Anura, Leptodactylidae) from the puna of Maraypata (Departamento de
1336 Huanuco, Peru). Zoologische Abhandlungen. Staatliches Museum für Tierkunde in Dresden 52, 57–64.
1337 Lehr, E. and Aguilar, C., 2003. A new species of *Phrynopus* (Amphibia, Anura, Leptodactylidae) from the puna of Maraypata (Departamento de
1338 Huánuco, Peru). Zoologische Abhandlungen. Staatliches Museum für Tierkunde in Dresden 53, 87–92.
1339 Lehr, E. and Aguilar, C., 2006. The taxonomic status of *Phrynopus pereger* Lynch 1975 (Amphibia, Anura, Leptodactylidae). Zootaxa 1284,
1340 53–60.
1341 Lehr, E. and Oróz, A., 2012. Two new species of *Phrynopus* (Anura: Strabomantidae) from the Cordillera de Carpish in central Peru
1342 (Departamento de Huánuco). Zootaxa 3512, 53–63.
1343 Lehr, E. and Rodríguez, D., 2017. Two new species of Andes Frogs (Craugastoridae: *Phrynopus*) from the Cordillera de Carpish in central Peru.
1344 Salamandra 53, 327–338.
1345 Lehr, E., Köhler, G. and Ponce, E., 2000. A new species of *Phrynopus* from Peru (Amphibia, Anura, Leptodactylidae). Senckenbergiana
1346 Biologica 80, 205–212.
1347 Lehr, E., Aguilar, C. and Köhler, G., 2002a. Two sympatric new species of *Phrynopus* (Anura: Leptodactylidae) from a cloud forest in the
1348 Peruvian Andres. J. Herpetol. 36, 208–216.

1349 Lehr, E., Rodríguez, D. and Córdova, J.H., 2002b. A new species of *Phrynopus* (Amphibia, Anura, Leptodactylidae) from the Cordillera de
1350 Carpish (Departamento de Huanuco, Peru). Zoologische Abhandlungen. Staatliches Museum für Tierkunde in Dresden 52, 65–70.
1351 Lehr, E., Müller, A. and Fritzsch, G., 2005a. Analysis of Andes frogs (*Phrynopus*, Leptodactylidae, Anura) phylogeny based on 12S and 16S
1352 mitochondrial rDNA sequences. Zool. Scr. 34, 593–603.
1353 Lehr, E., Lundberg, M. and Aguilar, C., 2005b. Three new species of *Phrynopus* from central Peru (Amphibia: Anura: Leptodactylidae). Copeia
1354 2005, 479–491.
1355 Lehr, E., Moravec, J. and Cusi, J.C., 2012. Two new species of *Phrynopus* (Anura, Strabomantidae) from high elevations in the Yanachaga-
1356 Chemillén National park in Peru (Departamento de Pasco). ZooKeys 235, 51–71.
1357 Lehr, E., von May, R., Moravec, J. and Cusi, J.C., 2017. A new species of *Phrynopus* (Amphibia, Anura, Craugastoridae) from upper montane
1358 forests and high Andean grasslands of the Pui Pui Protected Forest in central Peru. ZooKeys 713, 131–157.
1359 Lynch, J.D., 1975. A review of the Andean leptodactylid frog genus *Phrynopus*. Occas. pap. Mus. Nat. Hist. 35, 1–51.
1360 Lynch, J.D., 1986. New species of minute leptodactylid frogs from the Andes of Ecuador and Peru. J. Herpetol. 20, 423–431.
1361 Mamani, L. and Malqui, S., 2014. A new species of *Phrynopus* (Anura: Craugastoridae) from the central Peruvian Andes. Zootaxa 3838, 207–
1362 214.
1363 Padial, J.M., Chaparro, J.C., Castroviejo-Fisher, S., Guayasamín, J.M., Lehr, E., Delgado, A.J., Vaira, M., Teixeira, Jr, M., Aguayo, R. and De la
1364 Riva, I., 2012. A revision of species diversity in the Neotropical genus *Oreobates* (Anura: Strabomantidae), with the description of three
1365 new species from the Amazonian slopes of the Andes, and the proposal of candidate species. Am. Mus. Novit. 3752, 1–55.
1366 Rodríguez, L.O. and Catenazzi, A., 2017. Four new species of terrestrial-breeding frogs of the genus *Phrynopus* (Anura: Terrarana:
1367 Craugastoridae) from Río Abiseo National Park, Peru. Zootaxa 4273, 381–406.
1368 Trueb, L. and Lehr, E., 2008. A new species of *Phrynopus* (Anura, Strabomantidae) from Peru, with comments on the osteology of the genus.
1369 Phyllomedusa 7, 11–24.
1370 Venegas, P.J., Barboza, A.C., De la Riva, I. and Padial, J.M., 2018. A new species of *Phrynopus* from the northeastern Andes of Peru, its
1371 phylogenetic position, and notes on the relationships of Holoadeninae (Anura: Craugastoridae). Zootaxa 4446, 501–524.
1372 von May, R., Lehr, E. and Rabosky, D.L., 2018. Evolutionary radiation of earless frogs in the Andes: molecular phylogenetics and habitat shifts
1373 in high-elevation terrestrial breeding frogs. PeerJ 6, e4313.

Table S2. Primers used to amplify mitochondrial and nuclear genes fragments.

Gene fragment	Primer name	Direction	Primer sequence (5' to 3')	Reference
12S-tRNAval-16S	MVZ59	Forward	ATAGCACGTAAAAYGCTDAGATG	Graybeal, 1997
	tRNA-VAl	Reverse	GGTGTAAGCGARAGGCTTTKGTTAAG	Goebel et al., 1999
	12S-L13	Forward	TTAGAAGAGGCAAGTCGTAACATGGTA	Feller and Hedges, 1998
	16S-H10	Reverse	TGCTTACGCTACCTTTGCACGGT	Hedges, 1994
	16Sa-L	Forward	CGCCTGTTTATCAAAAACAT	Palumbi et al., 2002
	16Sb-H	Reverse	CCCGTCTGAACTCAGATCACGT	Palumbi et al., 2002
COI	AnF1 (T3)	Forward	ACHAAYCAYAAAGAYATYGG	Lyra et al., 2017
	AnR1 (T7)	Reverse	CCRAARAATCARAADARRTGTTG	Lyra et al., 2017
RAG-1	R1-GFF	Forward	GAGAAGTCTACAAAAAVGGCAAAG	Faivovich et al., 2005
	R1-GFR	Reverse	GAAGCGCCTGAACAGTTTATTAC	Faivovich et al., 2005
TYR	Tyr1C	Forward	GGCAGAGGAWCRTGCCAAGATGT	Bossuyt and Milinkovitch, 2000
	Tyr1G	Reverse	TGCTGGCRTCTCTCCARTCCCA	Bossuyt and Milinkovitch, 2000

References for this section:

Bossuyt, F. and Milinkovitch, M.C., 2000. Convergent adaptive radiations in Madagascan and Asian ranid frogs reveal covariation between larval and adult traits. Proc. Natl Acad. Sci. USA 97, 6585–6590.

Faivovich, J., Haddad, C.F.B., Garcia, P.C.A., Frost, D.R., Campbell, J.A. and Wheeler, W.C., 2005. Systematic review of the frog family Hylidae, with special reference to Hylinae: phylogenetic analysis and taxonomic revision. Bull. Am. Mus. Nat. Hist. 294, 1–240.

Feller, A.E. and Hedges, S.B., 1998. Molecular evidence for the early history of living amphibians. Mol. Phylogenetics Evol. 9, 509–516.

Graybeal, A., 1997. Phylogenetic relationships of bufonid frogs and tests of alternate macroevolutionary hypothesis characterizing their radiation. Zool. J. Linn. Soc. 119, 297–338.

Goebel, A.M., J.M. Donnelly, and M.E. Atz. 1999. PCR primers and amplification methods for 12S ribosomal DNA, the control region, cytochrome oxidase I, and cytochrome b in bufonids and other frogs, and an overview of PCR primers which have amplified DNA in amphibians successfully. Mol. Phylogenetics Evol. 11, 163–199.

Lyra, M.L., Haddad, C.F.B., de Azeredo-Espin, A.M.L., 2017. Meeting the challenge of DNA barcoding Neotropical amphibians: polymerase chain reaction optimization and new COI primers. Mol. Ecol. Resour. 17, 966–980.

Palumbi, S.R., Martins, A., Romano, S., Mc-Millan, W.O., Stice, L. and Grabawski, G., 2002. The Simple fool's guide to PCR, version 2.0. Department of Zoology and Kewalo Marine Laboratory, University of Hawaii, Honolulu. Privately published, compiled by S. Palumbi.

Figures

Figure 1. Living specimens of 18 species of *Phrynopus*: (A) *P. anancites*, (B) *P. badius*, (C) *P. barthlenae*, (D) *P. dagmarae*, (E) *P. dumicola*, (F) *P. heimorum*, (G) *P. horstpauli*, (H) *P. inti*, (I) *P. kauneorum*, (J) *P. mariellaleo*, (K) *P. miroslawae*, (L) *P. oblivius*, (M) *P. personatus*, (N) *P. peruanus*, (O) *P. pesantesi*, (P) *P. tautzorum*, (Q) *P. tribulosus*, and (R) *P. valquii*. Photos by E. Lehr (B, C, D, F, G, H, I, L, N, O, P, Q), A. Catenazzi (A, E, M); P. Venegas (J); J.C. Chaparro (K); G. Chávez (R).

Figure 2. Map of Peru showing the type location of species of *Phrynopus*. (1) *P. mariellaleo*; (2) *P. thompsoni*; (3) *P. capitalis*, *P. dumicola*, *P. personatus*; (4) *P. anancites*, *P. valquii*; (5) *P. remotum*; (6) *P. daemon*; (7) *P. lapioides*, *P. unchog*; (8).*P. lechryorhyncus*, *P. vestigiatus*; (9) *P. heimorum*, *P. horstpauli*; (10) *P. interstinctus*; (11) *P. kotosh*; (12) *P. dagmarae*, *P. kauneorum*; (13) *P. barthlanae*, *P. tautzorum*; (14) *P. miroslawae*; (15) *P. badius*; (16) *P. auriculatus*, *P. bracki*, *P. tribulosus*,; (17) *P. pesantesi*; (18) *P. bufoides*, *P. paucari*; (19) *P. juninensis*, *P. montium*; (20) *P. oblivius*, *P. peruanus*; (21) *P. inti*; (22) *P. chaparroi*.

Figure 3. (A) Strict consensus of 2 most parsimonious trees of 12,491 transformations for the total evidence analyses. (B) Maximum parsimony optimal tree of 12,479 transformations for the analyses excluding *Phrynopus thompsoni*. Numbers above branches indicate Goodman–Bremer values, and those under branches are Jackknife proportions.

Figure 4. Ancestral character states reconstructions of characters 74, 75, and 6 (from left to right) over one of the optimal phylogenetic hypotheses of Holoadeninae relationships. Reconstructions on the other optimal hypotheses are identical to the one depicted.

Figure 5. Ancestral character state reconstructions of characters 31 (left) and 30 (right) over one of the optimal phylogenetic hypotheses of Holoadeninae relationships. Reconstructions on the other optimal hypothesis are identical to the one depicted.

Figure 6. Ancestral character states reconstructions of characters 43, 41, and 42 (from left to right) over one of the optimal phylogenetic hypotheses of Holoadeninae relationships. Reconstructions on the other optimal hypotheses are identical to the one depicted.

Figure 7. Ancestral character states reconstructions of characters 50, 49, and 48 (from left to right) over one of the optimal phylogenetic hypotheses of Holoadeninae relationships. Reconstructions on the other optimal hypotheses are identical to the one depicted.

Figure S1. Maximum parsimony optimal trees of 12,491 transformations for the total evidence analyses.

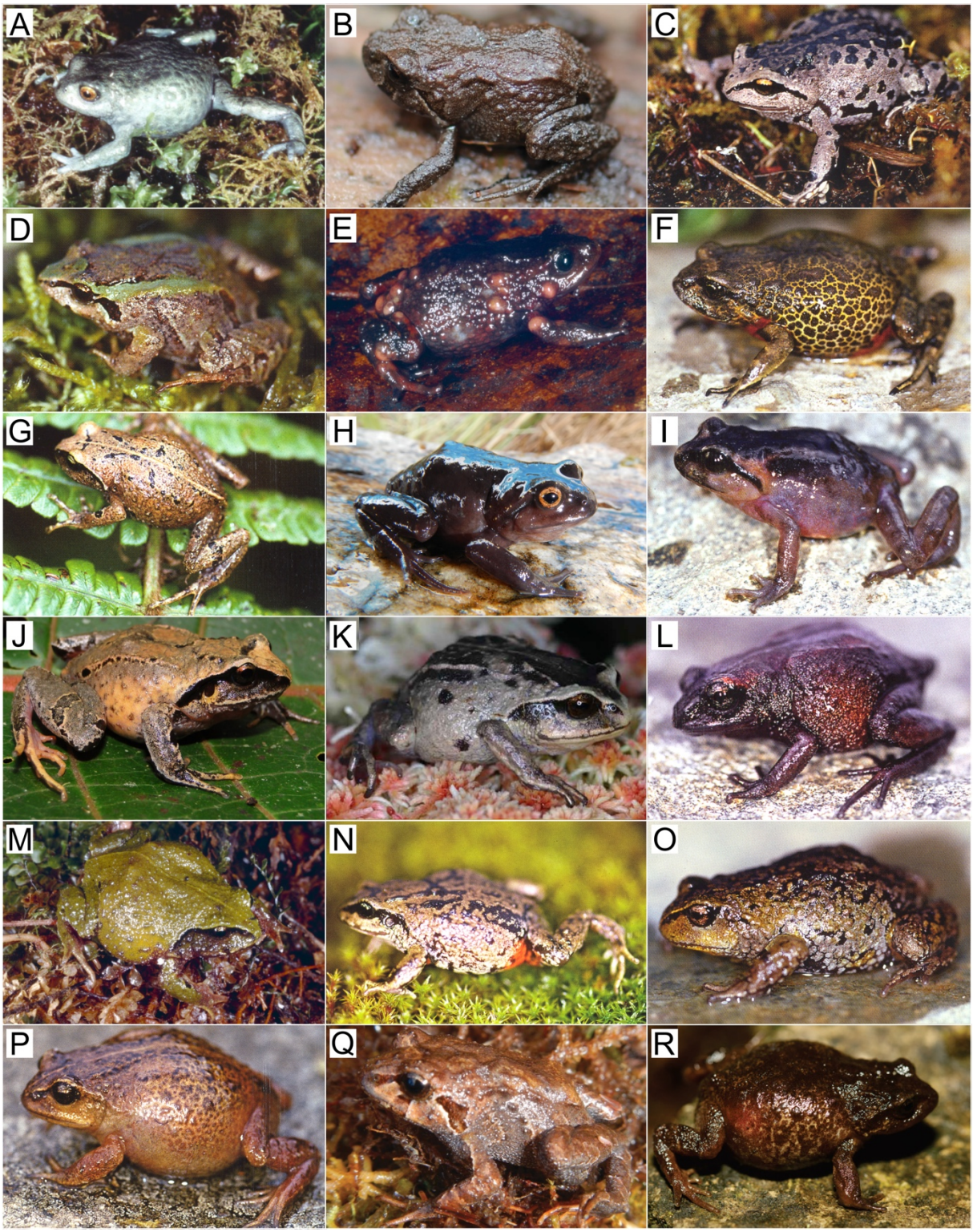

1430

1431 Figure 1

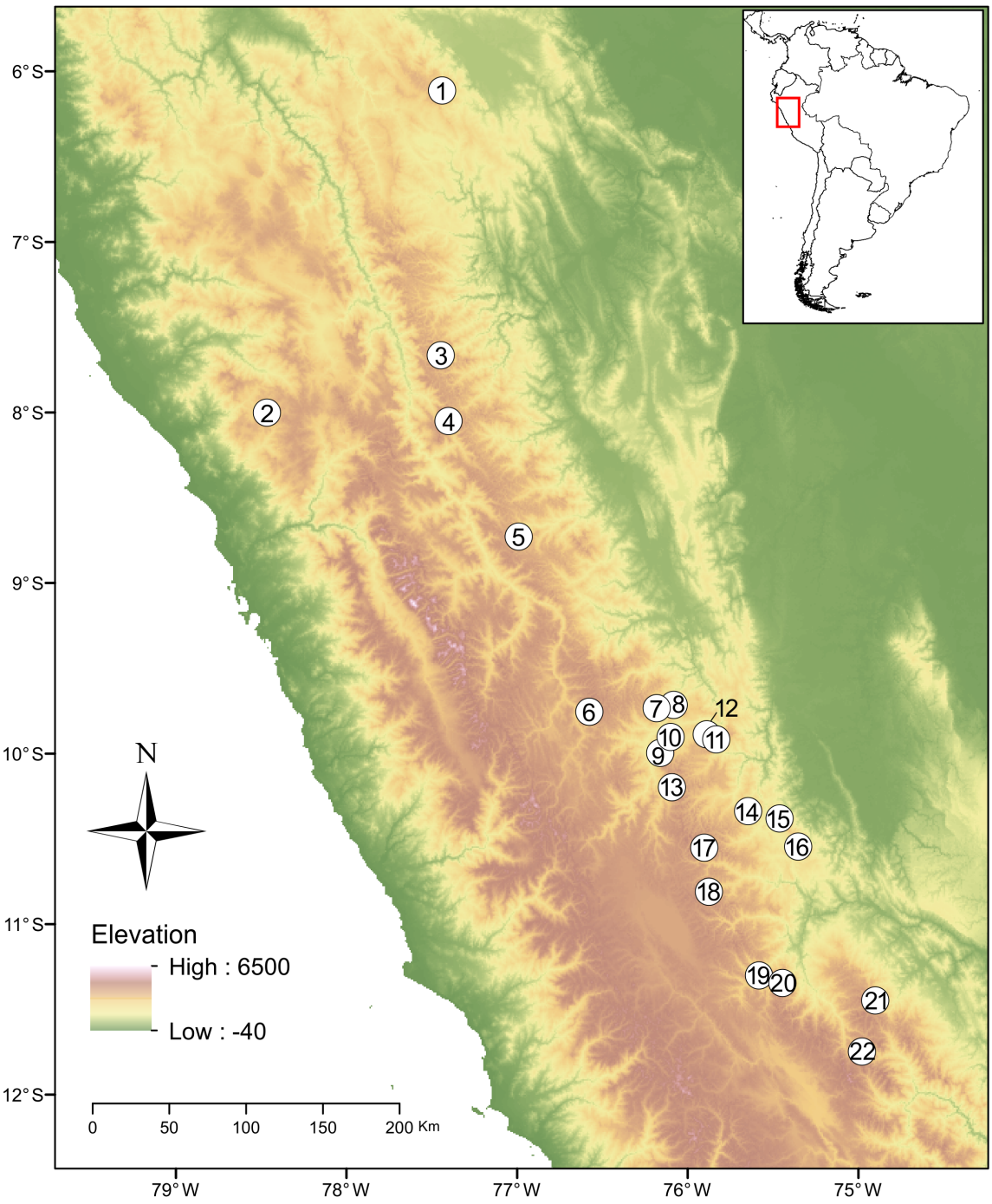

1432

1433 Figure 2

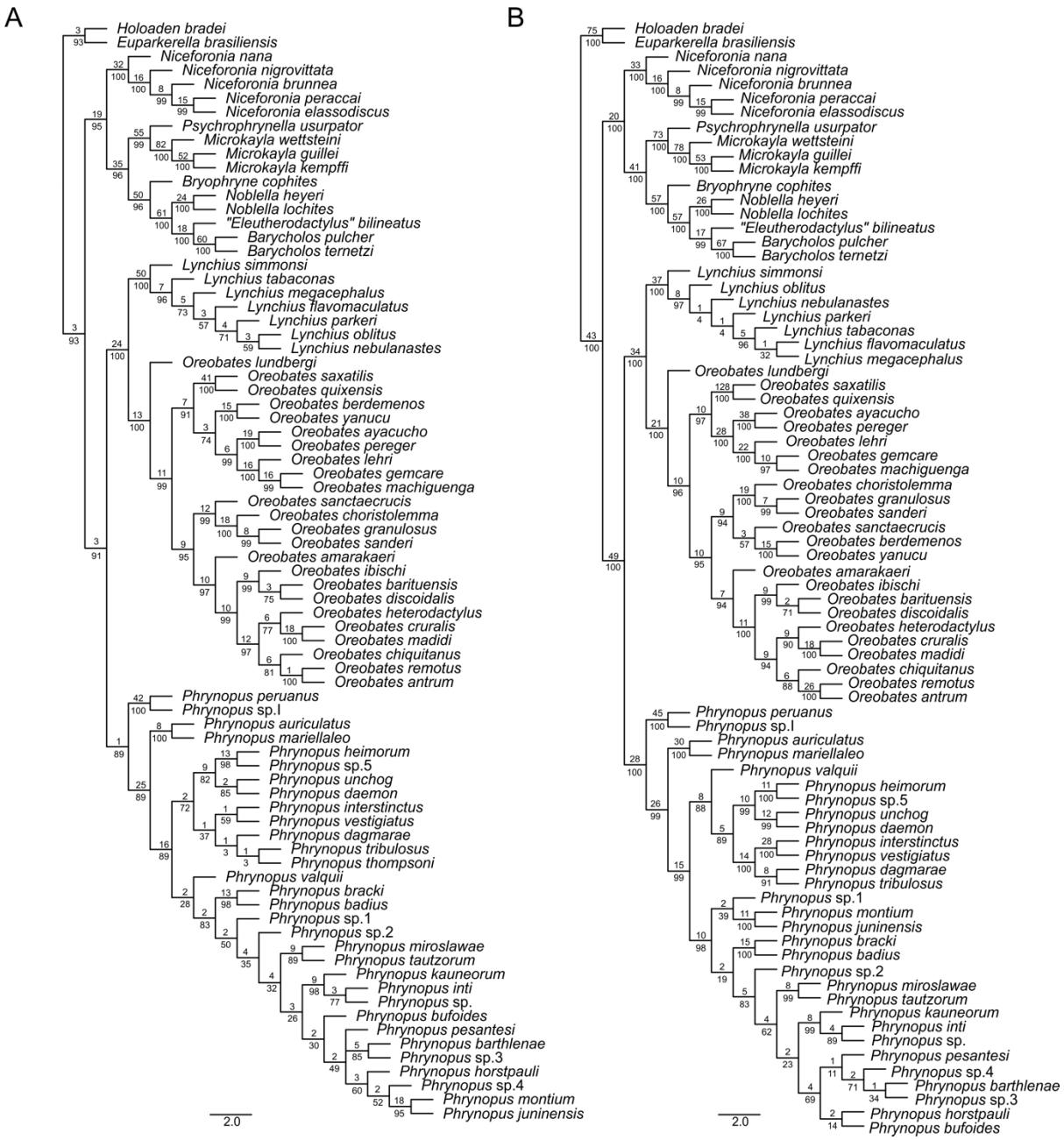

1434

1435 Figure 3

Holoaden bradei
Euparkerella brasiliensis
Niceforonia nana
Niceforonia nigrovittata
Niceforonia brunnea
Niceforonia peraccai
Niceforonia elassodiscus
Psychrophrynella usurpator
Microkayla wettsteini
Microkayla guillei
Microkayla kempffi
Bryophryne cophites
Noblella heyeri
Noblella lochites
"Eleutherodactylus" bilineatus
Barycholos pulcher
Barycholos ternetzi
Lynchius simmonsi
Lynchius tabaconas
Lynchius megacephalus
Lynchius flavomaculatus
Lynchius parkeri
Lynchius oblitus
Lynchius nebulanastes
Oreobates lundbergi
Oreobates saxatilis
Oreobates quixensis
Oreobates berdemenos
Oreobates yanucu
Oreobates ayacucho
Oreobates pereger
Oreobates lehri
Oreobates gemcare
Oreobates machiguenga
Oreobates sanctaecrucis
Oreobates choristolemma
Oreobates granulosus
Oreobates sanderi
Oreobates amarakaeri
Oreobates ibischi
Oreobates barituensis
Oreobates discoidalis
Oreobates heterodactylus
Oreobates cruralis
Oreobates madidi
Oreobates chiquitanus
Oreobates remotus
Oreobates antrum
Phrynopus peruanus
Phrynopus spl
Phrynopus auriculatus
Phrynopus mariellaleo
Phrynopus heimorum
Phrynopus sp.5
Phrynopus unchog
Phrynopus daemon
Phrynopus interstinctus
Phrynopus vestigiatus
Phrynopus dagmarae
Phrynopus tribulosus
Phrynopus thompsoni
Phrynopus valquii
Phrynopus bracki
Phrynopus badius
Phrynopus sp.1
Phrynopus sp.2
Phrynopus miroslawae
Phrynopus tautzorum
Phrynopus kauneorum
Phrynopus inti
Phrynopus sp.
Phrynopus bufoides
Phrynopus pesantesi
Phrynopus barthlenae
Phrynopus sp.3
Phrynopus horstpauli
Phrynopus sp.4
Phrynopus montium
Phrynopus juninensis
Finger pad
Absent
Present
Unknown
Finger circumferential groove
Absent
Present
Unknown
Shape of terminal phalange
T-shapped
Knobbed
Rounded
Pointed
Spade
Unknown

Figure 4

1438

1439 Figure 5

Holoaden bradei
Euparkerella brasiliensis
Niceforonia nana
Niceforonia nigrovittata
Niceforonia brunnea
Niceforonia peraccai
Niceforonia elassodiscus
Psychrophrynella usurpator
Microkayla wettsteini
Microkayla guillei
Microkayla kempffi
Bryophryne cophites
Noblella heyeri
Noblella lochites
"Eleutherodactylus" bilineatus
Barycholos pulcher
Barycholos ternetzi
Lynchius simmonsi
Lynchius tabaconas
Lynchius megacephalus
Lynchius flavomaculatus
Lynchius parkeri
Lynchius oblitus
Lynchius nebulanastes
Oreobates lundbergi
Oreobates saxatilis
Oreobates quixensis
Oreobates berdemenos
Oreobates yanucu
Oreobates ayacucho
Oreobates pereger
Oreobates lehri
Oreobates gemcare
Oreobates machiguenga
Oreobates sanctaecrucis
Oreobates choristolemma
Oreobates granulosus
Oreobates sanderi
Oreobates amarakaeri
Oreobates ibischi
Oreobates barituensis
Oreobates discoidalis
Oreobates heterodactylus
Oreobates cruralis
Oreobates madidi
Oreobates chiquitanus
Oreobates remotus
Oreobates antrum
Phrynopus peruanus
Phrynopus spl
Phrynopus auriculatus
Phrynopus mariellaleo
Phrynopus heimorum
Phrynopus sp.5
Phrynopus unchog
Phrynopus daemon
Phrynopus interstinctus
Phrynopus vestigiatus
Phrynopus dagmarae
Phrynopus tribulosus
Phrynopus thompsoni
Phrynopus valquii
Phrynopus bracki
Phrynopus badius
Phrynopus sp.1
Phrynopus sp.2
Phrynopus miroslawae
Phrynopus tautzorum
Phrynopus kauneorum
Phrynopus inti
Phrynopus sp.
Phrynopus bufoides
Phrynopus pesantesi
Phrynopus barthlenae
Phrynopus sp.3
Phrynopus horstpauli
Phrynopus sp.4
Phrynopus montium
Phrynopus juninensis
Dentigerous process of vomer
Absent
Broad
Thick
Unknown
Vomerine teeth
Absent
Present
Unknown
Anterior ala of vomer
Absent
Broad
Acute
Unknown

Figure 6

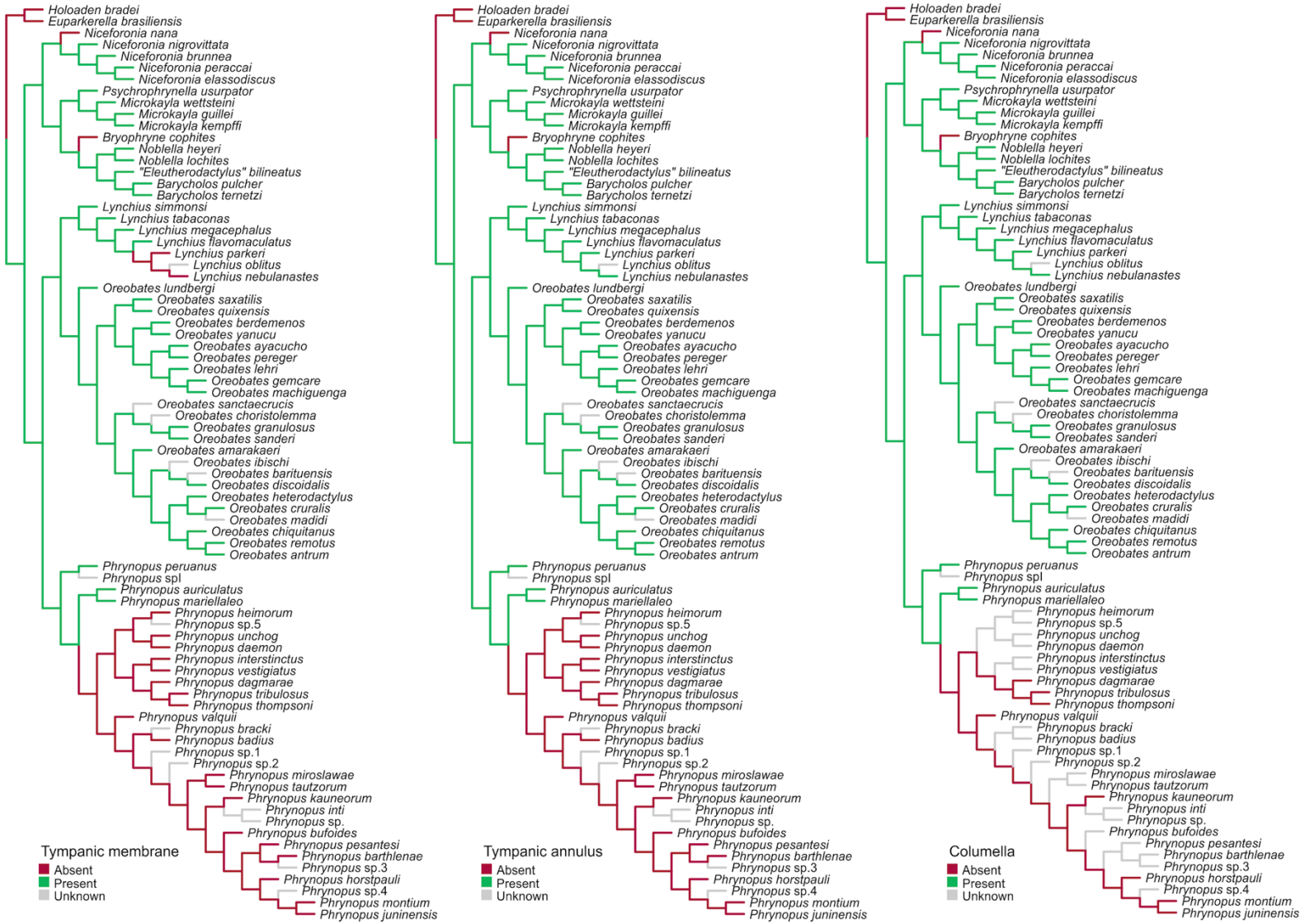

1442

1443 Figure 7

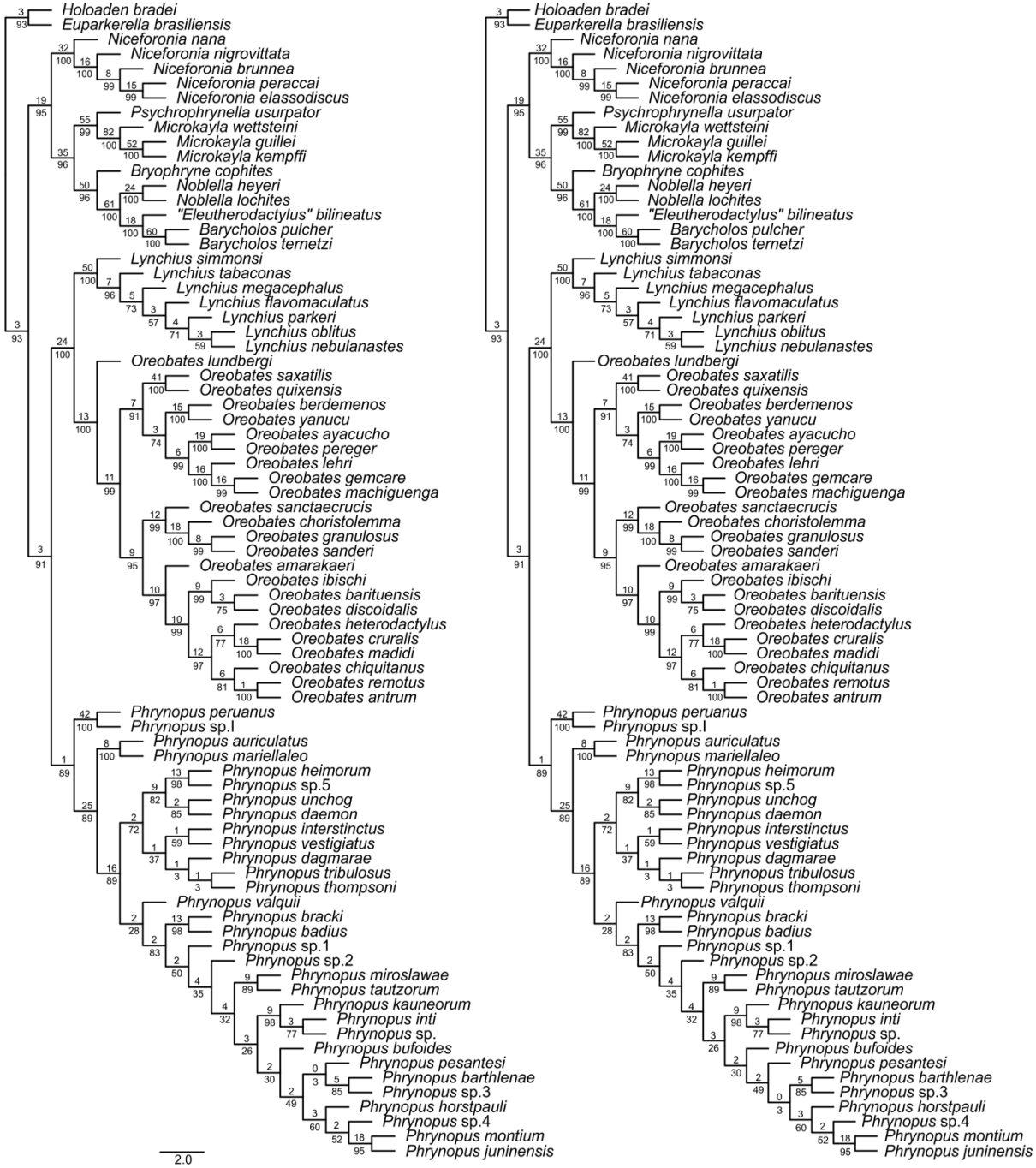

1444

1445 Figure S1

Appendices

Appendix 1. Phenotypic characters.

OSTEOLOGY

1. Hyale anterior process: absent = 0; present = 1. This character was used by Lynch (1971), who noted that the anterior process of hyale was lacking in half of the Neotropical genera of Leptodactylidae (at that time including species now split into14 families; De la Riva 2020).

2. Alary process of hyoid: absent = 0; present = 1. This character was used by Lynch (1971), who noted that the alary process of hyoid was absent in some genera of his Leptodactylidae (e.g. *Holoaden* and *Euparkerella*).

3. Shape of alary process of hyoid: narrow, stalk-like = 0; broad based = 1; wing-like = 2. This character corresponds to character 72 of Ponssa (2008).

4. Shape of extreme of posterolateral process of hyoid: acute = 0; expanded and concave = 1. This character corresponds to character 74 of Ponssa (2008).

5. Shape of posteromedial process of hyoid: distal and expanded = 0; uniform width = 1. This character corresponds to character 76 of Ponssa (2008).

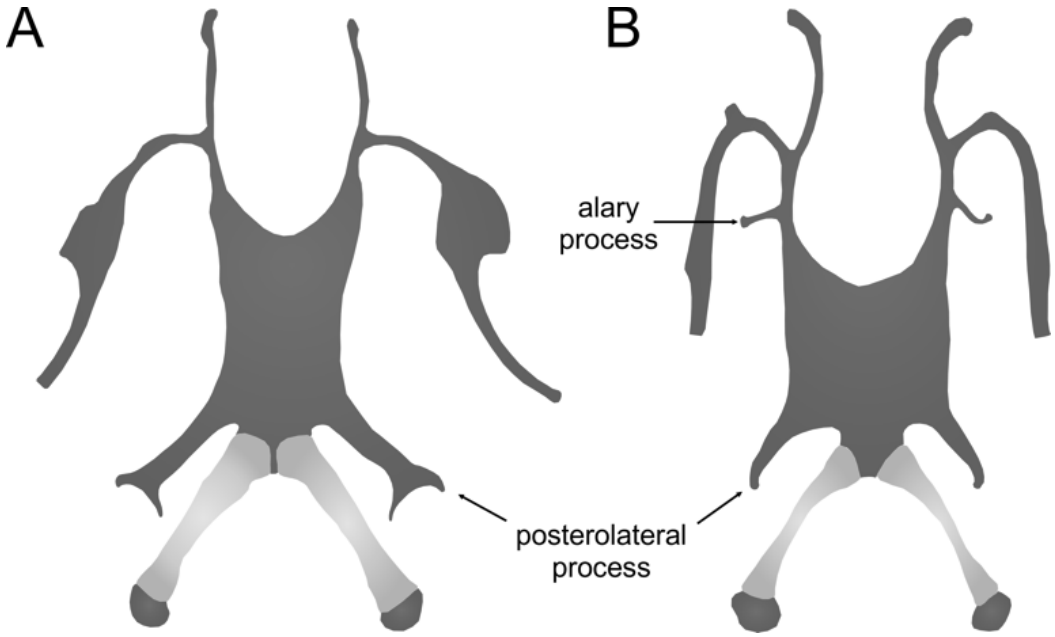

6. Shape of terminal phalanges: knobbed = 0 (G, H); spade = 1; t-shaped = 2 (A, B, C); pointed = 3(I); rounded = 4 (D, E, F). This character was used by Lynch (1971). The term 'spade' is used to describe what Lynch (1971) describes as "modified T-shaped" (his Figure 42; page 65).

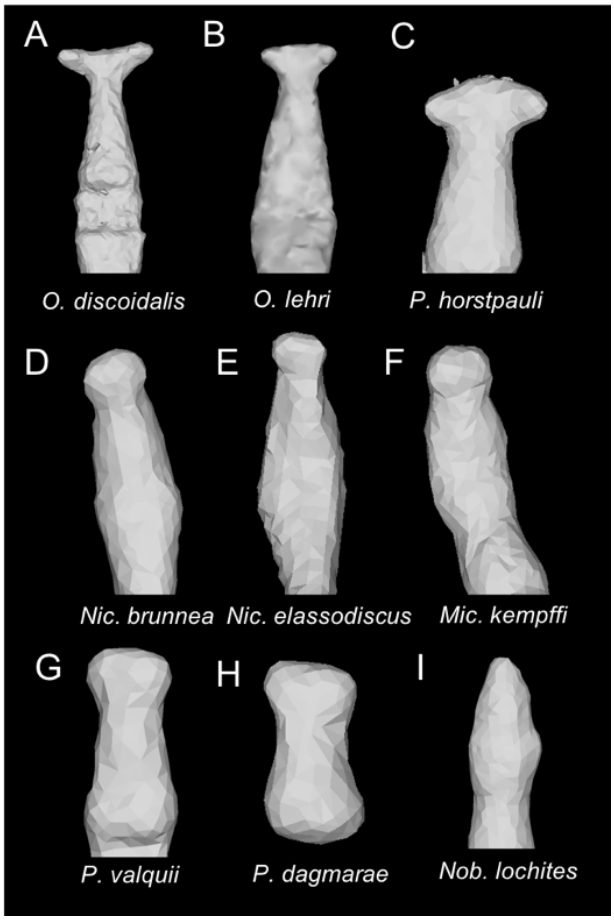

7. Angle of clavicles: directed laterally = 0; directed anteriorly = 1. This character corresponds to character 121 of Grant et al. (2006).

8. Omosternum: absent = 0; present = 1. This character corresponds to character 123 of Grant et al. (2006).

9. Shape of anterior terminus of omosternum: rounded or irregularly shaped = 0; distinctly bifid = 1. This character corresponds to character 125 of Grant et al. (2006).

10. Ossification of omosternum: entirely cartilaginous = 0; basally ossified (cartilaginous tip) = 1. This character corresponds to character 127 of Grant et al. (2006).

11. Shape of sternum: plate-like = 0; style = 1. This character was used by Lynch (1971) (his figure 34; page 59).

12. Distal (posterior) margin of sternum: medial notch present = 0; medial notch absent =1. This character corresponds to character 46 of Barrionuevo (2017).

13. Number of presacral vertebrae: 5 = 0; 6 = 1; 7 = 2; 8 = 3; 9 = 4.

14. Fusion of vertebra 8 and sacrum: free = 0; fused = 1. This character corresponds to character 144 of Grant et al. (2006).

15. Fusion of vertebrae 1 and 2: free = 0; fused = 1. This character corresponds to character 145 of Grant et al. (2006).

16. Fusion of vertebrae 2 and 3: free = 0; fused = 1. This character corresponds to character 146 of Grant et al. (2006).

17. Neural spine of vertebrae I-V: absent = 0; not imbricate = 1; imbricate = 2. This character was treated as additive and corresponds to character 78 of Ponssa (2008).

18. Dorsal ridge on urostyle: absent = 0; present = 1. This character was used by Reilly & Jorgensen (2010).

19. Dorsal ridge on ilia: absent = 0; present = 1. This character was used by Reilly & Jorgensen (2010).

20. Distal sacral-diapophyseal expansion: narrow/cylindrical = 0; expanded = 1. This character was used by Reilly & Jorgensen (2010).

21. Sacro-urostylic articulation: monocondylar = 0; bicondylar = 1. This character was used by Reilly & Jorgensen (2010).

22. Relation of frontoparietals in the parietal region: not fused = 0; fused = 1. This character corresponds to character 3 of Barrionuevo (2017).

23. Level of exposure of the frontoparietal fenestra: frontoparietals narrower than the fenestra = 0; frontoparietals equal or slightly wider than the fenestra = 1; frontoparietals in contact or jointed to each other, no frontoparietal fenestra = 2. This character was treated as additive and corresponds to character 5 of Barrionuevo (2017).

24. Frontoparietal-otoccipital relation: free = 0; fused = 1. This character corresponds to character 137 of Grant et al. (2006).

25. Notch dividing the anterior region of frontoparietal from the posterior one: absent = 0; present = 1. This character corresponds to character 51 of Ponssa (2008).

26. Exostosis on frontoparietals: absent = 0; present = 1.

27. Ridges on frontoparietals: absent = 0; present = 1.

28. Nasal-maxilla relation: separated = 0; in contact = 1. This character corresponds to character 134 of Grant et al. (2006).

29. Nasal-sphenethmoid relation: free. Separate = 0; overlapping or fused = 1. This character corresponds to character 135 of Grant et al. (2006).

30. Nasals relation: broadly separated. = 0; close to each other or in contact in the middle or anterior zone = 1; close to each other or in contact along its inner border = 2. This character corresponds to character 51 of Ponssa (2008).

31. Size and shape of nasals: large, quadrangular = 0 (B); medium-sized, claviform or triangular = 1(A); small, claviform or triangular = 2. This character corresponds to character 2 of Barrionuevo (2017).

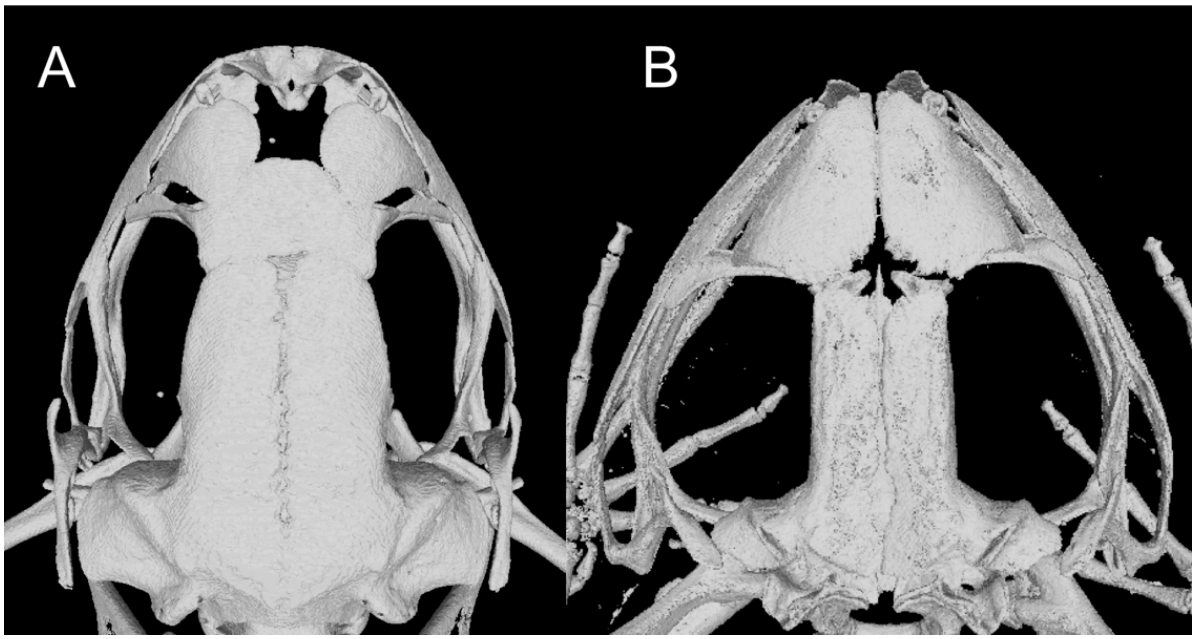

32. Orientation of alary process of premaxilla (in lateral view): directed anterolaterally = 0; directed dorsally = 1; directed posterodorsally = 2. This character was treated as additive and corresponds to character 131 of Grant et al. (2006).

33. Width of the base of the alary process of premaxillary in relation to its distal end in frontal view: base narrower than or equal to the distal (dorsal) end = 0; base wider than the distal (dorsal) end = 1. This character corresponds to character 8 of Barrionuevo (2017).

34. Orientation of alary process of premaxillary in frontal view: not divergent, the distal tip of alary process (dorsal) at the same level as the base = 0; divergent, the distal tip of alary process (dorsal) is directed laterally = 1. This character corresponds to character 7 of Barrionuevo (2017).

35. Premaxillary teeth: absent = 0; present = 1. This character corresponds to character 13 of Barrionuevo (2017).

36. Maxillary teeth: absent = 0; present = 1. This character corresponds to character 139 of Grant et al. (2006).

37. Pterygoid process of maxillary: absent = 0; present = 1. This character corresponds to character 12 of Barrionuevo (2017).

38. Quadratojugal-maxilla relation: overlapping = 0; separated = 1. This character corresponds to character 139 of Grant et al. (2006).

39. Cultriform process of parasphenoid: with keel = 0; without keel = 1. This character corresponds to character 59 of Ponssa (2008).

40. Length of the cultriform process of parasphenoid: short, not reaching the level of planum antorbitale = 0; long, reaching the level of planum antorbitale = 1. This character corresponds to character 27 of Barrionuevo (2017).

41. Vomerine teeth: absent = 0; present = 1.

42. Anterior ala of vomers: absent = 0; broad = 1; acute = 2. This character corresponds to character 65 of Ponssa (2008).

43. Dentigerous process of vomer: absent = 0; thick = 1; broad = 2; expanded = 3.

44. Palatines: absent = 0; present = 1.

45. Shape of palatines: straight = 0; curved or boomerang-shaped = 1. This character corresponds to character 23 of Barrionuevo (2017).

46. Zygomatic ramus of squamosal: elongate, slender, pointed = 0; shorter and less robust, but still well defined = 1; well defined, moderate length, abruptly directed ventrally = 2; inconspicuous, poorly differentiated = 3. This character corresponds to character 130 of Grant et al. (2006).

47. Quadratojugal: absent = 0; present = 1.

48. Tympanic annulus: absent = 0; present = 1.

49. Columella: absent = 0; present = 1.

50. Tympanic membrane: present = 0; absent = 1.

Following Pereyra et al., (2016), we made the following assumptions when scoring the presence/absence of the tympanic structures: (1) absence of the tympanic membrane and tympanic annulus when the columella is absent; (2) absence of the tympanic membrane when the tympanic annulus is absent; (3) presence of the tympanic annulus and columella when the tympanic membrane is present; and (4) presence of the columella when the tympanic annulus is present.

EXTERNAL MORPHOLOGY

Characters 51 to 89 were used by Duellman and Lehr (2009) to diagnose species of the genera *Bryophryne*, *Lynchius*, *Niceforonia*, *Noblella*, *Oreobates*, *Phrynopus*, *Pristimantis*, *Psychrophrynella*, and *Strabomantis* from Peru.

51. Enlarged eyelid tubercle: absent = 0; present = 1.

52. Postrictal tubercle: absent = 0; present = 1.

53. Ulnar tubercle: absent = 0; present = 1.

54. Heel tubercle: absent = 0; present = 1.

55. Tarsal tubercle: absent = 0; present = 1.

56. Middorsal tubercle: absent = 0; present = 1.

57. Cloacal tubercle: absent = 0; present = 1.

58. Sacral tubercle: absent = 0; present = 1.

59. Dorsolateral folds: absent = 0; present = 1.

60. Lateral folds: absent = 0; present = 1.

61. Interocular fold: absent = 0; present = 1.

62. Supratympanic fold: absent = 0; present = 1.

63. Paravertebral fold: absent = 0; present = 1.

64. Middorsal fold: absent = 0; present = 1.

65. Occipital-scapular fold: absent = 0; present = 1.

66. Discoidal fold: absent = 0; present = 1.

67. Thoracic fold: absent = 0; present = 1.

68. Vocal slits: absent = 0; present = 1.

69. Vocal sac: absent = 0; present = 1.

70. Nuptial pads: absent = 0; present = 1.

71. Finger lateral fringes: absent = 0; present = 1.

72. Finger webbing: absent = 0; present = 1.

73. Shape of fingers disc: not expanded = 0; expanded = 1.

74. Finger pads: absent = 0; present = 1.

75. Finger circumferential groove: absent = 0; present = 1.

76. Inner palmar tubercle: absent = 0; present = 1.

77. Outer palmar tubercle: absent = 0; present = 1.

78. Finger subarticular tubercles shape: absent = 0; present = 1.

79. Palmar supernumerary tubercles: absent = 0; present = 1.

80. Antebrachial tubercle: absent = 0; present = 1.

81. Toe lateral fringes: absent = 0; present = 1.

82. Toe webbing: absent = 0; present = 1.

83. Shape of toes discs: not expanded = 0; expanded = 1.

84. Toes pad: absent = 0; present = 1.

85. Inner metatarsal tubercle: absent = 0; present = 1.

86. Outer metatarsal tubercle: absent = 0; present = 1.

87. Toe subarticular tubercles shape: absent = 0; present = 1.

88. Plantar supernumerary tubercles: absent = 0; present = 1.

89. Cloacal sheath: absent = 0; present = 1.

90. Axillary glandular pads: absent = 0; present = 1. This character was used by Duellman and Lehr (2008).

91. Distal tubercle on finger IV: absent = 0; present = 1. This character corresponds to character 3 of Grant et al. (2006).

92. Metacarpal ridge: absent = 0; present = 1. This character corresponds to character 19 of Grant et al. (2006).

93. Morphology of male excrescences: nonspinous asperities = 0; uncornified spines = 1; large, cornified spines = 2. This character corresponds to character 23 of Grant et al. (2006).

94. Female excrescences on thumb: absent = 0; present = 1. This character corresponds to character 25 of Grant et al. (2006).

95. Tarsal keel: absent = 0; present = 1. This character corresponds to character 28 of Grant et al. (2006).

96. Morphology of tarsal keel: straight or very weakly curved, extending proximolateral from preaxial edge of inner metatarsal tubercle = 0; short, tubercle-like, curved or directed transversely across tarsus, not extending from metatarsal tubercle = 1; weak, short dermal thickening, not extending from metatarsal tubercle = 2. This character corresponds to character 29 of Grant et al. (2006).

97. Tarsal fringe: absent = 0; present = 1. This character corresponds to character 30 of Grant et al. (2006).

98. Metatarsal fold: absent = 0; present = 1. This character corresponds to character 46 of Grant et al. (2006).

99. Large intestine color: unpigmented = 0; pigmented anteriorly = 1; pigmented extensively = 2. This character corresponds to character 66 of Grant et al. (2006).

100. Adult testis (mesorchium) color: unpigmented = 0; pigmented medially only = 1; entirely pigmented = 2. This character corresponds to character 67 of Grant et al. (2006).

101. Color of mature oocytes: unpigmented (uniformly white or creamy yellow) = 0; pigmented (animal pale brown or black) = 1. This character corresponds to character 68 of Grant et al. (2006).

Appendix 2. Specimens examined in this study, including cleared and stained (CS) and scanned specimens (3DM).

Barycholos pulcher: AMNH 89707, AMNH 89714, AMNH 104345, KU 218156 (CS), KU 218158 (CS); *Barycholos ternetzi*: CFBH 26150, CFBH 23596, CFBH11599, CFBH 26105, CFBH 26108, CFBH 10260, CFBH 11595, CFBH 11600, CFBH 23818, CFBH 11601, CFBH 26038, CFBH 11594, CFBH 11597 (CS), CFBH 11598 (CS); *Bryophryne bakersfield*: MHNCP 5099, 5993, 5996, 5997, 6000, 6001, 6003, 6009, 6010, 6011, 6012, 6014, 6022, 7972; *Bryophryne bustamantei*: MHNCP 6018, 6019; *Bryophryne cophites*: AMNH 157025, 153092, 153094, 153091; MHNCP 4242, 4246, 4247, 4266, 4281, 4286; KU 138909 (CS), 173497 (CS), 173498 (CS); *Bryophryne hanssaueri*: MUSM 24557, 27567, 27568, 27608, 27610, 27611; *Bryophryne nubilosus*: MUSM 20970, 26310, 26311, 26312, 26316, 26317; *Bryophryne phuyuhampatu*: CORBIDI 18224, 18225, 18226; *Bryophryne quellokunka*: MHNCP 5374, 5375, 5380; *Bryophryne tocra*: MHNCP 5418, 5419, 5420, 5696; *Bryophryne wilakunka*: MHNCP 5425; "*Eleutherodactylus*" *bilineatus*: CFBH 23689, 34088, 34063, 34090, 32419, 37976, 23684 (CS), 35720 (CS); *Holoaden bradei*: AMNH 73548, 73549, KU 107087 (CS), 92868 (CS), 107088 (CS), MNRJ 22501 (CS), CFBH 36357, 252; *Euparkerella brasiliensis*: KU 93192 (CS), CFBH 39336, 26983, 253, 39340, 31334, 40840, 39335, 25984, 39333, 39338, 39337; *Holoaden bradei*: AMNH 73548, 73549, KU 107087 (CS), 92868 (CS), 107088 (CS), MNRJ 22501 (CS), CFBH 36357, 252; *Lynchius flavomaculatus*: KU 119721–24, 119737–42, 121354 142201–02, 202654–55, 218210, 119716–20, 119725–36, 119743 (CS), 141474–77, 142198–200, 165955–67, 166294 (CS), 202656; FMNH 197838, 197846, USNM 98929–30, 195393–424, 260788, BMNH 1947.2.16.11, 1947.2.16.12–14; *Lynchius nebulanastes*: KU 181407, 181392–406, 181408–14, 181415–16 (CS), 181841, 219806–819; *Lynchius oblitus*: MHNC 8598, 8599, 8601, 8602, 8606, 8614, 8625, 8626, 8652, 8672, 8673, 8674, 8675, 8676, 8677, 8689, 8690, MTD 45954; *Lynchius parkeri*: KU

135278, 135279–311, 135306 (CS), 181288–91, 181393, 219820, 181292–356, 181823, 181824 (CS), 181825–27, 181828 (CS), 181829, 196581–91, LSU 32172–32239; *Lynchius simmonsi*: KU 147068 (3DM), 147069, QCAZ 30829–30, 41639–40; *Lynchius tabaconas*: MHNC 8637, 8649, 8650; *Microkayla boettgeri*: MHNCP 5365; *Microkayla chapi*: MHNCP 5325, 5326, 5330, 5331; *Microkayla chilina*: MHNCP 5350, 5351, 5352, 5353, 5354, 5355; *Microkayla guillei*: AMNH 165109 (3DM); *Microkayla kempfii*: KU 220068, 220067 (3DM); *Microkayla wettsteini*: KU 183048, 183057, 183049, 183053, 183051, 183059, 154558, 183050, 183060, 183055, 183070 (CS), 183072 (CS); *Niceforonia brunnea*: KU 202652, 202653, 178258, 178259 (3DM), 202651; *Niceforonia elassodiscus*: KU 177284, 130272,177283, 143415 (3DM), 177282, 130271; *Niceforonia nana*: KU 169121, 169123, 169122, 169124, 169127, 169129, 170164 (CS), 169120, 169125, 169126, 169128; *Niceforonia nigrovittata*: AMNH 93509 (3DM), 93517, 93510, 103440, 96295, 96297; *Niceforonia peraccai*: KU 178267, 169131, 169130, 118137 (CS), 111430, 109171, 202657, 178266, 178265, 178264, 178263, 178262, 117796, 117795; *Noblella heyeri*: KU 196529, 196530, 196531 (CS); *Noblella lochites*: KU 147070 (3DM); *Noblella myrmecoides*: AMNH 102997, 97051, 153037; *Noblella pygmaea*: MUSM 26320, 24535, 24536; *Oreobates amarakaeri*: MHNCP 7049; *Oreobates antrum*: CFBH 34897, 39552, 39547, 39549, 39544, 39548, 39550 (CS), 39551, 39545 (CS); *Oreobates ayacucho*: MUSM 37858, 35548, 35552, 35549, 35553, 35551, MCZ 24362, 24363; *Oreobates berdemenos*: MACN 45641, 45651, 45639, 45661, 45673 45626 (CS); *Oreobates cruralis*: KU 215461, 207749; *Oreobates discoidalis*: KU 206435 (3DM), 154526, 182814, 182813, 182815, 154522, 206433 (CS), MACN 45698; *Oreobates gemcare*: AMNH 157013 (3DM), 153087, KU 173233, 173231 MHNCP 6687, 4564, 4602; *Oreobates granulosus*: AMNH 6060, 6062, 6063; *Oreobates chiquitanus*: MNRJ 106, MZUSP 85628, UFMT 10058, 19222–4, 1381–6, 7293 (CS), 7346, 7348–9, 7367, 719, 11111, 11113, 11114 (CS), 11115, 11116 (CS), 10526, 11112, 11117–20,

11108, 11109, 11110 (CS), 11107, 19220–3, 19225–31, 19239–41, 19245, 19224, 19242–44, 19232–8; *Oreobates lehri*: CM 158519 (3DM), 158523, 158535, 158505; *Oreobates lundbergi*: MUSM 17822; *Oreobates machiguenga*: MHNCP 6809; CM 158524 (3DM); *Oreobates pereger*: MUSM 13980, 19982, 19983, KU 151906 (CS); *Oreobates quixensis*: AMNH 84849, 84850, 103000, 102999, 22179, KU 149294 (CS), 146174 (CS); *Oreobates remotus*: MZUSP 141708, 141709–724; *Oreobates sanderi*: AMNH 6063, 6066 (3DM); *Oreobates saxatilis*: KU 212327, 212556, 212330, 217352, 217327, MUSM 8431, 8432; *Phrynopus auriculatus*: KU 291633, 291634 (3DM); *Phrynopus badius*: MUSM 31099; *Phrynopus barthlenae*: MUSM 20606, 20603, 20603, 20604, 20605, 20608, 20609; *Phrynopus bufoides*: MUSM 18074 (20358), 31246; *Phrynopus capitalis*: AMNH 134158; *Phrynopus chaparroi*: MHNCP 10983, 10982, 10984, 10985, 10981; *Phrynopus curator*: MUSM 31106; *Phrynopus daemon*: CORBIDI 15364; *Phrynopus dagmarae*: MUSM 20451, 20449, 20580, 20456, 20579, 20453, 20448, 20456, KU 196592 (3DM); *Phrynopus dumicola*: AMNH 134149, 134152; *Phrynopus heimorum*: MUSM 20441, 20442, 20443, 20444, 20446; *Phrynopus horstpauli*: MUSM 20424, 20437, 20435, 20434, 20426, 20436, 20435, 20430, 20439, KU 291400, 311453 (3DM); *Phrynopus interstinctus*: MUSM 29543, 29544, 29545; *Phrynopus juninensis*: MCZ 22851, 24361, 24360 (CS); *Phrynopus kauneorum*: MUSM 20459, 20451, KU 311451 (3DM); *Phrynopus lapidoides*: MUSM 32750; *Phrynopus mariellaleo*: CORBIDI 11668, 11669, 11657, 11692, 11707, 11796, 11799; *Phrynopus miroslawae*: MHNCP 6469; *Phrynopus montium*: MCZ 22858, 22859; *Phrynopus oblivius*: MUSM 19979, 19980, 19981, MCZ 24359 (CS), 109014 (CS), KU 206653 (CS); *Phrynopus paucari*: MUSM 20657; *Phrynopus personatus*: AMNH 134153; *Phrynopus peruanus*: MUSM 19977, 19978, MCZ 24318, 24311, 24319; *Phrynopus pesantesi*: MUSM 19857, 19860; *Phrynopus* sp. 1: CORBIDI 7382, 7385, 7380, 7383, 7387; *Phrynopus* sp. 2: CORBIDI 7379; *Phrynopus tautzorum*: MUSM 20613; *Phrynopus*

1716 *thompsoni*: KU 288712 (3DM); *Phrynopus tribulosus*: KU 291630 (3DM); *Phrynopus*
1717 *tribulosus*: MHNCP 6441; *Phrynopus unchog*: MUSM 32749, 32748; *Phrynopus valquii*:
1718 CORBIDI 14005, 14007, 13988, 13995, 13998-14001, 14003-04, KU 220918 (3DM);
1719 *Phrynopus vestigiatus*: MUSM 29542, CORBIDI 16090, 14958, 14599; *Psychrophrynella*
1720 *bagrecito*: KU 196512, 196519 (CS), 196522 (CS); *Psychrophrynella chirihampatu*: MHNCP
1721 14656, 14670, 14661, 14671, 14668, 14672, 14669; *Psychrophrynella glauca*: MHNCP
1722 16322; *Psychrophrynella usurpator*: MHNCP 4643, 4642, 8585, 4550, 4543, 14252, 4658,
1723 13166, KU 138939, 138936 (CS), 138925 (CS); AMNH 157028 (3DM).

1724 **Appendix 3**. GenBank accession numbers of species sampled in this study. Sequences
1725 produced in this study are highlighted in bold font. [sequences will be submitted to GenBank
1726 upon acceptance of the manuscript]

Species	16S	12S	RAG	TYR
Barycholos pulcher	EU186709	EU186727	EU186744	-
Barycholos ternetzi	DQ283094	-	-	DQ282921
Bryophryne cophites	EF493537	EF493537	EF493423	EF493508
"*Eleutherodactylus*" *bilineatus*	JX267324	JX267393	JX267556	JX267691
Euparkerella brasiliensis	JX267468	JX298276	JX267545	JX267682
Haddadus binotatus	EF493361	EF493361	EF493397	JX267685
Holoaden bradei	EF493366	EF493378	EF493449	EU186779
Lynchius flavomaculatus	EU186667	EU186667	EU186745	EU186766
Lynchius megacephalus	MK423938	-	-	-
Lynchius nebulanastes	EU186704	EU186704	-	-
Lynchius oblitus	KX470782	KX470777	KX470793	KX470800
Lynchius parkeri	EU186705	EU186705	MK423933	-
Lynchius simmonsi	JF810004	JF809940	JF809915	JF809894
Lynchius tabaconas	KX470780	KX470773	KX470789	KX470796
Microkayla guillei	AY843720	AY843720	-	DQ282995
Microkayla kempffi	MF186384	MF186308	MF186538	MF186566
Microkayla wettsteini	EU186696	EU186696	GQ345284	EU186776
Niceforonia brunnea	EF493357	EF493357	EF493422	EF493484
Niceforonia elassodiscus	EF493358	EF493358	-	-
Niceforonia nana	MH536808	MH532902	MN068027	MH542228
Niceforonia nigrovittata	MH538300	-	-	-
Niceforonia peraccai	EF493710	EF493710	EF493420	EF493485
Noblella heyeri	JX267541	JX267463	-	-
Noblella lochites	EU186699	EU186699	EU186756	EU186777
Oreobates amarakaeri	JF809996	JF809934	JF809913	JF809891
Oreobates antrum	MH025451	MH025427	MH025436	MH025445
Oreobates ayacucho	JF809970	JF809933	JF809912	JF809890
Oreobates barituensis	JF809999	JF809935	JF809914	JF809892
Oreobates berdemenos	KJ125507	-	-	-
Oreobates chiquitanus	EU192296	JF809923	JF809902	JF809882
Oreobates choristolemma	FJ539067	JF809921	JF809900	JF809881
Oreobates cruralis	EU186666	EU186666	EU186743	-
Oreobates discoidalis	FJ539068	FJ539073	JF809904	JF809884
Oreobates gemcare	JF809960	JF809930	JF809909	-
Oreobates granulosus	EU368897	JF809929	JF809908	JF809887
Oreobates heterodactylus	######	######	######	######
Oreobates ibischi	FJ438806	FJ438817	-	-

Oreobates lehri	JF809957	JF809927	JF809906	-
Oreobates lundbergi	JF809958	JF809928	JF809907	JF809886
Oreobates machiguenga	JF809969	JF809932	JF809911	JF809889
Oreobates madidi	FJ539070	FJ539075	JF809901	-
Oreobates pereger	JF809955	JF809926	JF809905	JF809885
Oreobates quixensis	EF493662	EF493828	DQ679273	JF809893
Oreobates remotus	JN688273	MH025425	MH025434	MH025443
Oreobates sanctaecrucis	JF809951	JF809924	JF809903	JF809883
Oreobates sanderi	EU368904	-	-	-
Oreobates saxatilis	EU186708	EU186726	EU186742	EU186763
Oreobates yanucu	KY111322	-	-	-
Phrynopus auriculatus	EF493708	EF493708	-	MF186582
Phrynopus badius	MG896571	MG896594	MG896618	-
Phrynopus barthlenae	MF186350	MF186292	-	-
Phrynopus bracki	EF493709	EF493709	EF493421	EF493507
Phrynopus bufoides	AM039645	AM039713	-	-
Phrynopus daemon	MG896574	MG896597	-	-
Phrynopus dagmarae	######	######	######	######
Phrynopus heimorum	MF186363	MF186302	-	MF186580
Phrynopus horstpauli	MF186364	MF186303	-	MF186584
Phrynopus interstinctus	MG896575	MG896598	MG896621	-
Phrynopus inti	MF651906	MF651913	MF651918	MF651921
Phrynopus juninensis	MG896576	MG896599	MG896622	-
Phrynopus kauneorum	AM039650	AM039718	-	-
Phrynopus mariellaleo	MH538299	-	MH538303	MH538306
Phrynopus miroslawae	MF186393	MF186312	MF186542	MF186585
Phrynopus montium	MG896578	MG896601	MG896624	-
Phrynopus peruanus	MG896580	MG896605	MG896627	MG896631
Phrynopus pesantesi	AM039656	AM039724	-	-
Phrynopus sp	AM039657	AM039725	-	-
Phrynopus sp. 1	######	-	######	######
Phrynopus sp. 2	######	######	######	######
Phrynopus sp. 3	######	######	######	######
Phrynopus sp. 4	######	-	-	-
Phrynopus sp. 5	######	-	-	-
Phrynopus spI	MG896589	MG896606	MG896629	-
Phrynopus tautzorum	AM039652	AM039720	-	-
Phrynopus tribulosus	EU186707	EU186725	MF186547	MF186578
Phrynopus unchog	MG896592	MG896609	-	-
Phrynopus valquii	######	######	######	######
Phrynopus vestigiatus	MG896593	MG896610	-	-
Psychrophrynella usurpator	EF493714	EF493714	EU186762	EU186780

1727

Species	COI	POMC	CYTB	28S
Barycholos ternetzi	-	JX298136	JX298401	DQ283496
Euparkerella brasiliensis	JX298357	JX298137	JX298402	-
Haddadus binotatus	KU494450	-	-	DQ283493
Lynchius nebulanastes	-	AY819154	-	-
Lynchius tabaconas	-	KX470787	-	-
Microkayla guillei	-	-	-	AY844323
Microkayla kempffi	-	MF186504	-	-
Microkayla wettsteini	-	GQ345266	-	GQ345139
Niceforonia brunnea	-	GQ345264	GQ345203	GQ345138
Oreobates berdemenos	-	-	KJ125511	-
Oreobates discoidalis	-	-	EU368883	-
Oreobates heterodactylus	-	-	EU368886	-
Oreobates madidi	-	-	EU368887	-
Oreobates quixensis	KU494611	AY819093	JX298404	-
Oreobates remotus	-	-	JN688276	-
Oreobates sanderi	-	-	EU368891	-
Phrynopus auriculatus	MF186466	-	-	-
Phrynopus badius	MG896611	-	-	-
Phrynopus barthlenae	MF186464	MF186519	-	-
Phrynopus bracki	-	GQ345263	GQ345202	GQ345137
Phrynopus dagmarae	######	-	-	-
Phrynopus heimorum	-	MF186515	-	-
Phrynopus horstpauli	MF186465	MF186518	-	-
Phrynopus interstinctus	MG896614	-	-	-
Phrynopus mariellaleo	-	MH538308	-	-
Phrynopus miroslawae	MF186463	MF186516	-	-
Phrynopus peruanus	MG896616	-	-	-
Phrynopus sp. 1	######	-	-	-
Phrynopus sp. 2	######	-	-	-
Phrynopus sp. 3	######	######	######	-
Phrynopus tribulosus	MF186469	MF186514	-	-
Phrynopus valquii	######	-	-	-
Phrynopus vestigiatus	MG896617	-	-	-
Psychrophrynella usurpator	-	-	GQ345205	-

1728

Species	CMYC-EX2	CMYC-EX3	H3	RHO
Barycholos ternetzi	KF625166	-	DQ284144	DQ283810
Euparkerella brasiliensis	KF625157	-	-	-
Haddadus binotatus	-	-	DQ284142	DQ283807
Lynchius nebulanastes	AY819320	-	-	-
Microkayla guillei	-	-	DQ284371	-

Microkayla wettsteini	GQ345153	-	GQ345219	-
Niceforonia brunnea	GQ345151	-	GQ345218	-
Oreobates quixensis	AY819178	AY819257	-	-
Phrynopus bracki	GQ345150	GQ345168	GQ345217	GQ345303
Phrynopus sp. 3	######	######	-	-

1729

Species	**NCX1**	**SLC8A3**	**SIA**	**CXCR4**
Microkayla wettsteini	GQ345237	GQ345335	GQ345316	GQ345189
Niceforonia brunnea	GQ345235	GQ345333	GQ345315	GQ345187
Phrynopus bracki	GQ345234	GQ345332	GQ345314	GQ345186
Phrynopus mariellaleo	MH538307	-	-	-

1730

1731 **Appendix S1**. Phenotypic dataset employed in the phylogenetic analyses of *Phrynopus*.

amarakaeri ??1?2????0000110000000000001100000000111100000111101 10??0?0000?
antrum 110?022102003000011010100000120100110011112110000001000000000100011 0?0101111111000011111001 0?00?00000
auriculatus ?????02?????3000?11010100000?011001100101221030000000100001101011110000000011010000011000111?01000000
ayacucho ??1?2????0000100000010010111100000000110000000110000 10?00?00000
badius ??0??????1?10100000010000011 1???0000011000000011000010?00?000?0
barthlenae ?????2????????????????????????????????????021????1?10100000000010001101100000110100000110100100 00?00000
berdemenos 1100022102003000111010200000120100110011112110000001000000000100011 1?0000101111000011111001 0?00?00000
bilineatus 10?102210200300011101020000012010011001111210300000100000000000001 1???0001111010000111100110?01200000
bradei 10?002210201300011101000000000110011001111210001110100000000100011000000101100000011100011 0?00?00000
brasiliensis ?0??0121????3000011010200000101100110010021103011100000000000010101 1???0000011010000011010000?00?00???
brunneus ????0421?2??3000211010200000120100110011112103000001000000100100111 0?0000011110000011100110?00?00000
bufoides ??0??????1?10000000000010001100100000110000000110000100 00?00000
cophites ????022100003000011010100001001100110010021110011101000000100000011??1000001101000001101001 0000?00000
cruralis ????022??2??3000111010200000120100110011112113000001000000000000011 10?0100111101000001111011 0?00?00000
daemon ??0??????1?10100100010000011 1???0000011000000011000010?00?000?0
dagmarae ????002?????3000011010200000?012001100111211130111000100001000000 11???0000011000000011000010??0?000?0
discoidalis 1101022102003000011010100000120000110011112100000001000000000100011 1100001111110000011110110?00?00000
elassodiscus ????0421?2??3000211010200000120101110011112113000001000000000000011 0?10001111110000111100110000?00000
flavomaculatus 10?002210201300011101020010012010011001111210000000100000010000011 1?0000011010000011000110?00?00000
gemcare ??1?2????0000100000010000011111000010111100001110001 10?00?00000
granulosus ??1?2????0000100000000010111111100010110100000110001 10?00?00000
guillei ????022?????3000111010200001101100110010021113000001000000100100011 1100000011000000011000110??0?0000?
heimorum ??0??????1?10000000000000011 1???0000011010000011000010?00?000?0
heyeri 10?003210200300001101020000000210011011000010500000100000000000001 10100000011010000111000110?01200000
horstpauli ????022?????3000011010200000?012001100100211100111000000001001001 1100100000110000000110001 1000?00000
interstinctus ??1??????1?10001000000010001 1???0000011010000011000010?00?000?0
juninensis ????022100013000011010100000101 1?011001002110301110000000000000001 1000000001100000001100001 0000?00000
kauneorum ????002?????3000?11010100000?011001100100211100111000000000010001 10?0000001100000001100 01?1000??0000
kempffi ????042?????3000111010200001101100110010021103000000000001000000011?10000001100000001100111 0?00?00000

lehri ?????22?????3000111010200000120001110011112100000001000000000100011?0000001101000001100011?00?00000
lochites ????0321?2??3000011010200001102100110110000105000001000000000000011???000001101010001100?10?012000?0
lundbergi ?????2?????????????????????????????????????1?2????000010000000001?001000101111000001111011?00?0000?
machiguenga ????022?????3000111010200000?201011100111121000000010000000000001????100001111010001111011?00?0000?
mariellaleo ??1?2????000010001001001001111???000001101100001100001?01000000
megacephalus ?????32?????3?0011?01?2??1111201??11?0??1?211?000001000???0??1?11??????0000110?00001100??1??????????
miroslawae ??0?1????1?10001100010010111???000001101000001101001?00?00000
montium 1100022120013000011010200000101200110010021110011100000000000000011001000001101000001101011?0?0000?
nana 110?042122003000111010200000120200110011112113011101000000000000011???000001100000001100011?00?000?0
nebulanastes 10?002210200300011101020000012020011001111210000010100000010010011???000001101000001100011?00?00000
nigrovittatus ????0421?2??3000211010200000120100110011112103000001000000100100111000000001101000111100011?00?000?0
parkeri 10?002210200300011101020010012020011001111211000010100000010000011 0?10000011010000011000110000?00000
peraccai 110?042122003000211010200000120100111011112113000001000000100100111000000001101000001100011?00?00000
pereger 1101022102003000111010200000120100110011112100000001000000100101111000000001101000001100001?00?00000
peruanus ??????21200?3000011010200000101200110010121113000000000000000010001101100000110000000110000?00?00000
pesantesi ??0??????1?10100000000010001100100000110100000110000100?0?0000?
pulcher 110?022102003000111010200000120100110011112103000001000000100100011111000111101000011101011?01200000
quixensis 1100022102003000111010200000120100110011112100000001100000000100111???10010111101000111011?00?000?0
sanderi ????022?????3000111010200000120100110011112100000001000000000101111111000101101000001101011?00?00000
saxatilis ??0000011000000001000 11???000001111100001111011?00?000?0
simmonsi ????032?????3000111010200000120100110011112110000001000000000101011 1??10000111100000111100?0?00?000?0
tabaconas ??1??????000010000001000011110000000011010000011000010?00?00???
tautzorum ??0??????1?10000000000100111???000001100000001100011?00?000?0
ternetzi 110?022102003000111010200000120100110011112103000001000000100100011 0?000010110101001110101?01200000
thompsoni ????002?????3000011010200000?011001100110211130111101000000110101111??000001101000001101011?00?000?0
tribulosus ?????02?????3000011010200000?011001100110211030111111110000000000??0?000000110100000110100?0??0?0000?
unchog ??0??????1?10101100010011011100000000110100000110100?0?00?0000?
usurpator 10?00201(1 2)00130000110102000000012101100100101140000010000000000010111100000011010000011000110?01000000
valquii ????002?????3000011010200000?011001100100211130111010000000010011 1???000001100000001100011?00?00000
vestigiatus ??1?1????1?1100100001010001111???000001101000001100001?00?000?0
wettsteini 1(0 1)0102210000300011101020000110110011001001110000000100000010010011111110000110100000110101 10?00?00000

bracki ????????????

A new terraranan genus from the Brazilian Atlantic Forest with comments on the systematics of Brachycephaloidea (Amphibia: Anura) †

Ana Paula Motta[1], Pedro Paulo Goulart Taucce[1], Célio Fernando Baptista Haddad[1], Clarissa Canedo[2,3]

[1]Laboratório de Herpetologia, Departamento de Biodiversidade e Centro de Aquicultura (CAUNESP), Instituto de Biociências, Universidade Estadual Paulista, Av. 24A 1515, CEP 13506-900, Rio Claro, São Paulo, Brazil.

[2]Departamento de Zoologia, Instituto de Biologia Roberto Alcantara Gomes, Universidade do Estado do Rio de Janeiro, Rua São Francisco Xavier, 524, Maracanã, 20550-013, Rio de Janeiro, Rio de Janeiro, Brazil.

[3]Setor de Herpetologia, Departamento de Vertebrados, Museu Nacional, Universidade Federal do Rio de Janeiro, Quinta da Boa Vista, 20940-040, Rio de Janeiro, Rio de Janeiro, Brazil.

Corresponding author: Ana Paula Motta, apmottah@gmail.com

Key-words: *Barycholos*, *Eleutherodactylus bilineatus*, *Noblella*, phylogeny, taxonomy

† Manuscrito aceito para publicação em *Journal of Zoological Systematics and Evolutionary Research*

ABSTRACT

"*Eleutherodactylus" bilineatus* has long been an enigma. Recent phylogenetic analyses have recovered this species as part of a clade including *Barycholos* and *Noblella*, but the relationship among these groups still remains contentious. In this study, we test the phylogenetic position and reassess the taxonomic status of this long-term *incertae sedis* species. We use phylogenetic analyses of nuclear and mitochondrial gene sequences and data for external morphology and osteology of "*E.*" *bilineatus* and its related genera. We recover the species as an independent lineage forming a fully-supported clade with *Barycholos* and *Noblella*. The combination of inferred relationships and morphological traits support the erection of a new genus that we name and diagnose. Our analyses also recover a non-monophyletic *Noblella* and the species of the genus, although morphologically similar, are part of different clades: one including species from central Andes and the other one including species from northern Andes. Moreover, distribution patterns point out connections among distant biogeographical areas of South America and a widespread distribution of an ancestor for the clade including *Barycholos*, "*E.*" *bilineatus*, and *Noblella*. We also compare the relationships among clades of Brachycephaloidea and, hence, the family and subfamily classifications in different studies. We show that the family classification is probably far from becoming stable, mostly due arbitrary selections of hierarchy of the clades. However, we show that by assigning a family to each of the highly-supported and frequently-recovered clades would render a more stable taxonomy of Brachycephaloidea.

1 INTRODUCTION

The species *Eleutherodactylus bilineatus* Bokermann, 1975 has long been an enigma. In its description, Bokermann (1975clearly stated that the new species was not related to any other known species from eastern Brazil and its relationship to other *Eleutherodactylus* Duméril & Bibron, 1841 was not clear. Lynch (1976) considered that the species could actually be a member of a genus other than *Eleutherodactylus*, since it resembled species of the genus *Adelophryne* Hoogmoed & Lescure, 1984 that were being described by Hoogmoed at that time. Nonetheless, after comparing the description of *E. bilineatus* to the material they were studying, Hoogmoed, Borges-Nojosa, & Cascon (1994) refused Lynch (1976)'s hypothesis and decided to keep Bokermann's generic allocation. *Eleutherodactylus bilineatus* has also been tentatively included in the *E. fitzingeri* group (Lynch, 1976). However, the species was anew considered of unknown affinity, and it was removed from the species group and not assigned to any other species group of the genus (Lynch & Myers, 1983; Lynch & Duellman, 1997).

The evolutionary history of *Eleutherodactylus* remained unknown for a long time. Molecular phylogenetic analyses for a large proportion of the group by Heinicke, Duellman, & Hedges (2007) found three major clades geographically defined (Caribbean Clade, Middle American Clade, and South American Clade), and a small clade from southeast Brazil represented by two species in the phylogeny (*Eleutherodactylus guentheri* and *E. parvus*). Due to its geographic isolation from other groups of *Eleutherodactylus*, 29 species from southeast Brazil, including *Eleutherodactylus bilineatus*, were removed from the genus and transferred to the resurrected genus *Ischnocnema* Reinhardt & Lütken, 1862 (Heinicke et al., 2007). Species of *Ischnocnema* were later grouped into five series (*I. guentheri*, *lactea*, *parva*, *ramagii*, and *verrucosa* species series), and *I. bilineata* was tentatively added to the *I. lactea*

1797 series based on its overall external morphology, since it had not yet been included in
1798 phylogenetic analyses (Hedges, Duellman, & Heinicke, 2008).
1799 The proposed composition of *Ischnocnema* was long based on poorly sampled
1800 phylogenies, as previous studies had included only up to five species out of the more than 30
1801 known species of *Ischnocnema*, and geographic distribution was the main criteria to assign
1802 species to the genus (Heinicke et al., 2007; Hedges et al., 2008). Canedo & Haddad (2012)
1803 were the first to test the phylogenetic position of *Eleutherodactylus bilineatus*. They used a
1804 molecular phylogenetic framework composed of 80% of the described species of
1805 *Ischnocnema* at the time, including representatives of all species series. Surprisingly, instead
1806 of being related to other species from the Atlantic forest of southeast Brazil,
1807 *Eleutherodactylus bilineatus* was found to be the sister species of a clade including the
1808 Andean genus *Noblella* Barbour, 1930 and *Barycholos* Heyer, 1969, a genus that comprises a
1809 species from Cerrado and another species from Ecuatorian Chocó (Canedo & Haddad, 2012).
1810 However, although *Eleutherodactylus bilineatus*, *Barycholos*, and *Noblella* formed a well-
1811 supported clade, the relationship of *Eleutherodactylus bilineatus* with the other two genera
1812 showed low support and the species was left as *incertae sedis* within the subfamily
1813 Holoadeninae (Canedo & Haddad, 2012).
1814 Many other phylogenetic analyses further recovered the clade including *Barycholos*,
1815 *Noblella,* and "*Eleutherodactylus*" *bilineatus* (De la Riva, Chaparro, Castroviejo-Fisher, &
1816 Padial, 2017; Guayasamin et al., 2017; Venegas, Barboza, De la Riva, & Padial, 2018; Santa-
1817 Cruz et al., 2019; Reyes-Puig et al., 2019). Nevertheless, the relationship between
1818 "*Eleutherodactylus*" *bilineatus* and those two genera still remains contentious. The species
1819 has been placed as either the sister of *Noblella* (De la Riva et al., 2017; Guayasamin et al.,
1820 2017; Venegas et al., 2018; Reyes-Puig et al., 2019) or of *Barycholos* and *Noblella* (De la
1821 Riva et al., 2017; Santa-Cruz et al., 2019). The low support for the relationship between those

1822 two genera and "*E*." *bilineatus* has prevented taxonomic decisions related to this species.
1823 Moreover, in some analyses, the inclusion of "*Eleutherodactylus*" *bilineatus* in any of its
1824 closest related genera, *Barycholos* or *Noblella*, would render a non-monophyletic grouping.
1825 An alternative solution to the inclusion of this species in either *Barycholos* or *Noblella* would
1826 be synonymizing *Barycholos* to *Noblella* and include "*E*." *bilineatus* within *Noblella*.
1827 However, this is also not a desirable solution because these two genera are morphologically
1828 different, each one having diagnosable morphological characters (Canedo & Haddad, 2012).
1829 Guayasamin et al. (2017) found "*Eleutherodactylus*" *bilineatus* sister to *Noblella* in both their
1830 maximum likelihood and Bayesian analyses and, besides the low support for this relationship,
1831 they placed the species in *Noblella*. Even though it was a new combination, the authors did
1832 not discuss or comment on the taxonomic placement of "*Eleutherodactylus*" *bilineatus* in
1833 *Noblella*.

1834 In this study, we test the phylogenetic position of "*Eleutherodactylus*" *bilineatus*,
1835 especially regarding its relationship with the Holoadeninae genera *Barycholos* and *Noblella*,
1836 and reassess the taxonomic status of this long-term *incertae sedis* species. We use
1837 phylogenetic analyses of nuclear and mitochondrial gene sequences and data for external
1838 morphology and osteology of "*Eleutherodactylus*" *bilineatus* and its related genera to support
1839 the recognition of a new genus of Holoadeninae.

1840

1841 **2 MATERIAL AND METHODS**

1842 **2.1 Molecular Analyses**

1843 **Taxon and gene sampling:** We follow the family taxonomy proposed by Padial, Grant, &
1844 Frost (2014). According to their classification, "*Eleutherodactylus*" *bilineatus*, as well as the
1845 genera *Barycholos* and *Noblella*, belong to the subfamily Holoadeninae of the family

Craugastoridae. We included all the species belonging to all genera of Holoadeninae that have molecular data available on GenBank, except species of *Qosqophryne* Catenazzi, Mamani, Lehr & von May, 2020. However, due to the taxonomic instability of families and subfamilies of Brachycephaloidea and the existence of an alternative classification (Heinicke, Lemmon, Lemmon, McGrath, & Hedges, 2018), we included terminals for the other two subfamilies of Craugastoridae. The subfamily Craugastorinae is represented by the genera *Craugastor* Cope, 1862, *Haddadus* Hedges, Duellman & Heinicke, 2008, and *Strabomantis* Peters, 1863, and Ceuthomantinae is represented by *Ceuthomantis* Heinicke, Duellman, Trueb, Means, MacCulloch & Hedges, 2009, *Pristimantis* Jiménez de la Espada, 1870, and *Yunganastes* Padial, Castroviejo-Fisher, Köhler, Domic & De la Riva, 2007. We also included genera of the families Brachycephalidae (*Brachycephalus* Fitzinger, 1826 and *Ischnocnema*) and Eleutherodactylidae (*Adelophryne*, *Diasporus* Hedges, Duellman & Heinicke, 2008, and *Eleutherodactylus*). We rooted all our analyses with the distant clade formed by the species *Fritziana fissilis* and *Agalychnis callidryas*. Our final dataset includes 135 species and 151 terminal taxa.

We chose the mitochondrial 12S rRNA, tRNA Val, and partial sequence of 16S rRNA genes, as well as nuclear genes recombination-activating gene 1 (RAG1) and tyrosinase precursor (tyr) to perform our analyses. These gene fragments were available to most of our terminals and have been successfully used in several phylogenetic studies of the Brachycephaoidea (e.g. Canedo & Haddad, 2012; Padial et al., 2014). Sequences for 12S, 16S, tRNAvaline, RAG, and TYR genes were newly produced for this study Accession numbers ######## to ########). Specimen voucher numbers for newly produced sequences and accession numbers for all sequences used in this study are listed in Table S1.

DNA extraction and sequencing: We extracted whole DNA from 99.5% ethanol preserved tissue (muscle or liver) following Lyra, Haddad, & Azeredo-Espin (2017) and performed PCR amplifications using Taq DNA Polymerase Master Mix (Ampliqon S/A, Denmark) and Axygene Maxygene thermocyclers. PCR program was a 3 min initial denaturing step at 95 °C, followed by 35–38 (nuclear 42–45) cycles of 20 s at 95 °C, 20 s at 50–56 °C, and 45 (fragments around 500 bp) or 80 s (fragments around 1000 bp), followed by a final extension step of 3 min at 68 °C. For the RAG 1 we used a nested-PCR program following Taucce et al. (2018). Primers and respective gene fragments are in Table 1.

Phylogenetic analyses: We conducted alignment with MAFFT v.730b (Katoh & Standley, 2013) using G-INS-i algorithm for the coding gene fragments (RAG1 and tyr) and the E-INS-i algorithm for the 12S, tVal, and 16S gene fragments. We performed an *a priori* partition scheme with the three mitochondrial loci and each codon position of the nuclear loci as different partitions, totaling nine partitions. We used PartitionFinder 2.1.1 (Lanfear, Frandsen, Wright, Senfeld, & Calcott, 2017) to search for the best partition scheme and respective best-fitting nucleotide substitution models under the Corrected Akaike Information Criterion (AICc; Hurvich & Tsai, 1989). PartitionFinder uses a maximum likelihood software in the analyses and we chose PhyML 3.0 (Guindon et al., 2010) for this purpose.

We performed tree searches using Bayesian inference (BI) and maximum likelihood (ML). We computed BI analysis in MrBayes 3.2.6 (Ronquist et al., 2012) using two independent runs of 3.0×10^7 generations, starting with random trees and four Markov chains (one cold), sampled every 3000 generations. We discarded 25% of generations and trees as burn-in and performed the run with unlinked character state frequencies, substitution rates of the GTR model, gamma shape parameters, and proportion of invariable sites between partitions. We used the standard deviation of split frequencies (< 0.01), Effective Sample Size

(ESS > 200), and Potential Scale Reduction Factor (PSRF; Gelman & Rubin, 1992; should approach 1.0 as runs converge) to assess convergence of the runs. We performed ML analysis in RAxML 8.2.12 (Stamatakis, 2014), searching the most likely tree 100 times and then we conducted 1,000 replicates of non-parametric bootstrap to assess support.

2.2 Morphology

The study of morphology was based on external morphology and osteology. Terminology for morphological characters used in the diagnosis and descriptions follows Duellman & Lehr (2009). Cranial and postcranial osteology follows the terminology in Trueb (1993). We followed Heyer (1975) for the shape of sternum (his character 32), Guayasamin (2004) for the shape of omosternum, and Ponssa (2008) for the shape of extreme of posterolateral process of hyoid (her character 74). The aim of comparisons is to provide evidence of divergence, hence we restricted comparisons to closely related species, which includes species of *Barycholos*, *Euparkerella* Griffiths, 1959, *Holoaden* Miranda-Ribeiro, 1920, and *Noblella* Northern Clade (*sensu* Reyes-Puig et al., 2019). Comparisons were based both on descriptions and examination of museum specimens, including types. Specimens examined are listed in Appendix. Museum abbreviations are those cited by Frost (2020).

3 RESULTS

3.1 Molecular analyses

The final alignment comprises 3,949 bp divided as follows: 12S rRNA (1,118 bp), tVal (75 bp), 16S rRNA (1,556 bp), RAG1 (645 bp), and tyr (555 bp). The optimal partition scheme includes eight partitions instead of the nine divided *a priori*, with the partitions including the second positions of RAG1 and tyr as a single partition. Partitions and respective nucleotide substitution models are in Table 2. In preliminary alignments, the tVal fragment of

1920 "*Eleutherodactylus*" *bilineatus* was only partially homologous to the tVal of other
1921 brachycephaloids. Because the fragment should be homologous in our whole matrix, we opted
1922 to exclude the whole region in "*E.*" *bilineatus* from our analyses.
1923 Our analyses recovered all genera monophyletic, except for *Noblella* and
1924 *Psychrophrynella* Hedges, Duellman & Heinicke, 2008, in both ML and BI analyses (Figure 1
1925 and Figure S1). *Noblella madreselva* is embedded in a clade including *Psychrophrynella*
1926 *chirihampatu*, *P. glauca*, and *P. usurpator*, rendering *Psychrophrynella* paraphyletic. The
1927 clade including *Noblella losamigos*, *N. madreselva*, *N. pygmaea*, and *N. thiuni* (*Noblella*
1928 Southern Clade *sensu* Reyes-Puig et al., 2019) and *Psychrophrynella chirihampatu*, *P.*
1929 *glauca*, and *P. usurpator* is sister to *Microkayla*, while the clade including *Noblella heyeri*, *N.*
1930 *lochites*, *N. myrmecoides*, *N. naturetrekii*, and *N. personina* (*Noblella* Northern Clade *sensu*
1931 Reyes-Puig et al., 2019) is related to *Barycholos* and "*Eleutherodactylus*" *bilineatus*.
1932 We recover the clade including *Barycholos*, "*Eleutherodactylus*" *bilineatus*, and
1933 *Noblella* Northern Clade with ML bootstrap support of 100% and posterior probability of
1934 100% in BI. "*Eleutherodactylus*" *bilineatus* clearly represents a divergent lineage that is not
1935 embedded in *Barycholos* nor in *Noblella* Northern Clade. Moreover, its relationships with
1936 *Barycholos* and *Noblella* Northern Clade differ in the ML and BI analyses. In ML,
1937 "*Eleutherodactylus*" *bilineatus* is sister to *Noblella* Northern Clade with low support (45%)
1938 and *Barycholos* is the sister group of this clade. In BI, "*Eleutherodactylus*" *bilineatus* is sister
1939 to a low-supported clade including *Barycholos* and *Noblella* Northern Clade (82%).
1940 The analysis of external morphology and osteology of "*Eleutherodactylus*" *bilineatus*
1941 indicates that the species does not belong to either *Barycholos* or *Noblella*. Even though it
1942 shares some features that are considered diagnosable for *Barycholos* or *Noblella*, the
1943 combination of characters found in "*Eleutherodactylus*" *bilineatus* clearly distinguishes it
1944 from species of these two genera. The phylogenetic position and morphological

distinctiveness of "*Eleutherodactylus*" *bilineatus* in comparison with its relatives support the placement of this species in a new genus that we name and diagnose below.

3.2 Systematics

Order Anura Oppel, 1811

Superfamily Brachycephaloidea Günther, 1858

Family Craugastoridae Hedges, Duellman, & Heinicke, 2008

Subfamily Holoadeninae Hedges, Duellman, & Heinicke, 2008

Eleutherodactylus bilineatus Bokermann, 1975

Eleutherodactylus (Eleutherodactylus) bilineatus: Lynch & Duellman, 1997

Ischnocnema bilineata: Heinicke et al., 2007

"*Eleutherodactylus*" *bilineatus*: Canedo & Haddad, 2012

Heyerus bilineatus: **New Genus**

Genus *Heyerus* Motta, Taucce, Haddad & Canedo **New Genus**

Type-species: *Heyerus bilineatus* (Bokermann, 1975) by original designation.

Etymology: The specific epithet is used as a noun in the genitive case and honors Dr. W. Ronald Heyer for his invaluable contributions on systematics, evolution, and biogeography of Neotropical amphibians.

Diagnosis: (1) Skin on dorsum smooth; no dorsolateral folds; (2) tympanic annulus and columella present; tympanic membrane distinct externally; (3) terminal discs on fingers and toes not expanded and not pointed; pads and circumferential grooves present on fingers and toes; terminal phalanges of fingers T-shaped; (4) short, tubercle-like inner tarsal fold present; (5) nasals large, quadrangular, and in contact along their inner border; (6) vomers bearing a

broad dentigerous process, separated from each other; vomerine teeth present; anterior alae of vomers broad; (7) alary process of hyoid absent; posterior border of posteromedial process of hyoid expanded and concave (Figure 3); (8) omosternum long and arrow-shaped; sternum bifurcated posteromedially (Figure 4).

Comparisons with other genera: *Heyerus* can be easily distinguished from its closest related genera *Barycholos*, *Euparkerella*, *Holoaden*, and *Noblella* Northern Clade (Table 3). The expanded and concave posterior border of posteromedial process of hyoid (Figure 3) is the only diagnostic character of *Heyerus* that is not shared by any other of those genera. However, that character is not known for any species of *Euparkerella*. The smooth dorsum without folds differentiates *Heyerus* from *Barycholos* (dorsal folds present in *Barycholos*) and *Holoaden* (dorsum heavily glandular in *Holoaden*). The presence of tympanic membrane, tympanic annulus and columella differentiates *Heyerus* from *Euparkerella* and *Holoaden* (tympanic membrane, tympanic annulus, and columella absent in *Euparkerella* and *Holoaden*). Terminal discs not pointed differs *Heyerus* from *Euparkerella* and *Noblella* Northern Clade whose terminal discs on fingers and toes are pointed. The T-shaped terminal phalanges of fingers differ *Heyerus* from *Euparkerella* (terminal phalanges with hook-like lateral processes in *Euparkerella*). An inner tarsal fold is present in *Heyerus* and its closest relatives, *Barycholos* and *Noblella* Northern Clade, but it is absent in *Euparkerella* and *Holoaden*. The large quadrangular nasals differentiate *Heyerus* from *Euparkerella*, *Holoaden*, and *Noblella* Northern Clade (nasals are medium sized in *Euparkerella* and *Holoaden*, and small in *Noblella* Northern Clade). Dentigerous processes and vomerine teeth are absent in *Euparkerella* and *Noblella* Northern Clade and present in *Heyerus*. The absence of alary process of hyoid differs *Heyerus* from *Barycholos* (alary process of hyoid present in *Barycholos*).

Distribution: *Heyerus bilineatus* is known from the Brazilian Atlantic Forest (sea level up to 900 meters) from the Paraguaçu River to the Jequitinhonha River in southern and central Bahia, northeastern Brazil (Dias, de Mira-Mendes, Souza-Costa, Juncá, & Solé, 2017).

4 DISCUSSION

Molecular and comparative morphological data supports the erection of a new monotypic genus of Holoadeninae, Craugastoridae. The new genus forms a fully supported clade with *Barycholos* and *Noblella* Northern Clade and shows a combination of morphological traits that distinguishes it from its relatives.

Integrative studies addressing the taxonomy of terraranan frogs have revealed that species believed to form a natural group are actually phylogenetically distant and many new genera of Brachycephaloidea have been recognized and named to accommodate species or a clade of species that represent independent lineages. In their major reorganization of direct-developing frogs, Hedges et al. (2008) recovered and erected many genera to include natural groups of species and, subsequently, four new genera of Brachycephaloidea were described (Heinicke et al., 2009; Heinicke, Barrio-Amorós, & Hedges, 2015; De la Riva et al., 2017; Catenazzi et al., 2020). Many of these genera contained less than five species when they were erected or described and, interestingly, subsequent studies revealed a much greater diversity in some of them. For example, *Bryophryne* Hedges, Duellman & Heinicke, 2008 included only two species in its description and is now composed of 11 species (Hedges et al., 2008; De la Riva et al., 2017; Catenazzi, Mamani, Lehr, & von May, 2020) and *Lynchius* was described to accommodate three species and now is composed of seven species (Hedges et al., 2008; Motta et al., 2016; Sánchez-Nivicela, Urgilés, Navarrete, Yánez-Muñoz, & Ron, 2019). Moreover, Trevisan et al. (2020) found a remarkable hidden diversity in the genus

Pristimantis from the northern Brazilian Atlantic Forest. Their analyses show that the populations of *Pristimantis* assigned to three nominal species, represent nine highly structured lineages that may correspond to undescribed species. In this regard, the diversity of *Heyerus* could be underestimated and future researches might reveal a higher number of species belonging to this genus. On the other hand, terraranan clades show a high heterogeneity in rate of diversification regardless of clades age (González-Voyer, Padial, Castroviejo-Fisher, De la Riva, & Vila, 2011) and some genera from the Brazilian Atlantic Forest, such as *Euparkerella*, *Holoaden*, and *Haddadus*, as well as *Barycholos* represent clades that have low species richness. Therefore, it is possible that *Heyerus* also constitutes a lineage or terraranan frogs with low species diversity, similar to its closely relative genera.

Inferred relationships and distribution patterns point out connections among distant biogeographical areas of South America (e.g. Atlantic Forest and the Andes; Cerrado and Chocó), and a widespread distribution of an ancestor for the clade including *Barycholos*, *Heyerus*, and *Noblella* Northern Clade (Hedges et al., 2008; Figure 5). A Northern Atlantic Forest–Andean connection is also supported by phylogenetic relationships of species in the terraranan genus *Oreobates* Jiménez de la Espada, 1872 (Teixeira Jr., Amaro, Recoder, Sena, & Rodrigues, 2012; Vaz-Silva, Maciel, de Andrade, & Amaro, 2018), and *Pristimantis* (Canedo & Haddad, 2012).

Inferred relationships also show that species with similar external morphology from central and northern Andes that have been included in the same genus are, in fact, part of different clades. The genus *Lynchius* Hedges, Duellman & Heinicke, 2008, for example, was erected by Hedges et al. (2008) to include three species from northern Andes that were considered part of *Phrynopus* Peters, 1873, an exclusively central Andean genus. Our analyses recover species of *Noblella* in two different clades, one including species from central Andes and the other one including species from northern Andes, that are not sister to

each other. Previous studies have found the same relationship (De la Riva et al., 2017; Catenazzi & Ttito, 2019; Santa-Cruz et al., 2019; Reyes-Puig et al., 2019; Catenazzi et al., 2020), but they refrain from proposing a new generic arrangement because the affinities of *Noblella peruviana* and *Psychrophrynella bagrecito*, the type species of *Noblella* and *Psychrophrynella*, remain unclear. Morphological evidence indicates that *P. bagrecito*, as well as most species of the genus, share a considerable number of traits with *N. peruviana* (De la Riva et al., 2017). In a scenario where these two species are part of the clade including *Noblella* Southern Clade and *Psychrophrynella* species, *Psychrophrynella* would become a junior synonym of *Noblella*, while *Phyllonastes* Heyer, 1977 would be the name available for the *Noblella* Northern Clade. An alternative scenario would place *N. peruviana* in the *Noblella* Northern Clade. In this case, species of *Noblella* Southern Clade would be transferred to *Psychrophrynella* and the name *Noblella* would apply to the *Noblella* Northern Clade. Therefore, it is crucial to infer the phylogenetic position of the type-species *Noblella peruviana* and *Psychrophrynella bagrecito* before making any taxonomic decision about these genera.

The classification of families and subfamilies of Brachycephaloidea has faced many changes since 2008, when Hedges et al. (2008) rearranged the taxonomy of the group. One reason for this instability is that the relationship among genera varies among the different analyzes, and authors have been including in the same family genera from clades that show low support and, therefore, have different relationships in different analyzes, rendering proposed families paraphyletic (see Hedges et al., 2008; Padial et al., 2014; Heinicke et al., 2018). Another important reason for the instability is that the decisions have been made based only on molecular data, and synapomorphies for clades representing different hierarchies (Family, Subfamily, and Genus) have not yet been proposed. This makes the selected

hierarchy of a clade (i.e., if the clade is considered a Family, Subfamily or Genus) arbitrary and contributes to the taxonomic instability in this group.

However, it is worth noting that, even considering different datasets and optimality criteria, there are clades that show high stability, i.e., clades that have been recovered with high support in all available analyzes that include representatives of all families of brachycephaloids: *Lynchius*, *Oreobates*, and *Phrynopus*; *Euparkerella* and *Holoaden*; *Pristimantis* and *Yunganastes*; *Barycholos*, *Bryophryne*, *Heyerus*, *Microkayla* De la Riva, Chaparro, Castroviejo-Fisher & Padial, 2017, *Noblella*, and *Psychrophrynella*.

Even though most of those stable clades are represented by the subfamilies of Strabomantidae in Heinicke et al. (2018), the family classification is probably far from becoming stable. The instability of the families Craugastoridae and Strabomantidae is mostly due to the position of the genus *Strabomantis*. When *Strabomantis* is recovered as sister group to a clade that comprises *Craugastor*, Strabomantidae is included in the synonym of Craugastoridae (Pyron & Wiens, 2011; Padial et al., 2014). When *Strabomantis* is recovered embedded in the Strabomantidae clade, and the clade comprising *Craugastor* is the sister clade to all other Strabomantidae, the two families are considered valid (Hedges et al., 2008; Heinicke et al., 2018; Jetz & Pyron, 2018) (Figure 6).

A solution to the instability in the family taxonomy of this group would be to split the subfamily Pristimantinae *sensu* Heinicke et al. (2018) into two families (one including *Pristimantis* and *Yunganastes*, and another including *Lynchius*, *Oreobates*, and *Phrynopus*) and elevate the subfamilies *sensu* Heinicke et al. (2018) to family rank. That classification would render all the families monophyletic in all available analyzes to date that have included representatives of all families of brachycephaloids. Ongoing studies of the anatomy of terraranan frogs (e.g., Taboada, Grant, Lynch, & Faivovich, 2013) are leading to the discovery of synapomorphies at different levels. In view of the relevance of including

morphological datasets for terraranan systematics, we reinforce the need of integration of various data sources for a more accurate classification of this group.

ACKNOWLEDGMENTS

We thank J. Pombal Jr. (MNRJ), T. Grant (MZUSP), R. Brown (KU), and R. Glor (KU) for allowing access to material under their care. AM thanks São Paulo Research Foundation (FAPESP) for her PhD. scholarship (grant #2017/08488-3). PPGT thanks FAPESP for his Postdoctoral fellowship (grant #2019/04076-8). FAPESP (grant #2013/50741-7) and Conselho Nacional de Desenvolvimento Científico e Tecnológico (CNPq; grant #306623/2018-8) provided financial support to CFBH. Rio de Janeiro Research Foundation (FAPERJ) provided financial support to CC (grants #E-26/210.034/2018; #E-26/010.100954/2018; #E-26/211.154/2019). M. Lyra helped with molecular procedures. We are grateful to Centro de Estudos de Insetos Sociais (São Paulo State University [UNESP]) for allowing us the use of the molecular laboratory. This research was supported by resources supplied by Núcleo de Computação Científica/Universidade Estadual Paulista Júlio de Mesquita Filho (NCC/UNESP) and Cyberinfrastructure for Phylogenetic Research.

REFERENCES

Bokermann, W. C. A. (1975 "1974"). Três espécies novas de *Eleutherodactylus* do sudeste da Bahia, Brasil (Anura, Leptodactylidae). *Revista Brasileira de Biologia*, 34, 11–18.

Bossuyt, F., & Milinkovitch, M. C. (2000). Convergent adaptive radiations in Madagascan and Asian ranid frogs reveal covariation between larval and adult traits. *Proceedings of the National Academy of Sciences of the United States of America*, 97, 6585–6590. https://doi.org/10.1073/pnas.97.12.6585

2117 Canedo, C., & Haddad, C. F. B. (2012). Phylogenetic relationships within anuran clade
2118 Terrarana, with emphasis on the placement of Brazilian Atlantic rainforest frogs genus
2119 *Ischnocnema* (Anura: Brachycephalidae). *Molecular Phylogenetics and Evolution*, 65,
2120 610–620. https://doi.org/10.1016/j.ympev.2012.07.016
2121 Catenazzi, A., & Ttito, A. (2019). *Noblella thiuni* sp. n., a new (singleton) species of minute
2122 terrestrial-breeding frog (Amphibia, Anura, Strabomantidae) from the montane forest
2123 of the Amazonian Andes of Puno, Peru. *PeerJ 7*, e6780, 1–15.
2124 https://doi.org/10.7717/peerj.6780
2125 Catenazzi, A., Mamani, L., Lehr, E., & von May, R. (2020). A new genus of terrestrial-
2126 breeding frogs (Holoadeninae, Strabomantidae, Terrarana) from southern Peru.
2127 *Diversity* 12, 1–17. https://doi:10.3390/d12050184
2128 De la Riva, I., Chaparro, J.C., Castroviejo-Fisher, S., & Padial, J.M. (2017). Underestimated
2129 anuran radiations in the high Andes: five new species and a new genus of
2130 Holoadeninae, and their phylogenetic relationships (Anura: Craugastoridae).
2131 *Zoological Journal of the Linnean Society*, 182, 129–172.
2132 https://doi.org/10.1093/zoolinnean/zlx020
2133 Dias, I. R., de Mira-Mendes, C. V., Souza-Costa, C. A., Juncá, F. A., & Solé, M. (2017). The
2134 advertisement call and comments on the distribution of *Eleutherodactylus*
2135 *bilineatus* Bokermann, 1975, an endemic frog of Bahia State, Brazil (Amphibia,
2136 Anura). *ZooKeys*, 677, 151–159. https://doi.org/10.3897/zookeys.677.12309
2137 Duellman, W. E., & Lehr, E. (2009). *Terrestrial-breeding frogs (Strabomantidae) in Peru*.
2138 Germany. 382 pp.
2139 Feller, A. E., & Hedges, S. B. (1998). Molecular evidence for the early history of living
2140 amphibians. *Molecular Phylogenetics and Evolution*, 9, 509–16.
2141 https://doi.org/10.1006/mpev.1998.0500

2142 Frost, D. R. (2020). Amphibian Species of the World: an Online Reference. Version 6.0.
2143 American Museum of Natural History American Museum of Natural History, New
2144 York, USA. Available from:
2145 http://research.amnh.org/herpetology/amphibia/index.html (accessed 21 July 2020).
2146 Gelman, A., & Rubin, D. B. (1992). Inference from iterative simulation using multiple
2147 sequences. *Statistical Science*, 7, 457–511.
2148 Goebel, A. M., Donnelly, J. M., & Atz, M. E. (1999). PCR primers and amplification methods
2149 for 12S ribosomal DNA, the control region, cytochrome oxidase I, and cytochrome b
2150 in bufonids and other frogs, and an overview of PCR primers which have amplified
2151 DNA in amphibians successfully. *Molecular Phylogenetics and Evolution*, 11, 163–
2152 199. https://doi.org/10.1006/mpev.1998.0538
2153 González-Voyer, A., Padial, J. M., Castroviejo-Fisher, S., De la Riva, I., & Vila, C. (2011).
2154 Correlates of species richness in the largest Neotropical amphibian radiation. *Journal*
2155 *of Evolutionary Biology*, 24, 931–942. https://doi.org/10.1111/j.1420-
2156 9101.2011.02243.x
2157 Graybeal, A. (1997). Phylogenetic relationships of bufonid frogs and tests of alternate
2158 macroevolutionary hypotheses characterizing their radiation. *Zoological Journal of the*
2159 *Linnean Society*, 119, 297–338.
2160 Guayasamin, J.M. (2004.) The *Eleutherodactylus orcesi* species group (Anura:
2161 Leptodactylidae): comparative osteology and comments on its monophyly.
2162 *Herpetological Monographs*, 18, 142–174. https://doi.org/10.1655/0733-
2163 1347(2004)018[0142:TEOSGA]2.0.CO;2
2164 Guayasamin, J. M., Hutter, C. R., Tapia, E. E., Culebras, J., Peñafiel, N., Pyron, R. A.,
2165 Morochz, C., Funk, W. C., & Arteaga-Navarro, A. F. (2017). Diversification of the

2166 rainfrog *Pristimantis ornatissimus* in the lowlands and Andean foothills of Ecuador.
2167 *PLoS One 12*, 3e0172615, 1–21. https://doi.org/10.1371/journal.pone.0172615
2168 Guindon, S., Dufayard, J. F., Lefort, V., Anisimova, M., Hordijk, W., & Gascuel, O. (2010).
2169 New algorithms and methods to estimate maximum-likelihood phylogenies: assessing
2170 the Performance of PhyML 3.0. *Systematic Biology*, 59, 307–332.
2171 https://doi.org/10.1093/sysbio/syq010
2172 Hedges, S. B. (1994). Molecular evidence for the origin of birds, *Proceedings of the National*
2173 *Academy of Sciences of the United States of America*, 91, 2621–2624.
2174 Hedges, S. B., W. E. Duellman, & Heinicke, M. P. (2008). New World direct-developing
2175 frogs (Anura: Terrarana): Molecular phylogeny, classification, biogeography, and
2176 conservation. *Zootaxa*, 1737, 1–182. https://doi.org/10.11646/zootaxa.1737.1.1
2177 Heinicke, M. P., Duellman, W. E., & Hedges, S. B. (2007). Major Caribbean and Central
2178 American frog faunas originated by oceanic dispersal. *Proceedings of the National*
2179 *Academy of Sciences*, 104, 10092–10097. https://doi.org/10.1073/pnas.0611051104
2180 Heinicke, M. P., Duellman, W. E., Trueb, L., Means, D. B., MacCulloch, R. D., & Hedges, S.
2181 B. (2009). A new frog family (Anura: Terrarana) from South America and an
2182 expanded direct-developing clade revealed by molecular phylogeny. *Zootaxa*, 2211,
2183 1–35. https://doi.org/10.5281/zenodo.189873
2184 Heinicke, M. P., Barrio-Amorós, C. L., & Hedges, S. B. (2015). Molecular and morphological
2185 data support recognition of a new genus of New World direct-developing frog (Anura:
2186 Terrarana) from an under-sampled region of South America. *Zootaxa*, 3986, 151–172.
2187 https://doi.org/10.11646/zootaxa.3986.2.1
2188 Heinicke, M.P., Lemmon, A. R., Lemmon, E. M., McGrath, K., & Hedges, S. B. (2018).
2189 Phylogenomic support for evolutionary relationships of New World direct-developing

2190 frogs (Anura: Terraranae). *Molecular Phylogenetics and Evolution*, 118, 145–155.
2191 https://doi.org/10.1016/j.ympev.2017.09.021
2192 Heyer, W. R. (1975). A preliminary analysis of the intergeneric relationships of the frog
2193 family Leptodactylidae. *Smithsonian Contributions to Zoology*, 199, 1–55.
2194 Heyer, W. R. (1977). Taxonomic notes on frogs from the Madeira and Purus rivers, Brasil.
2195 *Papéis Avulsos de Zoologia*, 31, 141–162.
2196 Hoogmoed, M. S., Borges-Nojosa, D. M., & Cascon, P. (1994). Three new species of the
2197 genus *Adelophryne* (Amphibia: Anura: Leptodactylidae) from northeastern Brazil,
2198 with remarks on the other species of the genus. *Zoologische Mededelingen. Leiden*,
2199 68, 271–300.
2200 Hurvich, C. M., & Tsa,i C. L. (1989). Regression and time series model selection in small
2201 samples. *Biometrika*, 76, 297–307.
2202 Jetz, W., & Pyron, R.A. (2018). The interplay of past diversification and evolutionary
2203 isolation with present imperilment across the amphibian tree of life. *Nature Ecology &*
2204 *Evolution*, 2, 850–858.
2205 Katoh, K., & Standley, D. M. (2013). MAFFT multiple sequence alignment software version
2206 7: Improvements in performance and usability. *Molecular Biology and Evolution*, 30,
2207 772–780. https://doi.org/10.1093/molbev/mst010
2208 Lanfear, R., Frandsen, P. B., Wright, A. M., Senfeld, T., & Calcott, B. (2017). Partitionfinder
2209 2: New methods for selecting partitioned models of evolution for molecular and
2210 morphological phylogenetic analyses. *Molecular Biology and Evolution*, 34, 772–773.
2211 https://doi.org/10.1093/molbev/msw260
2212 Lynch, J. D. (1976). The species groups of the South American frogs of the genus
2213 *Eleutherodactylus* (Leptodactylidae). *Occasional Papers of the Museum of Natural*
2214 *History, University of Kansas*, 61, 1–24.

2215 Lynch, J. D., & Myers, C. W. (1983). Frogs of the fitzingeri group of *Eleutherodactylus* in
2216 eastern Panama and Chocoan South America (Leptodactylidae). *Bulletin of the*
2217 *American Museum of Natural History*, 175, 481–572.
2218 Lynch, J. D., & Duellman, W. E. (1997). Frogs of the genus *Eleutherodactylus* in western
2219 Ecuador. *The University of Kansas Natural History Museum, Special Publications*, 23,
2220 1–23.
2221 Lyra, M.L., Haddad, C.F.B., & Azeredo-Espin, A.M.L. (2017). Meeting the challenge of
2222 DNA barcoding Neotropical amphibians: polymerase chain reaction optimization and
2223 new COI primers. *Molecular Ecology Resources*, 17, 966–980.
2224 https://doi.org/10.1111/1755-0998.12648
2225 Motta, A. P., Chaparro, J. C., Pombal Jr., J. P., Guayasamin, J. M., De la Riva, I., & Padial, J.
2226 M. (2016). Molecular phylogenetics and taxonomy of the Andean genus *Lynchius*
2227 Hedges, Duellman, and Heinicke, 2008 (Anura: Craugastoridae). *Herpetological*
2228 *Monographs*, 30, 119–142. https://doi.org/10.1655/HERPMONOGRAPHS-D-16-
2229 00002
2230 Padial, J.M., Grant, T., & Frost, D. R. (2014). Molecular systematics of terraranas (Anura:
2231 Brachycephaloidea) with an assessment of the effects of alignment and optimality.
2232 *Zootaxa*, 3825, 1–132. http://dx.doi.org/10.11646/zootaxa.3825.1.1
2233 Palumbi, S. R., Martin, A. P., Kessing, B. D., & McMillan, W. O. (1991). *Detecting*
2234 *population structure using mitochondrial DNA*. In: Hoelzel AR, ed. Genetic Ecology
2235 of Whales and Dolphins. Cambridge: International Whaling Comission, 203–215.
2236 Ponssa, M. L., (2008). Cladistic analysis and osteological descriptions of the frog species in
2237 the *Leptodactylus fuscus* species group (Anura, Leptodactylidae). *Journal of*
2238 *Zoological Systematics and Evolutionary Research*, 46, 249–266.
2239 https://doi.org/10.1111/j.1439-0469.2008.00460.x

2240 Pyron, R. A., & Wiens, J. J. (2011). A large-scale phylogeny of Amphibia including over
2241 2800 species, and a revised classification of extant frogs, salamanders, and caecilians.
2242 *Molecular Phylogenetics and Evolution*, 61, 543–583.
2243 https://doi.org/10.1016/j.ympev.2011.06.012
2244 Reyes-Puig, J. P., Reyes-Pui,g C., Ron, S. R., Ortega, J. A., Guayasamin, J. M., Goodrum, M.,
2245 Recalde, F., Vieira, J., Koch, C., & Yánez-Muñoz, M. H. (2019). A new species of
2246 terrestrial frog of the genus *Noblella* Barbour, 1930 (Amphibia: Strabomantidae) from
2247 the Llanganates-Sangay Ecological Corridor, Tungurahua, Ecuador. *PeerJ 7*,
2248 e7405, 1–26. https://doi.org/10.7717/peerj.7405
2249 Ronquist, F., Teslenko, M., van der Mark, P., Ayres, D. L., Darling, A., Hohna, S., Larget, B.,
2250 Liu, L., Suchard, M. A., & Huelsenbeck, J. P. (2012). MrBayes 3.2: efficient Bayesian
2251 phylogenetic inference and model choice across a large model space. *Systematic*
2252 *Biology*, 61, 539–542. https://doi.org/10.1093/sysbio/sys029
2253 Sánchez-Nivicela, J. C., Urgilés, V. L., Navarrete, M. J., Yánez-Muñoz, M. H., & Ron, S. R.
2254 (2019). A bizarre new species of *Lynchius* (Amphibia, Anura, Strabomantidae) from
2255 the Andes of Ecuador and first report of *Lynchius parkeri* in Ecuador. *Zootaxa*, 4567,
2256 1–24. https://doi.org/10.11646/zootaxa.4567.1.1
2257 Santa Cruz, R., von May, R., Catenazzi, A., Whitcher, C., López Tejeda, E., & Rabosky, D.
2258 L. (2019). A new species of terrestrial-breeding frog (Amphibia,
2259 Strabomantidae, *Noblella*) from the Upper Madre De Dios watershed, Amazonian
2260 Andes and lowlands of southern Peru. *Diversity*, 11, 1–20.
2261 https://doi.org/10.3390/d11090145
2262 Stamatakis, A. (2014). RAxML version 8: a tool for phylogenetic analysis and post-analysis
2263 of large phylogenies. *Bioinformatics*, 30, 1312–1313.
2264 https://doi.org/10.1093/bioinformatics/btu033

2265 Taboada, C., Grant, T., Lynch, J. D., & Faivovich, J. (2013). New morphological
2266 synapomorphies for the New World direct-developing frogs (Amphibia: Anura:
2267 Terrarana). *Herpetologica*, 69, 342–357. https://doi.org/10.1655/HERPETOLOGICA-
2268 D-13-00019
2269 Taucce P. P. G., Canedo, C., Parreiras, J. S., Drummond, L. O., Nogueira-Costa, P., Haddad,
2270 C. F. B. (2018). Molecular phylogeny of *Ischnocnema* (Anura: Brachycephalidae)
2271 with the redefinition of its series and the description of two new species. *Molecular*
2272 *Phylogenetics and Evolution*, 128, 123–146. https://doi:10.1016/j.ympev.2018.06.042
2273 Teixeira Jr., M., Amaro, R. C., Recoder, R. S., Sena, M. A., & Rodrigues, M. T. (2012). A
2274 relict new species of *Oreobates* (Anura, Strabomantidae) from the Seasonally Dry
2275 Tropical Forests of Minas Gerais, Brazil, and its implication to the biogeography of
2276 the genus and that of South American Dry Forests. *Zootaxa*, 3158, 37–52.
2277 http://dx.doi.org/10.5281/zenodo.209808
2278 Titus, T. A., & Larson, A. (1996). Molecular phylogenetics of desmognathine salmanders
2279 (Caudata: Plethodontidae): a reevaluation of evolution in ecology, life history, and
2280 morphology. *Systematic Biology*, 45, 451–472. https://doi.org/10.1093/sysbio/45.4.451
2281 Trevisan, C. C., Batalha-Filho, H., Garda, A. A., Menezes, L., Dias, I. R., Solé, M., Canedo,
2282 C., Juncá, F. A., & Napoli, M. F. (2020). Cryptic diversity and ancient diversification
2283 in the northern Atlantic Forest *Pristimantis* (Amphibia, Anura, Craugastoridae).
2284 *Molecular Phylogenetics and Evolution*, 148, 1055–7903.
2285 https://doi.org/10.1016/j.ympev.2020.106811
2286 Trueb, L., (1993). Patterns of cranial diversity among the Lissamphibia, in: Hanken, J., Hall,
2287 B.K. (Eds.), The Skull: Patterns of Structural and Systematic Diversity, Vol. 2.
2288 Chicago University Press, Chicago, pp. 255–343.

2289 Vaz-Silva, W., Maciel, N. M., de Andrade, S. P., & Amaro, R. C. (2018). A new cryptic
2290 species of *Oreobates* (Anura: Craugastoridae) from the seasonally dry tropical forest
2291 of central Brazil. *Zootaxa*, 4441, 89–108. https://doi.org/10.11646/zootaxa.4441.1.5
2292 Venegas, P. J., Barboza, A. C., De la Riva, I., & Padial, J. M. (2018). A new species
2293 of *Phrynopus* from the northeastern Andes of Peru, its phylogenetic position, and
2294 notes on the relationships of Holoadeninae (Anura: Craugastoridae).
2295 *Zootaxa*, 4446, 501–524. https://doi.org/10.11646/zootaxa.4446.4.5
2296 Walker, M., Lyra, M. L, Haddad, C. F. B. (2018). Phylogenetic relationships and cryptic
2297 species diversity in the Brazilian egg brooding tree frog, genus *Fritziana* Mello-Leitão
2298 1937 (Anura: Hemiphractidae). *Molecular Phylogenetics and Evolution*, 123, 59–72.
2299 http://dx.doi.org/10.1016/j.ympev.2018.02.012

2300 **TABLES**

2301 **Table 1**. Sequence primers used in this study.

Primer		Gene	Sequence	Reference
MVZ59	F	12S	ATAGCACGTAAAAYGCTDAGATG	Graybeal (1997)
12S L48	F	12S	ATGCAAGYMTCMGCRYCCCNGTGA	Walker et al. (2018)
12S F-H	R	12S	CTTGGCTCGTAGTTCCCTGGCG	Goebel et al. (1999)
12S A-L	F	12S	AAACTGGGATTAGATACCCCACTAT	Goebel et al. (1999)
12S H978	R	12S	CTTACCRTGTTACGACTTRCCT	Walker et al. (2018)
12S L13	F	12S	TTAGAAGAGGCAAGTCGTAACATGGTA	Feller and Hedges (1998)
16S Titus_1	R	16S	GGTGGCTGCTTTTAGGCC	Titus and Larson (1996)
16S L2A	F	16S	CCAAACGAGCCTAGTGATAGCTGGTT	Hedges (1994)
16S H10	R	16S	TGCTTACGCTACCTTTGCACGGT	Hedges (1994)
16S AR	F	16S	CGCCTGTTTATCAAAAACAT	Palumbi et al. (1991)
16S BR	R	16S	GACCTGGATTACTCCGGTCTGA	Palumbi et al. (1991)
R182	F	RAG1	GCCATAACTGCTGGAGCATYAT	Heinicke et al. (2007)
R270	R	RAG1	AGYAGATGTTGCCTGGGTCTTC	Heinicke et al. (2007)
RAG1FF2	F	RAG1	ATGCATCRAAAATTCARCAAT	Heinicke et al. (2007)
RAG1FR2	R	RAG1	CCYCCTTTRTTGATAKGGWCATA	Heinicke et al. (2007)
Tyr1B	F	Tyrosinase	AGGTCCTCYTRAGGAAGGAATG	Bossuyt and Milinkovitch (2000)
Tyr1E	R	Tyrosinase	GAGAAGAAAGAWGCTGGGCTGAG	Bossuyt and Milinkovitch (2000)
Tyr1C	F	Tyrosinase	GGCAGAGGAWCRTGCCAAGATGT	Bossuyt and Milinkovitch (2000)
Tyr1G	R	Tyrosinase	TGCTGGGCRTCTCTCCARTCCCA	Bossuyt and Milinkovitch (2000)

2302

Table 2. Best partition scheme and respective best-fitting molecular models. RAG1 = recombination activating gene, Tyr = tyrosinase, GTR = general time-reversible, K2P = Kimura two-parameter, and SYM = symmetrical.

Partition	Model
12S	GTR + Γ + I
tVal	GTR + Γ + I
16S	GTR + Γ + I
RAG1 1st position	GTR + Γ + I
RAG1 3rd position	K2P + Γ
Tyr 1st position	GTR + Γ + I
Tyr 3rd position	SYM + Γ
RAG1 and Tyr 2nd positions	GTR + Γ + I

Table 3. Comparison of characters used to diagnose *Heyerus*.

Characters	*Heyerus*	*Barycholos*	*Noblella* Northern clade	*Euparkerella*	*Holoaden*
Skin on dorsum	Smooth	Smooth	Smooth	Smooth	Granular
Dorsolateral folds	Absent	Present	Absent	Absent	Absent
Terminal discs shape	Not pointed	Not pointed	Pointed	Pointed	Not pointed
Terminal phalanges shape	T-shaped	T-shaped	Narrowly T-shaped	Hook-like lateral process	T-shaped
Tarsal fold	Present	Present	Present	Absent	Absent
Nasal size	Large	Large	Small	Medium	Medium
Dentigerous process of vomer	Present	Present	Absent	Absent	Present
Vomerine teeth	Present	Present	Absent	Absent	Present
Alary process of hyoid	Absent	Present	Absent	Absent	Absent
Posterior border of posterolateral process of hyoid	Expanded and Concave	Acute	Acute	–	Acute
Sternum shape	Bifurcated posteromedially	Bifurcated posteromedially	Bifurcated posteromedially	Not bifurcated	Not bifurcated
Tympanic annulus and columella	Present	Present	Present	Absent	Absent

FIGURES

Figure 1. The 50% majority rule consensus tree from Bayesian inference for 135 species and 151 terminal taxa of Brachycephaloidea, based on a dataset of 3949 aligned bp of fragments of genes 12S rRNA (1,118 bp), tVal (75 bp), 16S rRNA (1,556 bp), RAG1 (645 bp), and tyr (555 bp). Posterior probabilities are indicated at each node (asterisks represent values of 100%). Family and subfamily classifications proposed by Padial et al. (2014) and Heinicke et al. (2018) are presented on the right.

Figure 2. Adult female holotype (MZUSP 74681) and live specimen of *Heyerus bilineatus*. Photos: MZUSP and Mauro Teixeira Jr.

Figure 3. Ventral view of hyoid apparatus of (A) *Heyerus bilineatus* (CFBH 35720) and (B) *Barycholos ternetzi* (CFBH 11598). Expanded and concave posterolateral process is represented in (A) and acute posterolateral process is represented in (B). Bones are shown in pink and cartilages are shown in blue.

Figure 4. Pectoral girdle of (A) *Heyerus bilineatus* (CFBH 35720), (B) *Noblella heyeri* (KU 196531), and (C) *Holoaden luederwaldti* (MNRJ 3903). Sternum bifurcated posteromedially is represented in (A) and (B); sternum not bifurcated is represented in (C). Bones are shown in pink and cartilages are shown in blue.

Figure 5. The 50% majority rule consensus phylogram and map with type localities of species of the clade including the genera *Barycholos*, *Bryophryne*, *Euparkerella*, *Heyerus*, *Holoaden*, *Microkayla*, *Noblella*, and *Psychrophrynella*. Colors of clades and of points on the map

represent habitats where species and clades occur. Diamond shape represents the type locality of *Heyerus bilineatus*.

Figure 6. Relationships among families and subfamilies of Brachycephaloidea *sensu* Heinicke et al. (2018). Subfamilies of the family Strabomantidae are highlighted in blue. The clade including *Pristimantis* and *Yunganastes* is represented by Pristimantinae1, and the clade including *Lynchius*, *Oreobates*, and *Phrynopus* is represented by Pristimantinae2. Adapted from figure 8 in Padial et al. (2014).

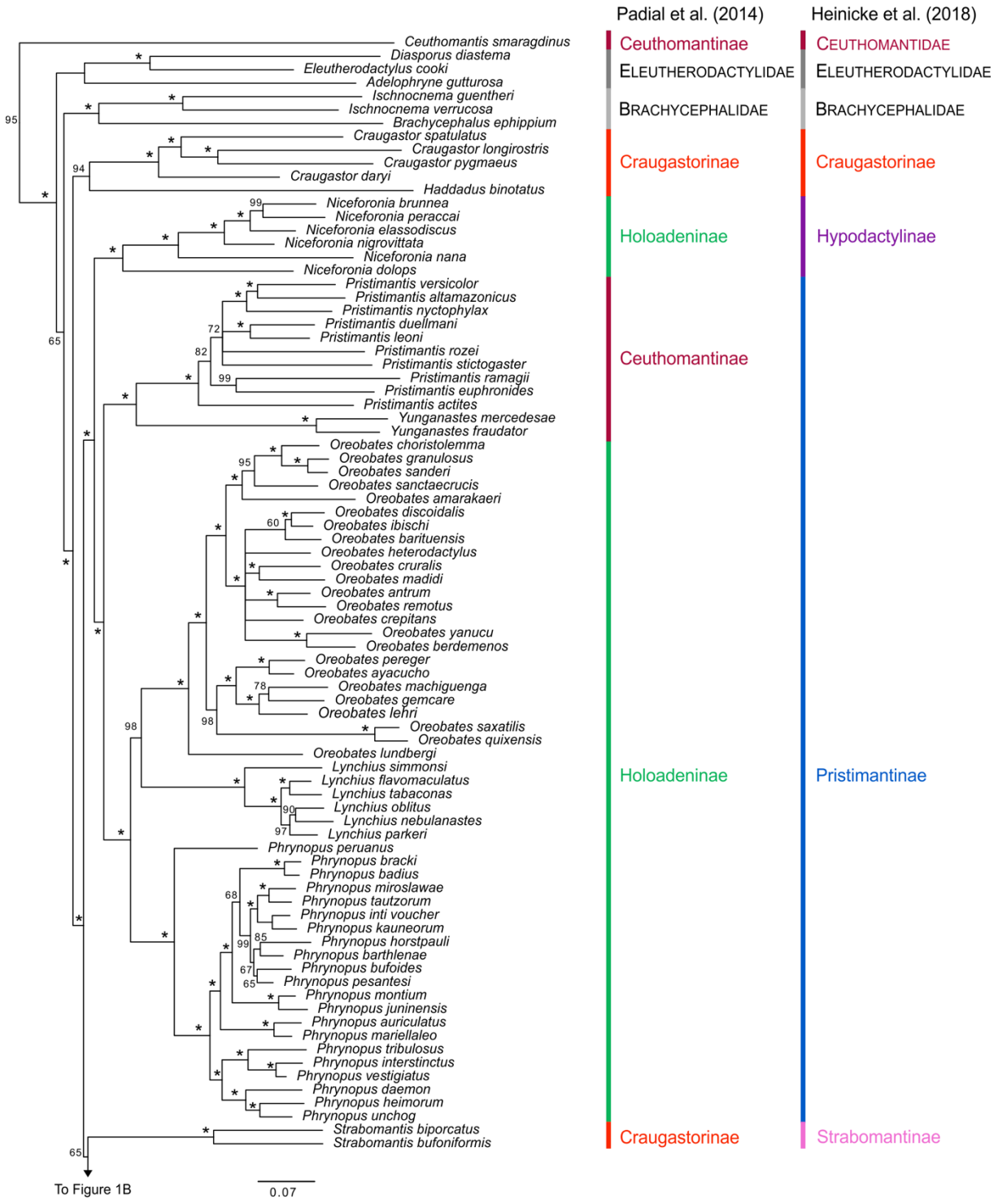
Padial et al. (2014)
Heinicke et al. (2018)
Ceuthomantinae
CEUTHOMANTIDAE
ELEUTHERODACTYLIDAE
ELEUTHERODACTYLIDAE
BRACHYCEPHALIDAE
BRACHYCEPHALIDAE
Craugastorinae
Craugastorinae
Holoadeninae
Hypodactylinae
Ceuthomantinae
Holoadeninae
Pristimantinae
Craugastorinae
Strabomantinae
Ceuthomantis smaragdinus
Diasporus diastema
Eleutherodactylus cooki
Adelophryne gutturosa
Ischnocnema guentheri
Ischnocnema verrucosa
Brachycephalus ephippium
Craugastor spatulatus
Craugastor longirostris
Craugastor pygmaeus
Craugastor daryi
Haddadus binotatus
Niceforonia brunnea
Niceforonia peraccai
Niceforonia elassodiscus
Niceforonia nigrovittata
Niceforonia nana
Niceforonia dolops
Pristimantis versicolor
Pristimantis altamazonicus
Pristimantis nyctophylax
Pristimantis duellmani
Pristimantis leoni
Pristimantis rozei
Pristimantis stictogaster
Pristimantis ramagii
Pristimantis euphronides
Pristimantis actites
Yunganastes mercedesae
Yunganastes fraudator
Oreobates choristolemma
Oreobates granulosus
Oreobates sanderi
Oreobates sanctaecrucis
Oreobates amarakaeri
Oreobates discoidalis
Oreobates ibischi
Oreobates barituensis
Oreobates heterodactylus
Oreobates cruralis
Oreobates madidi
Oreobates antrum
Oreobates remotus
Oreobates crepitans
Oreobates yanucu
Oreobates berdemenos
Oreobates pereger
Oreobates ayacucho
Oreobates machiguenga
Oreobates gemcare
Oreobates lehri
Oreobates saxatilis
Oreobates quixensis
Oreobates lundbergi
Lynchius simmonsi
Lynchius flavomaculatus
Lynchius tabaconas
Lynchius oblitus
Lynchius nebulanastes
Lynchius parkeri
Phrynopus peruanus
Phrynopus bracki
Phrynopus badius
Phrynopus miroslawae
Phrynopus tautzorum
Phrynopus inti voucher
Phrynopus kauneorum
Phrynopus horstpauli
Phrynopus barthlenae
Phrynopus bufoides
Phrynopus pesantesi
Phrynopus montium
Phrynopus juninensis
Phrynopus auriculatus
Phrynopus mariellaleo
Phrynopus tribulosus
Phrynopus interstinctus
Phrynopus vestigiatus
Phrynopus daemon
Phrynopus heimorum
Phrynopus unchog
Strabomantis biporcatus
Strabomantis bufoniformis
To Figure 1B
0.07

Figure 1A

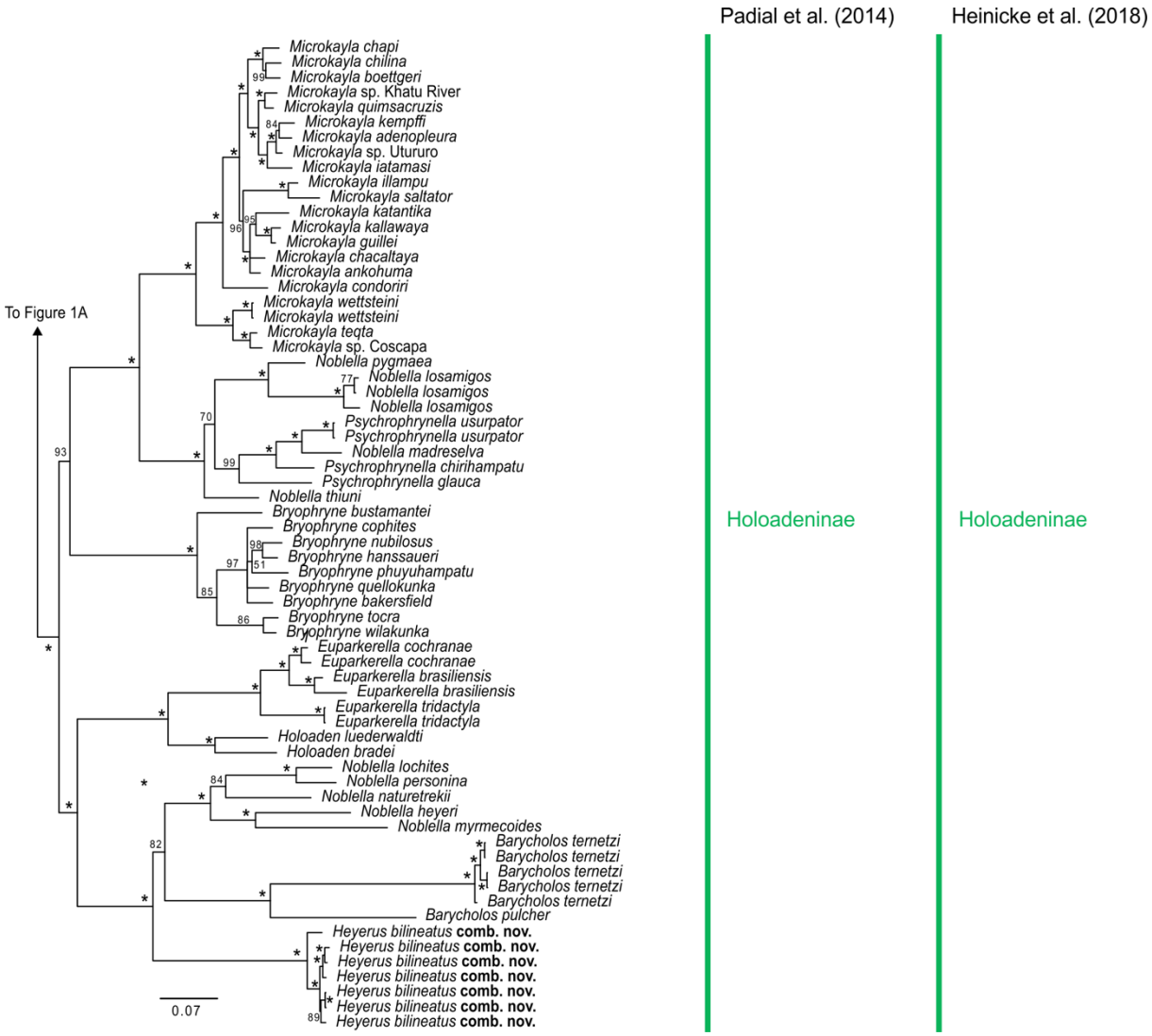
Padial et al. (2014)
Heinicke et al. (2018)
To Figure 1A
Microkayla chapi
Microkayla chilina
Microkayla boettgeri
Microkayla sp. Khatu River
Microkayla quimsacruzis
Microkayla kempffi
Microkayla adenopleura
Microkayla sp. Ututuro
Microkayla iatamasi
Microkayla illampu
Microkayla saltator
Microkayla katantika
Microkayla kallawaya
Microkayla guillei
Microkayla chacaltaya
Microkayla ankohuma
Microkayla condoriri
Microkayla wettsteini
Microkayla wettsteini
Microkayla teqta
Microkayla sp. Coscapa
Noblella pygmaea
Noblella losamigos
Noblella losamigos
Noblella losamigos
Psychrophrynella usurpator
Psychrophrynella usurpator
Noblella madreselva
Psychrophrynella chirihampatu
Psychrophrynella glauca
Noblella thiuni
Bryophryne bustamantei
Bryophryne cophites
Bryophryne nubilosus
Bryophryne hanssaueri
Bryophryne phuyuhampatu
Bryophryne quellokunka
Bryophryne bakersfield
Bryophryne tocra
Bryophryne wilakunka
Euparkerella cochranae
Euparkerella cochranae
Euparkerella brasiliensis
Euparkerella brasiliensis
Euparkerella tridactyla
Euparkerella tridactyla
Holoaden luederwaldti
Holoaden bradei
Noblella lochites
Noblella personina
Noblella naturetrekii
Noblella heyeri
Noblella myrmecoides
Barycholos ternetzi
Barycholos ternetzi
Barycholos ternetzi
Barycholos ternetzi
Barycholos ternetzi
Barycholos pulcher
Heyerus bilineatus comb. nov.
Heyerus bilineatus comb. nov.
Heyerus bilineatus comb. nov.
Heyerus bilineatus comb. nov.
Heyerus bilineatus comb. nov.
Heyerus bilineatus comb. nov.
0.07
Holoadeninae
Holoadeninae

Figure 1B

Figure 2

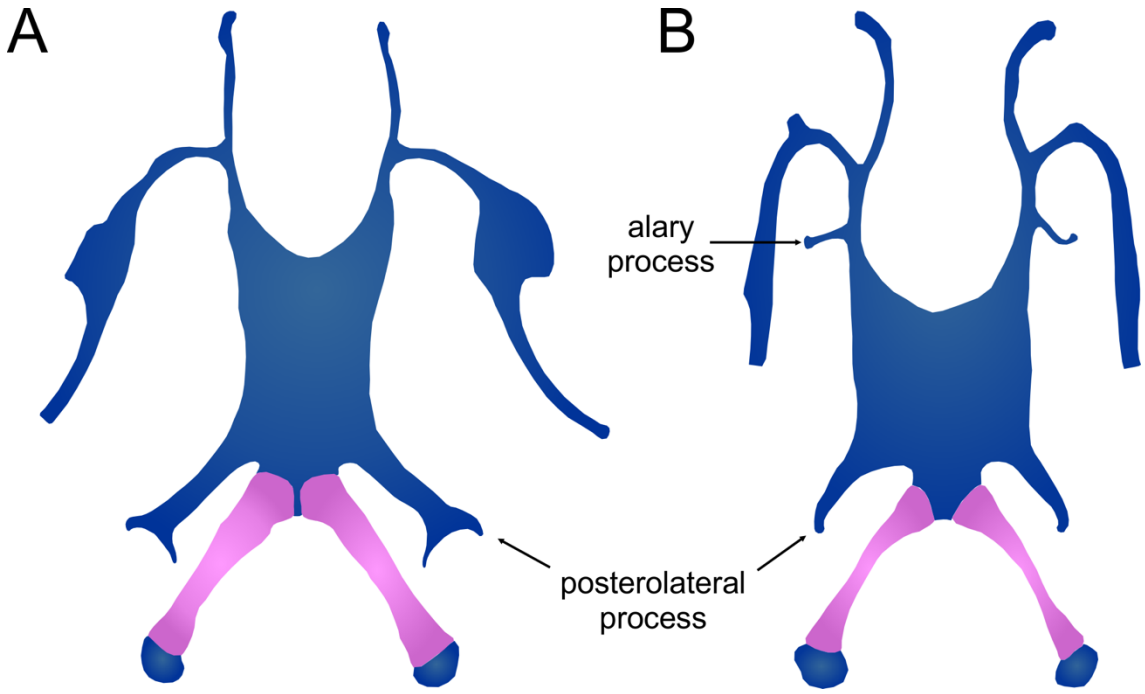

2347

2348 Figure 3

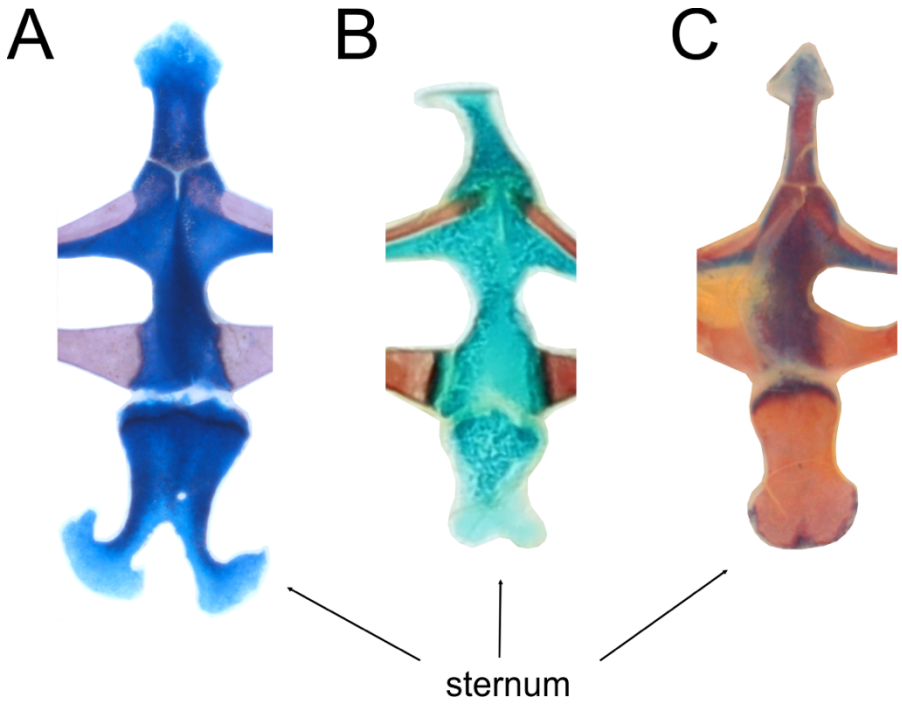

2349

2350 Figure 4

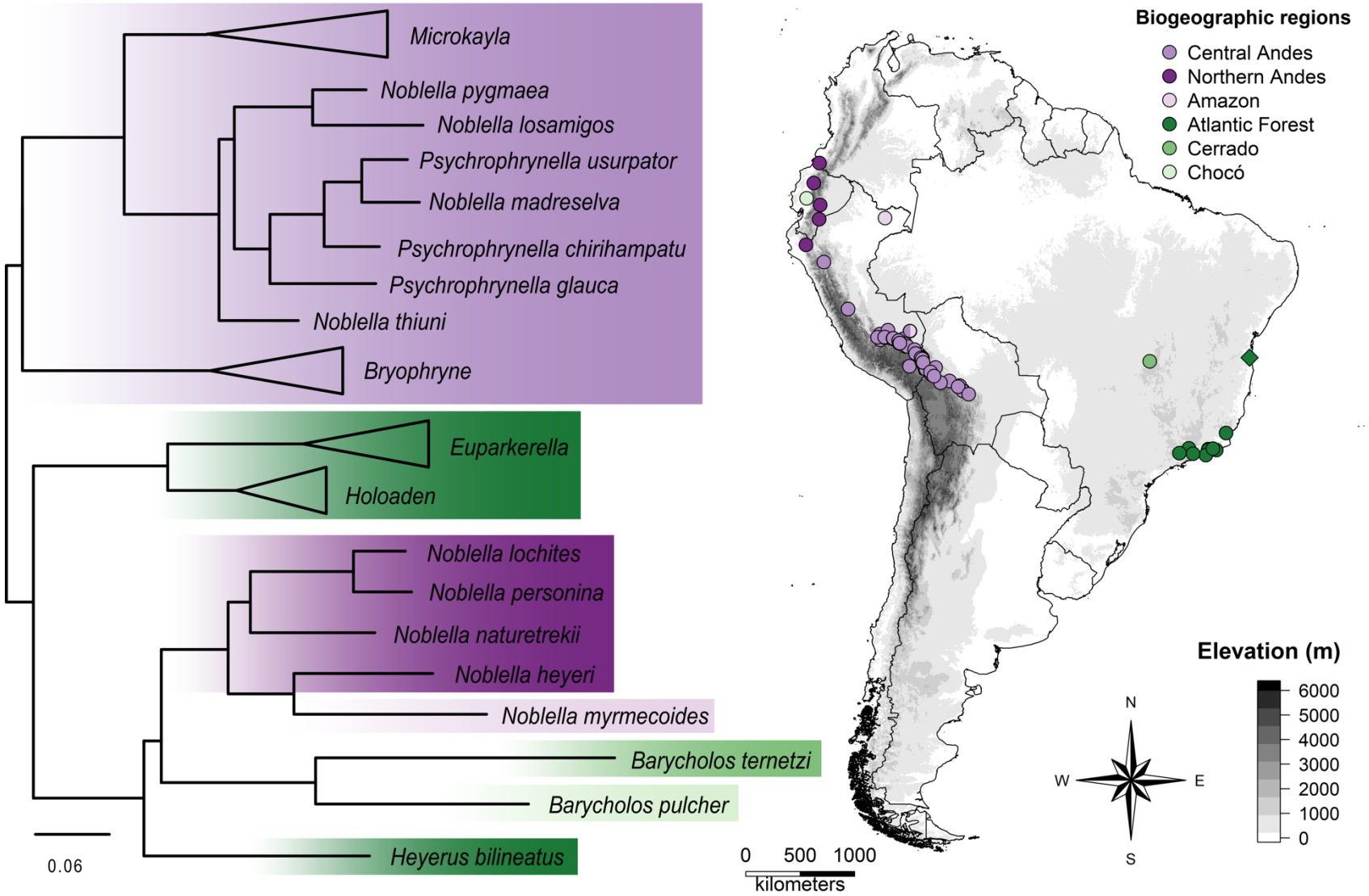

2351

2352 Figure 5

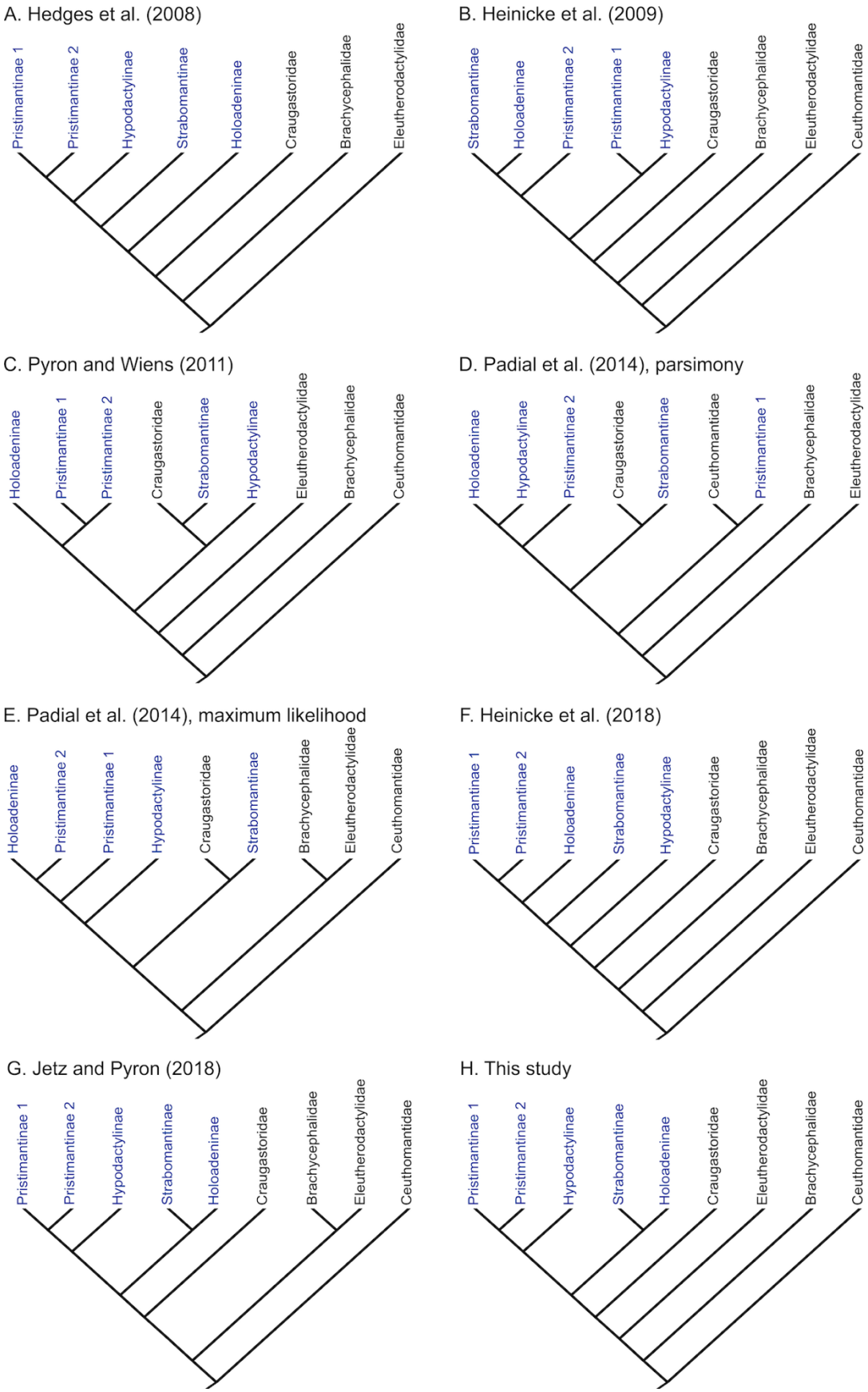

2353

2354 Figure 6

2355 **LIST OF SUPPORTING INFORMATION**

2356 **Table S1.** Genbank accession numbers of species sampled in this study. Sequences produced in this study are highlighted in bold font.

2357 [sequences will be submitted to GenBank upon acceptance of this manuscript]

Species	Voucher	12S–tVal–16S	RAG1	Tyr
Adelophryne gutturosa	ROM 39578	EU186679	EU186751	EU186772
Agaluchnis callidryas	—	DQ283423	EF493362	DQ283018
Barycholos pulcher	KU 217781	EU186727, EU186709	KX208662	EU186765
Barycholos ternetzi	CFBH 19426	JX267466	JX267543	JX267680
Barycholos ternetzi	CFBH 23511	KU495148	KF625108	KF625130
Barycholos ternetzi	CFBH 11596	########	########	########
Barycholos ternetzi	CFBH 11597	########	########	########
Barycholos ternetzi	CFBH 11598	########	########	########
Brachycephalus ephippium	CFBH 16807	HQ435679, HQ435693	HQ435721	HQ435735
Bryophryne bakersfield	MUBI 6022	MF186284, MF186341	MF186528	—
Bryophryne bustamantei	MHNC 6019	KT276286, KT276293	MF186544	MF186548
Bryophryne cophites	KU 173497	EF493537	EF493423	EF493508
Bryophryne hanssaueri	MUSM 27567	KY652642	KY681084	KY681063
Bryophryne nubilosus	MUSM 27882	KY652643	KY681085	KY681064
Bryophryne phuyuhampatu	CORBIDI 18224	MF419254	—	—
Bryophryne quellokunka	MNCN 43780	MF186309, MF186387	MF186526	—
Bryophryne tocra	MNCN 43786	MF186315, MF186396	MF186541	—
Bryophryne wilakunka	MUBI 5425	MF186291, MF186349	—	—
Ceuthomantis smaragdinus	ROM 40161	EU186677	EU186750	EU186771
Craugastor daryi	UTA-A 57940	EF493531	EF493452	EF493480
Craugastor longirostris	KU 177803	EF493395	EF493454	EF493482
Craugastor pygmaeus	UTA-A 55241	EF493711	EF493451	EF493479
Craugastor spatulatus	AMCC 118375	EU186674	EU186749	EU186770

Diasporus diastema	MVZ 203844	EU186682	EU186752	EU186773
Eleutherodactylus cooki	USNM 326784	EF493539	EF493413	EF493455
Euparkerella brasiliensis	—	JX267390, JX267468	JX267545	JX267682
Euparkerella brasiliensis	—	JX298276, JX298316	JX298185	JX298237
Euparkerella cochranae	MNRJ 56146	########	########	KF625114
Euparkerella cochranae	MNRJ 72082	########	########	KF625116
Euparkerella tridactyla	JFT 305	########	########	KF625109
Euparkerella tridactyla	JFT 346	########	—	KF625110
Fritziana aff. *fissilis*	MNRJ 44622	KR559917, KR270404, KR270421	KR138396	KR270390
Haddadus binotatus	MTR 13438	JX267346	JX267547	JX267684
Heyerus bilineatus	CFBH 23684	########	########	########
Heyerus bilineatus	CFBH 23689	########	########	########
Heyerus bilineatus	CFBH 32419	########	########	########
Heyerus bilineatus	CFBH 34063	########	########	########
Heyerus bilineatus	MNRJ 46476	JX267393, JX267324	JX267556	JX267691
Heyerus bilineatus	MNRJ 52873	JX267323	JX267555	—
Heyerus bilineatus	CFBH 35720	########	########	########
Holoaden bradei	USNM 207945	EF493378, EF493366	EF493449	EU186779
Holoaden luederwaldti	MZUSP 131872	EU186728, EU186710	EU186747	EU186768
Ischnocnema guentheri	CFBH 26993	JX267331, JX267501, JX267502	JX267611	JX267746
Ischnocnema verrucosa	CFBH 23685	JX267457, JX267538	JX267670	JX267810
Lynchius flavomaculatus	KU 218210	EU186667	EU186745	EU186766
Lynchius nebulanastes	KU 181408	EU186704	—	—
Lynchius oblitus	MHNC 8676	KX470778, KX870785	KX470794	KX470801
Lynchius parkeri	KU 181307	EU186705	—	—
Lynchius simmonsi	QZ 41639	JF809940, JF810004	JF809915	JF809894
Lynchius tabaconas	MHCN 8637	KX470773, KX470780	—	KX470796
Microkayla adenopleura	MNCN 44810	MF186283, MF186340	MF186537	MF186565

Microkayla ankohuma	MNKA 7280	MF186288, MF186346	—	MF186560
Microkayla boettgeri	MUBI 5363	MF186294, MF186353	—	MF186559
Microkayla chacaltaya	MNCN 42052	MF186357	MF186532	—
Microkayla chapi	MNCN 43762	MF186328, MF186417	MF186540	MF186562
Microkayla chilina	MNCN 43772	MF186327, MF186414	MF186539	MF186561
Microkayla condoriri	CBF 5989	MF186300, MF186360	MF186530	MF186550
Microkayla guillei	AMNH-A 165108	AY843720	—	DQ282995
Microkayla iatamasi	MNCN 42054	MF186304, MF186368	MF186536	MF186558
Microkayla illampu	CBF 5998	MF186369	MF186534	MF186549
Microkayla kallawaya	MNCN 42061	MF186376	—	MF186575
Microkayla katantika	CBF 6013	MF186307, MF186381	MF186533	MF186576
Microkayla kempffi	MNCN 43646	MF186308, MF186384	MF186538	MF186566
Microkayla quimsacruzis	MNCN 42063	MF186323, MF186405	—	—
Microkayla saltator	CBF 6033	MF186326, MF186410	—	—
Microkayla sp.	CBF 6564	MF186317, MF186399	—	MF186556
Microkayla sp.	MNCN 46980	MF186332, MF186426	—	MF186568
Microkayla sp.	MNCN 42034	MF186325, MF186409	MF186535	MF186563
Microkayla teqta	MNCN 45702	MF186318, MF186400	—	MF186552
Microkayla wettsteni	—	AM039711, AM039643	—	—
Microkayla wettsteni	CBF 6241	MF186338, MF186434	MF186531	MF186551
Niceforonia brunnea	KU178258	EF493357	GQ345282	EF493484
Niceforonia dolops	—	EF493394	EF493414	EF493483
Niceforonia elassodiscus	KU 178282	EF493358	—	—
Niceforonia nana	IAvHAm 13054	MH532902, MH536808	—	MH542228
Niceforonia nigrovittata	CORBIDI 9547	MH538300	—	—
Niceforonia peraccai	KU 178266	EF493710	EF493420	EF493485
Noblella heyeri	QCAZ 31471	JX267463, JX267541	—	—
Noblella lochites	KU 177356	EU186699	EU186756	EU186777

Noblella losamigos	AC94_09	MN336183	—	—
Noblella losamigos	MUSA 6302	MN100040	—	—
Noblella losamigos	MVZ 292687	MN366392	—	—
Noblella madreselva	CORBIDI 15770	MN056356	—	—
Noblella myrmecoides	QCAZ 40180	JX267464, JX267542	—	—
Noblella naturetrekii	QCAZ 71337	MK838467, MK838462	—	—
Noblella personina	QCAZ 58818	MK838468, MK838465	—	—
Noblella pygmaea	MUSM 24536	KY652645	KY681086	KY681066
Noblella thiuni	CORBIDI 18723	MK072732	—	—
Oreobates amarakaeri	MHNC 6975	JF809934 JF809996	JF809913	JF809891
Oreobates antrum	ZUFG 5888	MH025427, MH025451	MH025436	MH025445
Oreobates ayacucho	MNCN(IDlR5024)	JF809933 JF809970	JF809912	JF809890
Oreobates barituensis	MCN 1359	JF809935 JF809999	JF809914	JF809892
Oreobates berdemenos	FML 24623	KJ125509	—	—
Oreobates choristolemma	CBG 765	JF809921, FJ539072, FJ539067	JF809900	JF809881
Oreobates crepitans	ZUEC 14119	KJ125510	—	—
Oreobates cruralis	KU 215462	EU186666	EU186743	EU186764
Oreobates discoidalis	MNCN 43133	JF809925, FJ539073, FJ539068	—	JF809884
Oreobates gemcare	MHNC 6687	JF809930 JF809960	JF809909	—
Oreobates granulosus	MHNC 3396	JF809929, FJ539074, EU368897	JF809908	JF809887
Oreobates heterodactylus	MNK-A 7175	JF809923, FJ438816, EU192296, FJ438805	JF809902	JF809882
Oreobates ibischi	MNK-A 6612	FJ438817 FJ438806	—	—
Oreobates lehri	MUSM 27616	JF809927 JF809957	JF809906	—
Oreobates lundbergi	MTD 45902	JF809928 JF809958	JF809907	JF809886
Oreobates machiguenga	MHNC 6809	JF809932 JF809969	JF809911	JF809889
Oreobates madidi	MNK-A 7856	JF809922, FJ539075, FJ539070	JF809901	—
Oreobates pereger	MTD 46808	JF809926 JF809955	JF809905	JF809885
Oreobates quixensis	KU 178249	EF493828 EF493662	—	—

Oreobates remotus	MZUSP 141708	JN688273	—	—
Oreobates sanctaecrucis	MNK-A 5507	JF809924 JF809951	JF809903	JF809883
Oreobates sanderi	MNCN 42017	EU368904	—	—
Oreobates saxatilis	KU 212327	EU186726 EU186708	EU186742	EU186763
Oreobates yanucu	ZFMK 72569	KY111322	—	—
Phrynopus auriculatus	MUBI 6471	MF186290, MF186348	—	MF186582
Phrynopus badius	FMNH 282818	MG896594, MG896571	MG896618	—
Phrynopus barthlenae	MHNSM 20609	MF186292, MF186350	—	—
Phrynopus bracki	USNM 286919	EF493709	EF493421	EF493507
Phrynopus bufoides	—	AM039713, AM039645	—	—
Phrynopus daemon	MUSM 32747	MG896597, MG896574	—	—
Phrynopus heimorum	MTD 45621	MF186302, MF186363	MF186545	MF186580
Phrynopus horstpauli	MTD 44335	MF186303, MF186364	—	MF186584
Phrynopus interstinctus	MUSM 29543	MG896598, MG896575	MG896621	—
Phrynopus inti	UMMZ 245218	MF651913, MF651906	MF651918	MF651921
Phrynopus juninensis	MUSM 38324	MG896600, MG896577	MG896623	—
Phrynopus kauneorum	—	AM039718, AM039650	—	—
Phrynopus mariellaleo	CORBIDI 11658	MH538299	—	MH538306
Phrynopus miroslawae	MUBI 6469	MF186312, MF186393	MF186542	MF186585
Phrynopus montium	MUSM 33259	MG896601, MG896578	MG896624	—
Phrynopus peruanus	MUSM 38316	MG896605, MG896582	MG896626	MG896631
Phrynopus pesantesi	—	AM039724, AM039656	—	—
Phrynopus tautzorum	—	AM039720, AM039652	—	—
Phrynopus tribulosus	MUBI 7166	MF186330, MF186424	MF186547	MF186579
Phrynopus unchog	MUSM 32748	MG896608, MG896591	—	—
Phrynopus vestigiatus	MUSM 29542	MG896610, MG896593	—	—
Pristimantis actites	KU 217830	EF493696	EF493432	EF493494
Pristimantis altamazonicus	KU 215460	EF493670	EF493441	—

Pristimantis duellmani	WED 53050/KU 217998	AY326003	EF493438	EF493500
Pristimantis euphronides	BWMC 6918	EF493527	EF493427	EF493489
Pristimantis leoni	KU 218227	EF493684	EF493443	EF493495
Pristimantis nyctophylax	KU 177812	EF493526	EF493425	EF493487
Pristimantis ramagii	MNRJ 36751	JX267318	JX267658	JX267797
Pristimantis rozei	—	EF493691	EF493429	EF493491
Pristimantis stictogaster	KU 291659	EF493704	EF493445	EF493506
Pristimantis versicolor	KU 218096	EF493389	EF493431	EF493493
Psychophrynella usurpator	AC186_09	KY652662	KY672975	KY681083
Psycophrynella chirihampatu	MHNC 14664	KU884560	—	—
Psycophrynella glauca	CORBIDI 18729	MG837565	—	—
Psycophrynella usurpator	KU 173495	EF493714	—	—
Strabomantis biporcatus	CVULA 7073	EU186691	EU186754	EU186775
Strabomantis bufoniformis	SIUC 7062	DQ283165	—	DQ282942
Yunganastes fraudator	MNCN 43107	JF809938	JF809916	JF809895
Yunganastes mercedesae	ZFMK 72571	JF809939	JF809920	JF809899

2358

Figure S1. Maximum likelihood optimal tree of 135 species and 151 terminal taxa of Brachycephaloidea, based on a dataset of 3949 aligned bp of fragments of genes 12S rRNA (1,118 bp), tVal (75 bp), 16S rRNA (1,556 bp), RAG1 (645 bp), and tyr (555 bp). Bootstrap supports are indicated at each node (asterisks represent values of 100%). Family and subfamily classifications proposed by Padial et al. (2014) and Heinicke et al. (2018) are presented on the right.

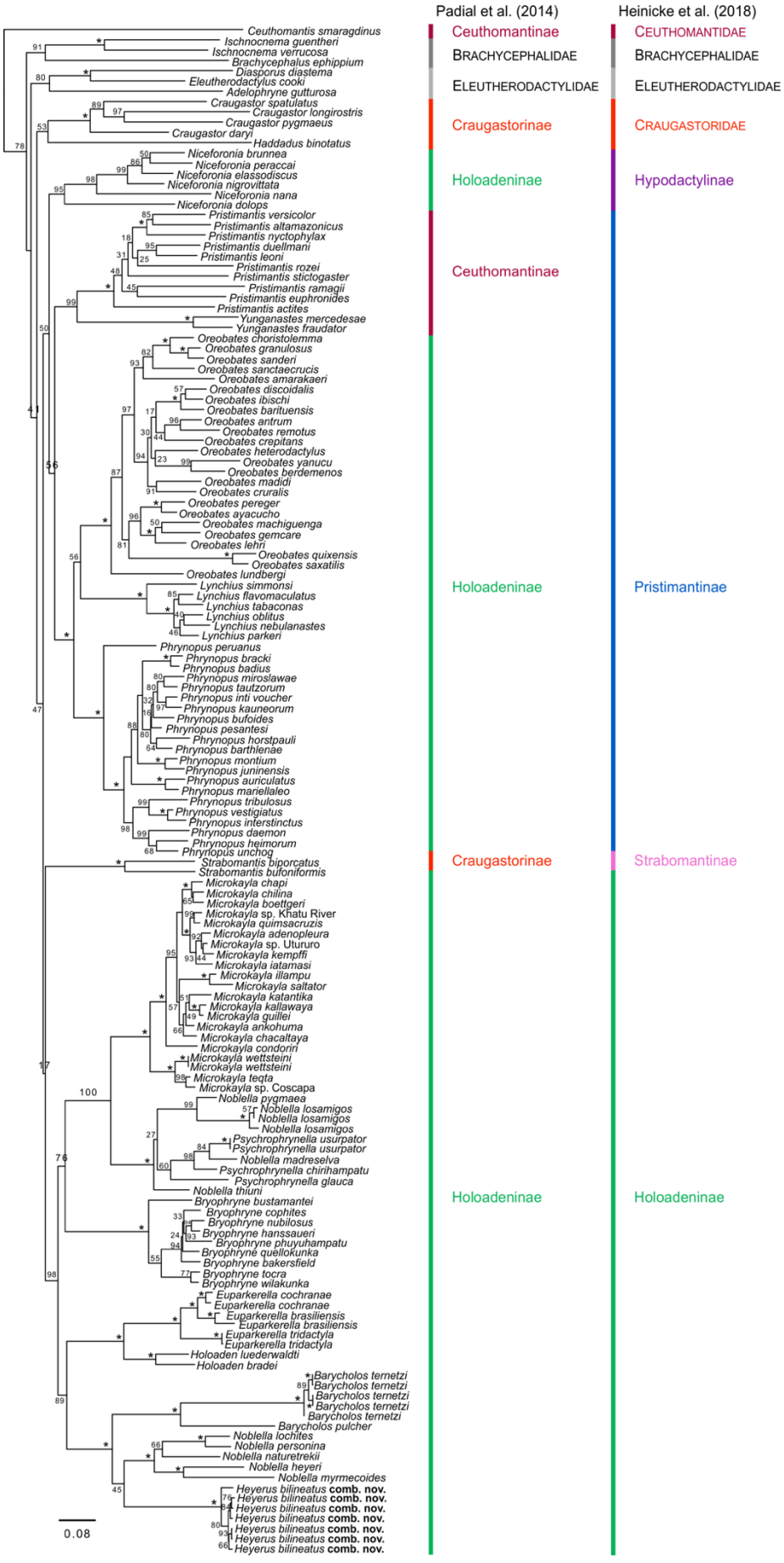
Padial et al. (2014)
Heinicke et al. (2018)
Ceuthomantinae
CEUTHOMANTIDAE
BRACHYCEPHALIDAE
BRACHYCEPHALIDAE
ELEUTHERODACTYLIDAE
ELEUTHERODACTYLIDAE
Craugastorinae
CRAUGASTORIDAE
Holoadeninae
Hypodactylinae
Ceuthomantinae
Holoadeninae
Pristimantinae
Craugastorinae
Strabomantinae
Holoadeninae
Holoadeninae
Ceuthomantis smaragdinus
Ischnocnema guentheri
Ischnocnema verrucosa
Brachycephalus ephippium
Diasporus diastema
Eleutherodactylus cooki
Adelophryne gutturosa
Craugastor spatulatus
Craugastor longirostris
Craugastor pygmaeus
Craugastor daryi
Haddadus binotatus
Niceforonia brunnea
Niceforonia peraccai
Niceforonia elassodiscus
Niceforonia nigrovittata
Niceforonia nana
Niceforonia dolops
Pristimantis versicolor
Pristimantis altamazonicus
Pristimantis nyctophylax
Pristimantis duellmani
Pristimantis leoni
Pristimantis rozei
Pristimantis stictogaster
Pristimantis ramagii
Pristimantis euphronides
Pristimantis actites
Yunganastes mercedesae
Yunganastes fraudator
Oreobates choristolemma
Oreobates granulosus
Oreobates sanderi
Oreobates sanctaecrucis
Oreobates amarakaeri
Oreobates discoidalis
Oreobates ibischi
Oreobates barituensis
Oreobates antrum
Oreobates remotus
Oreobates crepitans
Oreobates heterodactylus
Oreobates yanucu
Oreobates berdemenos
Oreobates madidi
Oreobates cruralis
Oreobates pereger
Oreobates ayacucho
Oreobates machiguenga
Oreobates gemcare
Oreobates lehri
Oreobates quixensis
Oreobates saxatilis
Oreobates lundbergi
Lynchius simmonsi
Lynchius flavomaculatus
Lynchius tabaconas
Lynchius oblitus
Lynchius nebulanastes
Lynchius parkeri
Phrynopus peruanus
Phrynopus bracki
Phrynopus badius
Phrynopus miroslawae
Phrynopus tautzorum
Phrynopus inti voucher
Phrynopus kauneorum
Phrynopus bufoides
Phrynopus pesantesi
Phrynopus horstpauli
Phrynopus barthlenae
Phrynopus montium
Phrynopus juninensis
Phrynopus auriculatus
Phrynopus mariellaleo
Phrynopus tribulosus
Phrynopus vestigiatus
Phrynopus interstinctus
Phrynopus daemon
Phrynopus heimorum
Phrynopus unchog
Strabomantis biporcatus
Strabomantis bufoniformis
Microkayla chapi
Microkayla chilina
Microkayla boettgeri
Microkayla sp. Khatu River
Microkayla quimsacruzis
Microkayla adenopleura
Microkayla sp. Ututuro
Microkayla kempffi
Microkayla iatamasi
Microkayla illampu
Microkayla saltator
Microkayla katantika
Microkayla kallawaya
Microkayla guillei
Microkayla ankohuma
Microkayla chacaltaya
Microkayla condorii
Microkayla wettsteini
Microkayla wettsteini
Microkayla teqta
Microkayla sp. Coscapa
Noblella pygmaea
Noblella losamigos
Noblella losamigos
Noblella losamigos
Psychrophrynella usurpator
Psychrophrynella usurpator
Noblella madreselva
Psychrophrynella chirihampatu
Psychrophrynella glauca
Noblella thiuni
Bryophryne bustamantei
Bryophryne cophites
Bryophryne nubilosus
Bryophryne hanssaueri
Bryophryne phuyuhampatu
Bryophryne quellokunka
Bryophryne bakersfield
Bryophryne tocra
Bryophryne wilakunka
Euparkerella cochranae
Euparkerella cochranae
Euparkerella brasiliensis
Euparkerella brasiliensis
Euparkerella tridactyla
Euparkerella tridactyla
Holoaden luederwaldti
Holoaden bradei
Barycholos ternetzi
Barycholos ternetzi
Barycholos ternetzi
Barycholos ternetzi
Barycholos pulcher
Noblella lochites
Noblella personina
Noblella naturetrekii
Noblella heyeri
Noblella myrmecoides
Heyerus bilineatus comb. nov.
Heyerus bilineatus comb. nov.
Heyerus bilineatus comb. nov.
Heyerus bilineatus comb. nov.
Heyerus bilineatus comb. nov.
Heyerus bilineatus comb. nov.
0.08

2365

APPENDIX

Specimens examined in this study, including cleared and stained specimens (CS).

Barycholos pulcher: AMNH 89707, AMNH 89714, AMNH 104345, KU 218156 (CS), KU 218158 (CS); *Barycholos ternetzi*: CFBH 26150, CFBH 23596, CFBH11599, CFBH 26105, CFBH 26108, CFBH 10260, CFBH 11595, CFBH 11600, CFBH 23818, CFBH 11601, CFBH 26038, CFBH 11594, CFBH 11597 (CS), CFBH 11598 (CS); *Euparkerella brasiliensis*: KU 93192 (CS), CFBH 39336, CFBH 26983, CFBH 253, CFBH 39340, CFBH 31334, CFBH 40840, CFBH 39335, CFBH 25984, CFBH 39333, CFBH 39338, CFBH 39337; *Euparkerella cochranae*: CFBH 272, CFBH 270, CFBH 273, CFBH 271, CFBH 35224, CFBH 274; *Euparkerella tridactyla*: CFBH 948, CFBH 1360, CFBH 950, CFBH 22526, CFBH 35672, CFBH 33134; *Heyerus bilineatus*: CFBH 23689, CFBH 34088, CFBH 34063, CFBH 34090, CFBH 32419, CFBH 37976, CFBH 23684 (CS), CFBH 35720 (CS); *Holoaden bradei*: AMNH 73548, AMNH 73549, KU 107087 (CS), KU 92868 (CS), KU 107088 (CS), MNRJ 22501 (CS), CFBH 36357, CFBH 252; *Holoaden luederwaldti*: AMNH 72334, MNRJ 3903 (CS), CFBH 19552, CFBH 19553, CFBH 19554, CFBH 19555, CFBH 19550, CFBH 19551, CFBH 19556, CFBH 29298, CFBH 9900, CFBH 9932, CFBH 9899, CFBH 9914; *Noblella heyeri*: KU 196529, KU 196530, KU 196531 (CS); *Noblella lochites*: KU 147070 and data from Heyer (1977); *Noblella myrmecoides*: AMNH 102997, AMNH 97051, AMNH 153037, and data from Heyer (1977); *Noblella pygmaea*: MUSM 26320, MUSM 24535, MUSM 24536.

Habitat rather than altitudinal shifts drive morphological evolution in a continental radiation of New World direct-developing frogs[†]

Ana Motta, Pedro Taucce, Célio Haddad

Laboratório de Herpetologia, Departamento de Biodiversidade e Centro de Aquicultura, Instituto de Biociências, Universidade Estadual Paulista, Av. 24A 1515, CEP 13506-900, Rio Claro, São Paulo, Brazil.

*Corresponding author: Ana Motta, apmottah@gmail.com

[†]Manuscrito em revisão no periódico *Amphibia-Reptilia*

Abstract. Bergmann's rule predicts a correlation between body size and temperature that is affected by both latitude and altitude. New World terrestrial breeding frogs of the superfamily Brachycephaloidea occur at elevations of up to 4500 m in the Andes, but support for Bergmann's rule in this group is limited. Habitat shifts also influence morphological traits, and phenotypic similarity of species that occur in similar habitats is considered evidence of convergent evolution. Several phylogenetically distant lineages of brachycephaloid frogs share similar ecological distributions and external morphologies, but correlations among these traits have not been tested explicitly. We investigate whether altitudinal and habitat shifts drive morphological evolution in a continental radiation of New World direct-developing frogs. We find that body size evolution does not support Bergmann's rule. Our results suggest, however, that habitat shifts drive morphological evolution in this group. Our analyses indicate that shifts from forest to grasslands in both lowland and highland environments resulted in morphological similarities across distantly related species. Specifically, occupation of Andean grasslands has involved evolutionary change toward decreased head and hindlimb length, while occupation of lowland grasslands and dry forests has involved evolutionary change toward expanded fingertips. We hypothesize that mechanical requirements might be responsible for convergence in this group and suggest that future analyses explore the relationship of body size and microhabitat use.

Keywords: Anura, Andes, Bergmann's rule, Brachycephaloidea, convergence, *Lynchius*, *Oreobates*, *Phrynopus*

Introduction

Environmental gradients are known to influence morphological traits, and a number of hypotheses have been formulated to explain factors shaping size variation in animals. Bergmann's rule predicts a correlation between body size and temperature because “smaller species would demand a warmer climate” (Bergmann, 1847). Even though the mechanisms (e.g. heat conservation, phylogenetic constraint, migration ability, starvation resistance, resource availability; Blackburn, Gaston and Loder, 1999) causing variation in body size are usually unknown, this pattern has been found in different groups of animals, including endotherms and ectotherms (see Blackburn, Gaston and Loder, 1999; Vinarski, 2014).

Terrestrial breeding frogs of the superfamily Brachycephaloidea, a group that comprises around one-third of New World frog species, have a broad distribution, from southern USA through Mexico and the Antilles to northern Argentina, in elevations up to 4500 m in the Andes (Frost, 2020; Padial, Grant and Frost, 2014). Nevertheless, the evaluation of Bergmann's rule in this group has been tested only recently, for the Andean genus *Phrynopus* (von May, Lehr and Rabosky, 2018). According to this study, species of *Phrynopus* show a cline in body size that agrees with Bergmann’s rule.

Habitat shifts also influence morphological traits, and phenotypic similarity of species that occur in similar habitats has long been considered evidence of convergent evolution through adaptation (Losos et al., 1998; Losos, 2011). In this sense, species from different lineages occupying equivalent ecological niches evolve similar features as a result of similar selection pressures, leading to convergent morphotypes (Wainwright and Reilly, 1994).

Correlation between body shape and habitat use or environmental niche is common across diverse lineages of Anura (Bossuyt and Milinkovitch, 2000; Blackburn et al., 2013; Moen, Irschick and Wiens, 2013; Vidal-Garcia et al., 2014; Vidal-Garcia and Keogh, 2015; Moen, Morlon and Wiens, 2016; Dugo-Cota et al., 2020). In this group, similar physiological

requirements can result in similar phenotypes. For example, frogs from dry regions are usually rotund to reduce surface area-to-volume ratios and minimize evaporative water loss (Thompson et al., 2005). Furthermore, habitat use also can be responsible for convergent morphotypes. For instance, arboreal species usually have long limbs and expanded tip of fingers and toes (Wells, 2007).

Andean highlands hold several phylogenetically distant lineages of brachycephaloid frogs that converge in their ecological distribution and external morphology. Species occupying this habitat share the “phrynopoid” morphology, characterized by small round bodies, short extremities, and rounded, non-expanded tip of fingers and toes (De la Riva, 2020; Fig. 1A, B). Likewise, species from xeric habitats in lowlands also share a morphotype (slender with long extremities and large discs on fingers; Fig. 1C, D) and support the idea that convergent evolution drives recurring patterns of morphological variation in this group (Motta et al., 2016).

The clade including the genera *Lynchius*, *Oreobates*, and *Phrynopus* has a broad diversity in morphological traits and a continental distribution in South America (Fig. 2). Species of this clade range in mean size from 13.4 mm to 57.1 mm, occur at elevations between 80 and 4280 m, and constitute an excellent study group to test Bergmann's rule. Moreover, its distribution encompasses a diverse number of Neotropical habitats. Some species occur in the high Andean humid grasslands above tree line, while most other species occur in montane forests of the eastern slopes of the Andes between 1000−2000 m elevations. There are, however, several species inhabiting warmer environments such as the Amazon lowlands, the Cerrado, and the dry Atlantic forests of eastern Brazil. Also, several species have colonized the highly seasonal inter-Andean dry valleys and the Yungas of northern Argentina. Interestingly, a terrestrial species of *Oreobates* from the high Andean grasslands (*O. ayacucho*) resembles species of *Phrynopus* that have relatively small and ecologically

restricted distributions in the high Andes (Fig. 1A, B). On the other hand, *Lynchius simmonsi*, a morphologically dissimilar species of the genus that occurs in montane forest below 2000 m, resembles species of *Oreobates* from montane forests and the Amazon lowlands (De la Riva, 2020). This pattern indicates that adaptation to similar environments perhaps led to similar transformations of traits in *Lynchius*, *Oreobates*, and *Phrynopus* (Padial et al., 2012; Motta et al., 2016).

We investigate whether altitudinal and habitat shifts drive morphological evolution in the clade including the genera *Lynchius*, *Oreobates*, and *Phrynopus*. We test two hypotheses: (1) body size is positively correlated with elevation and, hence, with decreasing environmental temperatures (Bergmann's rule), and (2) species occupying the same habitat are more similar to each other than to their relatives from other habitats (convergence).

Materials and Methods

To investigate variation in body size and shape, we took eight morphometric measurements: snout–vent length (SVL); head length (HL; from posterior margin of lower jaw to tip of snout); head width (HW; measured at level of rictus); width of disc of Finger III (F3); arm length (FA; from posterior margin of thenar tubercle to elbow); tibia length (TL); thigh length (TH; from vent to knee); foot length (FL; from proximal border of inner metatarsal tubercle to tip of fourth toe). Measurements were taken with digital calipers to the nearest 0.01 mm. We collected morphometric data for 39 species: 18 species of *Oreobates*, 16 species of *Phrynopus*, and five species of *Lynchius* (supplementary Table S1). Body size (SVL) data were also obtained from the literature. The final dataset for SVL includes 50 species: 22 species of *Oreobates*, 21 species of *Phrynopus*, and seven species of *Lynchius* (supplementary Table S2). To avoid the effect of sexual dimorphism, and because for many species only females were available, we included only females in our analyses.

We assembled data on minimum and maximum elevation and used elevational midpoints in our analyses (Table S1). Following Olson et al. (2001), we defined three habitats according to the biomes where focal species occur: Tropical and Subtropical Moist Broadleaf Forests (MF), Montane Grasslands and Shrublands (MG), and Tropical and Subtropical Dry Broadleaf Forests, Grasslands, Savannas and Scrublands (DF) (Table S2).

As data for species are not independent because of shared phylogenetic history (Blomberg, Garland and Ives 2003), a phylogenetic framework was included for all statistical analyses. We included 23 species of *Oreobates*, 21 species of *Phrynopus*, and seven species of *Lynchius* in the molecular phylogenetic analyses. The outgroup includes the Brachycephaloid species *Euparkerella brasiliensis*, *Niceforonia brunnea*, *Pristimantis curtipes*, *P. parectatus*, and *P. w-nigrum*. We reconstructed a dated species tree using the Bayesian coalescent species tree method StarBeast2 (Ogilvie, Bouckaert and Drummond, 2017) implemented in BEAST v.2.5.0 software package (Bouckaert et al., 2014). Our matrix includes legacy (GenBank) sequences of the mitochondrial 12S rRNA, tRNA Val, 16S rRNA, and cytochrome b oxidase (CYTB) genes and nuclear recombination activating gene 1 (RAG1), tyrosinase precursor (tyr), and proopiomelanocortin (POMC). Accession numbers for all sequences used in this study are listed in supplementary Table S3. We performed a search for the best-fitting nucleotide substitution model with bModelTest (Bouckaert and Drummond, 2017) also implemented in BEAST v.2.5.0 concomitantly with the species tree analysis. To date our species tree, we used a previously estimated substitution rate of 0.006/site/my for the 16S rRNA gene from another Brachycephaloid genus, *Ischnocnema* (Gehara et al., 2017). We assumed a relaxed clock with an uncorrelated lognormal distribution and a Yule model for the species tree. We did not estimate the relative rates among partitions to facilitate convergence. We ran the MCMC chain for 100,000,000 generations, sampling every 10,000 generations and discarding 10,000 as burn-in. We

checked convergence of the parameters using Tracer v.1.7.1 (Rambaut et al., 2018) and considered that a parameter converged when ESS was higher than 200. GenBank accession numbers for the taxa and genes sampled are included in Table S3.

We performed a phylogenetic size-correction using generalized least-squares (PGLS) regression analysis (Revell, 2009) to control for the effect of body size (independent variable) on all other measurements (dependent variables) using the Phytools package (Revell, 2012). The same package was used to calculate Pagel's lambda (Pagel, 1999) for each measured trait to test for phylogenetic dependence among measurements. All statistical analyses were conducted in R 3.2.3 (R Core Team, 2018).

To test for correlation in body size and elevation, we performed phylogenetic generalized least squares (PGLS) using the APE package (Paradis, Claude and Strimmer, 2004). We tested two different evolutionary models to investigate the processes that could best explain the evolution of these morphological traits: "Brownian motion (BM), a null model designed to represent a process of random walk with constant variance (described in detail in Freckleton, Harvey and Pagel 2002; O'Meara et al., 2006); and Ornstein-Uhlenbeck (OU) which adds to the random walk a tendency to evolve towards an "optimum value", generally considered to represent a biological scenario of stabilizing selection (Hansen, 1997; Butler and King, 2004)" (Ceccarelli et al., 2019). Akaike's information criterion (AIC) was used as a heuristic indicator for the fit of the different evolutionary models (Akaike, 1974). We performed these analyses in four different datasets: (1) species of *Lynchius*, *Oreobates*, and *Phrynopus* (LOP), (2) species of *Lynchius* only (LYN), (3) species of *Oreobates* only (ORE), and (4) species of *Phrynopus* only (PHR).

To test the relationship between body shape and habitat we used the size-corrected residuals of measurements. We performed phylogenetic principal components analysis (PCA) using Phytools to examine the distribution of habitat and taxa in phylomorphospace. We

performed a phylogenetic MANOVA in the Geiger package (Harmon et al., 2008) to test for significant differences in trait values among habitats. We used the Phytools package to perform phylogenetic ANOVA to test for differences in habitat group means for each measurement.

Results

Our analysis recovered a monophyletic *Phrynopus* sister to a clade including *Oreobates* and *Lynchius*, both also monophyletic (Fig. 2). We found intermediate to strong phylogenetic signal in all tested variables, with the exception of head width and arm length (estimated Pagel's lambda for each measurement is presented in Table 1).

The PGLS analyses showed a non-significant relationship between body size and elevation for all the PGLS analyses performed (Table 2; Fig. 3). We found that the BM model was the best fit for the ORE and LYN datasets, and the OU model was the best fit for the LOP and PHR datasets (Table 2).

Principal component analysis showed a great contribution of the two-first components, which summarized 87.8% of variation. The first principal component explained 77.3% of the variation in the data set and was highly correlated with tibia length (TB loading: -0.963). The second axis described 10.5% of the variation and was represented mainly by head width (HW loading: 0.819). The distribution of habitat on PCs 1 and 2 is presented in Fig. 4.

The phylogenetic MANOVA indicated significant differences in phylogenetic size-free trait residuals across habitats (F = 3.2497, P = 0. 01). Phylogenetic ANOVA showed that head length (P = 0.024), tibia length (P = 0.018), thigh length (P = 0.006), and foot length (P = 0.018) differ between species from Montane Grasslands and species from Moist Forests. Species from Dry Forests and Savannas differ from other species in the width of disc of Finger III (P = 0.012–0.02) (Fig. 5).

Discussion

In this study, we investigated whether body size variation in a widely distributed clade of Neotropical frogs supports Bergmann's rule. We also aimed to test for morphological convergence in this group. We found that body size evolution does not support Bergmann's rule in this group. On the other hand, habitat shifts drive morphological evolution in this continental radiation of direct-developing frogs.

Our results also show that, even though there is a tendency toward decreased body size at high elevations, body size did not differ significantly with elevation when we included species of *Lynchius*, *Oreobates*, and *Phrynopus* either under the BM model or under the OU model. The genera *Lynchius* and *Oreobates* show a tendency toward decreased body size at high elevations, while *Phrynopus* tends toward increased body size at high elevations. However, we also did not find a significant correlation between body size and elevation when analyzing each genus separately. Our findings contradict the previously postulated cline in body size that agrees with Bergmann's rule that has been found for species of *Phrynopus* (von May, Lehr and Rabosky, 2018).

Support for Bergmann's rule among anurans is still mostly contradictory (Ashton, 2002; Adams and Church, 2007). It has been proposed that in tropical areas, where water availability is more critical, water deficit might explain size variation better than temperature. In this case, species inhabiting dry areas are expected to be larger than species from wet regions (Olalla-Tárraga et al., 2009). However, even though some species of *Oreobates* inhabiting Cerrado and Dry Forests are among the largest ones, many species from moist forests are considerably larger than species from dry habitats and, thus, that might not be the better hypothesis to explain the variation in size in this group.

In frogs, the ratio of surface area to mass affects cutaneous respiration. Specifically, larger specimens have less efficient skin respiration (Szarski, 1964). The rarefied air in high

elevations can be considered an environmental constraint on body size in species occupying the high Andes and therefore might have an opposite effect on body size than that of temperature. Skin respiration efficiency can play a role on variation in size, contributing to species from high elevations to be small, and explain why this group does not follow Bergmann's cline.

In species of *Lynchius*, *Oreobates*, and *Phrynopus*, body shape changes with elevation: species from the high Andes are robust and round, while species from lowlands have slender bodies. Although we have found that body size does not correlate with elevation, it is also important to consider that changes in size might not be followed by changes in body mass if species have different body shapes (Blackburn, Gaston and Loder, 1999). In this sense, future studies can reveal a different pattern for body mass.

Our data show that the body shape displayed by forest species can work under a variety of environments. Species from MF occupy a large area in the phylomorphospace that completely overlaps the area occupied by species from DF and species from MF+MG. Moreover, species from MF+MG do not differ from species that occur only in MF in any of the traits analyzed. We also found that body shape of species from DF, species from MG, and species from MF+MG are less variable (i.e. occupy a smaller area in the phylomorphospace) than species that occur solely in MF. Provided that species occupied dry forests and montane grasslands from moist forests (Padial et al., 2012), the current body shape in species from DF and from MG probably still reflects adaptation to the ancestral environment (Moen, Morlon and Wiens, 2016).

Our analyses indicate that shifts from forest to grasslands in lowlands and highlands resulted in morphological similarities across distantly related species. Specifically, occupation of Andean grasslands has involved evolutionary change toward decreased head and hindlimb length, while occupation of lowland grasslands and dry forests has involved evolutionary

change toward expanded tip of fingers. Previous studies have discussed the similarity of species of the clade including *Lynchius*, *Oreobates*, and *Phrynopus* inhabiting the same habitats, and our results support the hypothesis that adaptation to high-altitude environments of the Andes and to more xeric habitats in the lowlands led to similar transformations of traits in this group (Padial et al., 2012; Motta et al., 2016; De la Riva, 2020). The study including species of the genus *Phrynopus* found the combination of shorter limbs and head in species living at higher elevations (von May, Lehr and Rabosky, 2018). Because there is a strong correlation between altitude and vegetation type in the altitudinal range of species of *Phrynopus* (De la Riva, 2020), we argue that our results agree with their findings. Similar morphology is also found in species of many other closely related terraranan genera (e.g. *Bryophryne*, *Microkayla*, and *Psychrophrynella*) that occur in Andean grasslands, including the wet puna from northern Peru to central Bolivia and paramos and subparamos from Ecuador to Venezuela (De la Riva et al., 2017; De la Riva, 2020). We believe future studies can reveal widespread convergence across additional lineages of terraranan frogs that independently occupied high-altitude environments of the Andes.

The evolution of round bodies with short limbs has been associated with arid environments, because the reduced area-to-volume ratio decreases water loss through evaporation (Tyler, 1989). However, our analyses show that species from DF do not share the general dry habitat morphotype. On the other hand, we found the dry habitat morphotype in species from MG, which occur in wet environments, where humidity levels are relatively high, and do not face the risk of desiccation as species from arid environments. Therefore, morphological convergence in species of *Lynchius*, *Oreobates*, and *Phrynopus* is not likely a result of physiological requirements to minimize evaporative water loss.

Colonization of similar microhabitats might also result in convergent phenotype. Body shape is strongly related to microhabitat use across major clades of anurans from different

continents (Moen, Irschick and Wiens, 2013; Moen, Morlon and Wiens, 2016), and that pattern is usually associated with the different mechanical requirements involved in exploring different microhabitats (Vidal-Garcia and Keogh, 2015). In the terraranan genus *Eleutherodactylus*, for example, the independent invasion of tree-, rock-, ground-, and water-related microhabitats resulted in morphological convergence in distantly related species, and ecomorphs are classified according to the microhabitat use (Dugo-Cota et al., 2019). Species of *Lynchius*, *Oreobates*, and *Phrynopus* occur in ground-related (e.g. leaf-litter and terrestrial) and rock-related (e.g. cave-dwelling and petricolous) microhabitats and, similarly to *Eleutherodactylus*, body shape could also be related to microhabitat use. Interestingly, many species from MF that use similar microhabitats as those from MG (moss and root mats) resemble species from MG in their overall shape. Therefore, mechanical requirements might also explain the convergence in species in this group and we suggest that future analyses explore the relationship of body size and microhabitat use.

Acknowledgments

For allowing access to material under their care we thank F. Burbrink, C. Raxworthy, and D. Kizirian (AMNH), P. Venegas (CORBIDI), R. Brown and R. Glor (KU), J. Hanken, J. Rosado, and J. Martinez (MCZ), J. Chaparro (MHNC), J. Pombal Jr. (MNRJ), C. Aguilar (MUSM), T. Grant (MZUSP), F. Franco (UFMT), F. Toledo (ZUEC). APM thanks São Paulo Research Foundation (FAPESP) for her PhD scholarship (grants #2017/08488-3 and #2019/09537-3). PPGT thanks FAPESP for his Postdoctoral fellowship (grant #2019/04076-8). FAPESP (grant #2013/50741-7) and Conselho Nacional de Desenvolvimento Científico e Tecnológico (CNPq; grant #306623/2018-8) provided financial support to CFBH. We thank K. Chovanec (KU) for polishing English language usage.

References

Adams, D.C., Church, J.O. (2008): Amphibians do not follow Bergmann's rule. Evolution **62**: 413–420.

Akaike, H. (1974): A New Look at the Statistical Model Identification. In: Selected Papers of Hirotugu Akaike. Springer Series in Statistics (Perspectives in Statistics). Parzen E., Tanabe, K., Kitagawa, G., Eds., New York, Springer.

Ashton, K.G. (2002): Do amphibians follow Bergmann's rule? Can. J. Zool. **80:** 708–716.

Bergmann, C. (1847): Ueber die Verhaltnisse der warmeokonomie der thiere zu ihrer grosse. Gottinger Stud. **3:** 595–708.

Blackburn, D.C., Siler, C.D., Diesmos, A.C., McGuire, J.A., Cannatella, D.C., Brown, R.M. (2013): An adaptive radiation of frogs in a Southeast Asian island archipelago. Evolution **67:** 2631–2646.

Blackburn, T.M., Gaston, K.J., Loder, N. (1999): Geographic gradients in body size: a clarification of Bergmann's rule. Divers. Distrib. **5:** 165–174.

Blomberg, S.P., Garland, T., Ives, A.R. (2003): Testing for phylogenetic signal in comparative data: Behavioral traits are more labile. Evolution **57:** 717-745.

Bossuyt, F., Milinkovitch, M.C. (2000): Convergent adaptive radiations in Madagascan and Asian ranid frogs reveal covariation between larval and adult traits. Proc. Natl. Acad. Sci. USA **97:** 6585–6590.

Bouckaert, R., Heled, J., Kühnert, D., Vaughan, T., Wu, C-H., Xie, D., Suchard, M.A., Rambaut, A., Drummond, A.J. (2014): BEAST 2: A Software Platform for Bayesian Evolutionary Analysis. PLoS Comput. Biol. **10:** e1003537.

Bouckaert, R., Drummond, A.J. (2017): bModelTest: Bayesian phylogenetic site model averaging and model comparison. BMC Evol. Biol. **17:** 17–42.

2694 Butler, M.A., King, A.A. (2004): Phylogenetic comparative analysis: a modeling approach for
2695 adaptive evolution. Am. Nat. **164:** 683–695.
2696 Ceccarelli, F.S., Koch, N.M., Soto, E.M., Barone, M.L., Arnedo, M.A., Ramírez, M.J. (2019):
2697 The Grass was Greener: Repeated Evolution of Specialized Morphologies and Habitat
2698 Shifts in Ghost Spiders Following Grassland Expansion in South America. Syst Biol.
2699 **68:** 63–77.
2700 De la Riva, I., Chaparro, J.C., Castroviejo-Fisher, S., Padial, J.M. (2017): Underestimated
2701 anuran radiations in the high Andes: five new species and a new genus of
2702 Holoadeninae, and their phylogenetic relationships (Anura: Craugastoridae). Zool. J.
2703 Linn. Soc. **182:** 129–172.
2704 De la Riva, I. (2020): Unexpected Beta-Diversity Radiations in Highland Clades of Andean
2705 Terraranae Frogs. In: Neotropical Diversification: Patterns and Processes. Rull, V.,
2706 Carnaval, A., Eds., Springer.
2707 Dugo-Cota, Á., Vilà, C., Rodríguez, A., Gonzalez-Voyer, A. (2019): Ecomorphological
2708 convergence in Eleutherodactylus frogs: a case of replicate radiations in the
2709 Caribbean. Ecol. Lett. **22:** 884–893.
2710 Freckleton, R.P., Harvey, P.H., Pagel, M. (2002): Phylogenetic analysis and comparative data:
2711 a test and review of evidence. Am. Nat. **160**: 712–726.
2712 Frost, D.R. (2020): Amphibian Species of the World: an Online Reference. Version 6.1
2713 (accessed on August 21, 2020). Electronic Database accessible at
2714 https://amphibiansoftheworld.amnh.org/index.php. New York: American Museum of
2715 Natural History.
2716 Gehara, M., Barth, A., Oliveira, E.F., Costa, M.A., Haddad, C.F., Vences, M. (2017): Model
2717 based analyses reveal insular population diversification and cryptic frog species in the

Ischnocnema parva complex in the Atlantic forest of Brazil. Mol. Phylogenet. Evol. **112**: 68–78.

Hansen, T.F. (1997): Stabilizing selection and the comparative analysis of adaptation. Evolution **51**: 1341–1351.

Harmon, L.J., Weir, J., Brock, C., Glor, R.E., Challenger, W. (2008): GEIGER: Investigating evolutionary radiations. Bioinformatics **24**: 129–131.

Losos, J.B. (2011): Convergence, Adaptation, and Constraint. Evolution **65**: 1827-1840.

Moen, D. S., H. Morlon, and J. J. Wiens. Testing convergence versus history: convergence dominates phenotypic evolution for over 150 million years in frogs. Syst. Biol. **65**: 146–160.

Losos, J.B., Jackman, T.R., Larson, A., de Queiroz, K., Rodriguez-Schettino, L. (1998): Contingency and determinism in replicated adaptive radiations of island lizards. Science **279**: 2115–2118.

Moen, D.S., Irschick, D.J., Wiens, J.J. (2013): Evolutionary conservatism and convergence both lead to striking similarity in ecology, morphology and performance across continents in frogs. Proc. Roy. Soc. Lond. B Biol. Sci. **280**: 2013–2156.

Moen, D.S., Morlon, H., Wiens, J.J. (2016): Testing Convergence Versus History: Convergence Dominates Phenotypic Evolution for over 150 Million Years in Frogs, Syst. Biol. **65**: 146–160.

Motta, A.P., Chaparro, J.C., Pombal, Jr., J.P., Guayasamin, J.M., De la Riva, I., Padial, J.M. (2016): Molecular phylogenetics and taxonomy of the Andean genus *Lynchius* Hedges, Duellman, and Heinicke, 2008 (Anura: Craugastoridae). Herpetol. Monogr. **30**: 119–142.

O'Meara, B.C., Ané, C., Sanderson, M.J., Wainwright, P.C. (2006): Testing for different rates of continuous trait evolution using likelihood. Evolution **60**: 922–933.

2743 Ogilvie, H.A., Bouckaert, R., Drummond, A.J. (2017): StarBEAST2 brings faster species tree
2744 inference and accurate estimates of substitution rates. Mol. Biol. Evol. **34**:
2745 2101–2114.
2746 Olalla-Tárraga, M.A., Diniz-Filho, J.A.F., Bastos, R.P., Rodríguez, M.A. (2009): Geographic
2747 body size gradients in tropical regions: water deficit and anuran body size in the
2748 Brazilian Cerrado. Ecography **32**: 581–590.
2749 Olson, D.M, Dinerstein, E., Wikramanayake, E.D., Burgess, N.D., Powell, G.V.N.,
2750 Underwood, E.C., D`Amico, J.A., Itouca, I., Strand, H.E., Morrison, J.C., Louckson,
2751 C.J., Allnutt, T.F., Ricketts, T.H., Kura, Y., Lamoreux, J.F., Wettengel., W., Hedao,
2752 P., Kassem, K.R. (2001): Terrestrial ecoregions of the world: a new map of life on
2753 Earth. BioScience **51**: 933–938.
2754 Padial, J.M., Chaparro, J.C., Castroviejo-Fisher, S., Guayasamín, J.M., Lehr, E., Delgado,
2755 A.J., Vaira, M., Teixeira, Jr, M., Aguayo, R., De la Riva, I. (2012): A revision of 20
2756 species diversity in the Neotropical genus *Oreobates* (Anura: Strabomantidae), with
2757 the description of three new species from the Amazonian slopes of the Andes, and the
2758 proposal of candidate species. Am. Mus. Novit. **3752**: 1–55.
2759 Padial, J.M., Grant, T., Frost, D.R. (2014): Molecular systematics of terraranas (Anura:
2760 Brachycephaloidea) with an assessment of the effects of alignment and optimality
2761 criteria. Zootaxa **3825**: 1–132.
2762 Pagel, M. (1999): Inferring the historical patterns of biological evolution. Nature **401**: 877–
2763 884.
2764 Paradis, E., Claude, J., Strimmer, K. (2004): APE: analyses of phylogenetics and evolution in
2765 R language. Bioinformatics **20**: 289–290.
2766 R Core Team (2018): R: A language and environment for statistical computing. Vienna,
2767 Austria: R Foundation for Statistical Computing. https://www.R–project.org/

2768 Rambaut, A., Drummond, A.J., Xie, D., Baele, G., Suchard, M.A. (2018): Posterior
2769 summarisation in Bayesian phylogenetics using Tracer 1.7. Syst. Biol. **67**: 901–904.
2770 Revell L.J. (2009): Size-correction and principal components for interspecific comparative
2771 studies. Evolution **63**: 3258–3268.
2772 Revell, L.J. (2012): phytools: An R package for phylogenetic comparative biology (and other
2773 things). Methods Ecol. Evol. **3**: 217–223.
2774 Szarski, H. (1964): The Structure of Respiratory Organs in Relation to Body Size in
2775 Amphibia. Evolution **18**: 118–126.
2776 Thompson, G., Withers, P., McMaster, K., Cartledge, V. (2005): Burrows of desert-adapted
2777 Frogs, Neobatrachus aquilonius and Notaden nichollsi. J. R. Soc. West. Aust. **88**: 17–
2778 23.
2779 Tyler, M.J. (1989): Australian Frogs. Australia, Viking O'Neil, Ringwood.
2780 Vidal-García, M., Byrne, P.G., Roberts, J.D., Keogh, J.S. (2014): The role of phylogeny and
2781 ecology in shaping morphology in 21 genera and 127 species of Australo-Papuan
2782 myobatrachid frogs. J. Evol. Biol. **27**: 181–192.
2783 Vidal-García, M., Keogh, J.S. (2015): Convergent evolution across the Australian continent:
2784 Ecotype diversification drives morphological convergence in two distantly related
2785 clades of Australian frogs. J. Evol. Biol. **28**: 2136–2151.
2786 Vinarski, M.V. (2014): On the applicability of Bergmann's rule to ectotherms: The state of
2787 the art. Biol. Bull. Rev. **4**: 232–242.
2788 von May, R., Lehr, E., Rabosky, D.L. (2018): Evolutionary radiation of earless frogs in the
2789 Andes: molecular phylogenetics and habitat shifts in high-elevation terrestrial
2790 breeding frogs. PeerJ **6**: e4313.
2791 Wainwright, P.C., Reilly, S.M. (1994): Ecological Morphology. Chicago, University of
2792 Chicago Press.

2793 Wells, K. (2007): The Ecology and Behavior of Amphibians. Chicago, The University of
2794 Chicago Press.

Tables

Table 1. Pagel's λ values for each trait used in the analysis of body shape. The estimated lambda represents the degree to which trait similarity is dependent upon evolutionary history (1 = trait similarity is directly correlated with evolutionary history; 0 = trait similarity is independent of phylogeny).

Trait	SVL	HL	HW	FA	TB	TH	FL	F3
Pagel's λ	0.6	0.4	0	0	0.94	0.93	0.77	1

Table 2. AIC and p-values for regression analyses considering *Lynchius* (LYN), *Oreobates* (ORE) and *Phrynopus* (PHR) species separately and including all species of the clade (LOP) under different evolutionary models (BM and OU).

Dataset	Model	AIC	p-value
LOP	BM	354.6999	0.3842
	OU	344.8992	0.2028
LYN	BM	53.0966	0.2898
	OU	55.0248	0.2967
ORE	BM	151.8109	0.1602
	OU	153.5855	0.1304
PHR	BM	155.0710	0.4816
	OU	147.2590	0.0645

Figure Legends

Figure 1. Species from Montane Grasslands (A) *Oreobates ayacucho* and (B) *Phrynopus pesantesi*; and species from Dry Forests and Cerrado (C) *O. crepitans* and (D) *O. remotus*. Photos by J. M. Padial (A), E. Lehr (B), and M. Teixeira Jr (C, D).

Figure 2. Phylogenetic relationship of species of *Lynchius*, *Oreobates*, and *Phrynopus*. Color on tips of terminals represent habitat where the species occur. Maps on the right represent the biome and elevational distributions of species. Abbreviations: Tropical and Subtropical Moist Broadleaf Forests (MF), Montane Grasslands and Shrublands (MG), and Tropical and Subtropical Dry Broadleaf Forests, Grasslands, Savannas and Scrublands (DF).

Figure 3. Relationships between body size and elevation in *Lynchius*, *Oreobates* and *Phrynopus* species. (A) Regression analysis considering all species of *Lynchius*, *Oreobates*, and *Phrynopus* and (B) considering species of each genus separately.

Figure 4. Phylomorphospace projection of *Lynchius*, Oreobates, and *Phrynopus* species based on body-size corrected data following a phylogenetic size-correction using generalized least-squares (GLS) regression analysis. Abbreviations: Tropical and Subtropical Moist Broadleaf Forests (MF), Montane Grasslands and Shrublands (MG), and Tropical and Subtropical Dry Broadleaf Forests, Grasslands, Savannas and Scrublands (DF).

Figure 5. Boxplots comparing measurements of body shape among different categories of habitat. Boxes represent the 25%/75% quartiles, and the median is shown with a horizontal line. Abbreviations for measurements: body size (SVL), foot length (FL), tibia length (TB), thigh length (TH), and finger III width (F3). Abbreviations: Tropical and Subtropical Moist

Broadleaf Forests (MF), Montane Grasslands and Shrublands (MG), and Tropical and Subtropical Dry Broadleaf Forests, Grasslands, Savannas and Scrublands (DF).

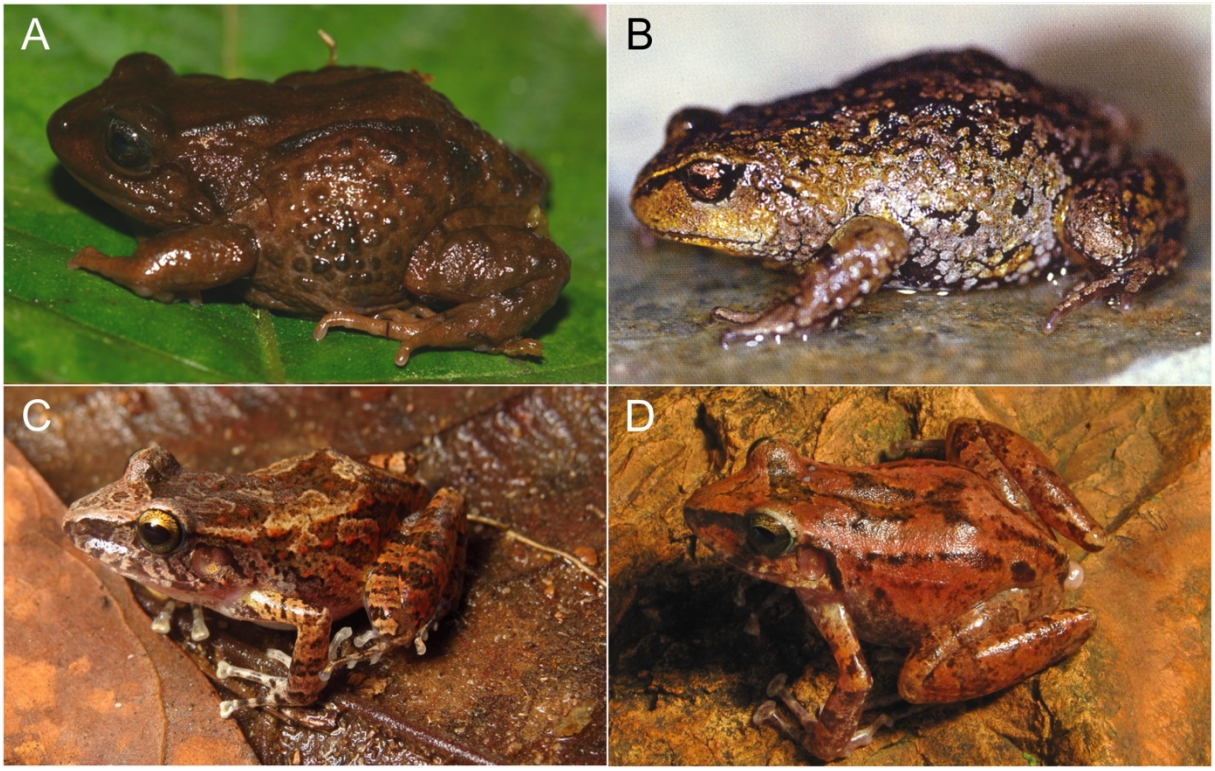

2832

2833 Figure 1

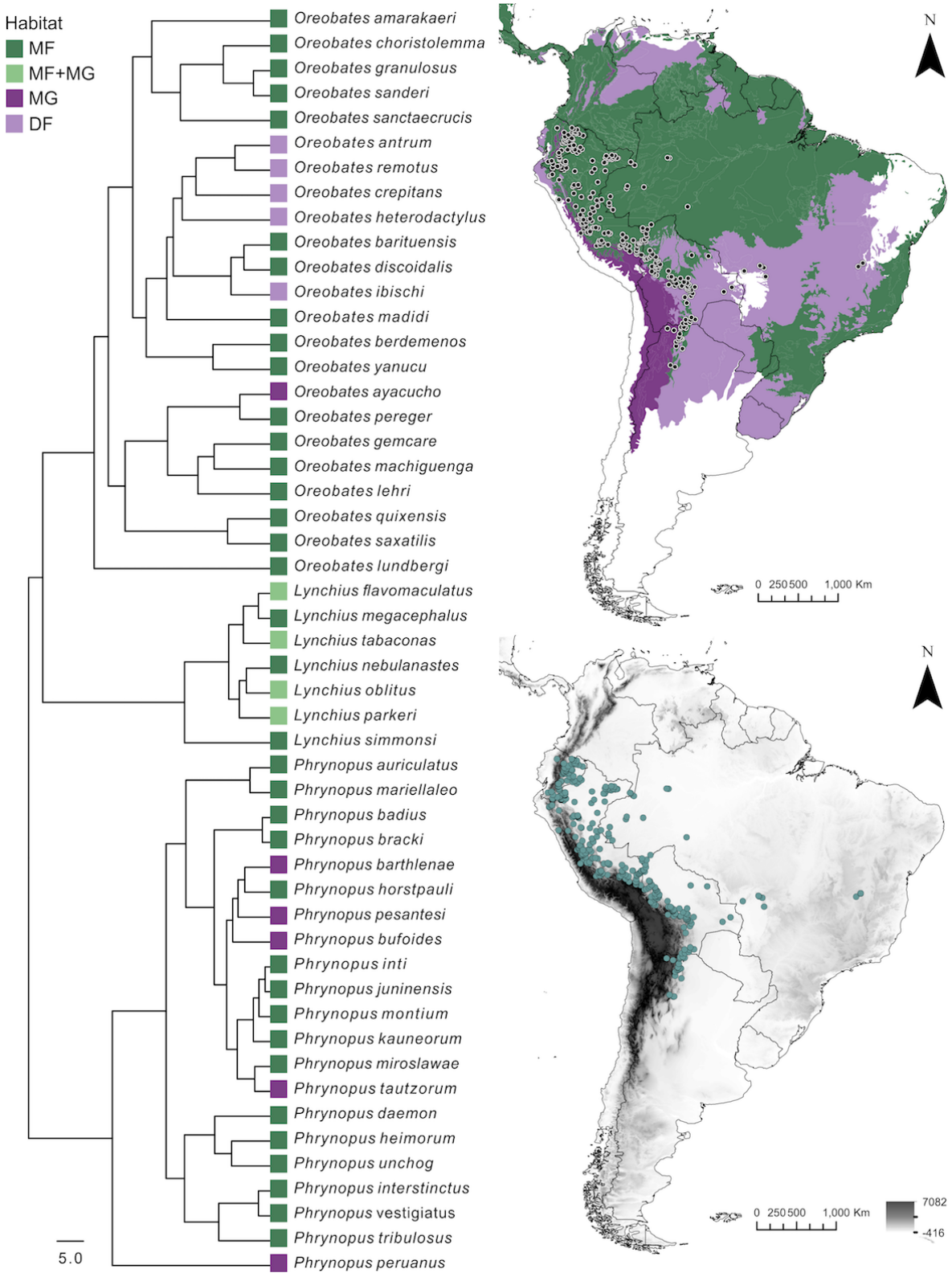

2834

2835 Figure 2

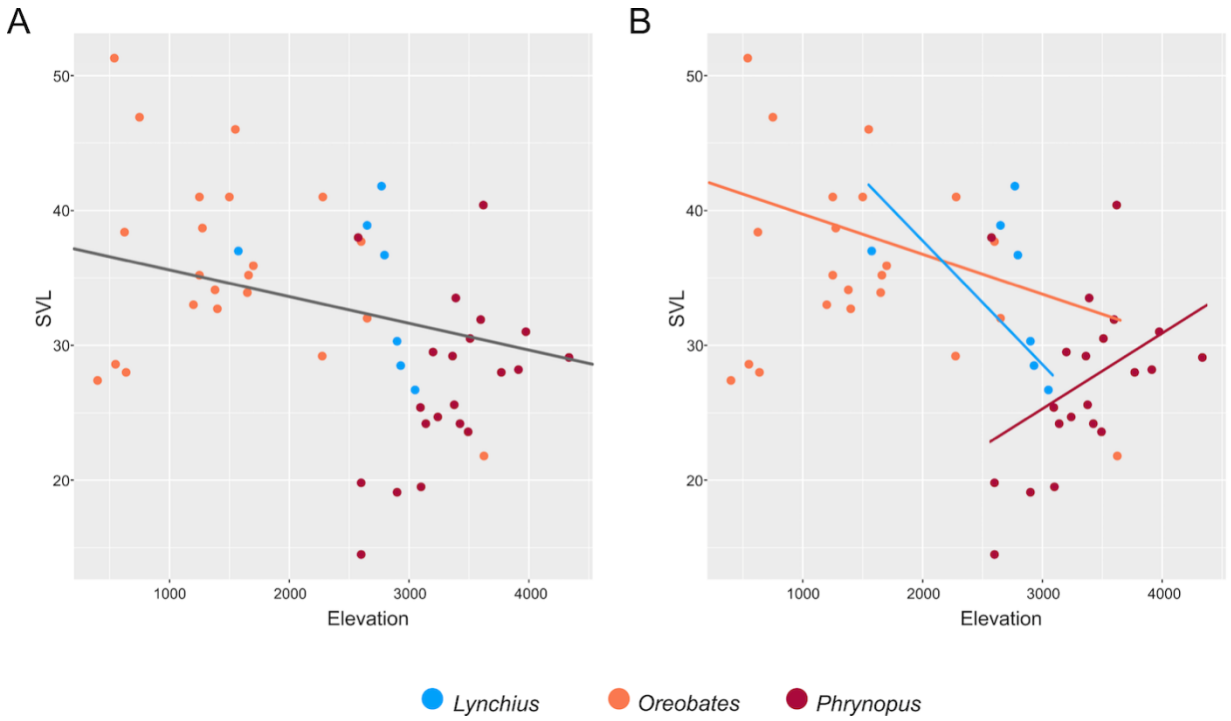

2836

2837 Figure 3

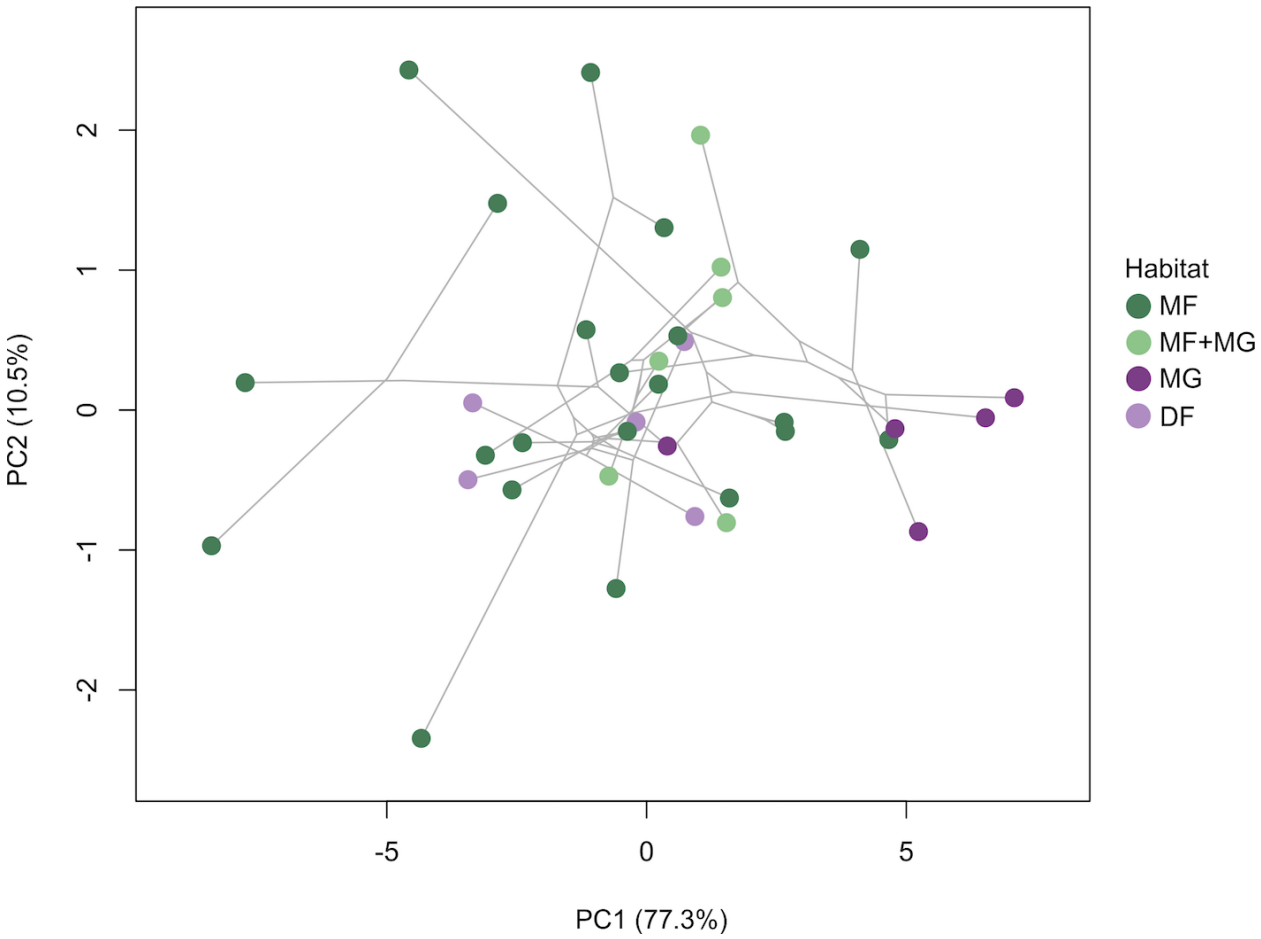

2838

2839 Figure 4

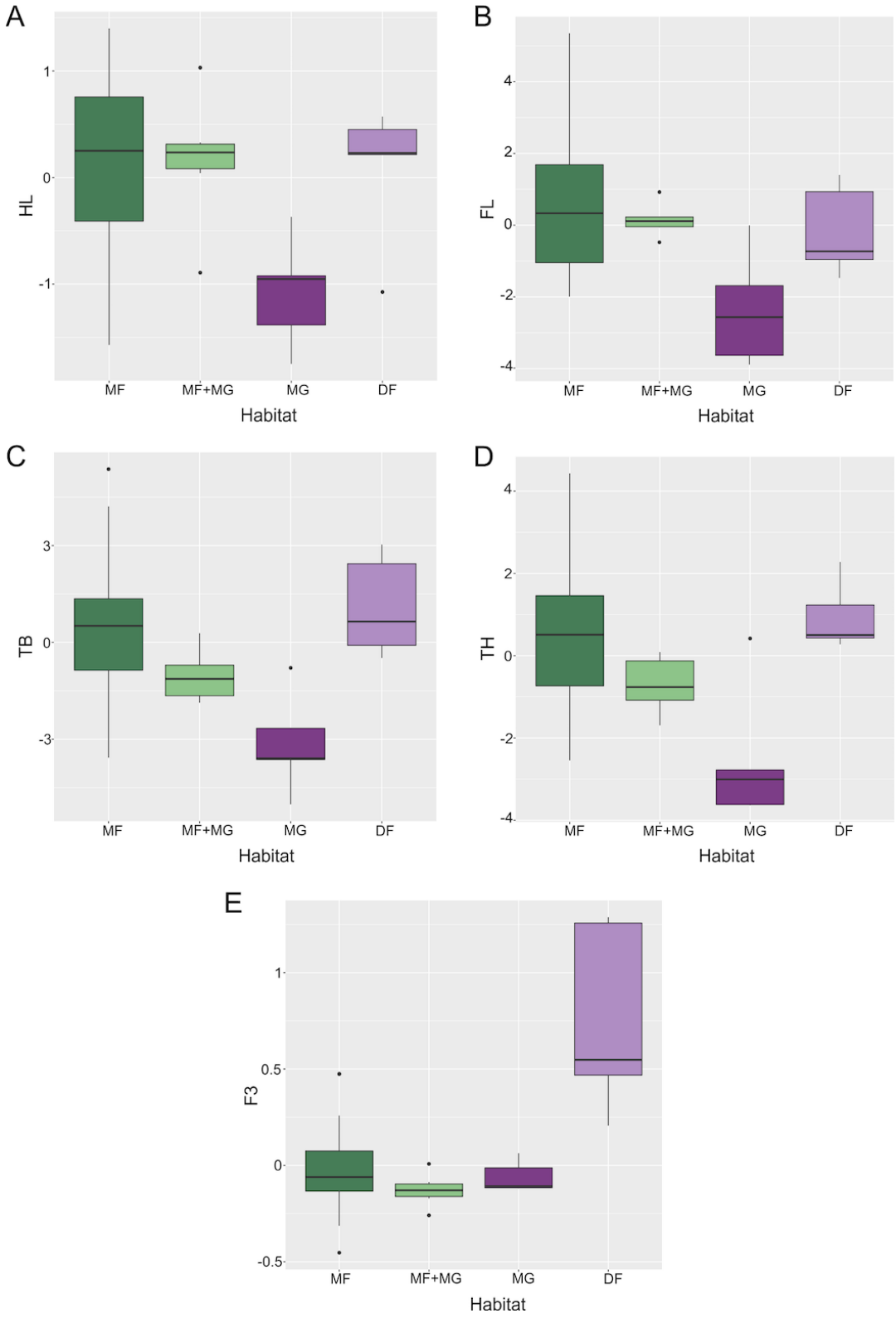

2840

2841 Figure 5

2842 **Supplementary material**

2843

2844 **Table S1.** Body size (SVL) and elevational midpoint for species included in the analyses. Species in bold represent species for which data on SVL
2845 was collected from the literature.

2846

Genus	Species	SVL	Elevation	References
Lynchius	*flavomaculatus*	38.9	2650	Motta et al. (2016)
Lynchius	***megacephalus***	41.8	2770	Sánchez-Nivicela et al. (2019)
Lynchius	*nebulanastes*	36.7	2795	Motta et al. (2016)
Lynchius	*oblitus*	26.7	3050	Motta et al. (2016)
Lynchius	*parkeri*	30.3	2900	Motta et al. (2016)
Lynchius	***simmonsi***	37	1575	Motta et al. (2016)
Lynchius	*tabaconas*	28.5	2930	Motta et al. (2016)
Oreobates	*antrum*	28	638	Vaz-Silva et al. (2018)
Oreobates	*ayacucho*	21.8	3625	Lehr (2007); Padial et al. (2012)
Oreobates	***barituensis***	34.1	1380	Vaira and Ferrari (2008)
Oreobates	***berdemenos***	35.2	1660	Pereyra et al. (2014)
Oreobates	*choristolemma*	41	1250	Padial, Chaparro and De la Riva (2008)
Oreobates	*crepitans*	28.6	550	
Oreobates	*discoidalis*	35.2	1250	Padial et al. (2008)
Oreobates	*gemcare*	37.7	2600	Padial et al. (2012)
Oreobates	*granulosus*	35.9	1700	Padial, Chaparro and De la Riva (2008)
Oreobates	*heterodactylus*	27.4	400	
Oreobates	*ibischi*	38.7	1275	Padial, Chaparro and De la Riva (2008)
Oreobates	*lehri*	32	2650	Padial et al. (2012)
Oreobates	*lundbergi*	41	2280	Padial et al. (2012)
Oreobates	*machiguenga*	32.7	1400	Padial et al. (2012)
Oreobates	***madidi***	33	1200	Padial, Gonzales-Álvarez and De la Riva (2005)

Oreobates	*pereger*	29.2	2275	Padial et al. (2012)
Oreobates	*quixensis*	51.3	540	Padial et al. (2012)
Oreobates	*remotus*	38.4	625	Teixeira et al. (2012)
Oreobates	*sanctaecrucis*	46	1550	Padial, Chaparro and De la Riva (2008)
Oreobates	***sanderi***	33.9	1650	Padial, Chaparro and De la Riva (2008)
Oreobates	*saxatilis*	46.9	750	Padial et al. (2012)
Oreobates	*yanucu*	41	1500	Köhler and Padial (2016)
Phrynopus	***auriculatus***	14.5	2600	Duellman and Hedges (2008)
Phrynopus	*badius*	19.1	2900	Lehr et al. (2012)
Phrynopus	*barthlenae*	31.9	3598	Duellman and Lehr (2009)
Phrynopus	***bracki***	19.8	2600	Hedges (1990); Von May, Lehr and Rabosky (2018)
Phrynopus	*bufoides*	31	3975	Duellman and Lehr (2009)
Phrynopus	*daemon*	24.7	3240	Chávez et al. (2015)
Phrynopus	*heimorum*	24.2	3425	Lehr (2001)
Phrynopus	*horstpauli*	33.5	3390	Duellman and Lehr (2009)
Phrynopus	*interstinctus*	24.2	3140	Lehr and Oróz (2012)
Phrynopus	***inti***	40.4	3620	Lehr et al. (2017)
Phrynopus	*juninensis*	30.5	3509	Von May, Lehr and Rabosky (2018)
Phrynopus	*kauneorum*	29.5	3200	Lehr, Aguilar and Köhler (2002)
Phrynopus	*mariellaleo*	38	2575	Venegas et al. (2018)
Phrynopus	*miroslawae*	29.2	3363	Chaparro, Padial and De la Riva (2008)
Phrynopus	***montium***	23.6	3493	Von May, Lehr and Rabosky (2018)
Phrynopus	*peruanus*	28.2	3913	Von May, Lehr and Rabosky (2018)
Phrynopus	***pesantesi***	29.1	4335	Von May, Lehr and Rabosky (2018)
Phrynopus	*tautzorum*	28	3770	Lehr and Aguilar, 2003
Phrynopus	*tribulosus*	25.4	3095	Von May, Lehr and Rabosky (2018)
Phrynopus	*unchog*	25.6	3377	Lehr and Rodríguez (2017)
Phrynopus	*vestigiatus*	19.5	3100	Lehr and Oróz (2012)

2847

2848 **Table S2.** Measurements and habitat coding for species included in the analyses.
2849

Genus	Species	SVL	HL	HW	FA	TB	TH	FL	F3	Habitat	References
Lynchius	*flavomaculatus*	38.9	14.4	13.9	9.4	20.1	18.6	20.2	0.7	MF+MG	Motta et al. (2016)
Lynchius	*nebulanastes*	36.7	13.8	13.4	9.2	19.5	18.7	20.7	0.8	MF	Motta et al. (2016)
Lynchius	*oblitus*	26.7	10.2	10.2	6	10.3	10.6	11.4	0.4	MF+MG	Motta et al. (2016)
Lynchius	*parkeri*	30.3	11.4	11.3	7.1	12.3	12.7	14	0.6	MF+MG	Motta et al. (2016)
Lynchius	*tabaconas*	28.5	10.8	10.4	6.1	12.3	12.5	13.2	0.5	MF+MG	Motta et al. (2016)
Oreobates	*antrum*	28	10.8	10	7.4	15.1	14.4	13.6	1.9	DF	Vaz-Silva et al. (2018)
Oreobates	*ayacucho*	21.8	7.7	6.9	4.9	7.8	8.9	8.9	0.3	MG	Padial et al. (2012)
Oreobates	*choristolemma*	41	15.4	15.1	9.5	21.9	19.8	20.4	1.5	MF	Padial et al. (2012)
Oreobates	*crepitans*	28.6	10.8	9.8	6.8	13.7	12.9	12.3	1.1	DF	
Oreobates	*discoidalis*	35.2	12.3	11.8	7.7	17.9	17.1	17.4	1.1	MF	Padial et al. (2012)
Oreobates	*gemcare*	37.7	15	14.5	8.6	24.4	21.5	23.9	1	MF	Padial et al. (2012)
Oreobates	*granulosus*	35.9	13.1	13.7	8.4	19.3	17.8	19.1	0.8	MF	Padial et al. (2012)
Oreobates	*heterodactylus*	27.4	10.7	9.8	6.8	15.3	13	13.7	0.8	DF	
Oreobates	*ibischi*	38.7	14.5	14.7	7.6	19.2	18.9	18.2	1.5	DF	Padial et al. (2012)
Oreobates	*lehri*	32	12.9	12.4	8.4	19.5	18.9	19.6	0.6	MF	Padial et al. (2012)
Oreobates	*lundbergi*	41	14.5	14.2	9.9	25.4	21.2	22.7	1.2	MF	Padial et al. (2012)
Oreobates	*machiguenga*	32.7	13.4	13.2	8.9	17	16.1	17.2	0.6	MF	Padial et al. (2012)
Oreobates	*pereger*	29.2	11.2	10.8	7	13.6	13.9	14.1	0.6	MF	Padial et al. (2012)
Oreobates	*quixensis*	51.3	19.8	20.5	11.5	27.8	25.8	26.1	0.9	MF	Padial et al. (2012)
Oreobates	*remotus*	38.4	13.1	12.8	10.3	19.4	18.5	17.5	2.2	DF	Padial et al. (2012)
Oreobates	*sanctaecrucis*	46	17.6	15.3	10.9	23.7	22.1	22.4	1.2	MF	Padial et al. (2012)
Oreobates	*saxatilis*	46.9	18.7	18.8	12.5	25.6	24.9	23.1	0.9	MF	Padial et al. (2012)
Oreobates	*yanucu*	41	15.4	15.1	9.5	21.9	19.8	20.4	1.5	MF	Köhler and Padial (2016)
Phrynopus	*badius*	19.1	7.4	6.8	3.9	7	7.2	7.6	0.4	MF	Von May, Lehr and Rabosky (2018)
Phrynopus	*barthlenae*	31.9	10.4	10.8	6.3	10.2	11.4	11.4	0.8	MG	Von May, Lehr and Rabosky (2018)

Phrynopus	*bufoides*	31	10.5	10.6	7	11	11.1	12.8	0.6	MG	Von May, Lehr and Rabosky (2018)
Phrynopus	*daemon*	24.7	8.4	8.1	5.4	8.2	9.3	9.6	0.4	MF	Von May, Lehr and Rabosky (2018)
Phrynopus	*heimorum*	24.2	8.4	8.2	4.3	8.3	8.9	9	0.4	MF	Von May, Lehr and Rabosky (2018)
Phrynopus	*horstpauli*	33.5	10.8	11.7	8.1	12.7	12.8	14.3	0.9	MF	Von May, Lehr and Rabosky (2018)
Phrynopus	*interstinctus*	24.2	8.8	8.8	4.5	9.8	10.4	10.1	0.5	MF	Von May, Lehr and Rabosky (2018)
Phrynopus	*juninensis*	30.5	12.3	12.5	7.9	12.6	12.4	14.4	0.7	MF+MG	Von May, Lehr and Rabosky (2018)
Phrynopus	*kauneorum*	29.5	11	11.2	7.3	12.7	12	14.1	0.6	MF	Von May, Lehr and Rabosky (2018)
Phrynopus	*mariellaleo*	38	15.2	16.5	10.6	21.5	21	20.5	0.8	MF	Venegas et al. (2018)
Phrynopus	*miroslawae*	29.2	9.7	11.4	7.2	10.2	10.8	11.4	0.4	MF	Von May, Lehr and Rabosky (2018)
Phrynopus	*peruanus*	28.2	9.5	9.5	5.6	9.2	8.6	8.9	0.5	MG	Von May, Lehr and Rabosky (2018)
Phrynopus	*tautzorum*	28	8.6	9.5	6	10	8.5	10.1	0.6	MG	Von May, Lehr and Rabosky (2018)
Phrynopus	*tribulosus*	25.4	8.5	9.2	4.5	10.2	8.9	11.1	0.4	MF+MG	Von May, Lehr and Rabosky (2018)
Phrynopus	*unchog*	25.6	9.2	8.3	5.4	8.9	9.7	10.1	0.4	MF	Von May, Lehr and Rabosky (2018)
Phrynopus	*vestigiatus*	19.5	7	6.7	4.1	8.6	8.6	9.2	0.3	MF	Von May, Lehr and Rabosky (2018)

2850

2851 **Table S3.** Genbank accession numbers of species sampled in this study.
2852

Species	Specimen	12S	16S	CYTB	POMC	RAG	TYR
Euparkerella brasiliensis	-	JX298276	KU495227	JX298402	JX298137	JX267545	JX298237
Lynchius flavomaculatus	KU218210	EU186667	EU186667	-	-	EU186745	EU186766
Lynchius megacephalus	MZUA633	-	MK423938	-	-	-	-
Lynchius nebulanastes	KU181408	EU186704	EU186704	-	AY819154	-	-
Lynchius oblitus	MHNC8614	KX470776	KX470783	-	-	-	KX470799
Lynchius oblitus	MHNC8674	KX470777	KX470784	-	-	-	KX470800
Lynchius oblitus	MHSNM19914	AM039708	AM039640	-	-	-	-
Lynchius oblitus	MTD45954	AM039707	AM039639	-	-	-	-
Lynchius parkeri	KU181307	EU186705	EU186705	-	-	-	-
Lynchius parkeri	QCAZ31466	MK423935	-	-	-	MK423933	-
Lynchius parkeri	QCAZ61015	MK423936	MK423937	-	-	MK423934	-
Lynchius simmonsi	QZ41639	JF809940	JF810004	-	-	JF809915	JF809894
Lynchius simmonsi	QZ41640	-	JF810005	-	-	-	-
Lynchius tabaconas	MHNC8637	KX470773	KX470780	-	KX470787	-	KX470796
Lynchius tabaconas	MHNC8650	KX470774	KX470781	-	-	-	KX470797
Niceforonia brunnea	KU178258	EF493357	EF493357	GQ345203	GQ345264	GQ345282	EF493484
Oreobates amarakaeri	CORBIDI18732	-	MH458942	-	-	-	-
Oreobates amarakaeri	MHNC6975	JF809934	JF809996	-	-	JF809913	JF809891
Oreobates amarakaeri	MHNC7017	-	JF809997	-	-	-	-
Oreobates amarakaeri	MHNC7049	-	JF809998	-	-	-	-
Oreobates antrum	ZUFG5888	MH025427	MH025451	-	-	MH025436	MH025445
Oreobates antrum	ZUFG5889	MH025428	MH025452	-	-	MH025437	MH025446
Oreobates antrum	ZUFG5890	MH025429	MH025453	-	-	MH025438	MH025447
Oreobates antrum	ZUFG8710	MH025430	MH025454	-	-	MH025439	MH025448
Oreobates ayacucho	MHNC6840	-	JF809971	-	-	-	-

Oreobates ayacucho	MNCNIDlR5024	JF809933	JF809970	-	-	JF809912	JF809890
Oreobates ayacucho	MNCNIDlR5026	-	JF809972	-	-	-	-
Oreobates barituensis	MCN1251	-	JF810001	-	-	-	-
Oreobates barituensis	MCN1359	JF809935	JF809999	-	-	JF809914	JF809892
Oreobates barituensis	MCN1360	-	JF810000	-	-	-	-
Oreobates berdemenos	FML24623	-	KJ125509	-	-	-	-
Oreobates berdemenos	LGE2530	-	KJ125507	KJ125511	-	-	-
Oreobates berdemenos	LGE2531	-	KJ125508	-	-	-	-
Oreobates choristolemma	CBG765	JF809921	FJ539067	-	-	JF809900	JF809881
Oreobates choristolemma	CBG768	-	EU368895	-	-	-	-
Oreobates crepitans	ZUEC14119	KJ125510	-	-	-	-	-
Oreobates discoidalis	MNCN43133	FJ539073	FJ539068	EU368883	-	JF809904	JF809884
Oreobates gemcare	MHNC6687	JF809930	JF809960	-	-	JF809909	-
Oreobates gemcare	MNCN44230	-	JF809961	-	-	JF809908	-
Oreobates granulosus	MHNC3396	JF809929	EU368897	-	-	-	JF809887
Oreobates heterodactylus	MNKA7175	JF809923	EU192296	EU368886	-	JF809902	JF809882
Oreobates heterodactylus	MNKA7177	-	EU368898	EU368885	-	-	-
Oreobates ibischi	MNKA6612	FJ438817	FJ438806	-	-	-	-
Oreobates lehri	HNC3223	-	JF809952	-	-	-	-
Oreobates lehri	MUSM27616	JF809927	JF809957	-	-	JF809906	-
Oreobates lehri	MTD45902	JF809928	JF809958	-	-	JF809907	JF809886
Oreobates lundbergi	MUSM19321	-	JF809959	-	-	-	-
Oreobates machiguenga	MHNC6809	JF809932	JF809969	-	-	JF809911	JF809889
Oreobates madidi	MNKA7856	FJ539075	FJ539070	EU368887	-	JF809901	-
Oreobates pereger	MTD46808	JF809926	JF809955	-	-	JF809905	JF809885
Oreobates pereger	MTD46809	-	JF809956	-	-	-	-
Oreobates quixensis	JMP1396	-	JF809993	-	-	-	-
Oreobates quixensis	JMP1571	-	JF809974	-	-	-	-

Oreobates quixensis	KU178249	EF493828	EF493662	-	-	-	-
Oreobates quixensis	KU218150	-	DQ679380	-	AY819093	-	-
Oreobates quixensis	MHNC8805	-	JF809992	-	-	-	-
Oreobates quixensis	MHNC8809	-	JF809977	-	-	-	-
Oreobates quixensis	MHNC8832	-	JF809976	-	-	-	-
Oreobates quixensis	MHNC8918	-	JF809973	-	-	-	-
Oreobates quixensis	MHNC8997	-	JF809975	-	-	-	-
Oreobates quixensis	MNCN43147	-	EU192297	EU368889	-	-	-
Oreobates quixensis	MNCNIDlR8051	-	JF809990	-	-	-	-
Oreobates quixensis	MNCNIDlR8156	-	JF809991	-	-	-	-
Oreobates quixensis	QZ25520	-	JF810002	-	-	-	-
Oreobates quixensis	QZ31186	-	JF810003	-	-	-	JF809893
Oreobates remotus	MZUSP141708	MH025425	JN688273	JN688276	-	MH025434	MH025443
Oreobates remotus	MZUSP141710	MH025422		JN688277	-	MH025431	MH025440
Oreobates remotus	MZUSP141711	MH025423		JN688278	-	MH025432	MH025441
Oreobates remotus	MZUSP141712	MH025424		-	-	MH025433	MH025442
Oreobates remotus	MZUSP141720	MH025426	JN688274	-	-	MH025435	MH025444
Oreobates remotus	MZUSP141721	-	JN688275	-	-	-	-
Oreobates sanctaecrucis	MNKA5507	JF809924	JF809951	-	-	JF809903	JF809883
Oreobates sanderi	MNCN42017	-	EU368904	EU368891	-	-	-
Oreobates saxatilis	JMP2634	-	JF809981	-	-	-	-
Oreobates saxatilis	JMP2635	-	JF809982	-	-	-	-
Oreobates saxatilis	JMP2636	-	JF809983	-	-	-	-
Oreobates saxatilis	JMP2637	-	JF809984	-	-	-	-
Oreobates saxatilis	JMP2640	-	JF809987	-	-	-	-
Oreobates saxatilis	JMP2641	-	JF809988	-	-	-	-
Oreobates saxatilis	JMP2666	-	JF809989	-	-	-	-
Oreobates saxatilis	KU212327	EU186726	EU186708	-	-	EU186742	EU186763

Oreobates saxatilis	MHNC6775	JF809931	JF809962	-	-	JF809910	JF809888
Oreobates saxatilis	MHNC6776	-	JF809963	-	-	-	-
Oreobates saxatilis	MHNC6777	-	JF809964	-	-	-	-
Oreobates saxatilis	MHNC9200	-	JF809978	-	-	-	-
Oreobates saxatilis	MHNC9202	-	JF809979	-	-	-	-
Oreobates saxatilis	MHNC9219	-	JF809980	-	-	-	-
Oreobates saxatilis	MHNC9220	-	JF809985	-	-	-	-
Oreobates saxatilis	MHNC9221	-	JF809986	-	-	-	-
Oreobates saxatilis	MNCN44412	-	JF809965	-	-	-	-
Oreobates saxatilis	MNCN44426	-	JF809966	-	-	-	-
Oreobates saxatilis	MNCN44427	-	JF809967	-	-	-	-
Oreobates saxatilis	MNCN44428	-	JF809968	-	-	-	-
Oreobates yanucu	ZFMK72569	-	KY111322	-	-	-	-
Phrynopus auriculatus	KU291634	EF493708	EF493708	-	-	-	-
Phrynopus auriculatus	MUBI6471	MF186290	MF186348	-	-	-	MF186582
Phrynopus badius	FMNH282818	MG896594	MG896571	-	-	MG896618	-
Phrynopus badius	MUSM31099	MG896595	MG896572	-	-	MG896619	-
Phrynopus barthlenae	-	AM039721	AM039653	-	-	-	-
Phrynopus barthlenae	MHNSM20609	MF186292	MF186350	-	MF186519	-	-
Phrynopus bracki	USNM286919	EF493709	EF493709	GQ345202	GQ345263	EF493421	EF493507
Phrynopus bufoides	-	AM039713	AM039645	-	-	-	-
Phrynopus daemon	MUSM32747	MG896597	MG896574	-	-	-	-
Phrynopus heimorum	-	AM039704	AM039636	-	-	-	-
Phrynopus heimorum	MTD45621	MF186302	MF186363	-	MF186515	-	MF186580
Phrynopus horstpauli	-	AM039715	AM039647	-	MF186517	-	-
Phrynopus horstpauli	MTD44335	MF186303	MF186364	-	MF186518	-	MF186584
Phrynopus interstinctus	MUSM29543	MG896598	MG896575	-	-	MG896621	-
Phrynopus inti	MUSM31203	-	MF651901	-	-	MF651916	-

Phrynopus inti	MUSM31968	MF651909	MF651902	-	-	MF651917	-
Phrynopus inti	MUSM31976	MF651910	MF651903	-	-	-	-
Phrynopus inti	MUSM31984	MF651911	MF651904	-	-	-	-
Phrynopus inti	UMMZ245218	MF651913	MF651906	-	-	MF651918	MF651921
Phrynopus inti	UMMZ245219	MF651914	MF651907	-	-	MF651919	-
Phrynopus juninensis	-	AM039728	AM039660	-	-	-	-
Phrynopus juninensis	MUSM33258	MF651915	MF651908	-	-	MF651920	-
Phrynopus juninensis	MUSM38323	MG896599	MG896576	-	-	MG896622	-
Phrynopus juninensis	MUSM38324	MG896600	MG896577	-	-	MG896623	-
Phrynopus kauneorum	-	AM039718	AM039650	-	-	-	-
Phrynopus mariellaleo	CORBIDI11657	-	MH538298	-	-	MH538302	MH538305
Phrynopus mariellaleo	CORBIDI11658	-	MH538299	-	-	MH538303	MH538306
Phrynopus mariellaleo	CORBIDI11669	-	MH538297	-	MH538308	MH538301	MH538304
Phrynopus miroslawae	MUBI6469	MF186312	MF186393	-	MF186516	MF186542	MF186585
Phrynopus montium	MUSM33259	MG896601	MG896578	-	-	MG896624	-
Phrynopus montium	MUSM33260	MG896602	MG896579	-	-	MG896625	-
Phrynopus peruanus	MTD46801	MG896603	MG896580	-	-	-	-
Phrynopus peruanus	MUSM38315	MG896604	MG896581	-	-	-	-
Phrynopus peruanus	MUSM38316	-	MG896582	-	-	MG896626	MG896631
Phrynopus peruanus	MUSM38317	-	MG896583	-	-	MG896627	MG896632
Phrynopus peruanus	MUSM38318	-	MG896584	-	-	MG896628	-
Phrynopus peruanus	MUSM38319	-	MG896585	-	-	-	-
Phrynopus peruanus	MUSM38320	-	MG896586	-	-	-	-
Phrynopus peruanus	MUSM38321	-	MG896587	-	-	-	-
Phrynopus peruanus	MUSM38322	-	MG896588	-	-	-	-
Phrynopus pesantesi	-	AM039724	AM039656	-	-	-	-
Phrynopus tautzorum	-	AM039720	AM039652	-	-	-	-
Phrynopus tribulosus	MUSM31106	MG896596	MG896573	-	-	MG896620	-

Phrynopus tribulosus	MUBI6441	MF186313	MF186394	-	MF186513	MF186546	MF186577
Phrynopus tribulosus	KU291630	EU186725	EU186707	-	-	-	-
Phrynopus tribulosus	MUBI6451	MF186329	MF186423	-	MF186514	-	MF186578
Phrynopus tribulosus	MUBI7166	MF186330	MF186424	-	-	MF186547	MF186579
Phrynopus unchog	MUSM32748	MG896608	MG896591	-	-	-	-
Phrynopus unchog	MUSM32749	MG896609	MG896592	-	-	-	-
Phrynopus vestigiatus	MUSM29542	MG896610	MG896593	-	-	-	-
Pristimantis curtipes	-	EF493513	EF493513	-	AY819062	KX525470	EF493497
Pristimantis parectatus	-	KY494222	KY494222	-	KY494200	KY494207	KY494220
Pristimantis w-nigrum	-	AY326004	AY326004	-	DQ158260	-	KT898370
Strabomantis biporcatus	CVULA7073	EU186691	EU186691	GQ345204	GQ345265	EU186754	EU186775

2853

References for this section:

Chaparro, J.C., Padial, J.M., De la Riva, I. (2008): Two sympatric new species of *Phrynopus* (Anura: Strabomantidae) from Yanachaga Chemillen National Park (central Peruvian Andes). Zootaxa **1761**: 49–58.

Chávez, G., Santa Cruz, R., Rodríguez, D., Lehr, E. (2015): Two new species of frogs of the genus *Phrynopus* (Anura: Terrarana: Craugastoridae) from the Peruvian Andes. Amphib. Reptile Conserv. **9**, 15–25.

Duellman, W.E., Hedges, S.B. (2008): Two minute species of *Phrynopus* (Lissamphibia: Anura) from the Cordillera Oriental in Peru. Zootaxa **1675**: 59–66.

Duellman, W.E., Lehr, E. (2009): Terrestrial-breeding frogs (Strabomantidae) in Peru. Münster, Germany: Nature und Tier Verlag.

Hedges, S.B. (1990): A new species of *Phrynopus* (Anura: Leptodactylidae). Copeia **1990**, 108–112.

Köhler, J., Padial, J.M. (2016): Description and phylogenetic position of a new (singleton) species of *Oreobates* Jiménez de la Espada, 1872 (Anura: Craugastoridae) from the Yungas of Cochabamba, Bolivia. Ann. Carnegie Mus. **8**: 23–38.

Lehr, E. (2001): A new species of *Phrynopus* (Anura: Leptodactylidae) from the eastern Andean slopes of central Peru. Salamandra **37**: 11–20.

Lehr, E. (2007): New eleutherodactyline frogs (Leptodactylidae: Pristimantis, *Phrynopus*) from Peru. Bull. Mus. Comp. Zool. **159**: 145–178.

Lehr, E., Aguilar, C. (2003): A new species of *Phrynopus* (Amphibia, Anura, Leptodactylidae) from the puna of Maraypata (Departamento de Huánuco, Peru). Zool. Abh. Staatl. Tierk. Dresden **53**: 87–92.

Lehr, E., Oróz, A. (2012): Two new species of *Phrynopus* (Anura: Strabomantidae) from the Cordillera de Carpish in central Peru (Departamento de Huánuco). Zootaxa **3512**: 53–63.

Lehr, E., Rodríguez, D. (2017): Two new species of Andes Frogs (Craugastoridae: *Phrynopus*) from the Cordillera de Carpish in central Peru. Salamandra **53**: 327–338.

Lehr, E., Aguilar, C., Köhler, G. (2002): Two sympatric new species of *Phrynopus* (Anura: Leptodactylidae) from a cloud forest in the Peruvian Andres. J. Herpetol. **36**: 208–216.

Lehr, E., von May, R., Moravec, J., Cusi, J.C. (2017): A new species of *Phrynopus* (Amphibia, Anura, Craugastoridae) from upper montane forests and high Andean grasslands of the Pui Pui Protected Forest in central Peru. ZooKeys **713**: 131–157.

Motta, A.P., Chaparro, J.C., Pombal, Jr., J.P., Guayasamin, J.M., De la Riva, I., Padial, J.M. (2016): Molecular phylogenetics and taxonomy of the Andean genus *Lynchius* Hedges, Duellman, and Heinicke, 2008 (Anura: Craugastoridae). Herpetol. Monogr. **30**: 119–142.

Padial, J.M., Gonzales-Álvarez, L., De la Riva, I. (2005): A new species of the *Eleutherodactylus discoidalis* group (Anura: Leptodactylidae) from Andean humid montane forests of Bolivia. Herpetologica **61**: 318–325.

Padial, J.M., Chaparro, J.C., De la Riva, I. (2008): Systematics of *Oreobates* and the *Eleutherodactylus discoidalis* species group (Amphibia, Anura), based on two mitochondrial DNA genes and external morphology. Zool. J. Linn. Soc. **152**: 737–773.

Padial, J.M., Chaparro, J.C., Castroviejo-Fisher, S., Guayasamin, J.M., Lehr, E., Delgado, A.J., Vaira, M., Teixeira Jr., M., Aguayo-Vedia, C.R., De la Riva, I. (2012): A revision of species diversity in the Neotropical genus *Oreobates* (Anura:

2904 Strabomantidae), with the description of three new species from the Amazonian
2905 slopes of the Andes. Am. Mus. Novit. **3752**: 1–55.
2906 Pereyra, M.O., Cardozo, D.E., Baldo, J.L.,, Baldo, D. (2014): Description and phylogenetic
2907 position of a new species of *Oreobates* (Anura: Craugastoridae) from northwestern
2908 Argentina. Herpetologica **70**: 211–227.
2909 Sánchez-Nivicela, J.C., Urgilés, V.L., Navarrete, M.J., Yánez-Muñoz, M.H., Ron, S.R.
2910 (2019): A bizarre new species of *Lynchius* (Amphibia, Anura,
2911 Strabomantidae) from the Andes of Ecuador and first report of *Lynchius parkeri* in
2912 Ecuador. Zootaxa **4567**: 1–24.
2913 Teixeira Jr., M., Amaro, R.C., Recoder, R.S., de Sena, M.A., Rodrigues, M.T. (2012): A
2914 relict new species of *Oreobates* (Anura, Strabomantidae) from the seasonally dry
2915 tropical forests of Minas Gerais, Brazil, and its implication to the biogeography of
2916 the genus and that of South American dry forests. Zootaxa **3158**: 37–52.
2917 Vaira, M., Ferrari, L. (2008): A new species of *Oreobates* (Anura: Strabomantidae) from
2918 the Andes of northern Argentina. Zootaxa **1908**: 41–40.
2919 Vaz-Silva, W., Maciel, N.M., de Andrade, S.P., Amaro, R.C. (2018): A new cryptic species
2920 of *Oreobates* (Anura: Craugastoridae) from the seasonally dry tropical forest of
2921 central Brazil. Zootaxa **4441**: 89–108.
2922 Venegas, P.J., Barboza, A.C., De la Riva, I., Padial, J.M. (2018): A new species
2923 of *Phrynopus* from the northeastern Andes of Peru, its phylogenetic position, and
2924 notes on the relationships of Holoadeninae (Anura: Craugastoridae).
2925 Zootaxa **4446**: 501–524.
2926 von May, R., Lehr, E., Rabosky, D.L. (2018): Evolutionary radiation of earless frogs in the
2927 Andes: molecular phylogenetics and habitat shifts in high-elevation terrestrial
2928 breeding frogs. PeerJ **6**: e4313.

Seção 2

Contribuições taxonômicas

On the identity of species of *Oreobates* (Anura: Craugastoridae) from central South America, with the description of a new species from Bolivia[†]

André Pansonato[1], Ana Motta[2,6], Pier Cacciali[3], Célio F. B. Haddad[2], Christine Strüssmann[1,4], and Martin Jansen[5]

[1]*Laboratório de Herpetologia, Centro de Referência da Biodiversidade Regional, Pós-Graduação em Ecologia e Conservação da Biodiversidade, Instituto de Biociências, Universidade Federal de Mato Grosso (UFMT). Av. Fernando Correa da Costa, 2367, Boa Esperança, 78060–900, Cuiabá, Mato Grosso, Brazil*

[2]*Departamento de Biodiversidade e Centro de Aquicultura (CAUNESP), Instituto de Biociências, Av. 24A, 1515, Bela Vista, 13506-900, Rio Claro, São Paulo, Brazil*

[3]*Instituto de Investigación Biológica del Paraguay, Del Escudo 1607, 1425 Asunción, Paraguay*

[4]*Faculdade de Medicina Veterinária, Universidade Federal de Mato Grosso (UFMT), Av. Fernando Correa da Costa, 2367, Boa Esperança, 78060–900, Cuiabá, Mato Grosso, Brazil*

[5]*Terrestrische Zoologie, Senckenberg Forschungsinstitut und Naturmuseum, Senckenberganlage 25, 60325 Frankfurt am Main, Germany*

[6]*Corresponding author. Email: apmottah@gmail.com*

[†] Manuscripto aceito para publicação no periódico *Journal of Herpetology*

Abstract.—The similar morphology of species in the genus *Oreobates* that inhabit rocky outcrops amidst the Seasonally Dry Tropical Forests and Cerrado savannas of central South America has led to taxonomic inaccuracies when only external morphology was considered. Therefore, researchers frequently fail to determine the true taxonomic status of some of these populations and attribute them to unidentified or misidentified species. Integrating different sources of data is of fundamental importance to understand the diversity of species in this group. Herein, we used external morphology (16 characters measured in 54 adult specimens), bioacoustics (238 advertisement calls of 19 specimens of *Oreobates* from six localities), and molecular evidence (based on 59 16S gene fragments representing 24 of the currently available names of *Oreobates*) to evaluate the taxonomic status and distribution range of *Oreobates* from 10 localities in central South America. We performed Phylogenetic analysis, Principal component analyses and discriminant function analyses to evaluate the taxonomic status of *Oreobates* in central South America. We redescribe *O. heterodactylus* based on a newly collected series of topotypes and additional material from other localities. We reassess the taxonomic status of *O. crepitans*, herein considered as a junior synonym of *O. heterodactylu*s. We also describe eastern Bolivian populations of *Oreobates* as a new species.

Key words: Amphibia; Bioacoustics; Brachycephaloidea; Seasonally Dry Tropical Forest; Morphology; Phylogeny; Taxonomy; Terrarana.

The genus *Oreobates* Jiménez de la Espada 1872 was described to accommodate a frog obtained at Quijos, Napo region, mid-northern Ecuador. It was originally considered as a cystignathid and remained as a monotypic genus for one century, until it was synonymized to *Ischnocnema* Reinhardt and Lütken, 1862 (Lynch, 1971; Lynch and Schwartz, 1971). Caramaschi and Canedo (2006) removed *Oreobates* from that synonymy and, besides the nominal form *Oreobates quixensis*, considered other four species originally allocated to *Ischnocnema* as belonging to the same genus. *Oreobates* is currently included in the family Craugastoridae (Pyron and Wiens, 2011; Padial et al., 2014; see also Streicher et al., 2018), although some authors still consider it as belonging to Strabomantidae (e.g., Heinicke et al., 2018). The genus now comprises 25 species (Frost, 2020), distributed from the Amazonian slopes of the Andes into the upper Amazon basin, from Colombia southwards to northern Argentina and east into savannas and dry forests from mid-eastern Brazil (Teixeira Jr. et al., 2012; Frost, 2020; Vaz-Silva et al., 2018). Frogs in the genus *Oreobates* occur in a wide variety of habitats, from the Andean Paramo grasslands through cloud, upper montane, lower montane, Amazonian lowland forests, Seasonally Dry Tropical Forests, to more open and xeric environments, such as Cerrado savannas (Teixeira Jr. et al., 2012; Köhler and Padial, 2016; Vaz-Silva et al., 2018).

Since the publication of the first molecular evaluation of the genus by Padial et al. (2008), several subsequent studies consistently attested the monophyly of *Oreobates* (e.g., Pyron and Wiens, 2011; Padial et al., 2012; Teixeira Jr. et al., 2012; Pereyra et al., 2014; Köhler and Padial, 2016; Vaz-Silva et al., 2018). However, intrageneric relationships still show some inconsistencies, and different authors point to the existence of cryptic/undescribed taxa as well (e.g., Padial et al., 2012; Köhler and Padial, 2016; Ferraro et al., 2018).

One of the taxonomic uncertainties within *Oreobates* refers to *Oreobates heterodactylus* (Miranda-Ribeiro 1937) and *Oreobates crepitans* (Bokermann 1965), both described from nearby localities in western Brazil (Padial et al., 2008; Padial et al., 2012). Individuals of both species have greatly expanded, truncate fingertips on Fingers III and IV, a condition found also in *Oreobates remotus* Teixeira-Jr, Amaro, Recoder, Sena & Rodrigues 2012 and *Oreobates antrum* Vaz-Silva, Maciel, Andrade & Amaro 2018. Although the relative proportion of the finger discs III and IV has been used to distinguish *O. crepitans* from *O. heterodactylus* in the past (Heyer and Muñoz, 1999), all four species of *Oreobates* described from Central South America share the presence of enlarged finger discs (Vaz-Silva et al., 2018), and this condition was considered a putative shared synapomorphy of this clade (Pereyra et al., 2014).

One of the aspects that until now prevented a better evaluation of the taxonomic status of *Oreobates crepitans* and *O. heterodactylus* is the lack of additional specimens – other than the faded types (see below) – from the type locality (or surrounding areas) of this latter species and unambiguously attributed to it. Heyer and Muñoz (1999) explicitly discussed this topic and for the first time provided coordinates for the type locality, but neither they nor subsequent authors dealing with *Oreobates* mentioned having visited the type locality of *O. heterodactylus* and/or obtained additional topotypes.

The two syntypes of *Oreobates heterodactylus*, housed at the Museu Nacional, Rio de Janeiro, Brazil, were obtained at the very beginning of the 20th century. At that time, aiming at the integration of innermost portions of the country located far away from the central administration in the Southeast, the Brazilian government created a commission for the implementation of telegraph lines between Rio de Janeiro and localities in some distant provinces in Amazonia. Members of the “Strategic Telegraph Commission from Mato Grosso to Amazonas” (1907-1915) – better known as the “Rondon Commission” – also

conducted scientific research in several areas such as Botany, Ethnography, Geography, Geology, and Zoology (de Sá et al., 2008), having described several new species. Among these was the frog *Teletrema heterodactylum* Miranda-Ribeiro 1937, of which two specimens were collected in 1908 near the city of São Luiz de Cáceres (nowadays Cáceres), approximately 200 km SW of Cuiabá (Hoehne, 1916; Miranda-Ribeiro, 1937). In the original description, Miranda-Ribeiro (1937) mentioned that both specimens were obtained at "gruta dita Fazendinha" (meaning a small cave - or grotto - called Fazendinha; Portuguese). When re-examining the types in 1962, Myers pointed that he could not find generic differences between Miranda-Ribeiro's *Teletrema* and the genus *Eleutherodactylus*, and proposed the new combination *Eleutherodactylus heterodactylus* (Myers, 1962).

Present uncertainties regarding the identity of *Oreobates crepitans* and *O. heterodactylus* were reinforced after the redescription of the latter species, as *Eleutherodactylus heterodactylus*, based on a sample comprised of Bolivian specimens only (Padial and De La Riva, 2005). Padial and De La Riva (2005) did not examine the two syntypes, previously referred as being in a bad condition of preservation (Heyer and Muñoz, 1999). These authors mention that the population from Bolivia could represent a third species, but that this assumption could not be corroborated due to the absence of new topotypical material and the bad preservation of the syntypes of *O. heterodactylus*. Indeed, the syntypes had been also examined by George Myers in 1944, less than a decade after the species description, and were described as being "somewhat shriveled" on that occasion (Myers, 1962:199).

The name *Eleutherodactylus heterodactylus* remained in use until Padial et al. (2008) included Bolivian samples – identified according to Padial and De La Riva (2005) – in molecular and morphological comparisons with known species of *Eleutherodactylus* and

of *Oreobates* and concluded for the validity and monophyly of the latter, having proposed the new combination *Oreobates heterodactylus*.

The other *Oreobates* species from the Brazilian state of Mato Grosso, originally described as *Eleutherodactylus crepitans*, was based on three specimens obtained at "São Vicente, Cuiabá" (Bokermann, 1965), nowadays within the limits of the municipality of Santo Antônio do Leverger. The species was synonymized to *Eleutherodactylus fenestratus* by Lynch (1980) and subsequently revalidated by Heyer and Muñoz (1999), who emphasized that the types were the only material known for the species. It was also treated as a *Pristimantis* (Heinicke et al., 2007) before Padial et al. (2012) removed it to its present generic allocation in the genus *Oreobates*. Strüssmann et al. (2011) described the topotypic call of *O. crepitans*, presented comments and pictures of the habitats and color variation in this species, and extended its distribution. However, considering the proximity of some of the reported populations of *O. crepitans* to the type locality of *O. heterodactylus*, those authors failed to analyze the variation in the relative proportions of the fingers among those populations. Indeed, some of the present taxonomic difficulties regarding the *Oreobates* species with greatly expanded fingertips on Fingers III and IV certainly arise from the lack of analyses of intraspecific variation in morphological, as well as in bioacoustic and molecular characteristics (Padial et al., 2012).

After careful literature review, interviews with local farmers, and field excursions to the city of Cáceres and surroundings, we were able to locate and visit the type locality of *Oreobates heterodactylus*. The place formerly called "Fazendinha" was subdivided over the course of time and the "gruta Fazendinha" is presently situated in a property named "Fazenda Hayashi" (Hayashi farm), where we obtained new specimens and advertisement call recordings. We also collected new material of *Oreobates* from additional populations in Brazil and Bolivia. This includes topotypic material of *Oreobates crepitans* and

specimens from a lowland Bolivian population previously identified as *O. heterodactylus sensu* Padial and De La Riva (2005). This latter material is recognized and described here as a new species. We used external morphology, bioacoustics and molecular evidence to evaluate the taxonomic status of *Oreobates* in central South America.

Material and Methods

We analyzed specimens of *Oreobates* from 10 localities from central South America (Fig. 1) in order to access their identity. These localities include (abbreviations used in the text in parentheses): Dolina Água Milagrosa, Cáceres, Mato Grosso, Brazil (DM); Gruta Fazendinha in Fazenda Hayashi, Cáceres, Mato Grosso, Brazil (GF; type locality of *O. heterodactylus*); Morro do Chapéu, Chapada dos Guimarães, Mato Grosso, Brazil (MC); Mata Fria, Chapada dos Guimarães, Mato Grosso, Brazil (MF); Fazenda União, Rosário Oeste, Mato Grosso, Brazil (RO); Estação Ecológica Serra das Araras, Porto Estrela, Mato Grosso, Brazil (SA); São Vicente, Santo Antônio do Leverger, Mato Grosso, Brazil (SV; type locality of *O. crepitans*); San Sebastián, Provincia Ñuflo de Chávez, Departamento Santa Cruz, Bolivia (SS); Serranía de Santiago, Cerro del Arco, Provincia Chiquitos, Departamento Santa Cruz, Bolivia (CA); Bella Boca, Provincia Ángel Sandoval, Departamento Santa Cruz, Bolivia (BB).

Molecular Data and Analysis.—We sampled 28 specimens of *Oreobates* from seven localities in Brazil and Bolivia (DM, GF, MF, SA, SV, SS, and CA) and generated new sequences for 25 of these specimens (Table 1), including topotypic specimens of *O. crepitans* and *O. heterodactylus*. Fragments of the mitochondrial 16S rRNA gene were sequenced for comparison with sequences from GenBank (Appendix 1). DNA was extracted from muscle stored in ethanol 98% at -12 to -27°C using the standard glass fiber plate protocol (Ivanova et al., 2006). Samples were washed for about 14 h in 50 µl of

diluted PBS buffer (1:9 of buffer and water respectively). Tissues were digested with vertebrate lysis buffer (60 µl per sample) and proteinase K (6 µl per sample) at 56°C for around 14 h. After extraction, DNA samples were eluted in 50 µL TE buffer.

Amplification via double-stranded PCR of mitochondrial 16S rRNA fragments was performed using the Eurofins MWG Operon primers 16sar-L (forward: 5'–CGCCTGTTTATCAAAAACAT–3') and 16sbr-H (reverse: 5'–CCGGTCTGAACTCAGATCACGT–3'), in an Eppendorf Mastercycler® pro. The PCR conditions were: (1) initial denaturation 2 min at 94ºC, (2) denaturation 35 s at 94ºC, (3) hybridization 35 s at 50ºC; (4) elongation 60 s at 72ºC and then back to (2) in 35 cycles; (5) final elongation 5 min at 72ºC. Cycle-sequencing and sequencing (BigDyeTerminator) were performed with the same forward and reverse primers mentioned above.

In total, 59 sequences were used, representing 24 of the currently available names of *Oreobates* (Frost, 2020) plus three candidate species detected by Padial et al. (2012) and the new species described herein (Appendix 1). Outgroup includes four species of *Lynchius*, and *Haddadus binotatus* was used to root the tree, according to the phylogenetic analyses by Hedges et al. (2008), Pyron and Wiens (2011), Padial et al. (2014), and Köhler and Padial (2016). The alignments of the sequences were performed in MAFFT 7 (Katoh et al., 2002; Katoh and Standley, 2013) through the webserver (available at http://mafft.cbrc.jp/alignment/server/). For the alignment of the 16S gene fragment, the Q-INS-i search strategy was included for the secondary structure of that gene (Katoh and Toh, 2008), which is considered appropriate for alignments that consist of large numbers of sequences (Katoh and Standley, 2013). The alignment, comprising 628 character columns, was visualized and exported with MSA Viewer (Yachdav et al., 2016). The best nucleotide substitution model for our dataset was identified using PartitionFinder2 (Lanfear et al., 2016), with linked branch lengths (supported by most of the phylogenetic programs).

Phylogenetic analyses were performed with the aligned sequences and with the implemented GTR+I+G best-fit model following the Akaike Information Criterion with a correction for finite sample sizes (AICc). Bayesian Inference analysis (BI) was performed with MrBayes 3.2 (Huelsenbeck and Ronquist, 2001; Ronquist and Huelsenbeck, 2003). Runs were performed in duplicate with 500,000 generations each, and trees sampled every 100 generations. Convergence were assessed graphically by checking the LnL values for stability, which was reached after about 25000 generations. Of each run, the first 1250 trees were discarded as "burn-in".

Maximum Likelihood (ML) analyses were performed using IQTree webserver (Trifinopoulos et al., 2016). To estimate clade support, a Maximum Likelihood (ML) analysis was run using 10,000 ultrafast bootstrap approximation (UFBoot) replicates with 10,000 maximum iterations and minimum correlation coefficient of 0.99 plus 10,000 replicates of Shimodaira-Hasegawa approximate likelihood ratio (SH-aLRT), which proved to be accurate with a high statistical power (Guindon et al., 2010). FigTree 1.3.1 was used for tree viewing (http://tree.bio.ed.ac.uk/software/figtree/). De Queiroz et al. (2002) were followed in the definition of weak (50–69 bootstrap percentages), moderate (70–89), and strong (90–100) support. However, it is emphasized that the goal of this study is to call attention to the degree of genetic differentiation among populations and not to provide an in-depth or comprehensive analysis of phylogenetic relationships within *Oreobates*, at any level. This would require more comprehensive data sets, e.g., including additional molecular markers.

For *Oreobates antrum*, *O. remotus*, and populations from Mato Grosso and Bolivia, the evolutionary genetic divergence were estimated for the 16S gene among sequences, computing uncorrected pairwise p-distances with Mega 6 (Tamura et al., 2013) to assess the degree of intra- and interspecific differences, using a Bootstrap estimation method of

10,000 replications. Additionally, on the full data set an initial species delimitation analysis was performed by using the automatic barcode gap discovery (ABGD) approach (Puillandre et al., 2012) through its web server (http://wwwabi.snv.jussieu.fr/public/abgd/abgdweb.html), setting the use of K80 Kimura measure of distance and Pmin=0.02 and Pmax=0.06 (values for Prior Intraspecific divergence that are more relevant for amphibians than the default setting).

Morphometry and Morphological Characters.—Terminology for morphological characters used in the diagnosis and descriptions follows Duellman and Lehr (2009). We measured 54 adult specimens (44 males and 10 females) with a digital caliper to the nearest 0.01 mm and rounded to one decimal to avoid pseudo precision. Abbreviations for measurements are as follows: snout–vent length, SVL; head length, HL; head width, HW; eye length, EL; eye to nostril distance, EN; internarial distance, IND; eye-eye distance, EE; tympanic membrane height, TYH; tympanic membrane length, TYL; width of disc of Finger III, F3; width of disc of Finger IV, F4; arm length, FA; tibia length, TL; thigh length, TH; foot length, FL; width of disc of Toe IV, T4. The terminology in color descriptions follows Köhler (2012), using photographs of live specimens.

Specimens were collected with permission of Instituto Chico Mendes de Conservação da Biodiversidade, Brazil (ICMBio 13429-2) and Ministerio de Medio Ambiente y Aqua, Bolivia (MMAyA-VMABCC-DGBAP 941). They were deposited in the Coleção Zoológica de Vertebrados, Universidade Federal de Mato Grosso (UFMT; Cuiabá, Mato Grosso, Brazil) and in the Senckenberg Naturmuseum und Forschungsinstitut (SMF; Frankfurt, Germany) (Appendix 2).

Bioacoustics.—We recorded the advertisement calls of individuals of *Oreobates* species using a digital recorder (either Marantz PMD 660 or Olympus DM-550), equipped with an external directional microphone (Yoga EM-9600 or Sennheiser ME 80

microphone). The recordings were taken in the field after identifying the emitter male. Digital recordings were sampled at a rate of 44.1 kHz, with 16-bit resolution. The files were subsequently saved as uncompressed .wav files and archived in the Banco de Registros Bioacústicos of the Laboratório de Herpetologia do Instituto de Biociências da Universidade Federal de Mato Grosso (LH; Cuiabá, Mato Grosso, Brazil), and in the Sektion Herpetologie at SMF. In addition to our own recordings, we also analyzed calls of *Oreobates* from Cerro del Arco (CA) stored in Fonoteca Zoológica, at the Museo Nacional de Ciencias Naturales (FonoZoo; Madrid, Spain; FonoZoo ID 19936; 20413–7).

We analyzed 238 advertisement calls of 19 specimens of *Oreobates* from six localities: four in the state of Mato Grosso, Brazil (DM; GF; SA; SV), and two in the Department Santa Cruz, Bolivia (SS; CA) (Appendix 3). Bioacoustic parameters were analyzed using Raven Pro 1.5 (Bioacoustics Research Program, 2014), with the following configuration: Hamming window function; brightness 50%; contrast 50%; DFT size 256 points, and time grid overlap 50%. The terminology in call descriptions is in accordance with Köhler et al. (2017), following the call-centered approach. We analyzed six quantitative parameters: call rate (calls/min), call duration (ms), number of pulses per call, dominant frequency (Hz), pulse duration (ms), and inter-pulse intervals (ms). Whenever possible, we also analyzed inter-call intervals, pulse rate, and number of harmonics. Call and pulse rate were calculated as the ratio of the absolute number of calls/pulses and the absolute duration in which these calls/pulses were emitted (Köhler et al., 2017). To produce spectrograms and waveforms, we used the R package “Seewave” (Sueur et al., 2008) and tuneR (Ligges et al., 2007) with the following settings: FFT size of 512 points, Hamming window, and 90% of overlap. In the Results section, numerical data (morphometric and bioacoustic) are presented as range (mean ± standard deviation). In comparisons, values and characteristics of the compared species are presented within parentheses.

Principal component analyses (PCA) and discriminant function analyses (DFA) were conducted in order to statistically evaluate the morphometric and acoustic differentiation between the populations of *Oreobates* compared herein. Because our sample of females is small and to meet statistical assumptions, PCA and DFA were ran with data from males only. The statistical analyses were performed on correlation matrices from 16 log-transformed morphometric and six bioacoustic characters, using R platform version 3.0.1 (R Development Core Team 2012). Bioacoustic comparisons through the DFA were performed using mean individual values.

Results

Molecular Characterization.—The analyses of molecular data revealed several distinct genetic clusters among the included *Oreobates* species (Fig. 1). Bayesian Inference analyses (BI) and Maximum Likelihood (ML) resulted in essentially the same topologies. The retrieved phylogeny (BI and ML) shows that Bolivian specimens from Cerro del Arco (CA) and San Sebastián (SS) are deeply nested together in a subclade with strong support (BI: 1 / ML: 100) within Andean populations including *O. barituensis*, *O. ibischi*, *O. discoidalis*, *O. berdemenos*, *O. yanucu*, *Oreobates* CaEU192295, *O. cruralis*, and *O. madidi* (support by Bayes: polytomy/bootstrap: 73). The sister clade (support: 0.5/49) is formed by *O. antrum*, *O. remotus* (from Central Brazil), and a clade comprising specimens from Dolina Água Milagrosa (DM), Gruta Fazendinha (GF), Mata Fria (MF), Estação Ecológica Serra das Araras (SA), and São Vicente (SV), all localities situated in the state of Mato Grosso, western Brazil

The results of mitochondrial gene distances show (1) intermediate between-group distances of DM, GF, MF, SA, and SV (3.0 to 4.8 %), and CA and SS (3.2%; Table 2); (2) high between-group distances between DM, GF, MF, SA, SV, and CA, SS (10.3 to 11.4 %;

Table 2); (3) high distances between *O. antrum* (8.0 to 11.7 %) and *O. remotus* (8.0 to 12.7 %; Table 2) to all other groups, and finally (4) the ABGD analysis on the full data set (including outgroups) revealed 25 groups including one composed of DM, GF, MF, SA, and SV populations by initial partition with prior intraspecific divergence (P) of 0.0129 % (results not shown).

Morphometry and Morphological Characters.—Specimens from western Brazilian populations are very similar regarding their external morphology and size, and morphology did not allow us to separate *Oreobates crepitans* and *O. heterodactylus* (including topotypic material). The prime characters used to separate these two species (shape and relative size of discs on Fingers III and IV, body size, and sexual dimorphism) proved to be useless for separation of species. Fingers III and IV have ovate expanded discs that can vary from greatly to moderately enlarged (Fig. 2) in specimens from different localities, but also from the same locality. Body size range does not vary among different populations (Table 3), even when comparing only the specimens from GF and SV (topotypic material, in both cases). Furthermore, no population demonstrates marked sexual size dimorphism.

Morphology allowed only for weak separation of Bolivian populations from Brazilian ones (Table 3), and no diagnostic character could be identified. Specimens from Bolivia are usually smaller and discs on Fingers III and IV are relatively less expanded.

The statistical analysis of morphometric data of sampled populations through a PCA evidenced a broad overlap in the multivariate space, reinforcing the idea of an overall similarity in the morphology of male specimens from the westernmost Brazilian populations of *Oreobates* (DM, GF, MC, MF, RO, SA, and SV). It also shows the morphometric distinctiveness of the Bolivian population from SS (Fig. 3A). The first two axes of the PCA explained 56% of the total morphometric variability in males and higher loadings corresponded to SVL, HL, F3, and F4. The DFA with morphometric

measurements assigned to the correct population/locality 100% of the specimens from SS, 40% from GF, 28% from DM and SA, and no specimen from MC, MF, RO, and SV (Table 4).

Advertisement Calls.—Fifty-three advertisement calls from three topotypes (SV) of *Oreobates crepitans* were analyzed. Call rate is 30.5–64.8 calls/min (46.3 ± 10.3). Each call is composed of two pulses (Fig. 4; Table 6), each one with at least three harmonics. Duration of each call varies from 33–56 ms (47 ± 7). The dominant frequency varies from 2067.2–4048.2 Hz (2952.9 ± 519.9). Pulse duration varies from 5–22 ms (11 ± 4) and inter-pulse intervals vary from 14–25 ms (20 ± 3). Another 48 advertisement calls from four specimens recorded at SA were analyzed. Call rate is 13.3–50.5 calls/min (27.6 ± 14.2). Each call is composed of two pulses (Fig. 4). Duration of each call varies from 31–73 ms (38 ± 7). The dominant frequency varies from 2239.5–3531.4 Hz (2725.7 ± 452.4). Pulse duration varies from 5–17 ms (8 ± 2) and inter-pulse intervals vary from 17–31 ms (22 ± 3).

Forty-two advertisement calls from four topotypes (GF) of *Oreobates heterodactylus* were analyzed (Table 6). Call rate is 62.7–85.7 calls/min (71.3 ± 7.8). Each call is composed of two pulses (Fig. 4), each one with at least four harmonics. Duration of each call varies from 27–57 ms (41 ± 6). The dominant frequency varies from 2670.1–3445.3 Hz (3199.5 ± 195.1) and is usually concentrated in the second harmonic. Pulses duration varies from 4–15 ms (9 ± 3) and inter-pulse intervals vary from 16–42 ms (22 ± 4).

Another 32 advertisement calls recorded in the locality DM were analyzed. Call rate is 38.3–68.6 calls/min (52.7 ± 11.8). Each call is composed of two pulses. Duration of each call varies from 36–46 ms (41 ± 2). The dominant frequency varies from 2928.5–

4134.4 Hz (3364.5 ± 352.1). Pulse duration varies from 5–15 ms (9 ± 2) and inter-pulse intervals vary from 17–27 ms (23 ± 3).

Sixty-three advertisement calls from six males from Bolivia (CA and SS) were analyzed. Call rate is 24–36 calls/min (29.8 ± 4). Each call (Fig. 4; Table 6) is composed of 5–9 pulses (6.2 ± 1.2), each pulse with 3–5 harmonics. Duration of each call varies from 111–237 ms (150 ± 33) and inter-call intervals vary from 1300–3349 ms (2179 ± 457). The dominant frequency varies from 2067.2–4306.6 Hz (3789.8 ± 644.5). Pulse rate is 36–49 pulses per second (41.8 ± 4.4). Pulse duration varies from 3–17 ms (7 ± 3) and inter-pulse intervals vary from 7–24 ms (17 ± 4).

Overall, advertisement calls of populations from DM and GF were similar to calls from SA and SV. However, they were distinct from calls of Bolivian populations. These results are revealed by the raw data of both spectral and temporal parameters (Fig. 4; Table 6), as well as by the PCA and DFA with bioacoustic data (Fig. 3B; Table 5). In the PCA, calls from DM, GF, SA, and SV widely overlap along the first function, while those from Bolivian populations (CA and SS) are clearly separated (Fig. 3B). The two principal components (PC) explained 71% of the total variation (eigenvalues >1.0). Highest loadings of the PC1 (54% variance) corresponded to the number of notes per call, call duration, and dominant frequency. The DFA with bioacoustic variables using all recorded males (from four Brazilian and two Bolivian populations) correctly assigned 100% of the individuals from GF and SA, 75% from CA, 50% from DM and SS, and no individual from SV (Table 5).

Taxonomic Conclusions.—The taxonomic re-assessment of some populations of *Oreobates* by integration of morphological, bioacoustic, and molecular data leads us to the following conclusions: (1) *O. heterodactylu*s and *O. crepitan*s are the same species, *Oreobates crepitans* (Bokermann 1965) being a junior synonym of *Oreobates*

heterodactylus (Miranda-Ribeiro 1937); (2) eastern Bolivian populations (SS) of *Oreobates*, including the populations used for the redescription of *O. heterodactylus* in Padial and De La Riva (2005)—Bella Boca–BB and Cerro del Arco–CA—represent a distinct and undescribed species. Hence, the redescription of *O. heterodactylus* from BB and CA does not correspond to the species described by Miranda-Ribeiro, and the species still demands a redescription based on freshly obtained topotypic specimens and calls.

In the following, *Oreobates heterodactylus* is redescribed based on a newly collected series of topotypes, and the Bolivian populations are described as a new species.

Redescription of *Oreobates heterodactylus* (Miranda-Ribeiro 1937)

(Figs. 2, 5, 6)

Teletrema heterodactylum: Miranda-Ribeiro 1937; syntypes: MN 106 (2 specimens); type locality: ‘‘gruta dita Fazendinha’’ Cáceres, Mato Grosso, Brazil

Eleutherodactylus heterodactylus: Myers 1962

Eleutherodactylus crepitans: Bokermann 1965; holotype: WCAB 16144 (now in MZUSP); type locality: São Vicente, Cuiabá, Mato Grosso, Brasil

Eleutherodactylus (*Eleutherodactylus*) *heterodactylus*: Lynch and Duellman 1997

Telatrema heterodactylum: Heyer and Muñoz 1999 (in error)

"*Eleutherodactylus*" *heterodactylus*: Heinicke et al. 2007

Pristimantis crepitans: Heinicke et al. 2007

Pristimantis (*Pristimantis*) *crepitans*: Hedges et al. 2008

Oreobates heterodactylus: Padial et al. 2008

Oreobates crepitans: Padial et al. 2012

Diagnosis.—A medium-sized *Oreobates* (SVL of adult females 25.2–32.6 mm, n = 9; adult males 22.2–29.9 mm, n = 41), characterized as follows: (1) skin on dorsal surfaces smooth with a few low tubercles scattered posteriorly; dorsolateral folds incomplete or absent; venter and throat smooth; groin smooth with or without small low tubercles; discoidal and thoracic folds present; (2) tympanic membrane and annulus distinct; tympanum large, its diameter 54–81% of eye diameter; supratympanic fold and postrictal tubercles present; (3) head slightly longer than wide (HW/HL 0.89–0.99); snout acuminate in dorsal view and rounded in lateral profile; canthus rostralis weakly concave in dorsal view; (4) cranial crests absent; upper eyelid without enlarged tubercles; (5) dentigerous process of vomers prominent, transverse, situated posteromedial to choanae; (6) males with vocal slits and nuptial pads; (7) hands with slender fingers, first finger longer than second; subarticular tubercles large, very prominent, and rounded; supernumerary tubercles present; tips of Fingers I and II narrowly round, those of Fingers III and IV elliptical (much wider than long, curved distally); pads present; circumferential grooves, lateral fringes, and hand webbing absent; palmar tubercle divided in two subunits, inner subunit much larger than outer; thenar tubercle rounded; (8) ulnar tubercle absent; ulna with white granules; (9) foot length 39–45% SVL; toe fringes and webbing absent; Toe III as long as Toe V; tips of toes narrowly rounded, lacking pads and circumferential grooves; inner metatarsal tubercle elongate; outer metatarsal tubercle subconical; subarticular tubercles large and conical; supernumerary tubercles present; (10) heel and tarsal tubercles absent; tarsus with white granules; (11) axillary glands present; (12) in life, dorsum reddish-brown with dark brown blotches and flecks; interorbital bar dark brown, sometimes continuous to dorsal longitudinal bars; middorsal stripe pale when present; venter pale; golden iris, metallic red laterally to the pupil; (13) advertisement call composed of two pulses and duration of 27–

73 ms (41 ± 7); call repetition rate of 13.3–85.7 calls/min (46 ± 18); and dominant frequency of 2067.2–4134.4 Hz (3014 ± 472.1).

Comparisons.—Regarding its external morphology, *Oreobates heterodactylus* differs from all other nominal species of *Oreobates*, except *O. antrum*, *O. discoidalis*, *O. remotus*, *O. yanucu*, and the new species from Bolivia by having greatly enlarged discs on Fingers III and IV (not enlarged or slightly enlarged in the other species). From *O. discoidalis* it can be distinguished by the presence of nuptial pads, absence of webbing on toes, and elliptical terminal tips of Fingers III and IV (nuptial pads absent, webbing rudimentary, terminal tips of Fingers III and IV truncate or ovate in *O. discoidalis*). From *O. yanucu*, it differs by its smooth skin on dorsum, elliptical terminal tips of Fingers III and IV, absence of webbing and ungual flaps on toes (skin of dorsum granular, terminal tips of Fingers III and IV truncate, basal webbing and distinct ungual flap on toes).

Oreobates heterodactylus mostly resembles *O. antrum*, *O. remotus*, and the new species from Bolivia in its external morphology. It differs from *O. antrum* by having nuptial pads and elliptical terminal tips of Fingers III and IV (nuptial pads absent; terminal tips of Fingers III and IV truncate). From *O. remotus*, it differs by having smaller size, nuptial pads, axillary glands, and elliptical terminal tips of Fingers III and IV (SVL of adult female 37.7 mm and adult males 29.6–33.1 mm; nuptial pads and axillary glands absent; terminal tips of Fingers III and IV truncate). It differs from *O. antrum* and the new species from Bolivia by having a shorter advertisement call (call duration 186–302 ms in *O. antrum* and 111–237 ms in the new species from Bolivia) composed of 2 pulses (5–11 pulses in *O. antrum* and 5–9 pulses in the new species from Bolivia).

Comments on the Type Locality and Natural History Notes.—Geographic coordinates of the type locality of *Oreobates heterodactylus* were first presented in Heyer and Muñoz (1999). These coordinates were said to have been provided by the zoologist

Paulo Emílio Vanzolini, a former taxonomist at the Museu de Zoologia (São Paulo, Brazil), also interested and very competent in tracing itineraries of traveler naturalists throughout Brazil. Vanzolini attributed the coordinates 16°00'S, 57°36'W to the type locality of *O. heterodactylus*. In their comments on this issue, Heyer and Muñoz (1999) also mentioned that Miranda-Ribeiro travelled to the type locality ("gruta Fazendinha") and "returned to Caceres in the same day and that 'Fazendinha' was near a place called Pirizal" (Heyer and Muñoz, 1999:7).

In the search of the exact place where the syntypes of *Oreobates heterodactylus* were collected, we interviewed residents and farmers in the town of Cáceres and surroundings and conducted two field expeditions (February 2012 and November 2016). We were able to trace the historical changes in the territorial limits, names, and ownership of the rural properties in the region once occupied by Fazendinha farm, from the time of the expeditions of Rondon Commission up to the present day. In spite of the diminutive ending of the word "Fazendinha" (which means a small farm), it was once a large farm, belonging to a farmer named Urbano Mesquita. The farm was subsequently subdivided, with parts of it being sold to different owners over the course of time, and the main settlements of the "Fazendinha" farm near Cáceres presently belong to the "Fazenda Monte Alto" (Monte Alto farm), while the "gruta Fazendinha" is presently situated in a neighboring property, the "Fazenda Hayashi" (Hayashi farm).

The coordinates given by Heyer and Muñoz (1999) in reality correspond to a farmhouse located in a flat, low-lying terrain in the municipality of Cáceres. The area is situated in the Paraguay River depression (elevations from 120 to 160 m.a.s.l.), halfway between the wetlands along the banks of the main river channel and a low mountain belonging to the "Província Serrana" (Cardoso et al., 2013). This is a corridor of parallel mountains (elevations from 280 to 600 m.a.s.l.) of Pre-Cambrian limestone which extends

along nearly 400 x 40 km, connecting the southern Amazonia to Cerrado savannas and to the Pantanal wetlands. Some of the formerly mapped occurrences of *O. heterodactylus* are distributed along these mountains (as *O. crepitans*; Strüssmann et al. 2011).

The botanist Frederico C. Hoehne, who also took part in some of the scientific expeditions under the Rondon Commission, reported that he made a visit to the "grutas da Fazendinha e do Pyrisal" (Hoehne, 1916:14) on 2 October 1908 in the company of Miranda-Ribeiro. It is clear from Hoehne's report that two caves were visited in the same day: "Fazendinha" and "Pyrisal". We could not locate a cave called "Pyrisal" (or "Pirizal", in modern Portuguese, a widely used toponym all over the Brazilian Pantanal wetlands, meaning a monodominant stand of "piri-piri", the macrophyte *Cyperus giganteus*, Cyperaceae). However, there is a low mountain nearly 10 km northeastward of Cáceres called "Serra do Pirizal", as well as homonymous, nearby stream and a farm. Both toponyms - Serra do Pirizal and Fazendinha - appear in an official topographic map, at a 1:250,000 scale, from the "Diretoria de Serviço Geográfico" - DSG, a Brazilian military mapping agency (DSG, 1982). Serra do Pirizal is also depicted in Cardoso et al. (2013), and at least part of it is located within the actual limits of the Fazenda Hayashi. In November 2016, the owner of this farm took us to a limestone hill where the "gruta Fazendinha" is located (16°1'10"S; 57°35'2"W) and where we collected and recorded individuals of *O. heterodactylus*.

We used the database on Brazilian caves available at the national register of speleological information ("Cadastro Nacional de Informações Espeleológicas" - CANIE) to check information on catalogued caves existing in the vicinities of Serra do Pirizal. The national cave research and conservation center ("Centro Nacional de Pesquisa e Conservação de Cavernas" - CECAV, Brasília, Brazil) is responsible for technical support and management of the CANIE database (https://www.icmbio.gov.br/cecav/canie.html).

We imported kmz data from CANIE into Google Earth and found that there are seven caves officially catalogued in the area: Dolina Água Milagrosa, Toca Dolina Água Milagrosa, Pita Canuto (or alternatively, Pita Canudo) I, Pita Canuto II, Loca da Revoada, Abrigo do Bicho Morto, and Caverna do Sítio Tarumã. Cardoso et al. (2013) mentioned ten caves located in the same area. Some of them are treated under the same names used in the CANIE, but others are additional to this database, including a cave named "Caverna do Cadeado", situated in the Serra do Pirizal (Cardoso et al., 2013). It was briefly visited in the 90's by a team of speleologists from CECAV and the local university. However, it was neither characterized in full nor officially catalogued, because the landowner had installed chains and a padlock ("cadeado", in portuguese) to block the entrance by car (J. Lima, CECAV, pers. comm.). The distance between Cáceres and Serra do Pirizal—2 km in a straight line and nearly 18 km from Cáceres on horseback—could be easily covered in a day. Besides, this could be done either using MT 343 or Rua Pirajá da Silva, two unpaved roads that already existed at the beginning of the 20th century. We used both, on different occasions, to access the Serra do Pirizal. The existence of such alternative, well-delimited trails to access the Pirizal and Caverna do Cadeado might be linked to the fact that the region was the scene of historical limestone mining. During our expedition to the "gruta Fazendinha" (Caverna do Cadeado), the owner of Fazenda Hayashi showed us the ruins of furnaces constructed by slaves for the calcination of limestone and production of quicklime. In view of these findings, the geological nature of the type locality of *Oreobates heterodactylus* also deserves some comments.

In the redescription of *Oreobates heterodactylus*, Padial and De La Riva (2005) mentioned that the two syntypes described by Miranda-Ribeiro were collected "in a sandstone cave near the town of Cáceres". Although this information had also previously appeared in Heyer and Muñoz (1999), the geological nature of the cave visited both by the

botanist Hoehne and by Miranda-Ribeiro was neither mentioned in the original report of the first (Hoehne, 1916), nor in the original description of *O. heterodactylus* (Miranda-Ribeiro, 1937). Individuals of this species indeed can occur in sandstone formations, such as in Chapada dos Guimarães and in portions of Estação Ecológica Serra das Araras (Strüssmann et al., 2011), a protected area situated nearly 60 km, in a straight line, from its type locality. However, our field records at Fazenda Hayashi, as well as available geological and speleological documents (e.g., Cardoso et al., 2013) attest that most caves near Cáceres are limestone caves, located in the karst landscapes of the southern Província Serrana. Moreover, in one of his many reports to the Rondon Commission, Miranda-Ribeiro (1916:28) explicitly mentioned the calcareous nature of the many caves in the region he explored.

Miranda-Ribeiro and Hoehne explored other caves in the vicinity of Cáceres. The first author briefly reported - without giving details on date and scientific results - having visited a place that most probably corresponds to Dolina Água Milagrosa (16°2'S; 57°31'W). This is a funnel-shaped, very deep sinkhole located between the Bebedouro and Morro Grande mountains, where we also collected and recorded some specimens of *Oreobates heterodactylus*. The aquifer upwelling at the bottom of the sinkhole does not have any surface contact with the nearby river drainages, is deeper than 180 m, and water color varies from generally green in the wet season to blue in the dry season (da Graça et al., 2017). The Dolina Água Milagrosa sinkhole is distinct enough to be treated by Miranda-Ribeiro (1937) merely as a “gruta”. Besides, it is located nearly 15 km on horseback from the Serra do Pirizal, so it would be impossible to travel and explore caves in both areas and to return to Caceres in the same day, as reported by Hoehne (1916). Therefore, we are convinced that the Dolina Água Milagrosa neither corresponds to the

Fazendinha nor to the Pirizal cave, and that both are located in the vicinities of the Serra do Pirizal.

According to the CANIE database, the nearest mapped cave to the Caverna do Cadeado is Loca da Revoada, situated nearly 5 km to the NE of it. Together with two other smaller caves, Locada da Revoada is situated in a low mountain depicted as Sítio Tarumã (Tarumã site/region) in the DSG map (DSG, 1982). In an unpublished report on the invertebrate fauna of the Loca da Revoada, Silva (2005) described it as being located amidst limestone outcrops at "Fazenda do Seu Dedé" (Dedé's farm; 15° 58' 54.599"S, 57° 34' 19.182"W , 208 m.a.s.l.), with its entrance surrounded by dry forest vegetation. Silva (2005) also mentioned the existence of a sinkhole inside the cave and of an extensive livestock pasture area nearly 60m from its entrance. This latter was described as quite steep, "requiring the use of rope or auxiliary equipment and vertical techniques for descending and ascending". Ascent to the cave interior was described as very difficult and even a team of experienced speleologists requested the help of representatives of the local military fire brigade of Cáceres to do so (Silva, 2005). It seems unlikely that the two scientists from the Rondon commission could have accessed the interior of this cave by their own, and besides the Dolina Água Milagrosa, we also dismiss the possibility that Loca da Revoada would correspond to the "gruta Fazendinha" of Miranda-Ribeiro (1937).

We have visited and collected specimens in almost all the localities from which *Oreobates heterodactylus* is presently known and in all of them the presence of rocky outcrops is conspicuous. In all these localities, the habitat characteristics match with those described for *O. crepitans* by Bokermann (1965), who stated that no one could expect to find frogs in such a rocky and dry place. During reproductive events, under fine rain or after heavy rains, males of *O. heterodactylus* were frequently seen calling from above or in small reentrances at the outcrops. Under these circumstances, population densities seem to

be high in most localities, and we here argue that this may be linked to the large availability of underground retreats. During the dry season, from July to September each year, these localities are subject to recurrent fires. There is no standing water, and even during heavy rains the runoff easily percolates into the rocky soil. Fires and the absolute absence – at any time – of puddles, ponds or other water collections at the surface level do not seem to negatively impact local populations of *O. heterodactylus*, and we hypothesize that reproduction of this and related species of *Oreobates* might occur in somewhat protected, possibly subterranean habitats. Despite the scarcity of surface water in the karst soils of the Provincia Serrana region, there is a well-developed underground (cryptorheic) drainage, evidenced by the numerous sinks and resurgences in the local riverbeds, sinkholes, grottos, caves, and caverns (Cardoso et al., 2013). Another possibility is that, when it rains, the water percolates amidst the superimposed rocks until it reaches an impermeable layer and sits there, creating wet habitats suitable for egg deposition and development. Indeed, reproduction of *Oreobates* species from rocky outcrops represents a largely unknown and very instigating field of research.

Species Description

Oreobates ***chiquitanus*** sp. nov.

(Figs. 7, 8, 9)

Eleutherodactylus heterodactylus: Padial and De La Riva 2005

Oreobates heterodactylus: Padial et al. 2008

Holotype.—SMF 88497 (field number MJ 1683), an adult male from “Centro de Investigaciones Ecológicas Chiquitos”, San Sebastián, 16°21’38”S, 62°0’8”W (datum =

WGS84), 466 m above sea level, Provincia Ñuflo de Chávez, Departamento Santa Cruz, Bolivia, collected on 25 November 2010 by Martin Jansen (Fig. 7).

Paratopotypes.—SMF 88498-9 (field number MJ 1684-5), two adult males collected on 25 November 2010 by Martin Jansen; SMF 88500 (MJ 1723), one female collected on 25 November 2010 by Martin Jansen.

Diagnosis.—A medium-sized *Oreobates* (SVL of adult female 27.4 mm; adult males 24.5–25.4 mm, n = 3), characterized as follows: (1) skin on dorsum, venter, and posterior surfaces of limbs smooth; cloacal region posteroventral to the cloaca shagreen; cloacal flap absent; dorsolateral folds present but ill-defined; ventral discoidal fold present, almost reaching the groin; thoracic fold present; (2) tympanic membrane and annulus distinct; tympanic membrane nearly round, large, diameter about ¾ of eye diameter; supratympanic fold present, well developed, extending to anterior level of insertion of forearm; two postrictal tubercles present, fused; (3) head slightly wider than long (HW/HL = 1.03), subacuminate in dorsal view and rounded in lateral profile; nostrils slightly protuberant, opening laterally; canthus rostralis distinct, weakly concave in dorsal view; loreal region slightly concave; lips rounded; (4) upper eyelid without tubercles; cranial crests absent; (5) dentigerous process of vomers elongate, length about two times the diameter of choanae, positioned posteromedially to choanae; choanae small, not concealed, slightly rounded, anterolaterally positioned in the roof of the mouth, separated by a distance of about six times their diameter; (6) males with vocal slits and nuptial pads; (7) hands with slender, long fingers; tips of Fingers I and II narrowly round, not enlarged laterally; tips of Fingers III and IV elliptical, distinctly enlarged, about 1.3 times the width of Fingers I and II; pads and circumferential grooves absent on Fingers I and II, weakly present on Fingers III and IV; lateral fringes and hand webbing absent; subarticular tubercles round, large, very prominent; supernumerary tubercles small, smaller than

subarticular tubercles; palmar tubercle elliptical, incompletely divided anteriorly in two subunits; thenar tubercle prominent, elliptical; (8) antebrachial and ulnar tubercles absent; (9) foot length 47.6–48.5 % SVL; Toes III and V reaching proximal margin of second subarticular tubercle of Toe IV; toe tips narrowly rounded, slightly enlarged; pads, circumferential grooves, lateral fringes, keels, and webbing absent on all toes; subarticular tubercles large and round; supernumerary tubercles present, conical, much smaller than subarticular tubercles; inner metatarsal tubercle ovoid, prominent, longer than wide, larger than outer metatarsal tubercle; outer metatarsal tubercle rounded; (10) heel lacking tubercles or folds; tarsal fold absent; (11) dorsal ground color Drab-Gray with a suggestion of Light Flesh Color and with many brown marks (well-demarcated Dusky Brown triangular interorbital, Light Neutral Gray-Dusky Brown arrow like middorsal); (12) advertisement call composed of 5–9 pulses (6.2 ± 1.1), with 3–5 harmonics; call rate 24–36 calls/min (29 ± 4), call duration 111–237 ms (150 ± 33), inter-call intervals 1300–3349 ms (2180 ± 456), and dominant frequency 2067.2–4306.6 Hz (3789.8 ± 644).

Description of Holotype.—An adult male, SVL 24.60 mm, with head slightly wider than long (HW/HL = 1.03), subacuminate in dorsal view and rounded in lateral profile; nostrils slightly protuberant, opening laterally; canthus rostralis distinct, weakly concave in dorsal view; loreal region slightly concave; lips rounded; upper eyelid without tubercles; cranial crests absent. Supratympanic fold present, well developed, extending to anterior level of insertion of forearm; tympanic membrane and tympanic annulus distinct; tympanic membrane nearly round, large, diameter about ¾ of eye diameter; two postrictal tubercles present, fused. Choanae small, not concealed, slightly rounded, anterolaterally positioned in the roof of the mouth, separated by a distance of about six times their diameter; dentigerous process of vomers present, positioned posteromedially to choanae, elongate, length about two times the diameter of choanae, oblique, separated medially from each

other by a distance nearly equal to the choana diameter. Tongue lanceolate, not notched posteriorly. Vocal slits present. Skin of dorsal and ventral surfaces, and posterior parts of hind limbs smooth; cloacal region posteroventral to the cloaca shagreen; cloacal flap absent; dorsolateral folds present but ill-defined; ventral discoidal fold present, almost reaching the groin; thoracic fold present. Arm and forearm slender. Hands with slender, long fingers; relative length of Fingers: III > IV > I > II; tips of Fingers I and II narrowly round, not enlarged laterally; tips of Fingers III and IV elliptical, distinctly enlarged, about 1.3 times the width of the Fingers I and II. Pads and circumferential grooves absent on Fingers I and II, weakly present on Fingers III and IV; lateral fringes and hand webbing absent. Subarticular tubercles round, large, very prominent; supernumerary tubercles small, round to conical, smaller than subarticular tubercles; palmar tubercle elliptical, incompletely divided anteriorly in two subunits, inner much larger than outer; thenar tubercle prominent, elliptical. Antebrachial and ulnar tubercles absent. Single, white, enlarged nuptial pad on thumb. Foot length 48.5% of SVL; Toes III and V reaching proximal margin of second subarticular tubercle of Toe IV; relative length of Toes IV > V > III > II > I; toe tips narrowly rounded, slightly enlarged. Pads, circumferential grooves, lateral fringes, keels, and webbing absent on all toes. Subarticular tubercles round, and large; supernumerary tubercles present, conical, much smaller than subarticular tubercles; inner metatarsal tubercle ovoid, prominent, longer than wide, larger than outer metatarsal tubercle; outer metatarsal tubercle rounded. Heel lacking tubercles or folds; tarsal fold absent.

Variation.—The only adult female (27.4 mm) has a larger SVL than adult males (24.6–25.4 mm). Other variations in size and proportions are shown on Table 3. There is little color variation in the dorsum among female and males, varying from Light Neutral

Gray with Dark Neutral Gray marks in males to Light Flesh Color Reddish in female (Fig. 8).

Coloration.—In life (Fig. 8), dorsal ground color Drab-Gray with a suggestion of Light Flesh Color and with many brown marks (well-demarcated Dusky Brown interorbital blotches, Light Neutral Gray-Dusky Brown arrow like middorsal mark); loreal region and upper lip with Dusky Brown bars; canthus rostralis Dusky Brown; supratympanic fold Sepia; tympanic membrane Medium Neutral Gray, annulus Cream Color; iris Dusky Brown with Light Yellow Ocher stipples; dorsal surface background color Light Flesh Color in thigh and shank, tarsus and foot, and forearm, with Dark Hair Brown bars. Ventral surfaces white; inner surfaces of forearm Dark Hair Brown. In preservative (Fig. 9), dorsal background color Light Neutral Gray with Dark Neutral Gray marks (e.g. interorbital blotches and arrow like middorsal mark), as other surface marks in head; dorsal surface background color Light Neutral Gray-Light Flesh Color in thigh and shank, tarsus and foot, and forearm, with Dark Neutral Gray bars. Ventral surfaces Cream White; inner surfaces of forearm Fawn Color.

Advertisement Call.—Sixty three (63) advertisement calls (Table 6) from six males of *Oreobates* ***chiquitanus*** sp. nov. recorded at two different localities in Bolivia (CA and SS) were analyzed. Call rate is 24–36 calls/min (29 ± 4). The call of the new species (Fig. 4) consists of 5–9 pulses (6.2 ± 1.1), each pulse with 3–5 harmonics. Duration of each call varies from 111–237 ms (150 ± 33) and inter-call intervals from 1300–3349 ms (2180 ± 456). The dominant frequency varies from 2067.2–4306.6 Hz (3789.8 ± 644) and corresponds to the second harmonic. Pulse rate is 36–49 pulses per second (41.8 ± 4.3). Pulse duration varies from 3–17 ms (7 ± 3) and inter-pulse intervals vary from 7–24 ms (17 ± 3).

Etymology.— The specific name refers to the occurrence of the species as an inhabitant of the Chiquitano dry forests. By naming the species we want to draw attention to the conservation of this forest type which is considered to be the world's best preserved Tropical Dry Forest, endemic to Bolivia and highly biodiverse, but currently being threatened mainly by deforestation and controlled burns for the expansion of cattle ranching and soybean agriculture. As an example, the Chiquitano region has lost 1.4 million hectares to fires – nearly 12% of its area before the fires – in the beginning of the second semester of 2019 (Romero-Muñoz et al., 2019). The impacts of this unprecedented ecological disaster, considered to be a result of intentional burning to convert forest to farmland, was not yet assessed on the many species of fauna and flora unique to this region.

Distribution.—Oreobates ***chiquitanus*** sp. nov. is currently known from its type locality, in Provincia Ñuflo de Chávez, and from Bella Boca, Provincia Ángel Sandoval, and Serranía de Santiago, Cerro del Arco, Provincia Chiquitos (Padial and De La Riva, 2005). All of these provinces are situated in Department Santa Cruz, eastern Bolivia (Fig. 1).

Natural History Notes and Conservation Issues.—All individuals included in the study herein were found in Chiquitano Dry Forest on the forest floor. Although this species does not seem to be directly associated with rocky habitats at the type locality, the presence of superimposed subterranean rocks is evident and granite outcrops are present in open formation as well as amidst the dry forest. Rocky outcrops are more evident and more abundant in the top and slopes of low, usually deforested hills situated along the margins of the Highway 10 (or Carretera Hardeman-Colonia Piraí), to the East of Concepción, located 25 km north of the type locality (CS, pers. obs.). The rocky landscape there is similar to

that occupied by the *Oreobates* species from the Brazilian Cerrado – *O. antrum*, *O. heterodactylus*, and *O. remotus*.

Oreobates ***chiquitanus*** sp. nov. is assumed to be associated with and restricted to the Chiquitano Dry Forest (sensu Ibisch and Mérida, 2004).

However, due to the sparse data available (i.e., insufficient information for a proper assessment of conservation status), *Oreobates* ***chiquitanus*** sp. nov. cannot be precisely placed into a formal threat category and in accordance with the IUCN criteria should be considered a "Data Deficient" taxon.

Comparisons.—Regarding its external morphology, *Oreobates* ***chiquitanus*** sp. nov. can be distinguished from the all other nominal species of *Oreobates* (character of comparative species in parenthesis) except *O. antrum*, *O. discoidalis*, *O. heterodactylus*, *O. yanucu*, and *O. remotus* by having greatly enlarged discs on Fingers III and IV (not enlarged or slightly enlarged). From *O. discoidalis* it can be distinguished by the presence of nuptial pads, absence of webbing on toes, and elliptical terminal tips of Fingers III and IV (nuptial pads absent, webbing rudimentary, terminal tips of Fingers III and IV truncate or ovate). From *O. yanucu*, it differs by its smooth skin on dorsum, elliptical terminal tips of Fingers III and IV, absence of webbing and ungual flaps on toes (skin of dorsum granular, terminal tips of Fingers III and IV truncate, basal webbing and distinct ungual flap on toes).

Oreobates ***chiquitanus*** sp. nov. mostly resembles in external morphology the other species of open formations: *O. antrum, O. heterodactylus*, and *O. remotus*. It differs from *O. remotus* by having smaller size, nuptial pads, and elliptical terminal tips of Fingers III and IV (SVL of adult female 37.7 mm and adult males 29.6–33.1 mm, nuptial pads absent, and terminal tips of Fingers III and IV truncate). *Oreobates* ***chiquitanus*** sp. nov. differs from *O. antrum* by its larger size, nuptial pads present, and subacuminate snout (SVL of

adult females 25.2–27.2 and adult males 20.6–24.1 mm, nuptial pads absent, acuminate-triangular snout). Presence of harmonics and lower call rate make the call of the new species different from that of *O. antrum* (absence of harmonics and 12.3–17.1 calls/min). *Oreobates* ***chiquitanus*** sp. nov. cannot be distinguished from *Oreobates heterodactylus* based on external morphology. However, advertisement call distinguishes the two species, with *O.* ***chiquitanus*** sp. nov. having a higher number of pulses per call (2 pulses) and call duration (27–73 ms).

Measurements of Holotype.—SVL 24.60 mm, HL 9.15 mm, HW 9.45 mm, EL 3.52 mm, EN 2.85 mm, IND 2.39 mm, EE 2.52 mm, TYH 2.1 mm, TYL 1.86 mm, F3 left 0.79 mm, F4 left 0.95 mm, F3 right 1.09 mm, F4 right 0.97 mm, FA 6.38 mm, TL 13.33 mm, TH 12.82 mm, FL 11.67 mm, and T4 0.56 mm.

Discussion

Taxonomic decisions.—*Oreobates heterodactylus* specimens are distributed in three clades: a well-supported clade that includes topotypes of *O. crepitans* and specimens from MF, another well-supported clade that includes topotypes of *O. heterodactylus* and specimens from DM, and an unsupported clade including specimens from SA. The genetic distance among specimens of the same clade ranges from 0.1% to 0.6%, while the distance among different clades range from 3.0% to 4.7%. *Oreobates* ***chiquitanus*** sp. nov. specimens are distributed in a clade that includes specimens from the type locality and another clade that includes specimens from CA, and the genetic distance between specimens from different localities is 3.2%. The intraspecific genetic distances are relatively low since the genetic distances among species of *Oreobates* show values ranging from 8.4% to 18.9% (Padial et al. 2012; this study). We consider that the genetic divergence and phylogenetic structure we found in *Oreobates* ***chiquitanus*** sp. nov. and in

O. heterodactylus reflect population genetic structure, probably shaped by distance, since specimens from close localities show lower genetic distance. Therefore, we neither consider the well-supported clades and genetic distance evidence against the synonymization of *O. crepitans* and *O. heterodactylus*, nor consider it an evidence to separate the populations of *O. chiquitanus* in two different species. Moreover, the synonymization of *Oreobates crepitans* and *O. heterodactylus* is supported by morphological and bioacoustic data analyses. The similarity in the morphology and advertisement calls of specimens from the Brazilian populations of *Oreobates* (DM, GF, MC, MF, RO, SA, and SV) was evidenced by the broad overlap in the multivariate space in the PCA analysis. Even the relative proportion of the discs on Fingers III and IV, which has been used to distinguish *O. crepitans* from *O. heterodactylus*, broad overlap in the multivariate space. A discriminant function analysis based on morphometric variables showed that the western Brazilian specimens in most cases could not be allocated into the populations/localities from which they came, differently from the Bolivian specimens that have been correctly allocated in 100% of the cases (Tab. 4)

Phylogeny.—Our analyses recovered the three relatively stable clades of *Oreobates* (Köhler and Padial, 2016): one clade with species from cloud forests and the Andes in Peru, one clade of species from the Yungas, and one clade with species from the Seasonally Dry Tropical Forests, Cerrado savannas, and montane forests.

The cloud forest-Andean clade comprises species from cloud forests in south-central Peru that have smooth skin, long fingers and toes, and low plantar tubercles (*Oreobates gemcare*, *O. lehri*, *O. machiguenga*, and *Oreobates* CaJF809995). This clade is sister to a clade of the high Andean species of *Oreobates* (*O. ayacucho* and *O. pereger*), which agrees with the hypothesis of montane forest origin of high Andean species, as it occurs on the related genus *Lynchius* (Motta et al., 2016).

The clade of Yungas species includes *Oreobates amarakaeri*, *O. choristolemma*, *O. granulosus*, *O. sanctaecrucis*, *O. sanderi*, and *Oreobates* CaEU368903, all species with granular skin, short fingers and toes, conspicuous plantar tubercles, and lack of expanded discs (Köhler and Padial, 2016). These features are also present in the basal species from Amazon lowlands, *O. quixensis* and *O. saxatilis*. However, these two clades have never been recovered as sister clades (Padial et al., 2012; Pereyra et al., 2014; Padial et al., 2014; Motta et al., 2016; Köhler and Padial, 2016).

Oreobates heterodactylus and *O.* ***chiquitanus*** sp. nov. are part of a clade that includes *O. antrum*, *O. barituensis*, *O. berdemenos*, *O. cruralis*, *O. discoidalis*, *O. ibischi*, *O. madidi*, *O. remotus*, *O. yanucu*, and *Oreobates* CaEU192295. Species of this clade are distributed in a variety of habitats ranging from Cerrado to tropical dry and montane forests and share the slender shape of body with soft skin (Köhler and Padial, 2016). Within this clade, the relationship among species from Seasonally Dry Tropical Forests and Cerrado savannas of central South America vary among recent studies. However, it is important to remember that *O.* ***chiquitanus*** sp. nov. has been included in previous phylogenetic analyses (e.g., Padial et al. 2012) under the name *O. heterodactylus sensu* Padial and De La Riva (2005), while *O. heterodactylus* (Miranda-Ribeiro, 1937) was represented by the terminal *O. crepitans* (e.g., Köhler and Padial, 2016). Taking this into consideration, analyses including only *O.* ***chiquitanus*** sp. nov. and *O. remotus* have recovered them as sister species (Teixeira Jr. et al., 2012; Padial et al., 2012, 2014), except for the maximum likelihood analyses of Padial et al. (2014), which recover *O.* ***chiquitanus*** sp. nov. as sister of a clade that includes *O. discoidalis*, *O. ibischi*, and *O. barituensis*, while *O. remotus* is sister to a clade formed by the former species plus a clade including *O. madidi* and *O. cruralis*. When *O. heterodactylus* is added to the analyses, ***O. chiquitanus*** sp. nov. and *O. remotus* have not been recovered as sister species (Pereyra et al., 2014; Köhler and Padial,

2016; Motta et al., 2016). Moreover, the relationship between *O. heterodactylus* and *O. remotus* also varies across analyses. These species form a clade in Pereyra et al. (2014) that is sister to *O.* ***chiquitanus*** sp. nov.. Maximum likelihood analysis in Motta et al. (2016) also recovers *O. heterodactylus* and *O. remotus* as sister species, while *O.* ***chiquitanus*** sp. nov. is sister to *O. berdemenos*. A clade formed by *O.* ***chiquitanus*** sp. nov. and *O. heterodactylus* is recovered by Köhler and Padial (2016) and by parsimony analyses of Motta et al. (2016). These latter authors also found *O. remotus* as sister to *O. berdemenos*, while Köhler and Padial (2016) found it as sister to a clade that includes *O. yanucu* and *O. berdemenos* (*O. yanucu* was not part of analyses in Motta et al., 2016).

In the description of *Oreobates antrum*, Vaz-Silva et al. (2018) found a clade that includes *O. antrum*, ***O. chiquitanus*** sp. nov., *O. heterodactylus* and *O. remotus*. Although they claim that this finding supports the existence of a clade endemic to Cerrado, we argue that this clade in fact supports the hypothesis of a connection Andes-Atlantic Forest through the Cerrado, mostly via enclaves of Seasonally Dry Tropical Forests.

Our analyses recovered a clade including *O. antrum*, *O. heterodactylus*, and *O. remotus*, while *O.* ***chiquitanus*** sp. nov. was inferred to as the sister species of a clade comprising *O. barituensis*, *O. discoidalis*, and *O. ibischi*, species of *Oreobates* that have the southernmost distribution in South America. The relationship found herein also supports the hypothesis of a connection between Andes-Atlantic Forest through the Cerrado, and indicate that diversification of the *Oreobates* species known from tropical dry forests might have taken place on two occasions independently.

Morphology.—Species of *Oreobates* are usually very diverse in their external morphology, including skin texture, body shape and size, relative length of limbs, and expansion of finger tips. Species that occur in the same habitat are usually more similar to each other than to those phylogenetically related to them, suggesting that convergent

evolution is responsible for morphological variation in this genus (Padial et al., 2012; Motta et al., 2016; Köhler and Padial, 2016). Species from tropical dry forests, neighboring formations of Cerrado and Atlantic Dry Forests, and from dry valleys of Andes are the only species of the genus that have the combination of slender body, long limbs, and expanded tips of fingers. This ecomorph has already been associated with species that occur in rocky habitats and caves in species of *Eleutherodactylus* (Hedges, 1989). It has been hypothesized that the shape of fingertips in these species is related to climbing habitats, as some specimens can be found on rocky substrates at up to 1.8 m above the ground (Vaz-Silva et al., 2018), and probably use rocky underground retreats as well (this paper).

The similar morphology of species of *Oreobates* that inhabit tropical dry forests and Cerrado savannas has led to taxonomic inaccuracies when only external morphology was considered. For example, a population of the recently described species *O. antrum* was previously identified as *O. remotus* (see Andrade et al., 2012) and its description was only made possible when acoustical and molecular data were also included in the comparisons (Vaz-Silva et al., 2018). Integrating different sources of data is of fundamental importance to understand the diversity of species in this group, as adaptation led to similar transformations of traits of external morphology in species of *Oreobates* (Motta et al., 2016).

We believe that the diversity of *Oreobates* in central South America is far from being known. By the time of the description of *O. remotus*, its type locality was more than 1.000 km distant from any other locality of known species of the genus. The description of *O. antrum* has already filled part of this gap and our accessing of the taxonomic problems regarding the other species from this part of the Neotropics shows that there is still much more to investigate and discover about this group.

Bioacoustics.—The general structure of the advertisement call of *Oreobates* species was described as "amplitude-modulated and highly pulsatile notes with little or no frequency modulation", and it was proposed as a putative synapomorphy of the genus (Padial et al., 2012). Further evidence for a phylogenetic signal in call characters of some terraranan groups including *Oreobates* was earlier found by Goicochea et al. (2010). On a fine scale, i.e. within *Oreobates* species, a phylogenetic signal might be obvious when comparing the specific pulse numbers in the subclade of the species from Cerrado, tropical dry and montane forest studied herein [acoustic measurements of all these species were presented recently by Vaz-Silva et al. (2018) in an overview]. The subclade including *O. antrum*, *O. heterodactylus*, and *O. remotus*) has calls that consist of two (*O. remotus* and *O. heterodactylus*) to eight (*O. antrum*) pulses per call. On the other hand, species of the subclade including *O.* ***chiquitanus*** sp. nov. (Fig. 2) have, in general, higher pulse numbers (5 to 32). Within this clade, *O.* ***chiquitanus*** sp. nov. (5-8 pulses per call) is similar to its closest relatives *O. barituensis* (5–6), *O. ibischi* (4–8), and *O. discoidalis* (8–13), whereas *O. madidi*, *O. cruralis* and *Oreobates* CaEU192295 have from 10 to more than 20 pulses per call.

Besides this potential phylogenetic signal, we can hypothesize that sexual selection might cover the phylogenetic signal within the subclades. Closely related and sympatric species seem to differ more in specific traits (e.g. pulse number) than allopatric species, probably in order to maintain species isolation. These effects might be responsible for the large differences in pulse numbers of sympatric *O. antrum* (5-9 pulses) / *O. remotus* (2 pulses) and *O. heterodactylus* (2 pulses) / *O.* ***chiquitanus*** sp. nov. (5–8 pulses). However, with more data at hand that group might serve as a model system to test these and other hypotheses on call evolution in frogs.

Strüssmann et al. (2011) described the call of *O. heterodactylus* consisting of two distinct notes. However, we herein follow the call-centered approach *sensu* Köhler et al. (2017) and thus suggest that the call of *O. heterodactylus* consists rather of two pulses instead of two notes (Fig. 6). Clearly, the use of an adequate and standardized terminology of units and traits of anuran advertisement calls is crucial to make inter-species comparisons reasonable in a taxonomic or evolutionary context (Köhler et al., 2017).

Acknowledgments.—We thank F. Franco, G. Köhler, J. Pombal Jr., and T. Grant for allowing access to material under their care at UFMT, SMF, MNRJ, and MZUSP, respectively; to J. M. Padial for recordings and for allowing access to bioacoustic samples deposited at "Fonoteca Zoológica" (FonoZoo.com), Museo Nacional de Ciencias Naturales (CSIC; Madrid, Spain), to A. Schulze and M. Campos Costa for field assistance. AP thanks "Coordenação de Aperfeiçoamento de Pessoal de Nivel Superior" (CAPES) for a postdoctoral fellowship (PNPD; process 20132816). CS thanks Conselho Nacional de Desenvolvimento Científico e Tecnológico for a research fellowship (CNPq #3123038/2018-1) and Senckenberg Forschungsinstitut und Naturmuseum (Frankfurt, Germany) for funding through the "Taxonomy Grant". AM thanks São Paulo Research Foundation for her PhD. scholarship (FAPESP #2017/08488-3) and Mohamed bin Zayed Species Conservation Fund for financial support. São Paulo Research Foundation (FAPESP #2013/50741-7) and Conselho Nacional de Desenvolvimento Científico e Tecnológico (CNPq #302518/2013-4) provided financial support to CFBH. P. Herrera and K. Rivero (Museo Noel Kempff Mercado, Santa Cruz de la Sierra) provided valuable assistance to obtain permits. Collecting permits were issued by "Instituto Chico Mendes de Conservação da Biodiversidade" (ICMBio/SISBio # 13429–1) and the Ministerio de Medio

Ambiente y Aqua, Bolivia (MMAyA-VMABCC-DGBAP 941). We thank J. D. Bagnall for polishing English language usage.

Literature cited

Andrade, S.P., W. Vaz-Silva, E. P. Victor-Júnior, D. L. Santos, and N. M. Maciel. 2012. Distribution extension, new state record and geographic distribution map of *Oreobates remotus* Teixeira-Jr, Amaro, Recoder, Sena and Rodrigues, 2012 (Amphibia, Anura, Strabomantidae) in Central Brazil. Herpetology Notes 5:275–276.

Bioacoustics Research Program 2014 Raven Pro: Interactive Sound Analysis Software. Version 1.5. [Computer software]. The Cornell Lab of Ornithology, Ithaca, New York, USA. Available from: http://www.birds.cornell.edu/raven.

Bokermann, W. C. A. 1965. Tres novos batraquios da região central de Mato Grosso, Brasil. Revista Brasileira de Biologia 25(3):257–264.

Caramaschi, U., and C. Canedo. 2006. Reassessment of the taxonomic status of the genera *Ischnocnema* Reinhardt and Lütken, 1862 and *Oreobates* Jiménez-de-la-Espada, 1872, with notes on the synonymy of *Leiuperus verrucosus* Reinhardt and Lütken, 1862 (Anura: Leptodactylidae). Zootaxa 54:43–54.

Cardoso, C. L., S. L. Melo, and E. S. Melo. 2013. Contribuição para estudo dos aspectos cársticos da província serrana de Cáceres-MT: estudo de caso da Gruta do Sobradinho. In: Rasteiro, M. A., and L. Morato (Orgs.). Congresso Brasileiro de Espeleologia, 32:253–260. http://www.cavernas.org.br/anais32cbe/32cbe_253-260.pdf.

da Graça, W. J., C. A. M. Oliveira, F. C. T. Lima, H. P. da Silva, and I. M. Fernandes. 2017. A new species of *Astyanax* (Characiformes: Characidae) from Dolina Água

3860 Milagrosa, Rio Paraguai basin, Mato Grosso, Brazil. Journal of Fish Biology 91(4):
3861 1123–1138. https://doi.org/10.1111/jfb.13405
3862 de Sá, D. M., M. R. Sá, and N. T. Lima. 2008. Telégrafos e inventário do território no
3863 Brasil: as atividades científicas da Comissão Rondon (1907-1915). História,
3864 Ciências, Saúde-Manguinhos 15(3):779–811. http://dx.doi.org/10.1590/S0104-
3865 59702008000300011.
3866 de Queiroz, A., R. Lawson, and J. A. Lemos-Espinal. 2002. Phylogenetic relationships of
3867 North American garter snakes (*Thamnophis*) based on four mitochondrial genes:
3868 how much DNA sequence is enough? Molecular Phylogenetics and Evolution
3869 22(2):315–329. https://doi.org/10.1006/mpev.2001.1074.
3870 Dexter, K. G., R. T. Pennington, A. T. Oliveira-Filho, M. L. Bueno, P. L. Silva de Miranda,
3871 and D. M. Neves. 2018. Inserting Tropical Dry Forests into the discussion on biome
3872 transitions in the Tropics. Frontiers Ecology and Evolution 104(6):1–7.
3873 https://doi.org/10.3389/fevo.2018.00104
3874 DSG – Diretoria de Serviço Geográfico. 1982. MIR-403. Folha SD.21-V-B. Cáceres.
3875 Escala 1:250.000.
3876 Duellman, W. E., and E. Lehr. 2009. Terrestrial-breeding frogs (Strabomantidae) in Peru.
3877 Natur und Tier Verlag, Münster, Germany, 382 pp.
3878 Ferraro, D. P., B. L. Blotto, D. Baldo, D. A. Barrasso, J. S. Barrionuevo, N. G. Basso, D. E.
3879 Cardozo, L. Cotichelli, J. Faivovich, M. O. Pereyra, and E. O. Lavilla. 2018.
3880 Sistemática y diversidad. Cuadernos de Herpetología 32 (Suppl. 1):05–56.
3881 Frost, D. R. 2020. Amphibian Species of the World: an Online Reference. Version 6.0.
3882 American Museum of Natural History American Museum of Natural History, New
3883 York, USA. Available from:

http://research.amnh.org/herpetology/amphibia/index.html (accessed 23 March 2020).

Goicochea, N., I. De la Riva, and J. M. Padial. 2010. Recovering phylogenetic signal from frog mating calls. Zoologica Scripta 39(2):141–154. https://doi.org/10.1111/j.1463-6409.2009.00413.x.

Guindon, S., J. F. Dufayard, V. Lefort, M. Anisimova, W. Hordijk, and O. Gascuel. 2010. New algorithms and methods to estimate maximum-likelihood phylogenies: assessing the Performance of PhyML 3.0. Systematic Biology 59(3):307–332. https://doi.org/10.1093/sysbio/syq010.

Hedges, S. B. 1989. An island radiation: allozyme evolution in Jamaican frogs of the genus *Eleutherodactylus* (Leptodactylidae). Caribbean Journal of Science 25:123–147.

Hedges, S. B., W. E. Duellman, W.E., and M. P. Heinicke. 2008. New World direct-developing frogs (Anura: Terrarana): Molecular phylogeny, classification, biogeography, and conservation. Zootaxa 1737:1–182.

Heinicke, M. P., W. E. Duellman, and S. B. Hedges. 2007. Major Caribbean and Central American frog faunas originated by oceanic dispersal. Proceedings of the National Academy of Sciences 104(24):10092–10097. https://doi.org/10.1073/pnas.0611051104.

Heinicke, M.P., A. R. Lemmon, E. M. Lemmon, K. McGrath, and S. B. Hedges. 2018. Phylogenomic support for evolutionary relationships of New World direct-developing frogs (Anura: Terraranae). Molecular Phylogenetics and Evolution 118:145–155. https://doi.org/10.1016/j.ympev.2017.09.021

Heyer, W. R., and A. M. Muñoz. 1999. Validation of *Eleutherodactylus crepitans* Bokermann, 1965, notes on the types and type locality of *Telatrema heterodactylum* Miranda-Ribeiro, 1937, and a description of a new species of *Eleutherodactylus*

from Mato Grosso, Brazil (Amphibia: Anura: Leptodactylidae). Proceedings of the Biological Society of Washington 112 (1):1–18.

Hoehne, F. C. 1916. Relatorios dos trabalhos de botanica e viagens executados durante os annos de 1908 e 1909. Commissão de Linhas Telegraphicas Estrategicas de Matto-Grosso ao Amazonas 20(4):1–54.

Huelsenbeck, J. P., and F. Ronquist. 2001. MRBAYES: Bayesian inference of phylogenetic trees. Bioinformatics 17(8):754–755. https://doi.org/10.1093/bioinformatics/17.8.754

Ibisch, P.L., and G. Mérida (Eds.). 2004. Biodiversity: the richness of Bolivia. State of knowledge and conservation. Editorial FAN, Santa Cruz de la Sierra, 644 pp.

Ivanova, N. V., J. R. Dewaard, and P. D. N. Hebert. 2006. An inexpensive, automation-friendly protocol for recovering high-quality DNA. Molecular Ecology Notes 6(4):998–1002. https://doi.org/10.1111/j.1471-8286.2006.01428.x

Katoh, K., and D. M. Standley. 2013. MAFFT multiple sequence alignment software version 7: Improvements in performance and usability. Molecular Biology and Evolution 30(4):772–780. https://doi.org/10.1093/molbev/mst010

Katoh, K., and H. Toh. 2008. Recent developments in the MAFFT multiple sequence alignment program. Briefings in Bioinformatics 9(4):286–298. https://doi.org/10.1093/bib/bbn013

Katoh, K., K. Mizawa, K. Kuma, and T. Miyata. 2002. MAFFT: a novel method for rapid multiple sequence alignment based on fast Fourier transform. Nucleic Acids Research 30(14):3059–3066. https://doi.org/10.1093/bib/bbn013

Köhler, G. 2012. Color Catalogue for Field Biologists. Herpeton, Offenbach, 49 pp.

Köhler, J., and J. M. Padial. 2016. Description and phylogenetic position of a new (singleton) species of *Oreobates* Jiménez De La Espada, 1872 (Anura:

3934 Craugastoridae) from the Yungas of Cochabamba, Bolivia. Annals of Carnegie
3935 Museum 84(1):23–38. https://doi.org/10.2992/007.084.0104.
3936 Köhler, J., M. Jansen, A. Rodríguez, P. J. R. Kok, L. F. Toledo, M. Emmrich, F. Glaw, C.
3937 F. B. Haddad, M. O. Rödel, and M. Vences. 2017. The use of bioacoustics in
3938 anuran taxonomy: theory, terminology, methods and recommendations for best
3939 practice. Zootaxa 4251(1):001-124. http://dx.doi.org/10.11646/zootaxa.4251.1.1
3940 Lanfear, R., P. B. Frandsen, A. M. Wright, T. Senfeld, and B. Calcott. 2016. Partitionfinder
3941 2: New methods for selecting partitioned models of evolution for molecular and
3942 morphological phylogenetic analyses. Molecular Biology and Evolution 34(3):772–
3943 773. https://doi.org/10.1093/molbev/msw260
3944 Ligges, U., O. Mersmann, S. Krey, and S. Schnackenberg. 2007. tuneR: Analysis of music.
3945 Available from: http://r-forge.r-project.org/projects/tuner/.
3946 Lynch, J. D. 1971. Evolutionary relationships, osteology, and zoogeography of
3947 leptodactyloid frogs. Miscellaneous Publication of the University of Kansas
3948 Museum of Natural History 53:1–238.
3949 Lynch, J. D. 1980. A taxonomic and distributional synopsis of the Amazonian frogs of the
3950 genus *Eleutherodactylus*. American Museum Novitates 2696:1–24.
3951 Lynch, J. D., and W. E. Duellman. 1997. Frogs of the genus *Eleutherodactylus* in western
3952 Ecuador. The University of Kansas Natural History Museum, Special Publications
3953 23:1–23. Available from:
3954 https://www.biodiversitylibrary.org/item/32832#page/7/mode/1up (accessed 04
3955 January 2019).
3956 Lynch, J. D., and A. Schwartz. 1971. Taxonomic disposition of some 19th century
3957 leptodactylid frog names. Journal of Herpetology 5:103–114.
3958 https://doi.org/10.2307/1562732.

3959 Miranda-Ribeiro, A. 1916. Relatorio dos trabalhos realizados durante o anno de 1908.
3960 Commissão de Linhas Telegraphicas Estrategicas de Matto-Grosso ao Amazonas
3961 27(4):1–40.
3962 Miranda-Ribeiro, A. 1937. Alguns batrachios novos das collecções do Museu Nacional. O
3963 Campo:66–69.
3964 Motta, A. P., J. C. Chaparro, J. P. Pombal Jr., J. M. Guayasamin, I. De la Riva, and J. M.
3965 Padial. 2016 Molecular phylogenetics and taxonomy of the Andean genus *Lynchius*
3966 Hedges, Duellman, and Heinicke 2008 (Anura: Craugastoridae). Herpetological
3967 Monographs 30:119–142. https://doi.org/10.1093/nar/gkw256
3968 Myers, G. S. 1962. The American leptodactylid frog genera *Eleutherodactylus*, *Hylodes*
3969 (=*Elosia*), and *Caudiverbera* (=*Calyptocephalus*). Copeia,1962:195–202.
3970 https://doi.org/10.2307/1439498.
3971 Padial, J.M., and I. De La Riva. 2005. Rediscovery, redescription, and advertisement call of
3972 *Eleutherodactylus heterodactylus* (Miranda Ribeiro, 1937) (Anura:
3973 Leptodactylidae), and notes on other *Eleutherodactylus*. Journal of Herpetology
3974 39(3):372–379. https://doi.org/10.1670/191-04A.1.
3975 Padial, J.M., J. C. Chaparro, and I. De La Riva. 2008. Systematics of *Oreobates* and the
3976 *Eleutherodactylus discoidalis* species group (Amphibia, Anura), based on two
3977 mitochondrial DNA genes and external morphology. Zoological Journal of the
3978 Linnean Society 152(4):737–773. https://doi.org/10.1111/j.1096-
3979 3642.2007.00372.x.
3980 Padial, J.M., J. C. Chaparro, S. Castroviejo-Fisher, J. M. Guayasamin, E. Lehr, A. J.
3981 Delgado, M. Vaira, M. Teixeira Jr., R. Aguayo, and I. De La Riva. 2012. A revision
3982 of species diversity in the Neotropical genus *Oreobates* (Anura: Strabomantidae),

3983 with the description of three new species from the Amazonian slopes of the Andes.
3984 American Museum Novitates 3752:1–55. https://doi.org/10.1206/3752.2
3985 Padial, J.M., T. Grant, and D. R. Frost. 2014. Molecular systematics of terraranas (Anura:
3986 Brachycephaloidea) with an assessment of the effects of alignment and optimality.
3987 Zootaxa 3825(1):1–132. http://dx.doi.org/10.11646/zootaxa.3825.1.1
3988 Pereyra, M.O., D. E. Cardozo, J. Baldo, and D. Baldo. 2014. Description and phylogenetic
3989 position of a new species of *Oreobates* (Anura: Craugastoridae) from Northwestern
3990 Argentina. Herpetologica 70(2):211–227.
3991 https://doi.org/10.1655/HERPETOLOGICA-D-13-00072
3992 Puillandre, N., A. Lambert, S. Brouillet, and G. Achaz. 2012. ABGD, Automatic Barcode
3993 Gap Discovery for primary species delimitation. Molecular Ecology 21(8):1864–
3994 1877. https://doi.org/10.1111/j.1365-294X.2011.05239.x.
3995 Pyron, R. A., and J. J. Wiens. 2011. A large-scale phylogeny of Amphibia including over
3996 2800 species, and a revised classification of extant frogs, salamanders, and
3997 caecilians. Molecular Phylogenetics and Evolution 61(2):543–583.
3998 https://doi.org/10.1016/j.ympev.2011.06.012
3999 Romero-Muñoz, A., M. Jansen, A. M. Nuñez, M. Toledo, R. V. Almonacid, and T.
4000 Kuemmerle. 2019. Fires scorching Bolivia's Chiquitano forest. Science
4001 366(6469):1082. https://doi.org/10.1126/science.aaz7264.
4002 Ronquist, F., and J. P. Huelsenbeck. 2003. MrBayes 3: Bayesian phylogenetic inference
4003 under mixed models. Bioinformatics 19(12):1572–1574.
4004 https://doi.org/10.1093/bioinformatics/btg180.
4005 Silva, F. J. 2005. Relatório do levantamento da fauna de invertebrados e caracterização
4006 bioespeleológica da Gruta do Jabuti, Município de Curvelândia e Loca da Revoada,
4007 Município de Cáceres – MT. Instituto Brasileiro do Meio Ambiente e dos Recursos

Naturais Renováveis / Centro Nacional de Pesquisa e Conservação de Cavernas, Brasília, DF, Brazil. Available from: https://dspace.icmbio.gov.br//jspui/handle/cecav/591 (accessed 30 April 2020).

Streicher, J.W., E. C. Miller, P. C. Guerrero, C. L. Correa-Quezada, J. C. Ortiz, A. J. Crawford, M. R. Pie, and J. J. Wiens. 2018. Evaluating methods for phylogenomic analyses, and a new phylogeny for a major frog clade (Hyloidea) based on 2214 loci. Molecular Phylogenetics and Evolution 119:128–143. https://doi.org/10.1016/j.ympev.2017.10.013.

Strüssmann, C., A. Pansonato, and D. Soares. 2011. Vocalização de anúncio e ampliação da distribuição de *Pristimantis crepitans* (Bokermann) (Amphibia, Anura, Strabomantidae). Iheringia, Série Zoologia 101(4):296–303. http://dx.doi.org/10.1590/S0073-47212011000300003.

Sueur, J., T. Aubin, and C. Simonis. 2008. Seewave, a free modular tool for sound analysis and synthesis. Bioacoustics 18(2):213–226. https://doi.org/10.1080/09524622.2008.9753600

Tamura, K., G. Stecher, D. Peterson, A. Filipski, and S. Kumar. 2013. MEGA6: Molecular evolutionary genetics analysis version 6.0. Molecular Biology and Evolution 30(12):2725–2729. http://dx.doi.org/10.1093/molbev/mst197

Teixeira Jr., M., R. C. Amaro, R. S. Recoder, M. A. Sena, and M. T. Rodrigues. 2012. A relict new species of *Oreobates* (Anura, Strabomantidae) from the Seasonally Dry Tropical Forests of Minas Gerais, Brazil, and its implication to the biogeography of the genus and that of South American Dry Forests. Zootaxa 3158:37–52. http://dx.doi.org/10.5281/zenodo.209808.

4031 Trifinopoulos, J., L. T. Nguyen, A. von Haeseler, and B. Q. Minh. 2016. W-IQ-TREE: a
4032 fast online phylogenetic tool for maximum likelihood analysis. Nucleic Acids
4033 Research 44:232–235. https://doi.org/10.1093/nar/gkw256.
4034 Vaz-Silva, W., N. M. Maciel, S. P. de Andrade, and R. C. Amaro. 2018. A new cryptic
4035 species of *Oreobates* (Anura: Craugastoridae) from the seasonally dry tropical
4036 forest of central Brazil. Zootaxa 4441:89–108.
4037 https://doi.org/10.11646/zootaxa.4441.1.5.
4038 Yachdav, G., S. Wilzbach, B. Rauscher, R. Sheridan, I. Sillitoe, J. Procter, S. E. Lewis, B.
4039 Rost, and T. Goldberg. 2016. MSAViewer: interactive JavaScript visualization of
4040 multiple sequence alignments. Bioinformatics 32(22):3501–3503.
4041 https://doi.org/10.1093/bioinformatics/btw474.

4042 **Tables**

4043 **Table 1.** GenBank accession number and locality for sequences of *Oreobates* produced in this study.

Voucher	GenBank ID	Locality
SMF 88497	MW029642	Bolivia: Santa Cruz, Province Ñuflo de Chávez San Sebastían
SMF 88499	MW029643	Bolivia: Santa Cruz, Province Ñuflo de Chávez San Sebastían
SMF 88500	MW029643	Bolivia: Santa Cruz, Province Ñuflo de Chávez San Sebastían
UFMT 10058	MW029622	Brazil: Mato Grosso, Santo Antônio do Leverger, São Vicente
UFMT 11114	MW029639	Brazil: Mato Grosso, Porto Estrela, Estação Ecológica Serra das Araras
UFMT 11116	MW029640	Brazil: Mato Grosso, Porto Estrela, Estação Ecológica Serra das Araras
UFMT 11118	MW029641	Brazil: Mato Grosso, Porto Estrela, Estação Ecológica Serra das Araras
UFMT 19217	MW029620	Brazil: Mato Grosso, Santo Antônio do Leverger, São Vicente
UFMT 19218	MW029621	Brazil: Mato Grosso, Santo Antônio do Leverger, São Vicente
UFMT 19225	MW029630	Brazil: Mato Grosso, Cáceres, Fazenda Hayashi "Gruta Fazendinha"
UFMT 19226	MW029631	Brazil: Mato Grosso, Cáceres, Fazenda Hayashi "Gruta Fazendinha"
UFMT 19231	MW029632	Brazil: Mato Grosso, Cáceres, Fazenda Hayashi "Gruta Fazendinha"
UFMT 19234	MW029633	Brazil: Mato Grosso, Cáceres, Dolina Água Milagrosa
UFMT 19235	MW029634	Brazil: Mato Grosso, Cáceres, Dolina Água Milagrosa

UFMT 19237	MW029635	Brazil: Mato Grosso, Cáceres, Dolina Água Milagrosa
UFMT 19239	MW029636	Brazil: Mato Grosso, Cáceres, Fazenda Hayashi "Gruta Fazendinha"
UFMT 19240	MW029637	Brazil: Mato Grosso, Cáceres, Fazenda Hayashi "Gruta Fazendinha"
UFMT 19245	MW029638	Brazil: Mato Grosso, Cáceres, Fazenda Hayashi "Gruta Fazendinha"
UFMT 7348	MW029623	Brazil: Mato Grosso, Chapada dos Guimarães, Mata Fria
ZUEC 14114	MW029624	Brazil: Mato Grosso, Santo Antônio do Leverger, São Vicente
ZUEC 14115	MW029625	Brazil: Mato Grosso, Santo Antônio do Leverger, São Vicente
ZUEC 14116	MW029626	Brazil: Mato Grosso, Santo Antônio do Leverger, São Vicente
ZUEC 14117	MW029627	Brazil: Mato Grosso, Chapada dos Guimarães, Mata Fria
ZUEC 14118	MW029628	Brazil: Mato Grosso, Chapada dos Guimarães, Mata Fria
ZUEC 14119	MW029629	Brazil: Mato Grosso, Chapada dos Guimarães, Mata Fria

4044

Table 2. Uncorrected between-group mean p-distances of the 16S mitochondrial rRNA gene of *Oreobates* populations from eastern Bolivia (SS – San Sebastián, Province Ñuflo de Chávez; CA – Province Chiquitos, Serranía de Santiago, Cerro del Arco) and Brazil [SV – São Vicente, Santo Antônio do Leverger (type locality of *O. crepitans*); MF – Mata Fria, Chapada dos Guimarães; SA – Estação Ecológica Serra das Araras, Porto Estrela; DM – Dolina Água Milagrosa, Cáceres; GF – Fazenda Hayashi "Gruta Fazendinha", Cáceres (type locality of *O. heterodactylus*)].

	O. antrum	SV	MF	CA	GF	DM	SA	*O. remotus*
SV	0.093							
MF	0.093	0.006						
CA	0.102	0.104	0.106					
GF	0.086	0.047	0.047	0.114				
DM	0.087	0.048	0.048	0.113	0.001			
SA	0.081	0.031	0.030	0.107	0.039	0.039		
O. remotus	0.080	0.097	0.095	0.127	0.098	0.100	0.094	
SS	0.117	0.106	0.109	0.032	0.112	0.112	0.103	0.131

Table 3. Morphometrics of *Oreobates* species from localities in the state Mato Grosso, Brazil [São Vicente, Santo Antônio do Leverger (SV; type-locality of *O. crepitans*); Mata Fria, Chapada dos Guimarães (MF); Morro do Chapéu, Chapada dos Guimarães (MC); Estação Ecológica Serra das Araras, Porto Estrela (SA); Fazenda União, Rosário Oeste (RO); Dolina Água Milagrosa, Cáceres (DM); Fazenda Hayashi "Gruta Fazendinha", Cáceres (GF; type locality of *O. heterodactylus*)], and Department Santa Cruz, Bolivia [San Sebastián, Province Ñuflo de Chávez (SS)]. Values are presented as mean ± standard deviation followed by range (minimum–maximum). *n* = number of specimens analyzed.

	SS		GF		DM	SA		RO	MC		MF		SV
	Males (*n*=3)	Female	Males (*n*=15)	Female (*n*=4)	Males (*n*=7)	Males (*n*=7)	Male	Female (*n*=3)	Males (*n*=5)	Female	Males (*n*=3)	Female	Males (*n*=4)
SVL	24.9±0.5 (24.6–25.4)	27.4	27.6±1.3 (24.9–29.7)	29.7±2.8 (26.1–32.6)	27.9±1.5 (26.6–29.9)	25.6±2.2 (22.2–29.6)	27.2	28.8±2.3 (27.4–31.5)	28.1±1.9 (25.1–30.0)	25.1	26.7±2.1 (24.3–27.9)	26.7	27.5±1.7 (25.0–28.7)
HL	8.9±0.2 (8.7–9.2)	10.7	10.1±0.6 (8.5–11.2)	11.4±0.7 (10.7–12.3)	10.2±0.5 (9.6–11.0)	10.1±0.8 (8.4–10.9)	10.6	10.5±0.4 (10.1–10.8)	10.3±0.4 (9.8–10.9)	9.9	10.5±0.7 (10.1–11.3)	10.3	10.3±0.9 (9.1–11.3)
HW	9.4±0.2 (9.1–9.6)	9.8	9.4±0.6 (8.2–10.7)	9.9±0.3 (9.7–10.4)	9.4±0.5 (9.1–10.4)	9.2±0.9 (7.6–10.4)	9.4	9.99±0.4 (9.6–10.3)	9.8±0.4 (9.1–10.3)	8.4	9.9±0.6 (9.3–10.4)	9.8	9.6±0.6) (8.8–10.1)
EL	3.6±0.4 (3.3–4.0)	3.2	3.6±0.3 (3.0–3.9)	3.5±0.2 (3.3–3.8)	4.0±0.2 (3.8–4.2)	3.5±0.3 (3.15–4.0)	3.5	3.5±0.2 (3.3–3.8)	3.6±0.2 (3.3–3.8)	2.9	3.5±0.3 (3.3–3.9)	3.5	3.7±0.2 (3.5–4.0)
EN	2.8±0.3 (2.5–3.0)	3.2	3.6±0.2 (3.4–3.9)	3.5±0.3 (3.3–3.8)	3.6±0.2 (3.4–3.9)	3.3±0.3 (3.0–3.8)	3.6	3.5±0.3 (3.3–3.8)	3.5±0.2 (3.3–3.7)	3.0	3.3±0.1 (3.3–3.5)	3.3	3.3±0.3 (2.9–3.6)
IND	2.3±0.1 (2.3–2.4)	2.7	2.2±0.2 (1.9–2.6)	2.45±0.3 (2.2–2.8)	2.3±0.1 (2.1–2.4)	2.2±0.3 (1.8–2.8)	2.4	2.45±0.3 (2.2–2.8)	2.3±0.3 (2.0–2.8)	2.1	2.2±0.03 (2.2–2.3)	2.3	2.0±0.2 (1.9–2.2)
EE	(2.6±0.2 (2.5–2.9)	3.1	4.9±0.3 (4.6–5.4)	5.4±0.2 (5.1–5.7)	4.9±0.2 (4.6–5.2)	4.9±0.5 (4.1–5.6)	5.4	5.1±0.4 (4.8–5.5)	4.9±0.3 (4.6–5.3)	4.7	4.9±0.4 (4.6–5.4)	5.1	4.9±0.3 (4.5–5.2)
TYH	2.2±0.1 (2.1–2.2)	2.2	2.4±0.2 (2.1–2.8)	2.5±0.1 (2.4–2.6)	2.7±0.1 (2.6–2.9)	2.5±0.3 (2.0–2.9)	2.6	2.5±0.3 (2.3–2.9)	2.6±0.2 (2.4–2.8)	2.3	2.5±0.2 (2.4–2.7)	2.5	2.3±0.1 (2.1–2.5)
TYL	1.9±0.0		2.3±0.2	2.3±0.1	2.5±0.2	1.86±0.04		2.5±0.3	2.5±0.2		2.5±0.3		2.2±0.1

	(1.9–1.9)	2.4	(1.8–2.8)	(2.1–2.5)	(2.1–2.7)	(2.1–3.0)	2.5	(2.2–2.9)	(2.3–2.9)	2.1	(2.3–2.9)	2.3	(2.1–2.5)
F3	0.8±0.1		1.2±0.1	1.2±0.2	1.2±0.1	1.2±0.2		0.9±0.2	1.2±0.1		1.0±0.3		1.0±0.1
	(0.7–0.9)	0.8	(1.0–1.6)	(1.0–1.5)	(1.1–1.4)	(0.8–1.4)	1.2	(0.8–1.0)	(1.1–1.2)	0.9	(0.8–1.4)	0.9	(0.9–1.1)
F4	0.8±0.2		1.2±0.1	1.3±0.1	1.2±0.1	1.2±0.1		1.0±0.3	1.2±0.1		1.1±0.3		1.0±0.1
	(0.7–1.0)	0.8	(1.1–1.4)	(1.1–1.5)	(1.1–1.4)	(1.0–1.4)	1.2	(0.8–1.2)	(1.1–1.4)	0.9	(0.8–1.3)	0.9	(0.9–1.1)
FA	6.1±0.4		6.5±0.3	6.7±0.5	6.5±0.5	6.3±0.4		7.2±0.4	6.5±0.2		6.5±0.2		6.4±0.5
	(5.7–6.4)	6.7	(5.9–6.9)	(6.3–7.3)	(5.5–7.1)	(5.5–6.8)	6.9	(6.8–7.6)	(6.3–6.6)	5.7	(6.3–6.6)	6.5	(5.9–7.1)
TL	13.3±0.1		12.8±0.7	13.6±0.9	13.0±0.7	13.1±1.0		14.0±0.8	13.3±0.5		13.3±0.1		13.2±0.5
	(13.3–13.4)	15.3	(11.6–13.9)	(12.7–14.5)	(12.2–14.3)	(11.6–14.6)	13.6	(13.4–14.9)	(12.6–13.9)	13.1	(13.2–13.5)	13.8	(12.7–13.9)
TH	12.5±0.3		11.9±06	12.5±0.6	12.1±1.1	11.8±0.9		13.2±1.5	12.9±0.6		12.4±0.5		12.0±1.16
	(12.3–12.8)	13.0	(10.9–13.1)	(11.7–13.0)	(10.2–14.0)	(10.6–13.6)	13.0	(11.7–14.8)	(12.2–13.8)	12.8	(11.9–12.9)	13.1	(10.8–13.0)
FL	12.0±0.3		11.5±0.6	12.1±0.8	11.8±0.7	11.8±0.9		12.6±0.9	12.2±0.6		11.8±0.09		11.9±0.3
	(11.7–12.3)	13.7	(10.3–12.3)	(11.8–13.6)	(10.8–12.9)	(10.5–13.2)	12.4	(11.8–13.6)	(11.4–12.9)	12.2	(11.8–12.0)	12.5	(11.4–12.2)
T4	0.6±0.1		0.7±0.1	0.7±0.1	0.7±0.1	0.8±0.1		0.8±0.1	0.7±0.1		0.7±0.1		0.7±0.1
	(0.6–0.6)	0.6	(0.5–1.1)	(0.6–0.8)	(0.5–0.8)	(0.7–1.0)	0.6	(0.65–0.9)	(0.6–0.8)	0.6	(0.7–0.8)	0.5	(0.6–0.9)

4058

Table 4. Summary of the number and percentage of male specimens of *Oreobates* spp. correctly classified into their original populations/localities (=True group), using the classification matrix of a Discriminant Function Analysis based on 16 morphometric variables. Populations/localities: Brazil: Dolina Água Milagrosa (DM), Gruta Fazendinha (GF), Morro do Chapéu (MC), Mata Fria (MF), Rosário Oeste (RO), Estação Ecológica Serra das Araras (SA), São Vicente (SV); Bolivia: Cerro del Arco (CA), San Sebastián (SS).

	True group							
	DM	GF	MC	MF	RO	SA	SV	SS
DM	2	2	2			1		
GF	5	6		1	1		2	
MC	3	1					1	
MF		1	1		1			
RO								
SA	1	2		1		2	1	
SV		1		1		2		
SS								4
Total number	7	15	5	3	0	7	4	4
%	28	40	0	0	0	28	0	100

Table 5. Summary of the number and percentage of male specimens of *Oreobates* spp. correctly classified into their original populations/localities (=True Group), using the classification matrix of a Discriminant Function Analysis based on six bioacoustic variables. Populations/localities: Brazil: Dolina Água Milagrosa (DM), Gruta Fazendinha (GF), Morro do Chapéu (MC), Mata Fria (MF), Rosário Oeste (RO), Estação Ecológica Serra das Araras (SA), São Vicente (SV); Bolivia: Cerro del Arco (CA), San Sebastián (SS).

	True Group					
	DM	GF	AS	SV	CA	SS
DM	1			1		
GF		4				
AS			4			
SV	1	1	1			
CA					3	1
SS					1	1
%	50	100	100	0	75	50
Total number	2	4	4	3	4	2

4073 **Table 6**. Numerical parameters of calls of *Oreobates* species from localities in the state of Mato Grosso, Brazil and Department Santa Cruz, Bolivia.

4074 Values are presented as mean ± standard deviation followed by range (minimum–maximum). *n* = number of calls analyzed.

Voucher	Voucher record	Air tempeature (ºC)	Number pulses/call	Call duration [ms]	Pulse duration [ms]	Inter–pulse intervals [ms]	Dominant frequency [Hz]	Call rate [calls/min]	Locality
UFMT 10058	LH 62 (*n*=20)	24	2	37±2 (33–40)	9±2 (6–12)	17±1 (14–19)	2850.9±223.4 2411.7–3186.9	56.6±11.6 (48.4–64.8)	São Vicente (SV)
UFMT 192179	LH 877 (*n*=8)	24	2	38±3 (34–43)	9±2 (5–13)	21±1 (19–22)	3380.7±468.9 2842.4–4048.2	43.9±7.3 (38.5–54.1)	São Vicente (SV)
UFMT 19218	LH 878 (*n*=25)	24	2	49±5 (39–56)	14±4 (9–22)	22±2 (18–25)	2897.5±639.6 2067.2–3617.6	42.5±12.1 (30.5–54.5)	São Vicente (SV)
No voucher	LH09B–01 (*n*=17)	23.4	2	33±1 (31–36)	7±1 (5–9)	20±2 (17–24)	2325.6±166.8 2239.5–2670.1	19.4±2.5 17.6–21.2	Porto Estrela (SA)
UFMT 11116	LH 07 (*n*=8)	24	2	42±13 (32–73)	8±2 (5–13)	23±2 (20–25)	3025.4±490.3 2239.5–3531.4	24.6	Porto Estrela (SA)
UFMT 11114	LH 08 (*n*=11)	24.3	2	42±5 (37–56)	10±3 (7–17)	22±4 (17–31)	3202.5±195.7 2670.1–3359.2	28.6±19.3 (50.5–67.5	Porto Estrela (SA)
UFMT 11115	LH 26 (*n*=12)	24.3	2	38±3 (33–42)	7±2 (5–12)	25±2 (23–29)	2655.7±317.7 2325.6–3359.2	32.9±17.8 (13.3–48)	Porto Estrela (SA)
UFMT 19238	LH 882 (*n*=12)	25.5	2	33±4 (27–38)	6±1 (4–9)	20±1 (18–22)	3129.4±76.5 3014.6–3186.9	67.9±7.4 (62.7–73.2)	Cáceres (GF)
UFMT 19241	LH 883 (*n*=3)	25.5	2	38±2 (36–39)	9±2 (6–11)	21±1 (20–22)	3014.6±344.5 2670.1–3359.2	69.2	Cáceres (GF)
UFMT 19240	LH 997 (*n*=22)	25.5	2	45±4 (38–57)	10±2 (7–15)	23±6 (16–42)	3316.1±83.1 3186.9–3445.3	68.6	Cáceres (GF)
UFMT 19226	LH 1288	25.5	2	46±3	11±2	23±3	2906.9±301.5	77.1±12.1	Cáceres (GF)

	(*n*=5)			(42–49)	(8–13)	(21–27)	(2756.2–3359.2)	(68.6–85.7)	
UFMT 19236	LH 881	25	2	41±2	10±2	19±1	3729.6±378.8	50.5±14.6	Cáceres (DM)
	(*n*=10)			(38–43)	(8–14)	(17–22)	3100.8–4134.4	(38.3–66.7)	
UFMT 19234	LH 1292	25	2	41±2	8±1	24±1	3198.6±170.8	54.4±11.3	Cáceres (DM)
	(*n*=22)			(36–46)	(5–10)	(21–27)	(2928.5–3445.3)	(43.3–68.5)	
SMF 88497	SMF 1683	26.3	6.7	137±15	4±1	19±1	3837.7±122.6	34.2	San Sebastián (SS)
	(*n*=29)		(6–8)	(122–166)	(3–5)	(17–21)	(3617.6–4048.2)		
No voucher	SMF 43	26.3	5.8±0.7	133±12	4±2	12±3	4277.9±44.5	29.2	San Sebastián (SS)
	(*n*=6)		(5–7)	(111–146)	(3–10)	(7–22)	(4220.5–4306.6)		
No voucher	FonoZoo 2634	23	7.8±0.7	208±15	10±1	18±1	3119.9±979	27.4±2.8	Cerro del Arco (CA)
	(*n*=9)		(7–9)	(191–237)	(7–12)	(15–20)	(2067.2–3962.1)	(24.8–30.4)	
No voucher	FonoZoo 5258	24	5.5±0.7	145±26	6±2	22±1	3143.8±1522	36.4	Cerro del Arco (CA)
	(*n*=2)		(5–6)	(126–163)	(4–9)	(21–24)	(2067.2–4220.5)		
No voucher	FonoZoo 5259	24	5	123±2	8±1	21±2	4029.1±37.9	25.6	Cerro del Arco (CA)
	(*n*=9)			(121–127)	(5–10)	(16–24)	(3962.1–4048.2)		
No voucher	FonoZoo 5260	23	5.7±0.4	145±14	9±3	18±4	4015.9±102.3	30.8	Cerro del Arco (CA)
	(*n*=8)		(5–6)	(122–157)	(5–17)	(8–23)	(3962.1–4220.5)		

4075

Figures legends

Fig. 1. A) Maximum Likelihood phylogram based on 628 bp of mitochondrial 16SrRNA gene sequences from 58 individuals of *Oreobates*. Bayesian Posterior Probabilities and bootstrap values of >45 are shown on branches. Outgroup not shown for graphical purposes. B) Geographical distribution of *Oreobates* from 10 localities from eastern South America. Abbreviations: São Vicente, Santo Antônio do Leverger (SV; type locality of *O. crepitans*); Mata Fria, Chapada dos Guimarães (MF); Morro do Chapéu, Chapada dos Guimarães (MC); Estação Ecológica Serra das Araras, Porto Estrela (SA); Fazenda União, Rosário Oeste (RO); Dolina Água Milagrosa, Cáceres (DM); Gruta Fazendinha, Fazenda Hayashi, Cáceres (GF; type locality of *O. heterodactylus*); San Sebastián, Provincia Ñuflo de Chávez (SS); Provincia Chiquitos, Serranía de Santiago, Cerro del Arco (CA); Provincia Ángel Sandoval, Bella Boca (BB). Inset map: South America.

Fig. 2. Variation in the relative proportions of tips of Fingers III and IV in populations of *Oreobates* from Mato Grosso, Brazil. A) MNRJ 106A from Cáceres (GF; holotype of *O. heterodactylus*); B) UFMT 19241 from Cáceres (GF); C) UFMT 11119 from Porto Estrela (SA); D) UFMT 19239 from Cáceres (GF); E) MNRJ 3985 from Santo Antônio do Leverger, São Vicente (SV; paratype of *O. crepitans*). Fingers expansion varies among specimens from different localities (e.g. B, C, and E) and among specimens from the same locality (e.g. A, B, and D).

Fig. 3. Scatter plots of principal component analysis (PCA) Component 1 versus PCA Component 2 scores of 16 morphometric (A) and six bioacoustic (B) variables for males of studied *Oreobates* populations from Brazil [Santo Antônio do Leverger, São Vicente (SV); Chapada dos Guimarães, Mata Fria (MF); Chapada dos Guimarães, Morro do Chapéu

(MC); Cáceres, Dolina Água Milagrosa (DM); Cáceres, Fazenda Hayashi, Gruta Fazendinha (GF); Porto Estrela, Estação Ecológica Serra das Araras (SA); Rosário Oeste, Fazenda União (RO)] and Bolivia [Provincia Ñuflo de Chávez, San Sebastián (SS); Provincia Ñuflo de Chávez, Cerro del Arco (CA)].

Fig. 4. Oscillogram and spectrogram (DFT size = 512 samples) of the advertisement call of *Oreobates* from Brazil and Bolivia: (A) voucher call LH 62, from specimen UFMT 10058, recorded on 26 November 2009, 21:20h, air temperature 24ºC, municipality of Santo Antônio do Leverger, São Vicente (SV), state of Mato Grosso, Brazil; (B) voucher call LH 08, from specimen UFMT 11114, recorded on 18 December 2009, 00:20h, air temperature 24.3ºC, municipality of Porto Estrela, Estação Ecológica Serra das Araras (SA), Mato Grosso, Brazil; (C) voucher call LH 882, from specimen UFMT 19238, recorded on 14 November 2016, 19:40h, air temperature 25.5ºC, municipality of Cáceres, Fazenda Hayashi Gruta Fazendinha (GF), Mato Grosso, Brazil; (D) voucher call MJ-1683, from specimen SMF 88497, recorded on 25 November 2010, 21:16h, air temperature 26.3ºC, Provincia Ñuflo de Chávez, San Sebastián (SS), Department Santa Cruz, Bolivia. FD = dominant frequency.

Fig. 5. Male topotype of *Oreobates heterodactylus* (UFMT 19241; SVL 25.0 mm) in dorsal, lateral, and ventral views.

Fig. 6. Live specimens of *Oreobates heterodactylus* from Mato Grosso State, mid-western Brazil: (A) adult male (UFMT 19239) from the type locality, Gruta Fazendinha, Fazenda Hayashi, Cáceres (GF); (B) adult male (UFMT 19234) from Dolina Água Milagrosa, Cáceres (DM); (C) adult female (UFMT 19243) and (D) adult male (UFMT 19240) from

Gruta Fazendinha, Fazenda Hayashi, Cáceres; (E) calling male (UFMT 19219) from São Vicente, Santo Antônio do Leverger (SV); (F) adult female (UFMT 11110) from Fazenda União, Rosário Oeste (RO).

Fig. 7. Holotype of *Oreobates* ***chiquitanus*** sp. nov. (SMF 88497; male; SVL 24.6 mm): (A) dorsal and (B) ventral view; (C) lateral view; (D) ventral view of right hand and (E) ventral view of right foot. Scale bar = 2 mm.

Fig. 8. Live specimens of *Oreobates* ***chiquitanus*** sp. nov. from San Sebastián, Provincia Ñuflo de Chávez, Department Santa Cruz, Bolivia: (A) holotype (SMF 88497) and (B) adult female (SMF 88500).

Fig. 9. Dorsal and ventral view of three paratypes of *Oreobates* ***chiquitanus*** sp. nov.: two adult males (SMF 88498-9) and one larger female (SMF 88500).

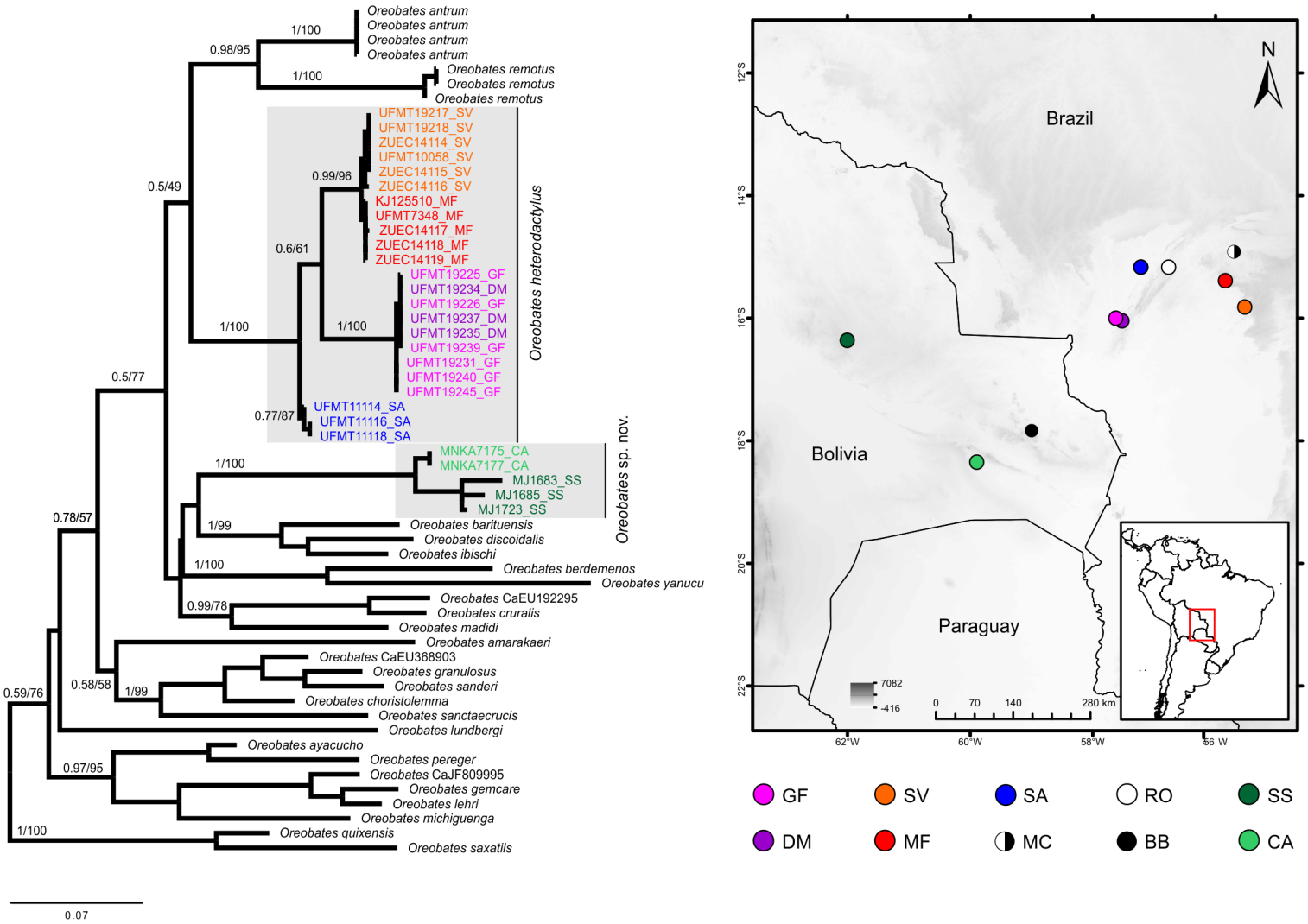

4140

4141 Figure 1

4142

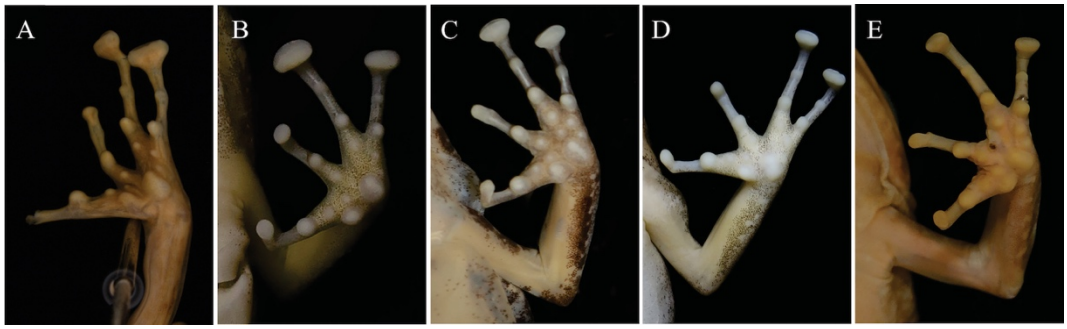

4143

4144 Figure 2

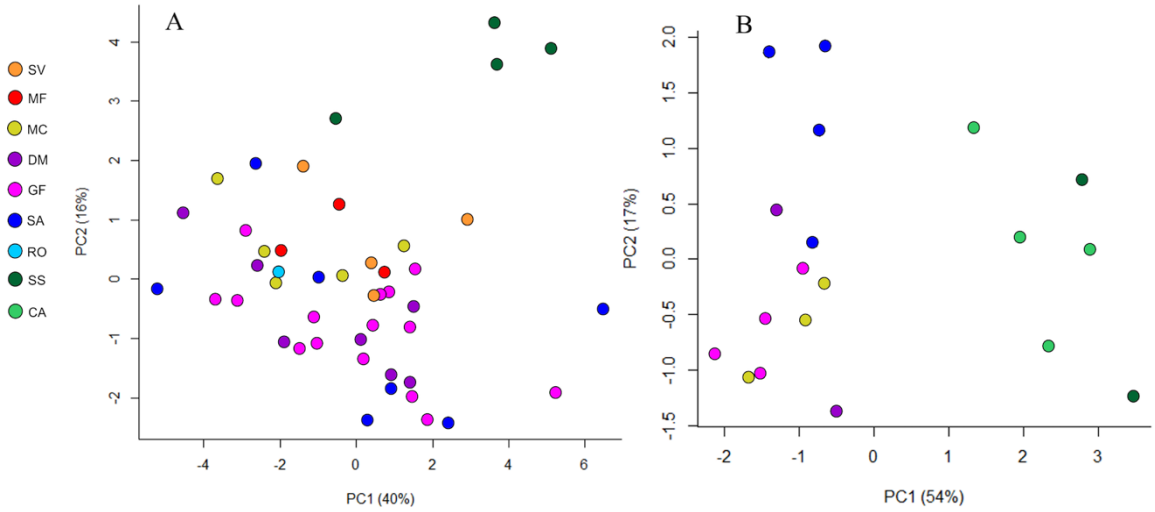

4145

4146 Figure 3

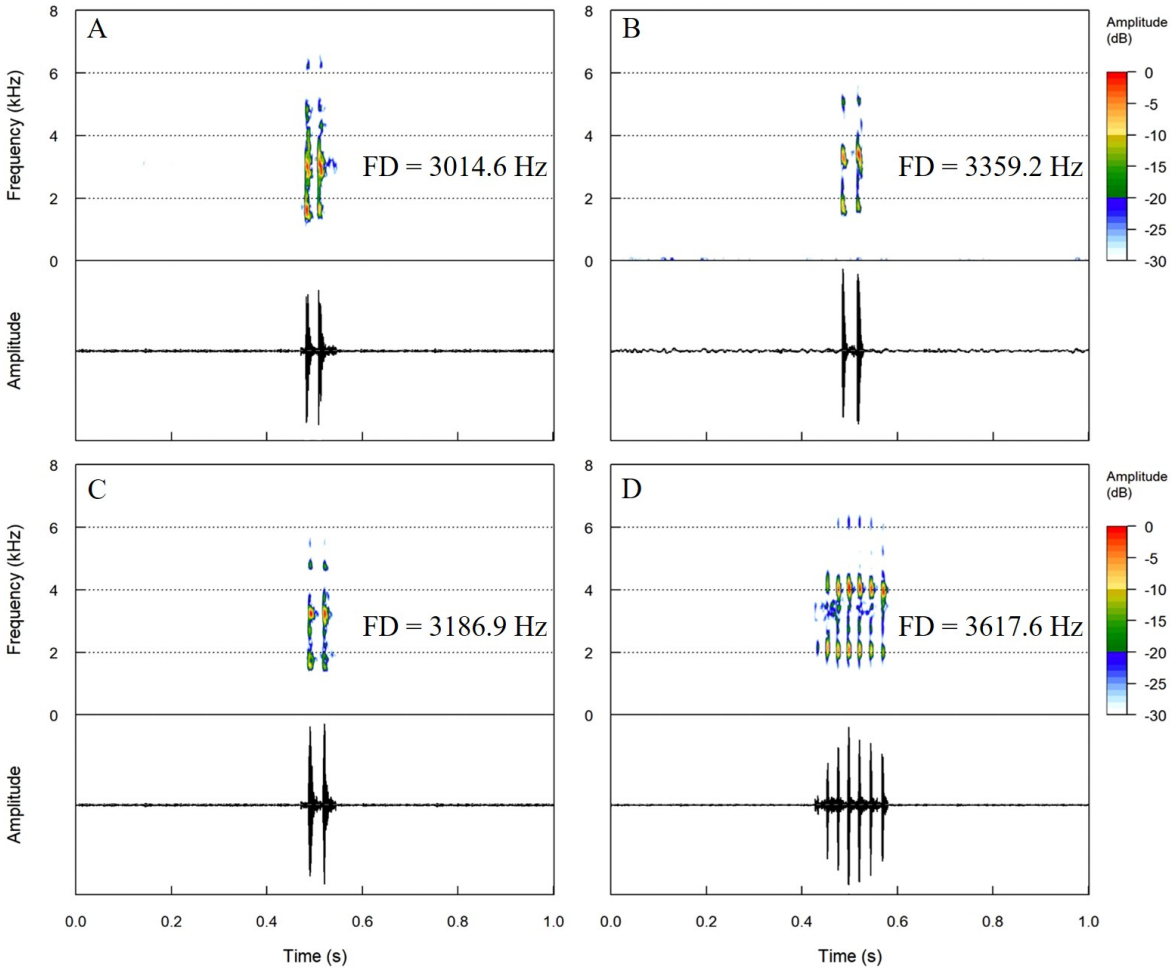

4147

4148 Figure 4

Figure 5

4151

4152 Figure 6

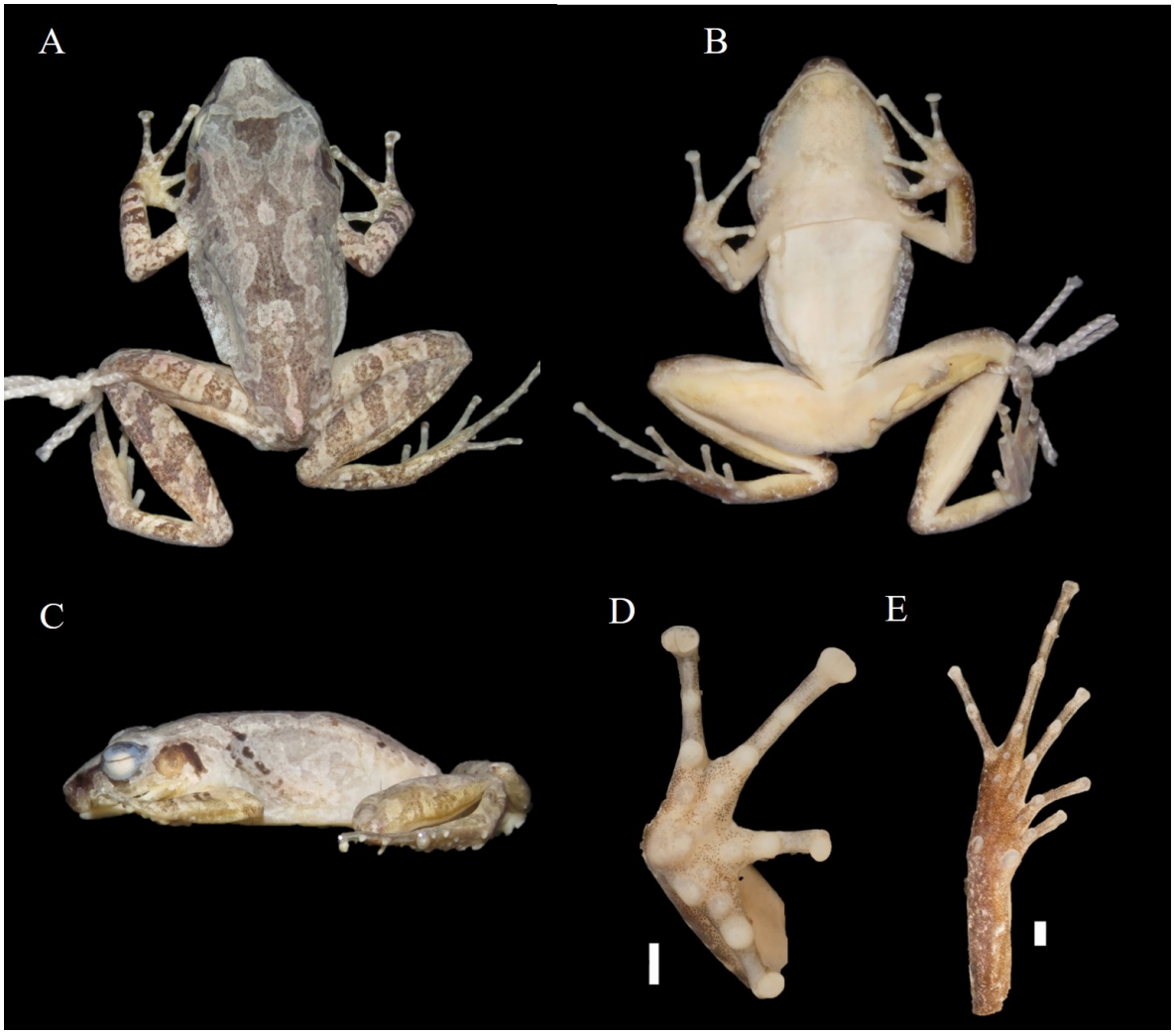

4153

4154 Figure 7

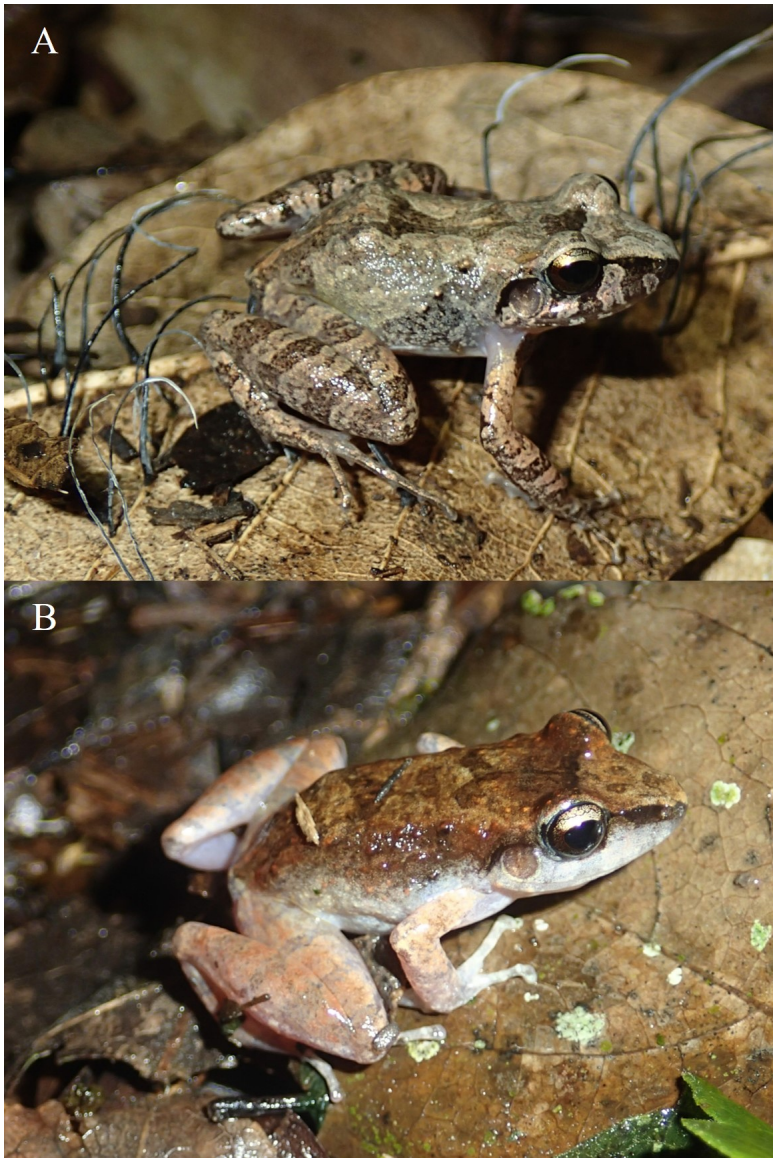

4155

4156 Figure 8

Figure 9

4159 **Appendix 1**. GenBank accession number for specimens sampled in this study.

Species	**GenBank No.**	**Locality**
Haddadus binotatus	EF493361	Brazil: Sao Paulo, Estacão Biologica de Boraceia
Lynchius flavomaculatus	EU186667	Ecuador: Loja, 19.4 km S Yangana
Lynchius nebulanastes	EU186704	Peru: Piura, El Tambo, 31.5 km E Canchaque
Lynchius parkeri	EU186705	Peru: Piura, 31 km SW Huancabamba
Lynchius simmonsi	JF810004	Ecuador: Zamora Chinchipe, Miazi Alto, Cordillera del Condor
Oreobates amarakaeri	JF809996	Peru: Cuzco, Distrito Camanti, Provincia Quispicanchi, Rio Nusiniscato
Oreobates antrum	MH025451	Brazil: Sao Domingos, GO
Oreobates antrum	MH025452	Brazil: Sao Domingos, GO
Oreobates antrum	MH025453	Brazil: Sao Domingos, GO
Oreobates antrum	MH025454	Brazil: Sao Domingos, GO
Oreobates ayacucho	JF809971	Peru: Ayacucho, Provincia La Mar, Entre Punqui y Anco
Oreobates barituensis	JF809999	Jujuy, Departamento Ledesma, Caimancito, 556 masl
Oreobates berdemenos	KJ125507	Argentina: Jujuy, Ledesma, Abra Colorada
Oreobates CaEU192295	EU192295	Bolivia: Santa Cruz, Camino a Bella Vista
Oreobates CaEU368903	EU368903	Bolivia: Cochabamba, Chaquisacha
Oreobates CaJF809995	JF809995	Peru: Cuzco, Distrito de Camanti, Provincia Quispicanchis
Oreobates chiquitanus	EU192296	Bolivia: Santa Cruz, Cerro del Arco, Serrania de Santiago

Oreobates chiquitanus	EU368898	Bolivia: Santa Cruz, Cerro del Arco, Serrania de Santiago
Oreobates cruralis	EU186666	Peru: Madre de Dios, Cuzco Amazonico, 15 km E Puerto Maldonado"
Oreobates discoidalis	EU368896	Bolivia: Tarija, Entre Rios, Chiquiaca
Oreobates gemcare	JF809961	Peru: Cuzco, Provincia Paucartambo, Esperanza, Valle de Kosnipata
Oreobates granulosus	EU368897	Peru: Puno, Santo Domingo, Carabaya
Oreobates ibischi	FJ438794	Bolivia: Santa Cruz, km 60 on Santa Cruz de la Sierra-Samaipata road
Oreobates lehri	FJ539069	Peru: Cusco, Kosnipata Valley
Oreobates lundbergi	JF809958	Peru: Pasco, Provincia Huanchon, from Auquimarca to Uchuerta
Oreobates machiguenga	JF809969	Peru: Cuzco, Provincia La Convención, Rio Kimbiri
Oreobates madidi	FJ539070	Bolivia: La Paz, Serrania Eslabon
Oreobates pereger	JF809955	Peru: Ayacucho, Provincia Lamar, Yanamonte, 2600 masl
Oreobates quixensis	EF493662	Ecuador: Sucumbios, Limoncocha
Oreobates remotus	JN688273	Brazil: Parque Nacional das Cavernas do Peruaçu, Januaria, MG
Oreobates remotus	JN688274	Brazil: Parque Nacional das Cavernas do Peruaçu, Januaria, MG
Oreobates remotus	JN688275	Brazil: Parque Nacional das Cavernas do Peruaçu, Januaria, MG
Oreobates sanctaecrucis	JF809951	Bolivia: Santa Cruz, Provincia Florida, La Yunga de Mairana
Oreobates sanderi	EU368904	Bolivia: La Paz, Santa Cruz de Valle Ameno
Oreobates saxatilis	JF809962	Peru: Cuzco, Provincia La Convención, Rio Kimbiri
Oreobates yanucu	KY111322	Bolivia: Cochabamba, Chapare, from Villa Tunari to Cochabamba

4160

Appendix 2: Specimens examined

Oreobates crepitans (junior synonym of *O. heterodactylus*).—Brazil: Mato Grosso: Santo Antônio do Leverger: São Vicente (15°49'8"S; 55°31'25"W) (holotype - MZUSP 85628; M: UFMT 10058, 19222–4); Chapada dos Guimarães: Mata Fria (15°23'9"S; 55°50'33"W) (M: UFMT 1381–6), Morro do Chapéu (14°54'60"S; 55°41'60"W), Manso (M: UFMT 7293, 7346, 7348–9, 7367); Porto Estrela: Estação Ecológica Serra das Araras (15°38'60"S; 57°12'60"W) (M: UFMT 719, 11111, 11113–6, 10526; F: UFMT 11112, 11117–20); Rosário Oeste: Fazenda União (15°9'60"S; 56°45'60"W) (M: UFMT 11108–10; F: UFMT 11107).

Oreobates heterodactylus.—Brazil: Mato Grosso: Cáceres: Fazenda Hayashi, Gruta Fazendinha (16°1'10"S; 57°35'2") (holotype – MNRJ 106; M: UFMT 19220–3, 19225–31, 19239–41, 19245; F: 19224, 19242–44), Dolina Água Milagrosa (16°2'36"S; 57°31'38"W) (M: UFMT 19232–8).

Oreobates remotus.—Brazil: Minas Gerais: Januária, Parque Nacional Cavernas do Peruaçu (holotype – MZUSP 141708; MZUSP 141709–724).

Appendix 3: Analyzed sound files

Oreobates ***chiquitanus*** sp. nov.—Bolivia: Department Santa Cruz: Provincia Ñuflo de Chávez (16°21'38"S; 62°0'8"W), San Sebastián (call from specimen SMF 88497); Provincia Chiquitos, Serranía de Santiago, Cerro del Arco (voucher FonoZoo 19936; 20413–7).

Oreobates crepitans (junior synonym of *O. heterodactylus*).—Brazil: Mato Grosso: Santo Antônio do Leverger, São Vicente (LH 62, specimen UFMT 10058; LH 877, specimen UFMT 192179; LH 878, specimen UFMT 19218); Porto Estrela, Estação Ecológica Serra

4185 das Araras (LH 09-B01, no voucher specimen; LH 07, specimen UFMT 11116; LH 08,
4186 specimen UFMT 11114; LH 26, specimen UFMT 11115).
4187 *Oreobates heterodactylus*.—Brazil: Mato Grosso: Cáceres, Fazenda Hayashi "Gruta
4188 Fazendinha" (LH 882, specimen UFMT 19238; LH 883, specimen UFMT 19241; LH
4189 1288, specimen UFMT 19226; LH 977, specimen UFMT 19240); Dolina Água Milagrosa
4190 (LH 881, specimen UFMT 19236; LH 1292, specimen UFMT 19234).

4191 **Two new species of terrestrial-breeding frogs (Anura: Brachycephaloidea) from**
4192 **Cordillera de Colán, Peru**

4193

4194 Pablo J. Venegas[a,b]*, Luis A. García-Ayachi[a,b], Jesús R. Ormeño[a,b,c], Santiago Bullard[a],
4195 Alessandro Catenazzi[a,b,d], and Ana P. Motta[e]

4196

4197 [a]*Instituto Peruano de Herpetologia (IPH), Lima, Peru;* [b]*Division de Herpetologia, Centro*
4198 *de Ornitologia y Biodiversidad (CORBIDI), Lima, Peru;* [c] *Huarango Nature –*
4199 *Conservamos Ica (CÓNICA). Ica, Perú;* [d]*Department of Biological Sciences, Florida*
4200 *International University, Miami, Florida, USA;* [e]*Departamento de Biodiversidade, Instituto*
4201 *de Biociências, Universidade Estadual Paulista (UNESP), Rio Claro, Brazil*

4202

4203 *corresponding author: sancarranca@yahoo.es

4204

4205 [†] Manuscrito submetido no periódico *Neotropical Biodiversity*

Two new species of terrestrial-breeding frogs (Anura: Brachycephaloidea) from Cordillera de Colán, Peru

We describe two new species of terrestrial-breeding frogs (Holodeninae) from the Cordillera de Colán, in northeastern Peru. We used Parsimony and Maximum Likelihood approaches to infer a molecular phylogeny on a dataset composed of 75 terminals, including three terminals representing the new species, and 4202 bp of concatenated mtDNA and nuDNA fragments. Our phylogenetic analyses support the placement of the two new species in *Lynchius* and *Oreobates*, respectively. The new species of *Lynchius* occurs in two localities from 1,977 to 2,006 m a.s.l., and is characterized by having a dorsum covered by conical tubercles and a brown dorsal coloration lacking a pattern of blotches on the hidden surfaces of flanks and hindlimbs. The new species of *Oreobates* is only known from one location at 2608 m a.s.l. and is characterized by the absence of axillary and inguinal glands, and the presence of white or cream blotches on the dark brown hidden surfaces of the body.

Keywords: Andes, Huancabamba Depression, *Lynchius*, *Oreobates*, Río Marañón

Introduction

The Huancabamba Depression, located in southern Ecuador and northern Peru approximately between 4°S–7°S, is a major structural and physiographic break in the Andes, and includes Abra de Porculla (2145 m a.s.l.), which is the lowest pass between Colombia and southern Chile [1]. The Huancabamba Depression is formed by a complex system of relatively low ridges, basins, and valleys [2] associated with a structural deflection of the Andean faults that corresponds to two major tectonic segments of the Andes [3]. The complex topography of this region is associated with drainages that separate distinct north-south mountain ranges. The Río Marañón, which changes direction from north to east at Huancabamba, forms the northern boundary of the Cordillera Central. Mountains south of the Marañón are drained by rivers that flow both northward into the Marañón (Río Chiriaco and Río Utcubamba), and southward into the Río Huallaga (Río Mayo), isolating mountaintop highland areas such as the Cordillera de Colán [2].

The Cordillera de Colán is a mountain ridge of moderate elevation (< 3700 m a.s.l.), and its herpetofauna is poorly known. An ornithological expedition by Louisiana State University in 1978 conducted the major herpetological survey in the Cordillera de Colán, and resulted in the discovery of several new species of amphibians that were later described by W. E. Duellman and colleagues (e.g., *Gastrotheca abdita* [4], *Hyloxalus spilotogaster* [5], *Pristimantis avicuporum* [2], *P. atrabracus* [2], *P. serendipitus* [2], *P. cuneirostris* [2], *P. metabates* [2], and *Telmatobius colanensis* [6]). In addition, other species independently discovered in the Cordillera de Colán were "*Colostethus*" *poecilonotus* [7], and *Hyloscirtus diabolus* [8]. However, the herpetofauna of these mountains is far from being well surveyed, and the true dimension of its amphibian biodiversity and endemicity remain unknown.

The New World terrestrial-breeding frogs are part of the superfamily Brachycephaloidea, which includes 1169 species (Frost 2020), representing about 33% of all New World frog species and nearly 17% of named species worldwide [9]. Nevertheless, species diversity in this group constantly grows with the discovery of new species when remote regions are surveyed, museum specimens are examined, or cryptic species complexes are phylogenetically analyzed (e.g. Elmer and Cannatella [10]; Ortega-Andrade and Venegas [11]; Motta et al. [12]; Rodríguez and Catenazzi [13]; Páez and Ron [14]; Santa-Cruz et al. [15]).

Brachycephalid frogs show a high degree of evolutionary convergence, especially throughout the Andes [16, 17]. Similar lifestyles related to high-Andean environments, such as grasslands and cloud forests, resulted in the convergent evolution of similar body shapes, posing a challenge for classifications based solely on morphology [16]. Species that occupy Andean highlands and share the "phrynopoid" morphology (i.e. characterized by small round bodies, short extremities, and rounded, non-expanded tips of fingers and toes) were considered part of *Phrynopus*, until the analyses of molecular data rejected the monophyly of the genus, revealing a scenario where high-elevation lineages have independent origins [16, 17, 18]. Most of the Andean Brachycephalid clades are included in the subfamily Holoadeninae, which contains 12 genera (*Barycholos, Bryophryne, Euparkerella, Holoaden, Lynchius, Microkayla, Niceforonia, Noblella, Oreobates, Phrynopus, Psychrophrynella,* and *Qosqophryne*) and 153 species [19], most of them restricted to the Andes from southern Ecuador to Bolivia [9, 12, 18, 20, 21].

We report the discovery of two new species of terrestrial-breeding frogs from Cordillera de Colán, a poorly sampled area in northern Peru. The new species resemble species of the genera *Lynchius*, *Oreobates*, and *Phrynopus* in their external morphology, and we use phylogenetic analyses of nuclear and mitochondrial genes to assess their

phylogenetic relationships, especially regarding Holoadeninae genera. We also combine morphological, molecular, and distribution data to support the recognition of the two species that we name and describe herein.

Materials and methods

Ethics and research

This study was carried out in accordance with the guidelines for use of live amphibians and reptiles in field research [22], compiled by the American Society of Ichthyologists and Herpetologists (ASIH) and the Society for the Study of Amphibians and Reptiles (SSAR). Specimens collected for this study are covered by the following research permits (given by the Ministerio de Agricultura and Servicio Nacional de Áreas Naturales Protegidas por el Estado) that include permanent scientific collection of live specimens: 004–2019–SERNANP–JEF, and 067–2019–MINAGRI–SERFOR–DGGSPFFS.

Morphology

The format for the descriptions follows Motta et al. [12] for *Lynchius*, and Padial et al. [23] for *Oreobates*. The terminology and definition of diagnostic characters follows Duellman and Lehr [24]. Specimens were preserved in 10% formalin and stored in 70% ethanol. We deposited all specimens in the herpetological collection of Centro de Ornitologia y Biodiversidad (CORBIDI), Lima, Peru. Sex was determined by the presence of vocal slits and by direct gonadal inspection. Measurements were taken with digital calipers and rounded to the nearest 0.1 mm. We measured SVL (snout–vent length), TL (tibia length), FL (foot length, distance from proximal margin of inner metatarsal tubercle to tip of Toe IV), HL (head length, obliquely from angle of jaw to tip of snout), HW (head width, at level of angle of jaw), ED (eye diameter, distance between the anterior and posterior

borders of the visible eye), IOD (interorbital distance, distance between the medial edge of the orbits), EW (upper eyelid width, length of the visible eye along the outer edge of eyelid), IND (internarial distance, distance between the inner edges of nares), EN (eye–nostril distance, distance between the anterior corner of orbit and the posterior margin of nares). Fingers and toes are numbered preaxially to postaxially from I to IV and I to V, respectively. Comparative lengths of Toes III and V were determined when both were adpressed against Toe IV; lengths of Fingers I and II were compared when adpressed against each other. We obtained data for comparison of *L. megacephalus* from Sánchez-Nivicela et al. [25]. Examined specimens and are listed in Appendix 1.

DNA extraction, amplification, and sequencing

We sequenced a fragment of the mitochondrial 16S rRNA gene. We extracted DNA from liver samples with a commercial extraction kit (IBI Scientific, Peosta, USA). We followed standard protocols [17] for extraction, amplification, and sequencing of DNA, using the same primers and amplification protocols of von May, Lehr and Rabosky [26]. We used a Proflex thermal cycler (Applied Biosystems), purified PCR products with Exosap-IT (ThermoFisher), and shipped purified samples to MCLAB (South San Francisco, CA, USA) for sequencing.

Phylogenetic analyses

To infer the phylogenetic relationship of the new species, we supplemented our sequences with sequences available on GenBank for species of *Lynchius* (n = 7), *Oreobates* (n = 24), and *Phrynopus* (n = 21). We also included species of all genera of Holoadeninae, except *Qosqophryne*: *Barycholos* (n = 2), *Bryophryne* (n = 1), *Euparkerella* (n = 1), *Holoaden* (n = 1), *Microkayla* (n = 3), *Noblella* (n = 3), *Niceforonia* (n = 6), *Psychrophrynella* (n = 1),

and the *incertae sedis* species "*Eleutherodactylus*" *bilineatus*. We rooted all our analyses with the distant species *Haddadus binotatus*. Our final sample includes 72 species, in addition to three terminals representing the two new species. We chose the mitochondrial 12S rRNA and partial sequence of 16S rRNA genes, as well as nuclear genes recombination-activating gene 1 (RAG1) and tyrosinase precursor (tyr) to perform our analyses. These gene fragments were available to most of our terminals and have been successfully used in several phylogenetic studies of the Brachycephaloidea [9, 17]. Specimen voucher numbers for newly produced sequences and accession numbers for all sequences used in this study are listed in Appendix 2.

We used parsimony and maximum likelihood optimization to generate phylogenetic hypotheses. For parsimony analyses, we partitioned sequences of the genes 12S, 16S, RAG1, and Tyr into fragments of equal length separated by conserved regions with no gaps and few or no nucleotide substitutions (following Motta et al. [12]). The conserved regions were identified after aligning the sequences in MAFFT v.7 (Katoh and Standley [27]; under the G-INS-i strategy) and we used Geneious 11.1.2 to visualize and edit the sequences. This strategy generated putatively homologous fragments where length variation among DNA sequences was only due to insertions and/or deletions of nucleotides, a requisite for tree-alignment in POY [28]. After the removal of gaps implied by MAFFT from sequence fragments, tree-alignment of unaligned sequences was performed under parsimony with equal weights for all classes of transformations using direct optimization [28, 29] and iterative pass optimization [30] algorithms in POY 5.1.1 [31]. We calculated Goodman–Bremer values for each supported clade in TNT using the optimal tree-alignment matrix and the parameters specified in the bremer.run macro. We also calculated parsimony jackknife frequencies from 1000 pseudoreplicates searches using driven searches, gaps treated as fifth state, and removal probability of 0.36 (≈ e–1) [32].

Multiple sequence alignments for maximum-likelihood analyses were performed in MAFFT online v7 using the G-INS-i strategy, which is considered appropriate for alignments that consist of large numbers of sequences [27, 33]. We applied the default transition:transversion cost ratio of 1:2, but changed the gap opening penalty to 1 time substitutions to avoid penalizing insertions and deletions more than we did in the parsimony analysis. The optimal maximum likelihood trees were estimated using 100 runs plus 1000 replicates of bootstrap in RAxML 8.2.10 [34] implemented in CIPRES under the GTR+G model for the combined matrix. Uncorrected p-distances were estimated in Mega v4.0 [34] for the aligned 16S fragment.

Taxonomy

We relied on the observation of morphological features and color patterns, as well as the inferred phylogenetic relationships, to justify our taxonomic conclusions. We considered the combination of these data to delimit species following a general lineage or unified species concept [36, 37].

Results

Phylogenetic relationships

Parsimony tree searches identified an optimal tree of 10,427 steps that was visited 5425 times during 1185 rounds of build + TBR, 23,656 of fusing, and 660 of ratchet. A round of swapping under iterative pass optimization recovered a single tree of 10,383 steps and a tree-alignment of 4202 characters. The optimal MAFFT similarity-alignment used in the maximum likelihood analysis comprises 3535 character columns and maximum likelihood score of the optimal tree was -47,278.957778.

Parsimony and maximum likelihood analyses recovered the genera *Lynchius*, *Oreobates*, and *Phrynopus* as monophyletic, but the relationships among these genera differed between the two analyses (Fig. 1). In parsimony, *Oreobates* and *Phrynopus* formed the sister group of *Lynchius*, while in maximum likelihood, *Phrynopus* was sister to *Lynchius* and *Oreobates*. Results from both analyses supported placement of the two new species in *Lynchius* and *Oreobates*, respectively.

Within *Lynchius*, the relationships among species are similar between parsimony and maximum likelihood analyses. In both analyses, the new species of *Lynchius* is sister to *L. simmonsi* (uncorrected p-distance = 9.8% for 16S), forming a clade that is the sister group of the remaining species of *Lynchius*.

Within *Oreobates*, the two phylogenies differed mostly regarding the position of *O. amarakaeri* and the new species. In parsimony, the new species is sister to *O. lundbergi* (uncorrected p-distance = 14.6% for 16S), forming a clade that is the sister group of the remaining species of *Oreobates* (Fig. 1A); while *Oreobates amarakaeri* is sister to a clade including *O. antrum*, *O. barituensis*, *O. berdemenos*, *O. crepitans*, *O. cruralis*, *O. discoidalis*, *O. heterodactylus*, *O. ibischi*, *O. madidi*, *O. remotes*, and *O. yanucu*. In maximum likelihood, the new species is sister to the clade including *O. antrum*, *O. barituensis*, *O. berdemenos*, *O. crepitans*, *O. cruralis*, *O. discoidalis*, *O. heterodactylus*, *O. ibischi*, *O. madidi*, *O. remotes*, and *O. yanucu*; while *O. amarakaeri* is sister to a clade including *O. choristolemma*, *O. granulosus*, *O. sanctaecrucis*, and *O. sanderi* (Fig. 1B).

The phylogenetic position and morphological distinctiveness of the newly collected specimens support description of the two new species, which we name and diagnose below.

***Lynchius waynehollomonae* sp. nov.**

Figures 2–3

Holotype

CORBIDI 20765, an adult male, from Uriarte (-5.490655, -78.368660; 1981 m), Aramango district, Bagua province, Amazonas department, Peru, collected by P.J. Venegas, L.A. García-Ayachi, J.C. Chávez and A. Marchelie on 13 August, 2019.

Paratype

CORBIDI 20755, 20767, 20770, 20778, adult males, collected with the holotype; CORBIDI 22583, an adult female, from Las Higueras (-5.669842, -78.32336; 1939 m), Cajaruro district, Utcubamba province, Amazonas department, Peru, collected by J. D. Ramos-Sandoval on December, 2019.

Diagnosis

A moderately large *Lynchius* (adult males SVL = 24.9–35.3 mm, n = 5; adult females SVL = 38.3 mm, n = 1) characterized as follows: (1) skin on dorsum of head, body, and limbs covered by conical tubercles heterogeneous in size and subconical and rounded tubercles on flanks; occipital folds absent; middorsal fold thin complete or incomplete when present; dorsolateral fold segmented formed by connected granular warts, when is present; venter smooth to weakly areolate on the last third; groin with minute tubercles; discoidal fold absent and thoracic folds present; (2) tympanic membrane prominent and annulus distinct, its diameter 51–58% of eye diameter; supratympanic fold thin; postrictal tubercles present, subconical; (3) head as wide as long or slightly wider than long (HW/HL = 1.1–1.2); snout round in dorsal and lateral views; canthus rostralis weakly concave in dorsal view; loreal region concave, sloping gradually toward the lips; lips not flared; (4) cranial crests absent; upper eyelid covered by small conical tubercles; (5) dentigerous process of vomers

prominent, oblique, situated posteromedial to choanae, each process bearing 5–7 teeth; (6) males with vocal slits on each side of the tongue and no nuptial pads; (7) fingers long and slender, first finger longer than second; subarticular tubercles prominent, subconical; supernumerary tubercles, prominent, round, smaller than subarticular tubercles; tips of fingers narrowly round; pads absent; circumferential grooves absent, narrow lateral fringes present, and hand webbing absent; (8) ulnar tubercle present, very low and rounded; (9) palmar tubercle prominent, slightly squarish, long as thenar tubercle and two times wider than it; thenar tubercle prominent, elliptical; (10) foot length 48–57% of SVL, narrow lateral fringes present and webbing absent; Toe III longer than Toe V; Toe III usually reaching the middle of second subarticular tubercle of Toe IV, Toe V reaching the proximal border of second subarticular tubercle of Toe IV; tips of toes narrowly rounded, lacking pads and circumferential grooves; (11) inner metatarsal tubercle ovate, prominent; outer metatarsal tubercle smaller, as the half of inner metatarsal tubercle, round, prominent; subarticular tubercles conical, prominent; supernumerary tubercles present, evident; (12) heel and tarsal tubercles present, conical and very small; (13) in life, dorsum rufous with dark brown markings; flanks brown with dark brown irregular stripes or blotches and a suprainguinal blotch; axilla, groins, and posterior surface of thighs brown without pattern; venter pale brown on the throat and chest with irregular brownish cream blotches and/or whitish irregular flecks; belly yellowish cream or dirty cream with pale brown reticulations; thighs yellowish cream or brownish cream with pale irregular flecks; shanks brown; tarsus brown with creamy brown flecks; iris black sprinkled with turquoise minute flecks and a golden ring around pupil; in preservative, dorsum grayish brown with dark brown markings and venter pale brown on throat with cream irregular flecks; belly and forelimbs cream with pale brown reticulations on belly; thighs creamy tan forward and brown back; shanks, tarsus and feet dark brown.

Comparison with other species

Among the seven known species of *Lynchius,* only *L. megacephalus* and *L. simmonsi* possess a dorsum with conical tubercles as *L. wayneholl*omonae. However, *L. megacephalus* can be readily distinguished from *L. wayneholl*omonae (characters in parenthesis) by having: dermal ridges on dorsum (absent), cranial crest (absent), finger I and II equal in size (finger I longer than II), palmar supernumerary tubercles low (prominent), plantar supernumerary tubercles absent (present), subarticular tubercles round (subconical), and light-blue sclera (gray sclera). Moreover, *L. wayneholl*omonae possess dorsolateral fold, absent in *L. megacephalus*. The new species differs from *L. simmonsi* (characters in parenthesis) by having: conical tubercles on dorsal surface heterogenous in size (uniformly sized), palmar tubercle not bifid (bifid), suprainguinal blotch (absent), and in life, venter pale brown on the throat with irregular brownish cream blotches or whitish irregular flecks and belly yellowish cream or dirty cream with pale brown reticulations (brown with small cream flecks).

Description of holotype

Head as wide as long (HW/HL 1.1); snout rounded in dorsal view and short, rounded in lateral profile; nostrils not protuberant, oriented laterally; canthus rostralis weakly concave in dorsal view, round in frontal profile; loreal region concave; lips not flared; upper eyelid with small conical tubercles of similar size; cranial crests absent. Supratympanic fold distinct; tympanic membrane prominent and tympanic annulus distinct; tympanic membrane nearly round, its length more than half of eye length; postrictal tubercles present, subconical. Choanae not concealed by palatal shelf of the maxillary arch when roof of mouth is viewed from below; choanae small, round, separated by a distance equal to six times the diameter of choana; dentigerous process of the vomers prominent, oblique,

situated posteromedial to choanae (posterior margin at level of choanae), their width approximately two times diameter of choanae, bearing five or seven vomerine teeth; vocal slits present. Skin of dorsal surfaces shagreen, sprinkled with conical tubercles on dorsum; flanks covered by subconical and conical tubercles; ventral surfaces smooth with the third posterior part weakly areolate; thighs areolate posteriorly in ventral view; occipital fold absent; middorsum folds present, thin; dorsolateral folds present, formed by connected granular warts, fragmented; discoidal fold absent; thoracic fold present. Ulnar tubercle present, small and rounded; palmar tubercle prominent, slightly squarish, two times wider than thenar tubercle; thenar tubercle prominent, elliptical; supernumerary tubercles prominent, rounded; subarticular tubercles subconical, slightly larger than supernumerary tubercles; finger tips narrowly rounded; pads and circumferential grooves absent; fingers with narrow lateral fringes and lacking webbing; nuptial pads absent; relative length of fingers: I > II < III > IV (Fig. 3C). Foot length 50% of SVL; heel and tarsus bearing small and low tubercles, lacking folds; inner metatarsal tubercle rounded, prominent, two times larger than outer metatarsal tubercle; outer metatarsal tubercle round, prominent; supernumerary tubercles present, weakly defined proximally and prominent distally; subarticular tubercles prominent, larger than supernumerary, subconical; toes with narrow lateral fringes and lacking webbing; toe tips narrowly rounded; pads and circumferential grooves absent; relative length of toes: I < II < III > V < IV (Fig. 3D); Toe V reaching proximal margin of second subarticular tubercle of Toe IV, and Toe III reaching to its middle.

Measurements of the holotype (in mm). SVL, 27.3; TL, 13.1; FL, 13.7; HL, 10.2; HW, 11.1; ED, 3.5; TY, 2.0; IOD, 2.8; EW 2.2; IND, 2.9; E–N, 3.2.

Color of holotype in life (Fig. 2 A-C). Dorsal surface rufous with brown blotches, irregular flecks and top of head brown with a brown interorbital bar with the anterior

margin rufous; flanks brown with a grayish hue, dark brown irregular stripes and blotches, including a suprainguinal blotch; ventrolateral region with yellowish cream blotches; sides of head brown suffused with whitish-cream, and bearing dark brown labial bars with creamy white margins and a dark brown blotch in the loreal region; supratympanic fold dark brown posteriorly; tympanic membrane brown in the middle with a paler ring; jaw brown with whitish speckles; forelimbs and hindlimbs with dark brown transversal bars and tarsus brownish cream with dark brown bars; axilla, groins and posterior surfaces of thighs uniformly brown. Ventral surface brown on the throat and chest with irregular brownish cream blotches and irregular whitish flecks; belly yellowish cream with pale brown reticulations; thighs yellowish cream with many paler irregular flecks; shanks brown; tarsus brown with creamy brown flecks; palms and soles brown. Iris black sprinkled with turquoise minute flecks and a golden ring around pupil.

Color of holotype in ethanol 70% (Fig. 3). Dorsal surface grayish brown with all its markings darker than the background; limbs brownish cream with dark brown bars. Ventral surface pale brown with creamy tan irregular flecks and speckles; belly cream with pale brown reticulations; forelimbs cream with brown speckles; thighs creamy tan forward and brown back; shanks, tarsus and feet dark brown.

Intraspecific variation

The four males and one female of the type series of *Lynchius* possess sexual dimorphism in size (Table 1), and males possess vocal slits. Dorsal background coloration and markings are similar in all specimens but the dorsum can be rufous or brown (CORBIDI 20778; Fig. 2 D-F).

Distribution and natural history observation

Lynchius wayneholllomonae is only known from two localities in the Río Utcubamba basin, northern extreme of Cordillera de Colán at elevations from 1,977 to 2,006 m a.s.l. (Amazonas Department, Peru) (Fig. 4). All specimens were collected by night in zones of abundant leaf litter on a mountain slope covered by humid montane forest [type of vegetation following Duellman and Pramuk [2]] near a cattle ranching pasture. The two known localities of *L. wayneholllomonae* lay in the Peruvian Yungas ecoregion (sensu Olson et al. [38]). Other species anurans collected with *L. wayneholllomonae* included *Noblella sp.*, *Pristimantis avicuporum*, *P. galdi, P. serendipitus*, and *Pristimantis* sp.

Etymology

The specific epithet *wayneholllomonae* is a noun in the genitive case and is a matronym for Wayne Hollomon Price (1943–2011), an American artist, licensed professional counselor and philanthropist, who was passionate about protecting the Earth's natural environments and wildlife. During her lifetime, Hollomon Price generously supported the protection and preservation of the rainforest, the natural environment, trees and endangered species, and she founded the Hollomon Price Foundation 12 years before her death. Since then, the foundation has continued Hollomon Price's work and legacy through its ongoing support of organizations focused on preserving people, biodiversity and ecosystems upon which all life depends, in ways that advance the lasting welfare of present and future generations. The Hollomon Price Foundation grew out of her love for the rainforest and its inhabitants, and the name *wayneholllomonae* honors her enduring legacy as a champion of protecting the rainforest.

***Oreobates colanensis* sp. nov.**

Figures 5–6

Holotype

CORBIDI 21191, an adult male, from Lechucita (-5.631091, -78.256952; 2608 m), Cajaruro district, Utcubamba province, Amazonas department, Peru, collected by J.R. Ormeño, P.J. Venegas, L.A. García-Ayachi, J.C. Chávez, S. Bullard and A. Marchelie on 23 November, 2019.

Paratype

CORBIDI 21295-96, adult males, from Lechucita (-5.630999, -78.256935; 2611 m), Cajaruro district, Utcubamba province, Amazonas department, Peru, collected by J.R Ormeño, S. Bullard, P.J. Venegas, L.A. García-Ayachi, J.C. Chávez and A. Marchelie on 2 December, 2019.

Diagnosis

A small species of *Oreobates* (SVL of adult male 21.9–22.5 mm, n = 3; adult females SVL unknow) characterized as follows: (1) skin of dorsum shagreen with many conical turbercles, flanks with many subconical tubercles on dorsolateral region but becoming rounded toward to ventrolateral region; occipital \ /-shaped fold present; dorsolateral fold present, formed by connected granular warts; venter smooth; posterior surfaces of thighs areolate, groin smooth; discoidal fold absent; postrictal tubercles present, rounded; (2) tympanic membrane and annulus distinct, large, about 36%–43% of length of eye; supratympanic fold present, ill-defined; (3) head as wide as long or slightly wider than long (HW/HL = 1.1–1.2); snout short, round in dorsal view and in lateral view; canthus rostralis concave in dorsal view, round in profile; (4) cranial crests absent; upper eyelid with scattered round tubercles; (5) dentigerous process of the vomers large, prominent, oval in

shape, situated posteromedial to choanae (posterior margin at level of choanae), their width about 1.2 times diameter of choanae, bearing 4 to 7 vomerine teeth; (6) males without vocal slits and vocal sacs; (7) hands with long and slender fingers, first finger barely longer than second; subarticular tubercles large and prominent, conical; supernumerary tubercles prominent, round, smaller than subarticular tubercles; fingertips round, barely enlarged, lacking circumferential grooves; lateral fringes and keels on fingers absent; (8) ulnar tubercles absent; (9) heel and tarsus bearing very low conical tubercles; (10) inner metatarsal tubercle ovate, prominent; outer metatarsal tubercle smaller than the inner metatarsal tubercle, subconical, prominent; subarticular tubercles, conical, prominent, supernumerary tubercles smaller than subarticular tubercles, prominent, round; (11) toes long and slender (foot length 48%–49% SVL), lateral fringes and webbing absent; toe V reaching to the middle of second subarticular tubercle of Toe IV, and Toe III reaching to its distal margin; tips of toes slightly enlarged, rounded, circumferential groove absent; (12) axillary glands absent; (13) in life, dorsum dark brown or reddish brown with brown flanks, ventrolateral region grayish brown with minute white flecks; dorsal markings not contrasted, occipital fold can be reddish brown; tiny whitish labial flecks or blotches present; axilla, groin, and hidden surfaces of hindlimbs with yellowish cream or white blotches; ventrally, throat brown with a reddish patch covering the middle, chest and ventral surface of forelimbs red, belly dark brown suffused with red with many white irregular flecks and small blotches, thighs red, shanks dark brown with cream blotches; iris gold with a brown stripe on the middle. In preservative, dorsum grayish brown; occipital and dorsolateral folds paler than the background color; blotches on axilla, groin, anterior and posterior surface of thighs white; ventrally, dark brown with dirty cream blotches and white flecks.

Comparison with other species

Among the 25 species of *Oreobates* currently known, *O. colanensis* can be readily distinguished by the absence of axillary and inguinal glands, and by the presence of white or cream blotches on the dark brown hidden surfaces of body as axilla, groins, anterior and posterior surfaces of thighs, and shanks. *Oreobates colanensis* also possess distinct dorsolateral folds, which are only present in *O. ayacucho, O. gemcare*, and *O. lehri*. However, *O. gemcare* and *O. lehri* differ by lacking conical tubercles on dorsum, while *O. ayacucho* differs by having finger I shorter than II (finger I barely or equal in size to finger II in *O. colanensis*). Furthermore, *O. gemcare* and *O. lehri* lack blotches or spots in the axillary region and groins (present in *O. colanensis*).

Oreobates colanensis and *O. lundbergi* are the only species in the genus that lack vocal slits, but *O. lunbergi* has smooth dorsum (bearing conical tubercles in *O. colanensis*) and lacks dorsolateral folds (present).

Description of holotype

Head as wide as (HW/HL 1.1); snout rounded in dorsal view and short, rounded in lateral profile; nostrils not protuberant, oriented laterally; canthus rostralis concave in dorsal view, round in frontal profile; loreal region concave; lips not flared; upper eyelid with few small granules; cranial crests absent. Supratympanic fold diffuse; tympanic membrane and annulus prominent; tympanic membrane nearly round, its length less than half of eye length; postrictal tubercles present, round. Choanae not concealed by palatal shelf of the maxillary arch when roof of mouth is viewed from below; choanae small, round, separated by a distance equal to five times the diameter of choana; dentigerous process of the vomers prominent, oblique, situated posteromedial to choanae (posterior margin at level of choanae), their width approximately one and a quarter times the diameter of choanae,

bearing 5 or 6 vomerine teeth. Skin on dorsum shagreen, with many low subconical tubercles, especially on the posterior half; flanks covered by small rounded tubercles; ventral surfaces smooth; thighs tuberculate posteriorly in ventral view; occipital fold \ /-shaped; middorsum bearing one thin fold, slightly visible; dorsolateral folds present, evident, fragmented; discoidal fold absent; thoracic fold present, weakly defined. Ulnar tubercle absent; palmar tubercle rounded, prominent, slightly larger than thenar tubercle; thenar tubercle prominent, elliptical; supernumerary tubercles prominent; subarticular tubercles rounded, larger than supernumerary tubercles; finger tips narrowly rounded; pads absent, circumferential grooves absent; fingers lacking lateral fringes and webbing; relative length of fingers: I > II < III > IV (Fig. 6C). Foot length 48% of SVL; heel and tarsus bearing very low conical tubercles, tarsus lacking folds; inner metatarsal tubercle oval, prominent, a bit larger than outer metatarsal tubercle; outer metatarsal tubercle round; supernumerary tubercles present, distinct; subarticular tubercles prominent, subconical; toes lacking lateral fringes and webbing; toe tips rounded, barely expanded; pads and circumferential grooves absent; relative length of toes: I < II < III > V < IV (Fig. 6D); Toe V reaching to the middle of second subarticular tubercle of Toe IV, and Toe III reaching to its distal margin.

Measurements of the holotype (in mm): SVL, 21.9; TL, 10.8; FL, 10.6; HL, 7.6; HW, 8.4; ED, 2.6; TY, 1.1; IOD, 2.2; EW 1.8; IND, 2.5; E–N, 2.1.

Color of holotype in life (Fig. 5 A-D). Dorsal surface dark brown; rostrum with a white vertical stripe in the middle; top of snout paler than dorsum; canthal stripe broad, darker than background; labials bars broad, darker than background with thin white borders; jaw dark brown with some white speckles; supratympanic fold darker than background; occipital fold reddish brown; dorsolateral folds slightly paler than background; flanks grayish brown with white flecks on the ventrolateral region; axillar

region, groin, and anterior and posterior surface of thighs with cream blotches; forearm reddish brown; tibia with darker bars; tarsus brownish cream with dark brown bars; dorsal surface of feet and toes pale brown. Ventrally, throat brown with a reddish patch covering the middle, chest and ventral surface of forelimbs; belly dark brown suffused with red with many white flecks, thighs red, shanks dark brown with cream blotches, palms and soles dark brown. Iris gold with a brown stripe in the middle.

Color of holotype in ethanol 70% (Fig. 6). Dorsal surface grayish brown; top of head turn paler than the background, head markings darker than the dorsum as in life, occipital folds turn brownish cream and dorsolateral folds grayish brown; flanks dark brown, hidden surfaces brown and the blotches turn white; forearms turn brownish cream, tarsus and feet turn dirty cream with dark brown bars, and toes dirty cream. Ventral surface dark brown but reddish colorations turn creamy tan, flecks and blotches remain white, and shanks dark brown with white blotches.

Intraspecific variation

All type specimens have similar sizes and proportions (Table 2). Coloration is identical in all specimens but specimen CORBIDI 21295 has a reddish brown dorsum (Fig 5 E-F).

Distribution and natural history

Oreobates colanensis is only known from the Refugio Lechucita, in the eastern slope of Cordillera de Colán, in the Río Utcubamba basin at an elevation of 2,608 m a.s.l. (Amazonas Department, Peru) (Fig. 7). The Refugio Lechucita lies in the Peruvian Yungas ecoregion (sensu Olson et al. [38]). All individuals were collected by night in the leaf litter of a slope covered by primary humid montane forest [types of vegetation following Duellman and Pramuk [2]]. The other syntopic species of anurans were *Noblella* sp., *P.*

corrugatus, *P.* sp., and *Rhinella arborescandens*.

Etymology

The specific epithet "*colanensis*" refers to the mountains where we discovered the species, the Cordillera de Colán.

Discussion

The clade containing *Lynchius*, *Oreobates*, and *Phrynopus* represents an interesting radiation of frogs in both their morphology and distribution. The within-genus morphological diversity also occurs across genera. For example, in their external morphology, the high Andean species *O. ayacucho* and *O. pereger* are more similar to species of *Phrynopus* and Andean species of *Lynchius* than to their *Oreobates* relatives, and were initially considered to be members of *Phrynopus* (see Lynch [39]; Cannatella [40]; Lehr [41]). Similarly, *Lynchius simmonsi* from the cloud forests on the easternmost ridges of the Amazonian Andes was initially considered to be an *Oreobates*, due to its similarity to species of *Oreobates* from montane forests and the Amazon lowlands [42]. Interestingly, when we collected specimens of *Lynchius wayneholllomonae*, we believed they represented a new species of *Oreobates*, since it also resembles *Oreobates* species from montane forests and the Amazon lowlands. Instead, the new species is sister to *L. simmonsi*, and this clade supports the hypothesis of convergent evolution along elevation gradients in *Lynchius*, *Oreobates*, and *Phrynopus* [12].

The two new species improves our understanding on the distribution of *Lynchius* and *Oreobates* in the Andes. The Huancabamba Depression has long been considered as a major biogeographic barrier to the north-south dispersal of some Andean organisms [43, 44, 45] and a migration corridor for others [46]. The Huancabamba Depression may have

4693 influenced the radiation of several Andean genera of lizards, such as *Andinosaura,*
4694 *Macropholidus, Petracola, Pholidobolus, Riama*, and *Stenocercus* [43, 45, 48, 49, 50, 51,
4695 52, 53]. For amphibians, the Huancabamba Depression is the southernmost limit for the
4696 radiation of *Lynchius* [12] and may be the northernmost limit for *Phrynopus* (see Chávez et
4697 al. [54]; Venegas et al. [21]). In addition, with the discovery of *O. colanensis* the
4698 Huancabamba Depression is now the northernmost limit for Andean species of *Oreobates*.
4699 According with Quintana et al. [46], the Huancabamba area was at sea level by the Eocene,
4700 while other portions of Andes were already uplifted, and it was not until the Middle
4701 Miocene that the Andes emerged to form the Huancabamba Depression. With most species
4702 of *Lynchius* restricted to the Huancabamba Depression, it is plausible that the rise of the
4703 Andes along the Huancabamba Depression influenced the evolution and diversification of
4704 this genus, probably acting as a center of origin and diversification.

4705 The relatively low-elevation mountains at the Huancabamba Depression created a
4706 mixture of montane environments [2], which terrestrial-breeding frogs such as *Lynchius*
4707 could easily colonize, promoting its diversification. With the exception of *L. simmonsi*, a
4708 species restricted to the Cordillera del Condor in Ecuador, species of *Lynchius* reach
4709 elevations above 2000 m, where bush-like elfin forests and paramos gradually replace
4710 montane forests [12]. *Lynchius wayneholllomonae* is the first species of *Lynchius* found
4711 south of the Huancabamba Depression and occurring exclusively in the Peruvian Yungas
4712 (see Olson et al. [38]).

4713 Species of *Oreobates* are broadly distributed, and occur from the dry Atlantic
4714 forests in eastern Brazil, across the Cerrado of central Brazil and the western Amazonian
4715 lowland forests, as well as the Andean montane forests from northern Argentina to Central
4716 Peru [23]. *Oreobates quixensis* and *O. saxatilis* are the only species known to occur in
4717 northern Peru, along the Amazonian lowlands and Andean hills up to 1000 m (see Padial *et*

al. [23]). Only five species of *Oreobates* possess an Andean distribution mostly above 2000 m (*O. ayacucho*, *O. gemcare*, *O. lehri*, *O. lundbergi*, and *O. pereger*, and they are restricted to a region between 10º and 14º of latitude of the Amazonian versant of the Andes in the Cordillera Oriental of Peru [23, 24]. *Oreobates colanensis* represents the northernmost high-Andean species of *Oreobates*, extending the distribution of the genus in the high Andes by more than 600 km north (Fig. 7).

Our knowledge of species diversity for the genera *Lynchius*, *Oreobates*, and *Phrynopus* has greatly improved as a result of recent systematic researches focusing on this group [12, 17, 21, 22, 25]. More than one third of the 69 species of this clade were described in the last decade [19], and many more are awaiting to be named [12, 23; 25] However, the diversity of species is still underestimated, and many areas of the Andes and the adjacent lowlands suitable for the existence of species of *Lynchius*, *Oreobates*, and *Phrynopus* remain to be surveyed. Future surveys in other poorly sampled areas in the cordilleras of Peru will certainly reveal further new species in this clade.

Acknowledgments

We are especially grateful with the Servicio Nacional de Áreas Naturales Protegidas por el Estado (SERNANP), especially with the professional personnel of the Santuario Nacional Cordillera de Colán: Christian Olivera, Johnny D. Ramos, Gerlys Fernandez, and Abner García for its logistic support. We thank A. Marchelie for his photographs of Bosque Quemado. We also thank Axel Marchelie and Juan C. Chávez for the company and field assistance. APM thanks São Paulo Research Foundation (FAPESP) for her PhD. scholarship (grant #2017/08488-3).

Author contribution

PJV, LAGA, AC, and APM conceived and designed the study. PJV wrote the manuscript. AC, APM and LAGA reviewed and improved the manuscript. LAGA gathered morphological data. JROB and SB collected the type series and field data of *Oreobates colanensis*. APM made the molecular analysis and phylogenetic trees.

Disclosure statement

The authors have no conflicts of interest to disclose.

Funding

This research was funded by the Critical Ecosystem Partnership Fund (CEPF) (project number CEPF–109938) through the Fondo de Promoción de las Áreas Naturales Protegidas del Perú (PROFONANPE), and the Global Genome Initiative (GGBN-GGI).

References

1. Peñaherrera del Aguila C. Atlas del Perú. Lima: Instituto Geográfico Nacional; 1989.
2. Duellman WE, Pramuk JB. Frogs of the genus *Eleutherodactylus* (Anura: Leptodactylidae) in the Andes of Northern Peru. Natural History Museum The University of Kansas. 1999 30 July;13:1–78. DOI: https://doi.org/10.5962/bhl.title.16169.
3. Sillitoe RH. Tectonic segmentation of the Andes: implications for magmatism and metallogeny. Nature. 1974;250(5467):542–545. DOI: https://doi.org/10.1038/250542a0.
4. Duellman WE. Two new species of marsupial frogs (Anura: Hylidae) from Peru. Copeia. 1987:903–909. DOI: https://doi.org/10.2307/1445553.
5. Duellman WE. Frogs of the genus *Colostethus* (Anura; Dendrobatidae) in the Andes of northern Peru. 2004. DOI: https://doi.org/10.5962/bhl.title.8467.
6. Wiens JJ. Systematics of the Leptodactylid Frog genus *Telmatobius* in the Andes of northern Peru. Occas Pap of the Mus of Nat Hist, The Univ of Kans, Lawrence, Kans. 1993 24 November;162:1–76.
7. Rivero JA. New *Colostethus* (Amphibia, Dendrobatidae) from South America. Breviora. 1991;493:1–28.
8. Rivera–Correa M, Garcia–Burneo K, Grant T. A new Red-Eyed of stream treefrog of *Hyloscirtus* (Anura: Hylidae) from Peru, with comments on the taxonomy of the genus. Zootaxa. 2016 Jan 4;4061(1):29–40. DOI: https://doi.org/10.11646/zootaxa.4061.1.3. PubMed PMID: 27395477.
9. Padial JM, Grant T, Frost DR. Molecular systematics of terraranas (Anura: Brachycephaloidea) with an assessment of the effects of alignment and optimality criteria. Zootaxa. 2014;3825(1):1–132. DOI: https://doi.org/10.11646/zootaxa.3825.1.1.
10. Elmer KR, Cannatella DC. Three new species of leaflitter frogs from the upper Amazon forests: cryptic diversity within *Pristimantis* "*ockendeni*" (Anura: Strabomantidae) in Ecuador. Zootaxa. 2008;1784(1):11–38. DOI: https://doi.org/10.11646/zootaxa.1784.1.2.
11. Ortega-Andrade HM, Venegas PJ. A new synonym for *Pristimantis luscombei* (Duellman and Mendelson 1995) and the description of a new species of

Pristimantis from the upper Amazon basin (Amphibia: Craugastoridae). Zootaxa. 2014;3895(1):31–57. DOI: https://doi.org/10.11646/zootaxa.3895.1.2.

12. Motta AP, Chaparro JC, Pombal JJP, et al. Molecular phylogenetics and taxonomy of the Andean genus *Lynchius* Hedges, Duellman, and Heinicke 2008 (Anura: Craugastoridae). Herpetological Monographs. 2016;30(1):119–142. DOI: https://doi.org/10.1655/HERPMONOGRAPHS-D-16-00002.

13. Rodríguez LO, Catenazzi A. Four new species of terrestrial-breeding frogs of the genus *Phrynopus* (Anura: Terrarana: Craugastoridae) from Río Abiseo National Park, Peru. Zootaxa. 2017;4273(3):381–406. DOI: https://doi.org/10.11646/zootaxa.4273.3.4.

14. Páez NB, Ron SR. Systematics of *Huicundomantis*, a new subgenus of *Pristimantis* (Anura, Strabomantidae) with extraordinary cryptic diversity and eleven new species. 2019;868. DOI: https://doi.org/10.3897/zookeys.868.26766.

15. Santa-Cruz R, von May R, Catenazzi A, et al. A new species of terrestrial-breeding frog (Amphibia, Strabomantidae, *Noblella*) from the upper Madre de Dios watershed, Amazonian Andes and lowlands of southern Peru. Diversity. 2019;11(9):145.

16. De la Riva I. Unexpected beta-diversity radiations in highland clades of Andean Terraranae frogs. Neotropical Diversification: Patterns and Processes: Springer; 2020. p. 741–764.

17. Hedges SB, Duellman WE, Heinicke MP. New World direct-developing frogs (Anura: Terrarana): molecular phylogeny, classification, biogeography, and conservation. Zootaxa. 2008;1737(1):1–182. DOI: https://doi.org/10.11646/zootaxa.1737.1.1.

18. De la Riva I. Bolivian frogs of the genus *Phrynopus*, with the description of twelve new species (Anura: Brachycephalidae). Herpetological Monographs. 2007;21(1):241–277. DOI: https://doi.org/10.1655/07-011.1.

19. Frost DR. Amphibian Species of the World: an Online Reference. Version 6.1: American Museum of Natural History, New York, USA.; 2020 [cited 2020 10 July]. Available from: https://amphibiansoftheworld.amnh.org/index.php

20. Catenazzi A, Mamani L, Lehr E, et al. A new genus of terrestrial-breeding frogs (Holoadeninae, Strabomantidae, Terrarana) from southern Peru. Diversity. 2020;12(5):184. DOI: https://doi.org/10.3390/d12050184.

21. Venegas PJ, Barboza AC, Riva I, et al. A new species of *Phrynopus* from the northeastern Andes of Peru, its phylogenetic position, and notes on the relationships of Holoadeninae (Anura: Craugastoridae). Zootaxa. 2018 Jul 19;4446(4):501–524. DOI: https://doi.org/10.11646/zootaxa.4446.4.5. PubMed PMID: 30313872.

22. Beaupre SJ, Jacobson ER, Lillywhite HB, et al. Guidelines for use of live amphibians and reptiles in field and laboratory research. Second ed: The American Society of Ichthyologists and Herpetologists; 2004. p. 1–43.

23. Padial JM, Chaparro JC, Castroviejo-Fisher S, et al. A revision of species diversity in the Neotropical genus *Oreobates* (Anura Strabomantidae), with the description of three new species from the Amazonian slopes of the Andes. American Museum Novitates. 2012; 3752:55. DOI: https://doi.org/10.1206/3752.2.

24. Duellman WE, Lehr E. Terrestrial breeding frogs (Strabomantidae) in Peru. Natur und Tier - Verlag GmbH; 2009.

25. Sanchez-Nivicela JC, Urgiles VL, Navarrete MJ, et al. A bizarre new species of *Lynchius* (Amphibia, Anura, Strabomantidae) from the Andes of Ecuador and first report of *Lynchius parkeri* in Ecuador. Zootaxa. 2019;4567(1):1–24. DOI: https://doi.org/10.11646/zootaxa.4567.1.1.

26. von May R, Lehr E, Rabosky DL. Evolutionary radiation of earless frogs in the Andes: molecular phylogenetics and habitat shifts in high-elevation terrestrial breeding frogs. PeerJ. 2018;6:e4313. DOI: https://doi.org/10.7717/peerj.4313.

27. Katoh K, Standley DM. MAFFT multiple sequence alignment software version 7: improvements in performance and usability. Molecular biology and evolution. 2013;30(4):772–780. DOI: https://doi.org/10.1093/molbev/mst010.

28. Wheeler WC, Aagesen L, Arango CP, et al. Dynamic homology and phylogenetic systematics: a unified approach using POY. American Museum of Natural History; 2006.

29. Wheeler W. Optimization alignment: the end of multiple sequence alignment in phylogenetics? Cladistics. 1996;12(1):1–9. DOI: https://doi.org/10.1111/j.1096-0031.1996.tb00189.x.

30. Wheeler WC. Iterative pass optimization of sequence data. Cladistics. 2003;19(3):254-260. DOI: https://doi.org/10.1111/j.1096-0031.2003.tb00368.x.

31. Varón A, Vinh LS, Wheeler WC. POY version 4: phylogenetic analysis using dynamic homologies. Cladistics. 2010;26(1):72–85. DOI: https://doi.org/10.1111/j.1096-0031.2009.00282.x.

32. Farris JS, Albert VA, Källersjö M, et al. Parsimony jackknifing outperforms neighbor-joining. Cladistics. 1996;12(2):99–124. DOI: https://doi.org/10.1111/j.1096-0031.1996.tb00196.x.

33. Katoh K, Kuma K-i, Toh H, et al. MAFFT version 5: improvement in accuracy of multiple sequence alignment. Nucleic acids research. 2005;33(2):511–518. DOI: https://doi.org/10.1093/nar/gki198.

34. Stamatakis A. RAxML version 8: a tool for phylogenetic analysis and post-analysis of large phylogenies. Bioinformatics. 2014;30(9):1312–1313. DOI: https://doi.org/10.1093/bioinformatics/btu033.

35. Tamura K, Dudley J, Nei M, et al. MEGA4: molecular evolutionary genetics analysis (MEGA) software version 4.0. Molecular biology and evolution. 2007;24(8):1596–1599. DOI: https://doi.org/10.1093/molbev/msm092.

36. de Queiroz K. The general lineage concept of species, species criteria, and the process of speciation. In: Howard DJ, Berlocher SH, editors. Endless Forms: Species and Speciation: Oxford University Press; 1998. p. 57–75.

37. de Queiroz K. Species concepts and species delimitation. Syst Biol. 2007 Dec;56(6):879–886. DOI: https://doi.org/10.1080/10635150701701083. PubMed PMID: 18027281.

38. Olson DM, Dinerstein E, Wikramanayake ED, et al. Terrestrial ecoregions of the world: A new map of life on earth. BioScience. 2001;51(11):933-938. DOI: https://doi.org/10.1641/0006-3568(2001)051[0933:TEOTWA]2.0.CO;2.

39. Lynch JD. A review of the Andean leptodactylid frog genus *Phrynopus*. Occas Pap of the Mus of Nat Hist, The Univ of Kans, Lawrence, Kans. 1975;35, 1–51.

40. Cannatella DC. Two new species of the leptodactylid frog genus *Phrynopus*, with comments on the phylogeny of the genus. Occas Pap of the Mus of Nat Hist, The Univ of Kans, Lawrence, Kans. 1984;113, 1–16.

41. Lehr E. A new species of *Phrynopus* from Departamento Cusco, southern Peru (Anura: Brachycephalidae). Zootaxa. 2007;1618:61–68. DOI: https://doi.org/10.11646/zootaxa.1618.1.3.

42. Caramaschi U, Canedo C. Reassessment of the taxonomic status of the genera *Ischnocnema* Reinhardt and Lütken, 1862 and *Oreobates* Jiménez-de-la-Espada, 1872, with notes on the synonymy of *Leiuperus verrucosus* Reinhardt and Lütken, 1862 (Anura: Leptodactylidae). Zootaxa. 2006;1116(1):43–54. DOI: https://doi.org/10.11646/zootaxa.1116.1.3.

43. Cadle JE. Systematics of lizards of the genus *Stenocercus* (Iguania: Tropiduridae) from Northern Perú: New species and comments on relationships and distribution patterns. Proc of the Acad of Nat Sci of Phila. 1991;143:1–96. DOI: http://www.jstor.org/stable/4064994

44. Duellman WE. The South American Herpetofauna: Its Origin, Evolution, and Dispersal. Museum of Natural History The University of Kansas. 1979;Monograph 7. DOI: https://doi.org/10.5962/bhl.title.3207.

45. Vuilleumier F. Pleistocene speciation in birds living in the high Andes. Nature. 1969;223(5211):1179–1180. DOI: https://doi.org/10.1038/2231179a0.

46. Quintana C, Pennington RT, Ulloa CU, et al. Biogeographic barriers in the Andes: Is the Amotape—Huancabamba zone a dispersal barrier for dry forest plants? 1. Annals of the Missouri Botanical Garden. 2017;102(3):542–550. DOI: https://doi.org/10.3417/D-17-00003A.

47. Doan TM. A south-to-north biogeographic hypothesis for Andean speciation: evidence from the lizard genus *Proctoporus* (Reptilia, Gymnophthalmidae). Journal of Biogeography. 2003;30(3):361–374. DOI: https://doi.org/10.1046/j.1365-2699.2003.00833.x.

48. Doan TM, Castoe TA. Phylogenetic taxonomy of the Cercosaurini (Squamata: Gymnophthalmidae), with new genera for species of *Neusticurus* and *Proctoporus*. Zoological Journal of the Linnean Society. 2005;143(3):405–416. DOI: https://doi.org/10.1111/j.1096-3642.2005.00145.x.

49. Kizirian D, Bayefsky-Anand S, Eriksson A, et al. A new *Petracola* and re-description of *P. ventrimaculatus* (Squamata: Gymnophthalmidae). Zootaxa. 2008;1700(1):53–62. DOI: https://doi.org/10.11646/zootaxa.1700.1.4.

50. Sánchez-Pacheco SJ, Nunes PMS, Marques-Souza S, et al. Formal recognition of the species of *Oreosaurus* (Reptilia, Squamata, Gymnophthalmidae) from the Sierra Nevada de Santa Marta, Colombia. ZooKeys. 2017 (691):149. DOI: https://doi.org/10.3897/zookeys.691.13595.

51. Torres–Carvajal O. Phylogeny and biogeography of a large radiation of Andean lizards (Iguania, *Stenocercus*). Zool Scr. 2007;36(4):311–326. DOI: https://doi.org/10.1111/j.1463-6409.2006.00284.x.

52. Torres-Carvajal O, Mafla-Endara P. Evolutionary history of Andean *Pholidobolus* and *Macropholidus* (Squamata: Gymnophthalmidae) lizards. Molecular

Phylogenetics and Evolution. 2013;68(2):212–217. DOI: https://doi.org/10.1016/j.ympev.2013.03.013.

53. Torres-Carvajal O, Venegas PJ, Sales Nunes PM. Description and phylogeny of a New species of Andean lizard (Gymnophthalmidae: Cercosaurinae) from the Huancabamba Depression. South American Journal of Herpetology. 2020;18(1). DOI: https://doi.org/10.2994/SAJH-D-18-00069.1

54. Chávez G, Santa-Cruz R, Rodríguez D, et al. Two new species of frogs of the genus *Phrynopus* (Anura: Terrarana: Craugastoridae) from the Peruvian Andes. Amphibian and Reptile Conservation. 2015;9(1):15–25.

4931 **Tables**

4932 **Table 1.** Variation of measurements (in mm) and proportions of the type series of *Lynchius*
4933 *waynehollomonae*. See text for abbreviations.

	Males (n = 5)	Female CORBIDI 22583
SVL	24.9–27.8 (26.6 ± 1.17)	35.3
TL	13.1–14.7 (13.6 ± 0.64)	16.6
FL	13.7–15.1 (14.3 ± 0.58)	17.0
HL	8.9–10.2 (9.6 ± 0.53)	11.8
HW	10.3–11.2 (10.8 ± 0.38)	13.6
ED	3.2–3.6 (3.4 ± 0.12)	4.1
IOD	2.4–2.8 (2.6 ± 0.17)	3.5
EW	2.2–2.3 (2.2 ± 0.05)	2.9
IND	2.4–2.9 (2.6 ± 0.19)	2.9
E-N	2.8–3.2 (3 ± 0.12)	3.6
TY	1.8–2 (1.9 ± 0.1)	2.2
TL/SVL	0.48–0.54 (0.51 ± 0.03)	0.47
FL/SVL	0.5–0.57 (0.54 ± 0.03)	0.48
HL/SVL	0.35–0.37 (0.36 ± 0.01)	0.34
HW/SVL	0.4–0.42 (0.41 ± 0.01)	0.38
HW/HL	1.08–1.16 (1.13 ± 0.03)	1.15
E-N/ED	0.82–0.92 (0.87 ± 0.04)	0.86
EW/IOD	0.79–0.95 (0.87 ± 0.07)	0.82
TY/ED	0.51–0.58 (0.55 ± 0.03)	0.53

4934

Table 2. Variation of measurements (in mm) and proportions of the type series of *Oreobates colanensis*. See text for abbreviations.

	Males			
	CORBIDI 21191	CORBIDI 21295	CORBIDI 21296	Min-Max (mean)
SVL	21.9	22.5	22.1	21.9–22.5 (22.2)
TL	10.8	11.4	11.5	10.8–11.5 (11.2)
FL	10.6	10.8	10.8	10.6–10.8 (10.8)
HL	7.6	7.8	7.6	7.6–7.8 (7.7)
HW	8.4	8.9	8.7	8.4–8.9 (8.7)
ED	2.6	2.8	2.6	2.6–2.8 (2.7)
IOD	2.2	2.7	2.7	2.2–2.7 (2.5)
EW	1.8	2.0	1.8	1.8–2 (1.9)
IND	2.5	2.8	2.4	2.4–2.8 (2.6)
E-N	2.1	2.4	2.5	2.1–2.5 (2.3)
TY	1.1	1.2	1.0	1–1.2 (1.1)
TL/SVL	0.49	0.51	0.52	0.49–0.52 (0.51)
FL/SVL	0.48	0.48	0.49	0.48–0.49 (0.48)
HL/SVL	0.35	0.35	0.34	0.34–0.35 (0.35)
HW/SVL	0.38	0.39	0.40	0.38–0.4 (0.39)
HW/HL	1.10	1.14	1.16	1.1–1.16 (1.13)
E-N/ED	0.82	0.87	0.95	0.82–0.95 (0.88)
EW/IOD	0.80	0.75	0.65	0.65–0.8 (0.73)
TY/ED	0.43	0.43	0.36	0.36–0.43 (0.41)

Figures

Figure 1. Phylogenetic trees resulting from the analysis of data sets of 4202 aligned bp (POY) and 3535 aligned bp (MAFFT) and composed of the mitochondrial genes 12S and 16S, and fragments of the nuclear protein-coding genes RAG1 and Tyr. (A) Maximum parsimony optimal tree of 10,427 transformations. Numbers above branches indicate Goodman–Bremer values, and those under branches are Jackknife proportions. (B) Maximum likelihood optimal tree (log likelihood -47,278.957778) and bootstrap node values.

Figure 2. Two living adult males of *Lynchius wayneholl*omonae sp. nov. **(**A-C) Dorsolateral, dorsal and ventral views of holotype, CORBIDI 20765, 27.3 mm SVL. (D-F) Dorsolateral, dorsal and lateral views of the paratype, CORBIDI 20778, 24.9 mm SVL. Photographs by Axel Marcheli.

Figure 3. Preserved *Lynchius wayneholl*omonae sp. nov. (holotype) in dorsal view (A), ventral view (B), palm (C), sole (D), and head in lateral view (E). Scale 5 mm. Photographs by LAGA.

Figure 4. Distribution of species of the genus *Lynchius* in Ecuador and Peru. Green circles with black center are major cities for reference.

Figure 5. Two living adult males of *Oreobates colanensis* sp. nov. (A) Dorsolateral view, (B) lateral view showing the pattern on hidden surfaces, (C) dorsal view showing the pattern on the posterior surface of thighs, and (D) ventral view of holotype, CORBIDI

21191, 21.9 mm SVL. (E-F) Dorsolateral and ventral views of the male paratype, CORBIDI 21295, 22.5 mm SVL. Photographs by Axel Marcheli.

Figure 6. Preserved *Oreobates colanensis* sp. nov. (holotype) in dorsal view (A), ventral view (B), palm (C), sole (D), and head in lateral view (E). Scale 5 mm. Photographs by LAGA.

Figure 7. Distribution of Andean species of the genus *Oreobates*. Green circles with black center are major cities for reference. Green circles with black center are major cities for reference.

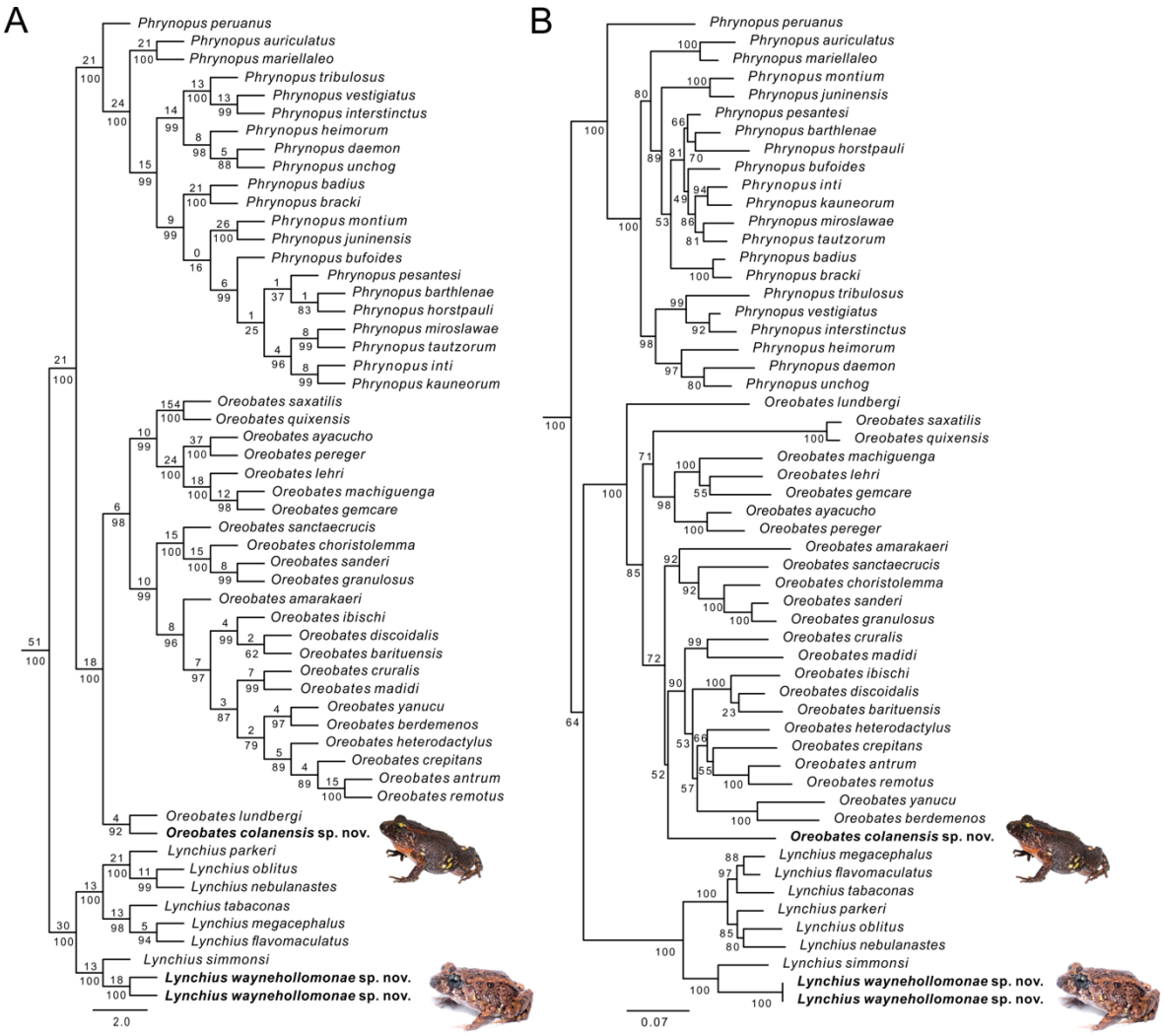

4972

4973 Figure 1

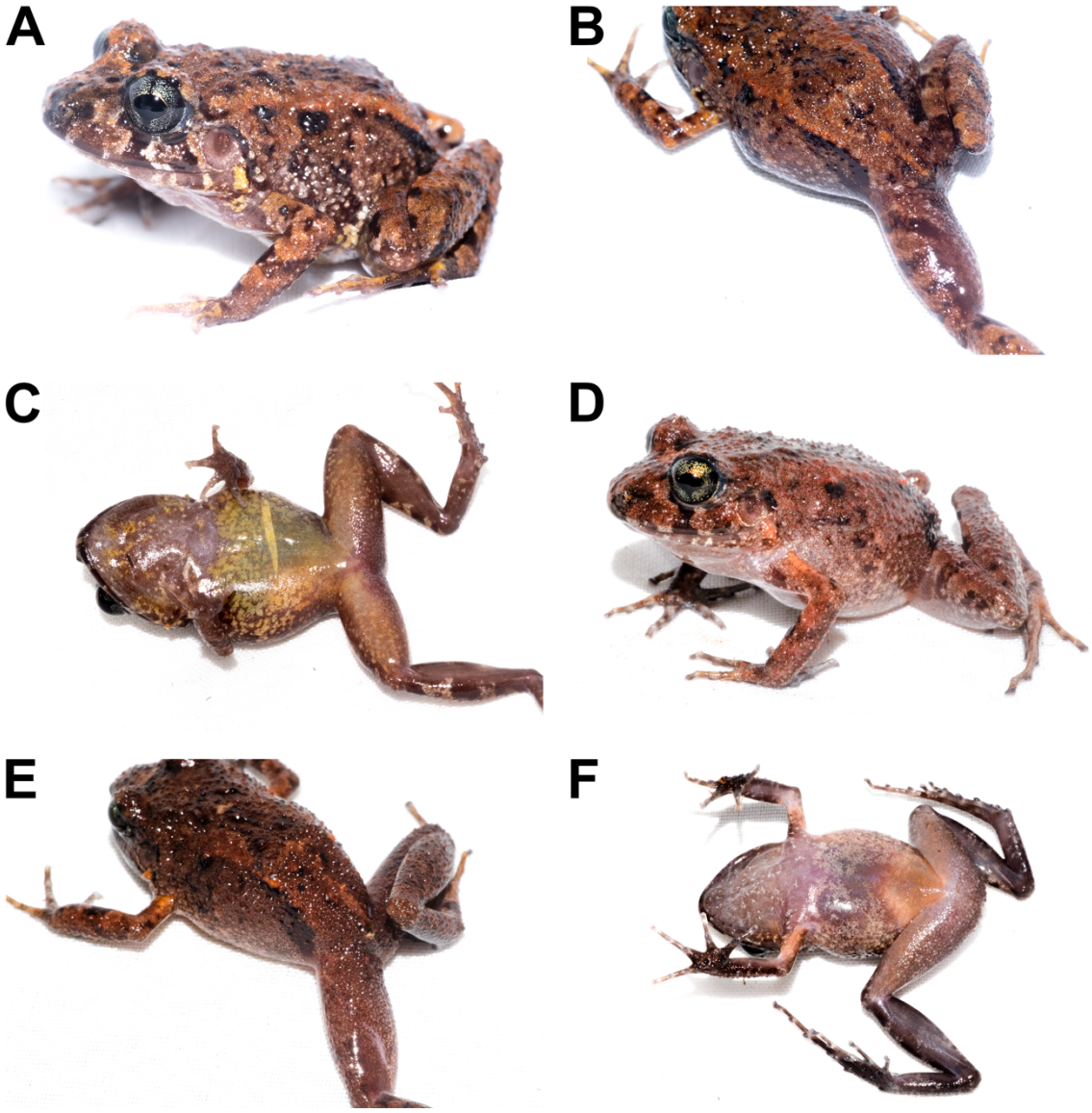

4974

4975 Figure 2

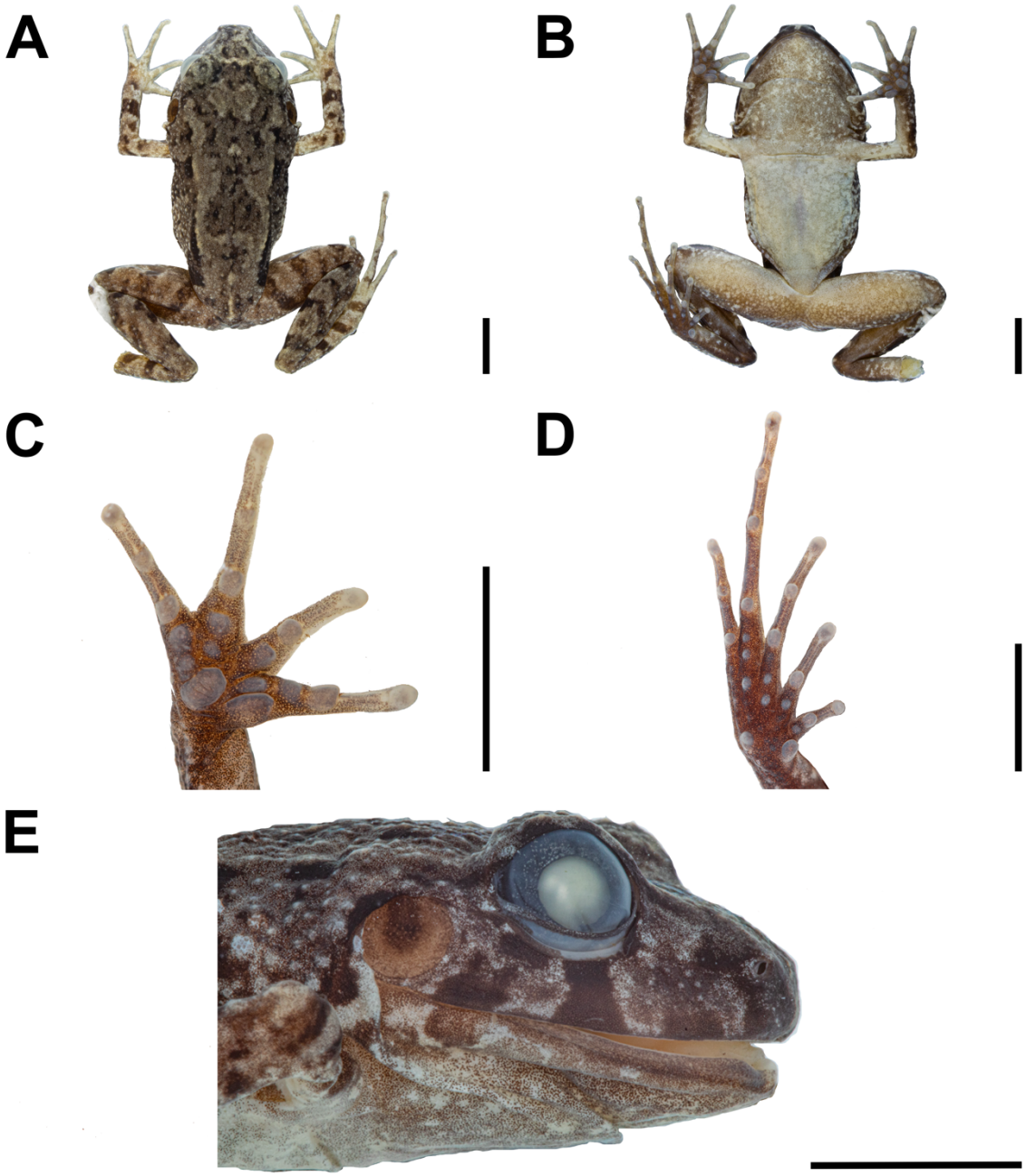

4976

4977 Figure 3

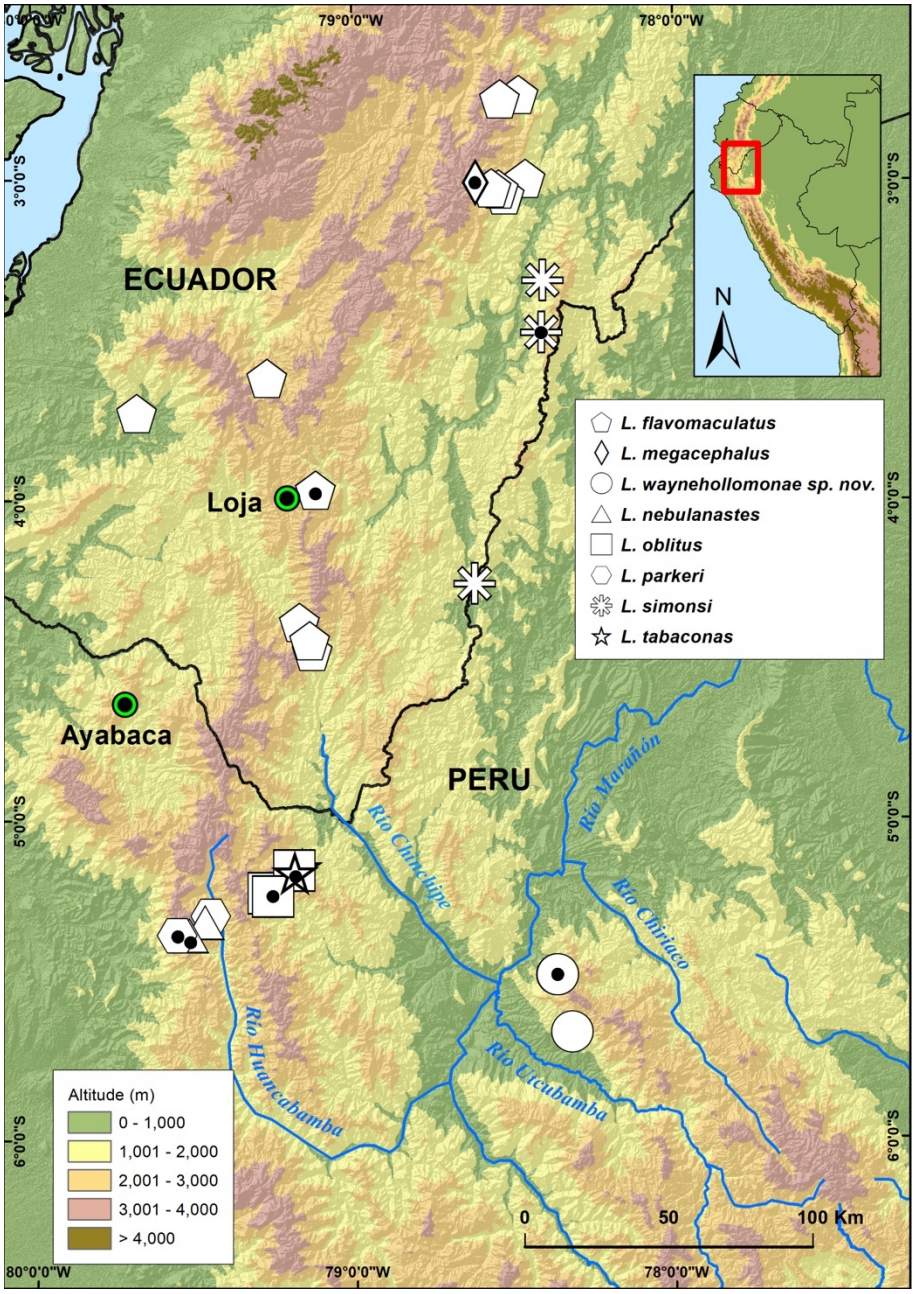

4978

4979 Figure 4

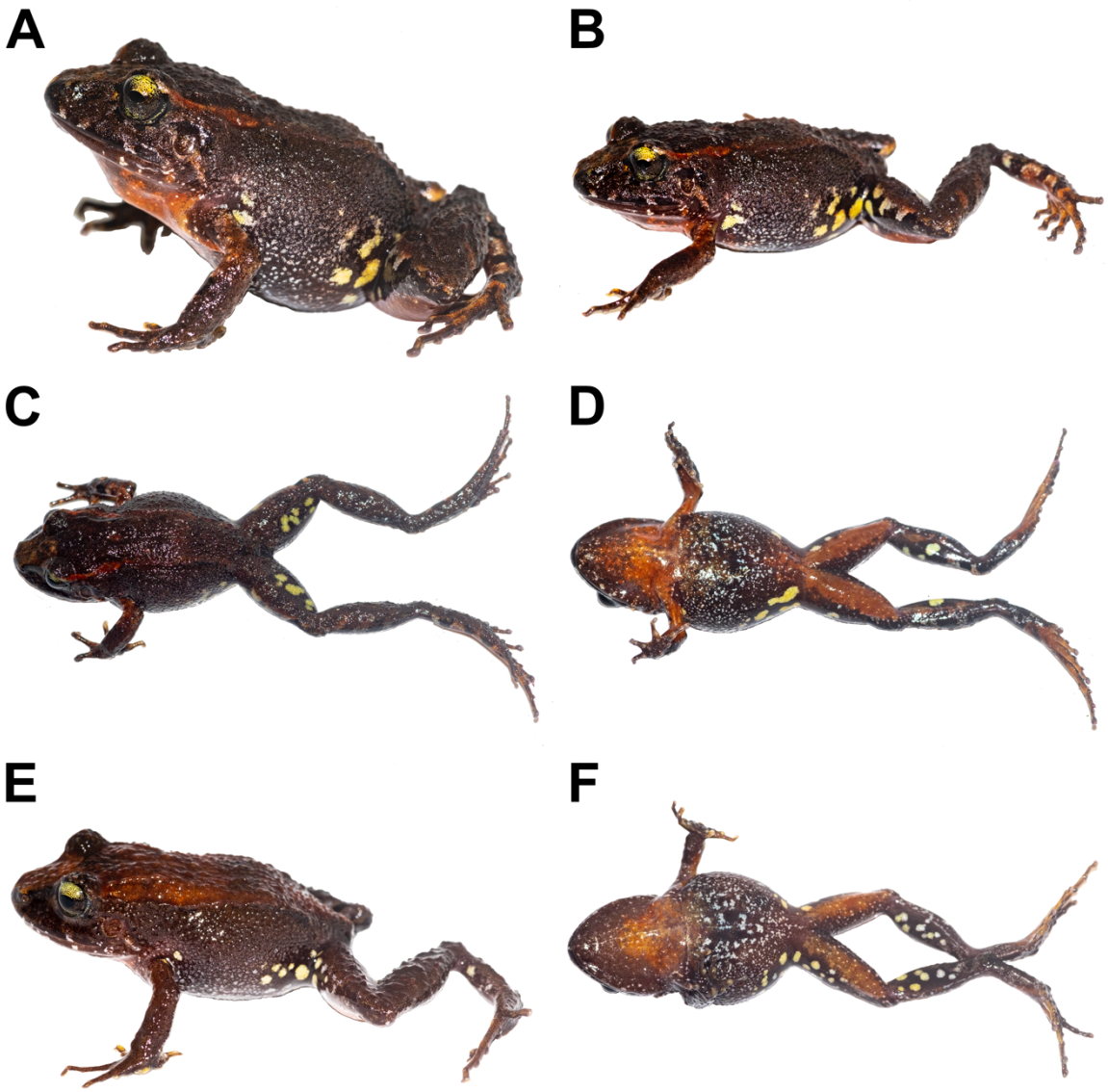

4980

4981 Figure 5

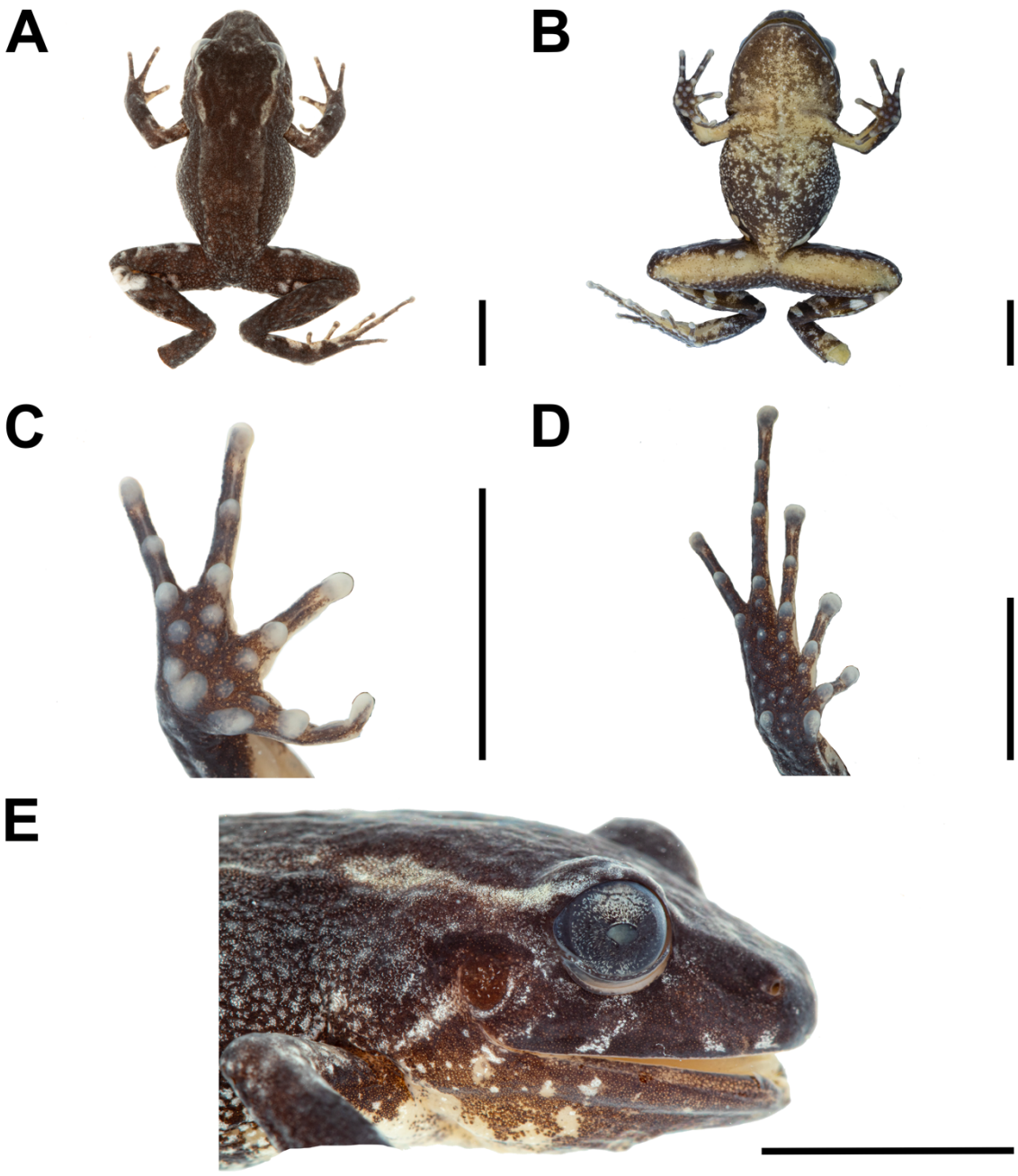

4982

4983 Figure 6

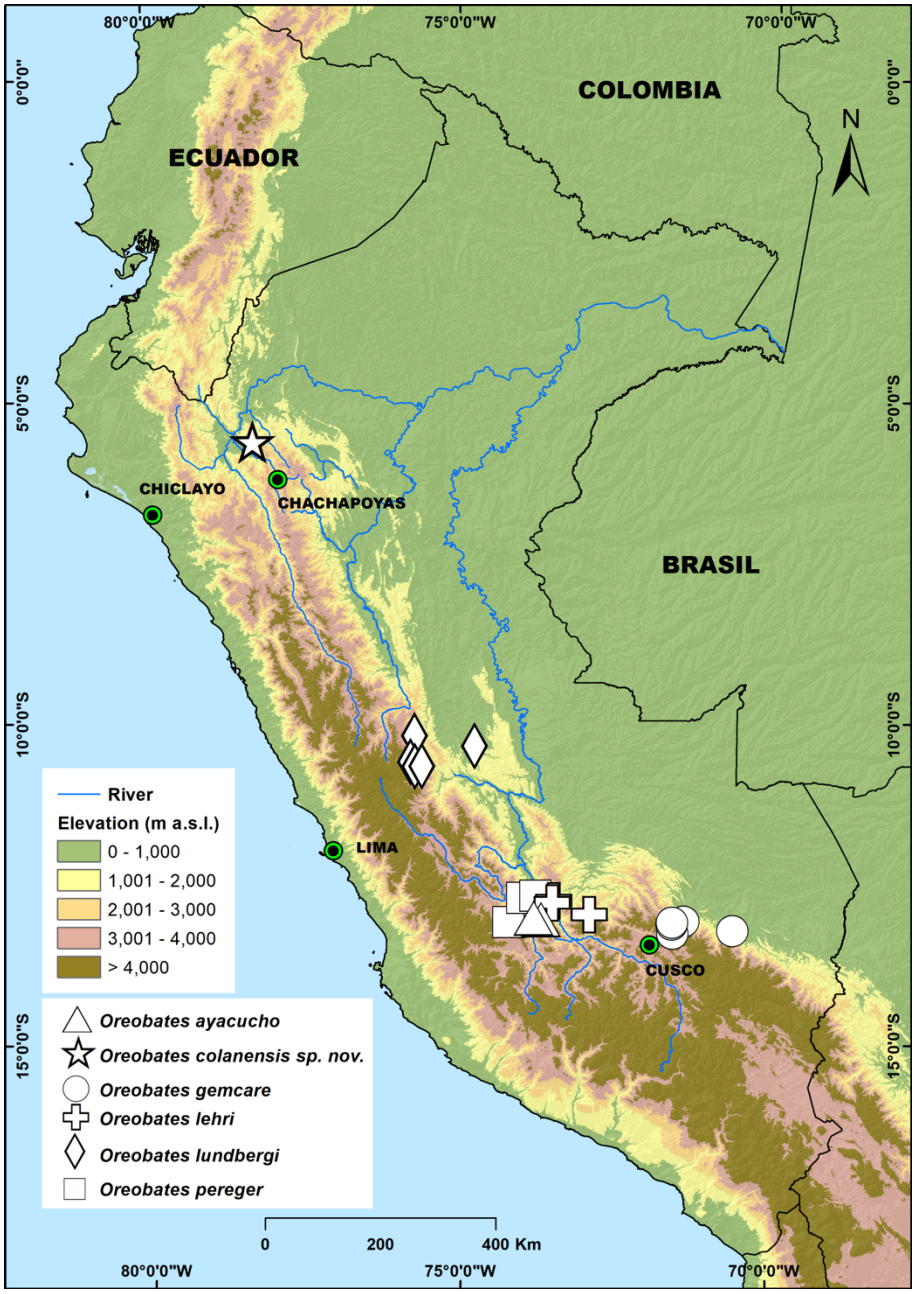

4984

4985 Figure 7

Appendix 1. Material examined.

Lynchius flavomaculatus: KU 119721–24, 119737–42, 121354 142201–02, 202654–55, 218210, 119716–20, 119725–36, 141474–77, 142198–200, 165955–67, 202656; FMNH 197838, 197846, USNM 98929–30, 195393–424, 260788, BMNH 1947.2.16.11, 1947.2.16.12–14; Lynchius nebulanastes: KU 181407, 181392–406, 181408–14, 181841, 219806–819; Lynchius oblitus: MHNC 8598, 8599, 8601, 8602, 8606, 8614, 8625, 8626, 8652, 8672, 8673, 8674, 8675, 8676, 8677, 8689, 8690, MTD 45954; Lynchius parkeri: KU 135278, 135279–311, 181288–91, 181393, 219820, 181292–356, 181823, 181825–27, 181829, 196581–91, LSU 32172–32239; Lynchius simmonsi: KU 147068, 147069, QCAZ 30829–30, 41639–40; Lynchius tabaconas: MHNC 8637, 8649, 8650; Oreobates antrum: CFBH 34897, 39552, 39547, 39549, 39544, 39548, 39551; Oreobates ayacucho: MUSM 37858, 35548, 35552, 35549, 35553, 35551, MCZ 24362, 24363; Oreobates berdemenos: MACN 45641, 45651, 45639, 45661, 45673; Oreobates cruralis: KU 215461, 207749; Oreobates discoidalis: KU 206435, 154526, 182814, 182813, 182815, 154522, MACN 45698; Oreobates gemcare: AMNH 157013, 153087, KU 173233, 173231 MHNCP 6687, 4564, 4602; Oreobates granulosus: AMNH 6060, 6062, 6063; Oreobates heterodactylus: MNRJ 106, MZUSP 85628; Oreobates lehri: CM 158519, 158523, 158535, 158505; Oreobates lundbergi: MUSM 17822; Oreobates machiguenga: MHNCP 6809; CM 158524; Oreobates pereger: MUSM 13980, 19982, 19983; Oreobates quixensis: AMNH 84849, 84850, 103000, 102999, 22179; Oreobates remotus: MZUSP 141708, 141709–724; Oreobates sanderi: AMNH 6063, 6066 (3DM); Oreobates saxatilis: KU 212327, 212556, 212330, 217352, 217327, MUSM 8431, 8432.

5009 **Appendix 2.** Genbank accession numbers of species sampled in this study. Sequences
5010 produced in this study are highlighted in bold font. [sequences will be submitted to
5011 GenBank upon acceptance of manuscript]

Species	**16S**	**12S**	**RAG**	**TYR**
Barycholos pulcher	EU186709	EU186727	EU186744	-
Barycholos ternetzi	DQ283094	-	-	DQ282921
Bryophryne cophites	EF493537	EF493537	EF493423	EF493508
"Eleutherodactylus" bilineatus	JX267324	JX267393	JX267556	JX267691
Euparkerella brasiliensis	JX267468	JX298276	JX267545	JX267682
Haddadus binotatus	EF493361	EF493361	EF493397	JX267685
Holoaden bradei	EF493366	EF493378	EF493449	EU186779
Lynchius flavomaculatus	EU186667	EU186667	EU186745	EU186766
Lynchius megacephalus	MK423938	-	-	-
Lynchius wayneholl omonae	########	-	-	-
Lynchius wayneholl omonae	########	-	-	-
Lynchius nebulanastes	EU186704	EU186704	-	-
Lynchius oblitus	KX470782	KX470777	KX470793	KX470800
Lynchius parkeri	EU186705	EU186705	MK423933	-
Lynchius simmonsi	JF810004	JF809940	JF809915	JF809894
Lynchius tabaconas	KX470780	KX470773	KX470789	KX470796
Microkayla kempffi	MF186384	MF186308	MF186538	MF186566
Microkayla guillei	AY843720	AY843720	-	DQ282995
Microkayla wettsteini	EU186696	EU186696	-	EU186776
Niceforonia brunnea	EF493357	EF493357	EF493422	EF493484
Niceforonia dolops	EF493394	EF493394	EF493414	EF493483
Niceforonia elassodiscus	EF493358	EF493358	-	-
Niceforonia nana	MH536808	MH532902	MN068027	MH542228
Niceforonia nigrovittata	MH538300	-	-	-
Niceforonia peraccai	EF493710	EF493710	EF493420	EF493485
Noblella heyeri	JX267541	JX267463	-	-
Noblella lochites	EU186699	EU186699	EU186756	EU186777
Noblella myrmecoides	JX267542	JX267464	-	-
Oreobates amarakaeri	JF809996	JF809934	JF809913	JF809891
Oreobates antrum	MH025451	MH025427	MH025436	MH025445
Oreobates ayacucho	JF809970	JF809933	JF809912	JF809890
Oreobates barituensis	JF809999	JF809935	JF809914	JF809892
Oreobates berdemenos	KJ125507	-	-	-
Oreobates choristolemma	FJ539067	JF809921	JF809900	JF809881
Oreobates colanensis	########	-	-	-
Oreobates crepitans	KJ125510	-	-	-
Oreobates cruralis	EU186666	EU186666	EU186743	-

Oreobates discoidalis	FJ539068	FJ539073	JF809904	JF809884
Oreobates gemcare	JF809960	JF809930	JF809909	-
Oreobates granulosus	EU368897	JF809929	JF809908	JF809887
Oreobates heterodactylus	EU192296	JF809923	JF809902	JF809882
Oreobates ibischi	FJ438806	FJ438817	-	-
Oreobates lehri	JF809957	JF809927	JF809906	-
Oreobates lundbergi	JF809958	JF809928	JF809907	JF809886
Oreobates machiguenga	JF809969	JF809932	JF809911	JF809889
Oreobates madidi	FJ539070	FJ539075	JF809901	-
Oreobates pereger	JF809955	JF809926	JF809905	JF809885
Oreobates quixensis	EF493662	EF493828	-	JF809893
Oreobates remotus	JN688273	MH025425	MH025434	MH025443
Oreobates sanctaecrucis	JF809951	JF809924	JF809903	JF809883
Oreobates sanderi	EU368904	-	-	-
Oreobates saxatilis	EU186708	EU186726	EU186742	EU186763
Oreobates yanucu	KY111322	-	-	-
Phrynopus auriculatus	EF493708	EF493708	-	MF186582
Phrynopus badius	MG896571	MG896594	MG896618	-
Phrynopus barthlenae	MF186350	MF186292	-	-
Phrynopus bracki	EF493709	EF493709	EF493421	EF493507
Phrynopus bufoides	AM039645	AM039713	-	-
Phrynopus daemon	MG896574	MG896597	-	-
Phrynopus heimorum	MF186363	MF186302	-	MF186580
Phrynopus horstpauli	MF186364	MF186303	-	MF186584
Phrynopus interstinctus	MG896575	MG896598	MG896621	-
Phrynopus inti	MF651906	MF651913	MF651918	MF651921
Phrynopus juninensis	MG896576	MG896599	MG896622	-
Phrynopus kauneorum	AM039650	AM039718	-	-
Phrynopus mariellaleo	MH538299	-	MH538303	MH538306
Phrynopus miroslawae	MF186393	MF186312	MF186542	MF186585
Phrynopus montium	MG896578	MG896601	MG896624	
Phrynopus peruanus	MG896580	MG896605	MG896627	MG896631
Phrynopus pesantesi	AM039656	AM039724	-	-
Phrynopus tautzorum	AM039652	AM039720	-	-
Phrynopus tribulosus	EU186707	EU186725	MF186547	MF186578
Phrynopus unchog	MG896592	MG896609	-	-
Phrynopus vestigiatus	MG896593	MG896610	-	-
Psychrophrynella usurpator	EF493714	EF493714	EU186762	EU186780

5012

New distribution records of *Oreobates antrum* Vaz-Silva, Maciel, Andrade, and Amaro, 2018, a cave-associated species from the Seasonally Dry Tropical Forest in the Brazilian Cerrado (Anura: Brachycephaloidea: Craugastoridae) †

Ana P. Motta[1,*], Mariana Lyra[1], Thiago Gazoni[2], Patrícia P. Parise-Maltempi[2], Célio F. B. Haddad[1]

[1]Universidade Estadual Paulista (UNESP), Instituto de Biociências, Departamento de Zoologia e Centro de Aquicultura (CAUNESP), CP 199, 13506-900 Rio Claro, São Paulo, Brazil

[2]Universidade Estadual Paulista (UNESP), Instituto de Biociências, Departamento de Biologia, CP 199, 13506-900 Rio Claro, São Paulo, Brazil

[*]Corresponding author. E-mail: apmottah@gmail.com

† Manuscrito publicado no periódico *Herpetology Notes,* 13: 561–563 (2020)

The genus *Oreobates* Jiménez de la Espada, 1872 comprises 25 species widely distributed in tropical South America across a disparate and diverse array of ecoregions, from the wet montane grasslands of the Andes up to 4.500 m to the Amazonian lowland forests, or the seasonal dry tropical forests of the Cerrado biome (Padial et al., 2012; Teixeira et al., 2012; Pereyra et al., 2014; Kohler and Padial, 2016; Vaz-Silva et al., 2018). Five species are known to occur in Brazil: *O. antrum* Vaz-Silva, Maciel, Andrade, and Amaro, 2018, *O. crepitans* (Bokermann, 1965), *O. heterodactylus* (Miranda-Ribeiro, 1937), *O. quixensis* Jiménez de la Espada, 1872, and *O. remotus* Teixeira, Amaro, Recoder, Sena, and Rodrigues, 2012. *Oreobates quixensis* has broad distribution in Amazonian lowlands, while the other four species occupy Cerrado and dry Atlantic forests and are associated to rocky outcrops and caves.

Oreobates antrum was recently described from a complex of caves in the municipality of São Domingos, northeastern region of the state of Goiás, Central Brazil. The species is known only from its type-locality; specimens were recorded from two caves located at 8 km apart (Vaz-Silva et al., 2018). In the present study, we report two new records of *O. antrum*, including the first record of the species in the state of Tocantins, Brazil.

Field work was conducted in the municipality of Aurora do Tocantins, state of Tocantins, Brazil, on 12 August 2011. All collected specimens were anesthetized and killed with 10 % lidocaine, fixed in 10 % formaldehyde, and stored in 70 % ethanol. Specimens are housed in the Coleção de Anfíbios Célio F. B. Haddad, Departamento de Zoologia, Universidade Estadual Paulista (CFBH), municipality of Rio Claro, state of São Paulo, Brazil. We also re-examined one specimen identified as *O. remotus* (CFBH 34897) collected at Gruta dos Revolucionários, municipality of Posse, state of Goiás (14.291°S, 46.259°W) on 20 June 2012, since *O. antrum* had been misidentified as *O. remotus* before

its description. Specimens identity was obtained by comparing them with the original description of *O. antrum* and *O. remotus*, and by analysing molecular data (data not published and not included herein).

We found and collected eight specimens (CFBH 39544-45, 39547-52) at Gruta das Rãs, municipality of Aurora do Tocantins municipality (12.693°S, 46.406°W). Specimens were found inside the cave at 0-0.5 m above the floor. Many specimens were laying very close to each other on a stalagmite and one specimen was caught climbing it (Figure 1). Morphological analyses of specimens support the identification of this population, as well as the specimen CFBH 34897 from Gruta dos Revolucionários, as *O. antrum*. Specimens present 10 of the set of 11 characters included in the species diagnosis. The only character that has not been confirmed refers to the advertisement call, since we were not able to record calling males. The two new records extend the distribution range of *O. antrum* to approximately 100 km north and 75 km south from its type locality (Figure 2).

Unlike its sister species *Oreobates remotus*, which occurs in wet limestone outcrops in forest environments (Teixeira et al., 2012), *O. antrum* has only been found inside caves in Cerrado. *Oreobates antrum* seems to be strongly associated to caves and probably reproduces inside them, an idea supported by the fact that males were heard calling inside caves and no specimen of *O. antrum* has been found outside caves (Vaz-Silva et al., 2018).

The use of caves by anurans is not an unusual behaviour, but most species are known to use caves as a shelter when under unfavourable external environmental conditions. In Brazil, the use of caves is more frequent when caves are inserted in arid and semiarid biomes, such as Caatinga and Cerrado, probably due to the risks of high temperatures and low humidity of those biomes (Matavelli et al., 2015).

However, other species of Brachycephaloidea are known to use caves not only as a refuge, but also for reproduction. For example, the Jamaican frog *Eleutherodactylus*

cundalli Dunn, 1926 and the Puerto Rican frog *E. cooki* Grant, 1932 spend most part of their lives in caves, leaving them mainly during the night to forage. Calling males, gravid females, clutches, and froglets of those species have been found inside caves (Rogowitz and Sanchez-Rivoleda, 1999; Diesel et al., 1995).

These new geographic distribution data presented here suggest that, besides the species-specific environmental requirements in this group, species of *Oreobates* from Cerrado biome may have wider distribution, which can be confirmed by additional sampling in this biome and its caves.

Acknowledgments. APM and MLL thanks São Paulo Research Foundation (FAPESP) for their scholarships (#2017/08488-3; #2017/26162-8). TG thanks Coordenação de Aperfeiçoamento de Pessoal de Nível Superior (CAPES) for his PhD fellowship. Conselho Nacional de Desenvolvimento Científico e Tecnológico (CNPq #473264/212-9) provided financial support to PPPM. FAPESP (#2013/50741-7) and CNPq (#302518/2013-4) provided financial support to CFBH. Permit (#30202-2) was provided by Instituto Chico Mendes de Conservação da Biodiversidade (ICMBio–SISBIO).

References

Diesel, R., Bäurle, G., Vogel, P. (1995): Cave breeding and froglet transport: a novel pattern of anuran brood care in the Jamaican frog, *Eleutherodactylus cundalli*. **Copeia** 1995: 354–360.

Köhler, J., Padial, J.M. (2016): Description and phylogenetic position of a new (singleton) species of *Oreobates* JiméNez De La Espada, 1872 (Anura: Craugastoridae) from the Yungas of Cochabamba, Bolivia. Annals of Carnegie Museum **84**: 23–38.

5103 Matavelli, R., Campos, A.M., Feio, R.N., Ferreira, R.L. (2015): Occurrence of anurans in
5104 Brazilian caves. Acta Carsologica 44: 107–120.
5105 Padial, J.M., Chaparro, J.C., Castroviejo-Fisher, S., Guayasamín, J.M., Lehr, E., Delgado,
5106 A.J., Vaira, M., Teixeira Jr, M., Aguayo, R., De la Riva I. (2012): A revision of
5107 species diversity in the Neotropical genus *Oreobates* (Anura: Strabomantidae), with
5108 the description of three new species from the Amazonian slopes of the Andes, and
5109 the proposal of candidate species. American Museum Novitates **3752**: 1–55.
5110 Pereyra, M.O., Cardozo, D., Baldo, J.L., Baldo, D. (2014): Description and phylogenetic
5111 position of a new species of *Oreobates* (Anura: Craugastoridae) from northwestern
5112 Argentina. Herpetologica **70**: 211–227.
5113 Rogowitz G.L., Sanchez-Rivoleda, J. (1999): Locomotor performance and aerobic capacity
5114 of the cave coqui, *Eleutherodactylus cooki*. Copeia **1999**: 40–48.
5115 Teixeira Jr., M., Amaro, R.C., Recoder, R.S., De Sena, M.A., Rodrigues, M.T. (2012) A
5116 relict new species of *Oreobates* (Anura, Strabomantidae) from the Seasonally Dry
5117 Tropical Forests of Minas Gerais, Brazil, and its implication to the biogeography of
5118 the genus and that of South American Dry Forests. Zootaxa **52**: 37–52.
5119 Vaz-Silva, W., Maciel, N.M., de Andrade, S.P., Amaro, R.C. (2018): A new cryptic species
5120 of *Oreobates* (Anura: Craugastoridae) from the seasonally dry tropical forest of
5121 central Brazil. Zootaxa **4441**: 89–108.
5122

Figures

Figure 1. Specimens of *Oreobates antrum* found on a stalagmite at Gruta das Rãs, municipality of Aurora do Tocantins, state of Tocantins, Brazil.

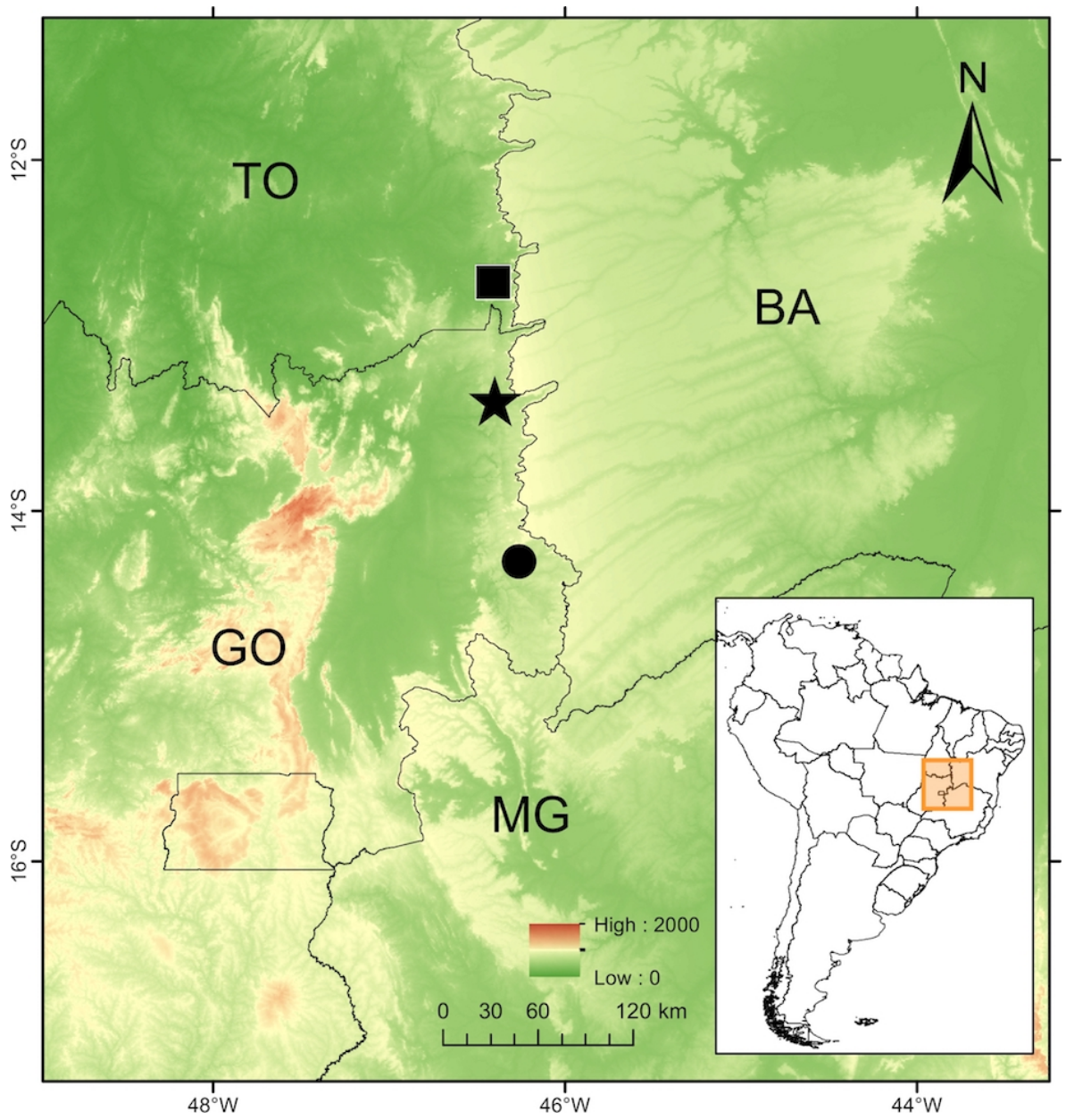

Figure 2. Geographic distribution of *Oreobates antrum*. Star: municipality of São Domingos, state of Goiás (type locality). Circle: Gruta dos Revolucionários, municipality of Posse, state of Goiás (new record). Square: Gruta das Rãs, municipality of Aurora do Tocantins, state of Tocantins (new record).

Conclusões Gerais

- Apresentamos uma análise filogenética de evidência total sem precedentes em caracteres e táxons, combinando 15 genes e 101 caracteres fenotípicos para 79 espécies de Holoadeninae. Nossas análises recuperaram o gênero *Phrynopus* monofilético, irmão do clado incluindo os gêneros *Lynchius* e *Oreobates*. Encontramos baixo suporte para *Phrynopus*. No entanto, mostramos que isso se deve ao comportamento "wildcard" de *P. thompsoni*, um terminal com dados faltantes. Com base na hipótese filogenética resultante, identificamos sinapomorfias para *Phrynopus* e gêneros relacionados. Discutimos a evolução da orelha média relacionada à comunicação acústica e da cintura pélvica relacionada à locomoção em Holoadeninae. Também discutimos a convergência de características nos gêneros que compartilham a morfologia "phrynopoid". Mostramos que a evolução repetida de estados de caráter é um fenômeno comum em Holoadeninae e não se restringe a grupos andinos. Além disso, embora muito tenha sido discutido sobre convergência em Holoadeninae, os eventos envolvem o mesmo estado ancestral dando origem ao mesmo estado derivado, constituindo um exemplo de paralelismo. Nosso estudo fornece uma base sólida para uma maior exploração e compreensão da evolução morfológica em terrarana.
- Análises filogenéticas incluindo caracteres moleculares, juntamente com dados de morfologia externa e osteologia de "*E.*" *bilineatus*, suportam a descrição de um novo gênero para acomodar esta espécie que nomeamos e diagnosticamos neste trabalho. Nossas análises recuperaram "*E.*" *bilineatus* como uma linhagem independente formando um clado altamente suportado com *Barycholos* e *Noblella*. Nossas análises também recuperam o gênero *Noblella* não monofilético e as espécies do gênero, embora morfologicamente semelhantes, fazem parte de diferentes clados: um

incluindo espécies dos Andes centrais e outro incluindo espécies dos Andes do norte. Além disso, os padrões de distribuição apontam conexões entre áreas biogeográficas distantes da América do Sul e uma distribuição generalizada de um ancestral para o clado incluindo *Barycholos*, "*E.*" *bilineatus* e *Noblella*. Também comparamos as relações entre os clados de Brachycephaloidea e, portanto, as classificações de família e subfamília em diferentes estudos. Mostramos que a classificação de famílias provavelmente está longe de se estabilizar, principalmente devido a seleções arbitrárias de hierarquia dos clados. No entanto, mostramos que a atribuição de uma família a cada um dos clados altamente sustentados e frequentemente recuperados tornaria a taxonomia de Brachycephaloidea mais estável.

- Investigamos se as mudanças altitudinais e de habitat conduzem à evolução morfológica em uma radiação continental de sapos de desenvolvimento direto da região Neotropical (*Lynchius*, *Oreobates* e *Phrynopus*). Descobrimos que a evolução do tamanho do corpo não suporta a regra de Bergmann. Nossos resultados sugerem, no entanto, que as mudanças de habitat conduzem a evolução morfológica neste grupo. Nossas análises indicam que mudanças de floresta para Puna nos Andes e para ambientes secos de baixada resultaram em semelhanças morfológicas entre espécies distantemente relacionadas. Especificamente, a ocupação do ambiente Puna envolveu mudança evolutiva em direção à diminuição do comprimento da cabeça e dos membros posteriores, enquanto a ocupação de ambientes secos de baixada envolveu mudança evolutiva em direção à expansão das pontas dos dedos. Nós hipotetizamos que os requisitos mecânicos podem ser responsáveis pela convergência neste grupo e sugerimos que futuras análises explorem a relação entre o formato do corpo e o uso de micro-habitat.

- Avaliamos o status taxonômico e a área de distribuição de populações de *Oreobates* de 10 localidades na região central da América do Sul. Realizamos análises filogenéticas, análises de componentes principais e análises de funções discriminantes para avaliar o status taxonômico destas populações. Como resultado, redescrevemos *O. heterodactylus* com base em uma série de topótipos recém coletados e material adicional de outras localidades. Reavaliamos o status taxonômico de *O. crepitans*, considerado sinônimo júnior de *O. heterodactylus*. Também descrevemos as populações de *Oreobates* no leste da Bolívia como uma nova espécie.
- Descrevemos duas novas espécies de Holodeninae da Cordillera de Colán, no nordeste do Peru. A primeira espécie pertence ao gênero *Lynchius* e ocorre em duas localidades de 1.977 a 2.006 m a.s.l., enquanto a segunda espécie pertence ao gênero *Oreobates* e só é conhecida em um local a 2.608 m a.s.l. *Lynchius. wayneholomonae* é a primeira espécie de *Lynchius* encontrada ao sul da Depressão de Huancabamba e ocorrendo exclusivamente nas Yungas peruanas. *O. colanensis* representa a espécie de *Oreobates* no extremo norte dos Andes, estendendo em mais de 600 km ao norte a distribuição do gênero em altitudes acima de 2000 m nos Andes.
- Foram encontrados e coletados espécimes na Gruta dos Revolucionários, Posse, Goiás e na Gruta das Rãs, Aurora do Tocantins, Tocantins. Análises morfológicas dos espécimes corroboram a identificação destas populações como *O. antrum* e os dois novos registros estendem a faixa de distribuição da espécie para aproximadamente 100 km ao norte e 75 km ao sul de sua localidade-tipo.